

**Reliable mass spectrometric techniques for
new insights into the kallikrein-kinin system –
modern bioanalytical peptide quantitation of an
endogenous cascade**

Inaugural-Dissertation

zur Erlangung des Doktorgrades
der Mathematisch-Naturwissenschaftlichen Fakultät
der Heinrich-Heine-Universität Düsseldorf

vorgelegt von

Tanja Gangnus
aus Schwetzingen

Düsseldorf, Dezember 2021

aus dem Institut für Klinische Pharmazie und Pharmakotherapie
der Heinrich-Heine-Universität Düsseldorf

Gedruckt mit der Genehmigung der
Mathematisch-Naturwissenschaftlichen Fakultät der
Heinrich-Heine-Universität Düsseldorf

Berichtersteller:

1. Prof. Dr. Stephanie Lärer

2. Prof. Dr. Georg Kojda

Tag der mündlichen Prüfung: 02. Dezember 2021

I. Erklärung zur Dissertation

Hiermit versichere ich an Eides statt, dass die vorgelegte Dissertation mit dem Titel:

Reliable mass spectrometric techniques for new insights into the kallikrein-kinin system – modern bioanalytical peptide quantification of an endogenous cascade

von mir selbstständig und ohne unzulässige fremde Hilfe unter Beachtung der Grundsätze zur Sicherung guter wissenschaftlicher Praxis an der Heinrich-Heine-Universität Düsseldorf erstellt worden ist. Die Dissertation wurde in der vorgelegten oder in ähnlicher Form noch bei keiner anderen Institution eingereicht. Ich habe bisher keinen erfolglosen Promotionsversuch unternommen.

Düsseldorf, den 15.12.2021

Tanja Gangnus

II. Danksagungen

Während des Erstellens und Schreibens dieser Dissertation habe ich viel Unterstützung und Hilfe erhalten. Ich sage deshalb „Herzlichen Dank“...

...Frau Prof. Dr. Stephanie Läer, meiner Promotionsbetreuerin, für die Möglichkeit meine Promotion am Institut der Klinischen Pharmazie durchzuführen und den damit verbundenen Erfahrungen, die ich sammeln durfte. Danke für die Förderung meines wissenschaftlichen Interesses und den Raum meine eigenen Ideen zu verfolgen und zu verwirklichen.

...Herrn Prof. Dr. Georg Kojda für die Übernahme meiner Mentorenschaft und die stets freundliche Unterstützung. Weiterhin danke ich für die fachkundige Betreuung und die stete Bereitschaft zum differenzierten wissenschaftlichen Austausch, der meine Arbeit bereichern konnte.

...Herrn Dr. Björn Burckhardt für die Betreuung meiner Dissertationsarbeit und die immerwährende Unterstützung. Stets aufschlussreiches Feedback hat mich dazu gebracht, mein Denken zu schärfen und meine Arbeit auf ein höheres Niveau zu bringen. Danke für die mehrfache Durchsicht dieser Arbeit und deren kritische Betrachtung. Danke für den moralischen Beistand und menschlichen Halt, die es mir erst ermöglicht haben diese Arbeit zu vollenden.

...meinen aktuellen und ehemaligen Kollegen und Kolleginnen am Institut für Klinische Pharmazie, die mich auf dem Weg meiner Promotion begleitet haben und durch wissenschaftliche Diskussionen und Ratschläge, aber auch Aufmunterung und Motivation letztendlich zur Fertigstellung dieser Arbeit beigetragen haben.

...meinen Freunden, die mich auf der einen Seite auf meinem Weg unterstützt und begleitet haben, aber auch in den richtigen Momenten für die nötige Ablenkung gesorgt haben.

...meiner Familie und insbesondere meinen Eltern Heike und Bernd und meiner Schwester Verena, die mich immer in jeglicher Hinsicht unterstützt und ermutigt hat und die mir meinen bisherigen Lebensweg ermöglichten.

III. Zusammenfassung

Dem Kallikrein-Kinin System (KKS) wird eine zentrale Rolle bei zahlreichen Erkrankungen zugeschrieben. Dies wurde jüngst im Rahmen der Pandemie COVID-19 untermauert, bei der früh ein Bradykinin-Sturm ursächlich für die Pathologie postuliert wurde. Somit ist ein besseres Verständnis der (patho)physiologischen Bedeutung des KKS essentiell, um die Rationale für die Entwicklung neuer therapeutischer Angriffspunkte innerhalb des KKS zu schaffen. Aufgrund des Mangels verlässlicher bioanalytischer Assays für Kininpeptide sollten im Rahmen dieser Arbeit umfassende und regulatorisch konforme bioanalytische Plattformen auf Basis der Massenspektroskopie erarbeitet und klinisch angewendet werden.

Im Vordergrund der Arbeit stand die Etablierung bioanalytischer massenspektrometrischer Plattformen für die simultane und verlässliche Quantifizierung der Kininpeptide Bradykinin, Kallidin, Des-Arg(9)-bradykinin, Des-Arg(10)-kallidin, Bradykinin 1-7, Bradykinin 2-9 und Bradykinin 1-5 in Plasma und respiratorischen Lavageflüssigkeiten. Die bekannten Limitationen der bisher häufig angewandten Immunoassays durch Kreuzreaktionen wurden durch den Einsatz von hocheffizienten und orthogonalen Trennungstechniken überwunden. Die Erfassung der niedrigen endogenen Peptidspiegel wurde erfolgreich durch eine Optimierung der Ionisationseffizienz und Reduktion der unspezifischen Peptidadsorption mittels statistischer Versuchsplanung ermöglicht. Der umfassenden Methodenentwicklung schloss sich eine Validierung der Assays entsprechend internationaler bioanalytischer Leitlinien aus 150 µl Plasma und 100 µl respiratorischer Lavageflüssigkeiten mit sensitiven Quantifizierungsgrenzen von bis zu 2 pg/mL für die Kininpeptide an.

Aufbauend widmete sich diese Arbeit auch der systematischen Untersuchung präanalytischer Variablen, die wiederum für bis zu $\frac{3}{4}$ aller Quantifizierungsfehler in der Bioanalytik verantwortlich sein können. Durch die Identifizierung bedeutender Einflussfaktoren auf artifizielle Veränderungen von Plasmakininpiegeln während der Blutabnahme und -aufbereitung konnte ein standardisiertes präanalytisches Protokoll entwickelt werden. In einer proof-of-concept Untersuchung war die Anwendung des Protokolls in Kombination mit der bioanalytischen Plattform durch Detektion niedriger endogener Kininlevel (<5 pg/mL) mit geringer interindividueller und Inter-Tagesvariabilität charakterisiert.

Die entwickelten massenspektrometrischen Plattformen wurden abschließend in klinischen Studien angewendet. Umfassende Kininprofile wurden in 28 gesunden Erwachsenen erhoben, um verlässliche Daten für Kontrollgruppen zu erheben. Darüber hinaus konnte zusammen mit internationalen Forschungsteams aus Leuven und Nijmegen in klinischen Studien mit COVID-19 Patienten erstmalig gezeigt werden, dass das KKS wesentlich an der Pathologie von COVID-19 beteiligt ist. Der umgehende Einsatz der entwickelten Methoden lieferte einen wertvollen Beitrag auf dem aktuell gesellschaftlich hochrelevanten Feld der Corona-Forschung.

IV. Summary

The kallikrein-kinin system (KKS) is considered to play a central role in numerous diseases. This was recently underscored in the context of the COVID-19 pandemic, in which a bradykinin storm was postulated early to be causative for the disease pathology. Thus, a better understanding of the (patho)physiological significance of the KKS is essential to provide the rationale for the development of new therapeutic targets within the KKS. Due to the lack of reliable bioanalytical assays for kinin peptides, comprehensive and guideline compliant bioanalytical platforms based on mass spectroscopy were intended to be developed and clinically applied within the scope of this thesis.

The focus of the work was the establishment of bioanalytical mass spectrometric platforms for the simultaneous and reliable quantification of the kinins bradykinin, kallidin, des-Arg(9)-bradykinin, des-Arg(10)-kallidin, bradykinin 1-7, bradykinin 2-9 and bradykinin 1-5 in plasma and respiratory lavage fluids. The known limitations of previously commonly used immunoassays by cross-reaction have been overcome by the use of highly efficient and orthogonal separation techniques. The detection of low endogenous peptide levels was successfully enabled by optimising ionisation efficiency (factor of 7.7) and reducing non-specific peptide adsorption (factor of 26.6) using design of experiments. The comprehensive method development was followed by validation of the assays according to international bioanalytical guidelines applying 150 μ L of plasma and 100 μ L of respiratory lavage fluids with sensitive quantification limits of down to 2 pg/mL for the kinin peptides.

Based on this, this work was also dedicated to the systematic investigation of pre-analytical variables, which in turn can be responsible for up to $\frac{3}{4}$ of all quantification errors in bioanalysis. By identifying significant factors causing artificial changes in plasma kinin levels during blood collection and processing, a standardised pre-analytical protocol was developed. In a proof-of-concept study, the application of the protocol in combination with the bioanalytical platform was characterised by detection of low endogenous kinin levels (<5 pg/mL) with limited inter-individual and inter-day variability.

The developed mass spectrometric platforms were finally applied within clinical studies. Comprehensive kinin profiles were collected in 28 healthy adults to provide reliable data for control groups. In addition, in cooperation with international research teams from Leuven and Nijmegen, clinical studies with COVID-19 patients demonstrated for the first time that the KKS is significantly involved in the pathology of COVID-19. The prompt application of the developed methods provided a valuable contribution to the currently socially highly relevant field of corona research.

V. Table of Contents

I. Erklärung zur Dissertation	III
II. Danksagungen.....	IV
III. Zusammenfassung.....	V
IV. Summary	VI
V. Table of Contents	VII
VI. List of Abbreviations.....	XI
VII. List of Tables	XIII
VIII. List of Figures.....	XIV
1. Introduction	1
1.1. The kallikrein-kinin system.....	1
1.1.1. Metabolism of kinins.....	1
1.1.2. Pharmacology of kinins	3
1.1.3. Current status of bioanalysis of kinins	4
1.2. Coronavirus disease 2019.....	6
1.3. Ethical considerations regarding bioanalysis of kinins in the critically ill.....	9
1.4. Issues and challenges in bioanalytical peptide quantification with focus on kinins	11
1.4.1. Sampling and biological sample handling	11
1.4.2. Non-specific peptide adsorption	12
1.4.3. <i>Ex vivo</i> stability	13
1.4.4. Sample purification from biological fluids	14
1.4.5. Liquid chromatography coupled with tandem mass spectrometry.....	15
1.4.6. Method development and optimization.....	17
1.4.7. Method validation	19
2. Aim of the thesis	20
3. Improving sensitivity for the targeted mass spectrometric analysis of bradykinin using a design of experiments approach	21
3.1. Background	21
3.2. Materials and Methods	23
3.2.1. Chemicals and reagents.....	23
3.2.2. Preparation of kinin stock and working solutions.....	23
3.2.3. Sample preparation	24
3.2.4. Design of experiments.....	24
3.2.5. Applicability of optimizations	28
3.2.6. Instrumentation.....	28
3.2.7. Software packages.....	29
3.3. Results and Discussion	30

3.3.1. Optimisation of mobile phase composition	30
3.3.2. Optimisation of injection solvent and sample collection material.....	34
3.3.3. Applicability	39
3.4. Conclusion	41
4. Targeted mass spectrometric platform for the comprehensive determination of peptides in the kallikrein-kinin system in plasma.....	42
4.1. Background	42
4.2. Materials and Methods	44
4.2.1. Preparation of kinin stock and working solutions.....	44
4.2.2. Human blood samples.....	44
4.2.3. Sample preparation	44
4.2.4. Liquid chromatography coupled with tandem mass spectrometry.....	45
4.2.5. Method development for kinin quantitation in plasma	46
4.2.6. Validation of kinin quantitation in plasma	46
4.2.7. Applicability of kinin quantitation in plasma	49
4.3. Results.....	50
4.3.1. Method development for kinin quantitation in plasma	50
4.3.2. Validation of kinin quantitation in plasma	51
4.3.3. Applicability of kinin quantitation in plasma	57
4.4. Discussion	59
4.5. Conclusion	63
5. Tackling reliable determination of peptides of the kallikrein-kinin system in human plasma	64
5.1. Background	64
5.2. Materials and Methods	67
5.2.1. Human samples	67
5.2.2. Investigations on extent and time-course of artificial kinin alterations.....	67
5.2.3. Impact of protease inhibitors on <i>ex vivo</i> kinin stability.....	67
5.2.4. Effect of blood sampling and handling on kinin quantification	69
5.2.5. Effect of specimen handling on kinin quantification.....	70
5.2.6. Validation and applicability of the standardized protocol.....	71
5.2.7. Liquid chromatography coupled to tandem mass spectrometry monitoring of kinins	71
5.2.8. Quality control system	71
5.2.9. Statistical analysis	72
5.3. Results.....	73
5.3.1. Investigations on extent and time-course of artificial kinin alterations.....	73
5.3.2. Impact of protease inhibitor on <i>ex vivo</i> kinin stability.....	74
5.3.3. Effect of blood sampling and handling on kinin quantification	77
5.3.4. Effect of specimen handling on kinin quantification.....	79
5.3.5. Validation and applicability of the standardized protocol.....	80
5.4. Discussion	82
5.5. Conclusion	84

6. Sensitive mass spectrometric determination of kinins in respiratory saline lavage fluid in light of COVID-19	85
6.1. Background	85
6.2. Materials and Methods	88
6.2.1. Chemicals and reagents.....	88
6.2.2. Preparation of kinin stock and working solutions.....	88
6.2.3. Sample preparation	88
6.2.4. Liquid chromatography coupled with tandem mass spectrometry.....	89
6.2.5. Method development for kinin quantitation in saline lavage fluids.....	90
6.2.6. Validation of kinin quantitation in saline	90
6.2.7. Applicability of kinin quantitation in nasal lavage fluid	92
6.3. Results.....	93
6.3.1. Method development for kinin quantitation in saline lavage fluids.....	93
6.3.2. Validation of kinin quantitation in saline	93
6.3.3. Applicability of kinin quantitation in nasal lavage fluid	100
6.4. Discussion	102
6.5. Conclusion	105
7. Mass spectrometric study of variation in kinin peptide profiles in nasal fluids and plasma of adult healthy individuals	106
7.1. Background	106
7.2. Materials and methods	108
7.2.1. Study design.....	108
7.2.2. Blood sampling.....	108
7.2.3. Sampling of nasal lavage fluid.....	108
7.2.4. Estimating endogenous kinin levels in nasal epithelial lining fluid.....	109
7.2.5. Mass spectrometric kinin quantification.....	110
7.2.6. Data analysis.....	110
7.3. Results.....	111
7.3.1. Study population.....	111
7.3.2. Endogenous kinin profiles in plasma	111
7.3.3. Kinin profiles applying inappropriate sampling conditions in plasma.....	113
7.3.4. Kinin profiles in nasal lavage fluids of healthy volunteers	113
7.3.5. Estimating endogenous kinin levels in nasal epithelial lining fluid.....	115
7.3.6. Comparison of kinin profiles in plasma and nasal fluids.....	116
7.4. Discussion	117
7.5. Conclusion	119
8. Investigation of kinin peptides in biological fluids of COVID-19 patients	120
8.1. Background	120
8.2. A dysregulated kallikrein-kinin system in COVID-19 patients.....	123
9. Overall conclusion and perspective	125
10. Acknowledgement and funding	130
11. References	131

12. Appendix	151
13. Curriculum vitae	164
14. List of publications	165
14.1. Publications in international peer-reviewed journals.....	165
14.2. Publications in revision in international peer-reviewed journals	166
14.3. Publications under consideration in international peer-reviewed journals	166
14.4. Oral presentations	166
14.5. Poster presentations.....	166
14.6. Awards.....	167

VI. List of Abbreviations

ACE:	Angiotensin-converting-enzyme
ACN:	Acetonitrile
AEBSF:	4-(2-aminoethyl)benzolsulfonylfluoride
ANOVA:	Analysis of variance
APP:	Aminopeptidase P
ARDS:	Acute respiratory distress syndrome
B₁ receptor:	Bradykinin receptor type 1
B₂ receptor:	Bradykinin receptor type 2
BALF:	Bronchoalveolar lavage fluid
BK:	Bradykinin
C1INH:	C1-esterase inhibitor
COVID-19:	Coronavirus disease 2019
CP:	Carboxypeptidase
Cps:	counts per second
CV:	Coefficient of variation
Da:	Dalton
DMSO:	Dimethyl sulfoxide
DoE:	Design of experiments
DPP IV:	Dipeptidylpeptidase IV
ECE:	Endothelin-converting enzyme
EDTA:	Ethylenediaminetetraacetic acid
EG:	Ethylene glycol
EMA:	European Medicines Agency
EP:	Endopeptidase
FA:	Formic acid
GRAVY:	Grand average of hydropathicity index
FDA:	US Food and Drug Administration
HDMB:	Hexadimethrine bromide
HMWK:	High molecular weight kininogen
¹H-NMR:	Proton nuclear magnetic resonance
HPLC:	High-performance liquid chromatography
ICH:	International Council for Harmonisation
IQR:	Interquartile range
IS:	Internal standard
KAL:	Kallidin
KKS:	Kallikrein-kinin system
LB:	Protein low binding
LC:	Liquid chromatography
LC-MS/MS:	Liquid chromatography coupled with tandem mass spectrometry
LLOQ:	Lower limit of quantification
LMWK:	Low molecular weight kininogen
LoD:	Limit of detection
log D:	Normalized distance to target
MCX:	Mixed-mode strong cation exchange

MPO-DNA:	Myeloperoxidase deoxyribonucleic acid
MRM:	Multiple reaction monitoring
MS:	Mass spectrometry
m/z:	mass-to-charge ratio
n.a.:	Not applicable
NEP:	Neprilysin
NET:	Neutrophil extracellular traps
NELF:	Nasal epithelial lining fluid
NLF:	Nasal lavage fluid
PA:	Propionic acid
PEP:	Prolylendopeptidase
PMSF:	Phenylmethanesulfonyl fluoride
PP:	Polypropylene
PRCP:	Prolylcarboxypeptidase
PS:	Polystyrene
Q:	Quadrupole
Q²:	Goodness of prediction
QC:	Quality control
R²:	Goodness of fit
RAAS:	Renin-angiotensin-aldosterone System
RBC:	Red blood cells
RE:	Relative error
RNA:	Ribonucleic acid
s:	seconds
SARS-CoV-2:	Severe acute respiratory syndrome coronavirus 2
SD:	Standard deviation
SE:	Standard error
S/N:	Signal-to-noise ratio
SPE:	Solid phase extraction
TFA:	Trifluoroacetic acid
TNF α:	Tumor necrosis factor α
ULOQ:	Upper limit of quantification
V:	Volt
WCX:	Weak cation exchange

VII. List of Tables

Table 1.	Overview of available liquid chromatography coupled to tandem mass spectrometry assays for kinins in plasma, serum or whole blood.....	16
Table 2.	Kinin-specific transitions and voltage parameters for mass spectrometric detection	45
Table 3.	Accuracy and precision results for kinins in plasma	52
Table 4.	Absolute matrix effect, coefficient of variation of internal standard normalized matrix factor and recovery for all kinin peptides in plasma	53
Table 5.	Parallelism of the kinins in plasma.....	54
Table 6.	Results of the kinin stability assessments in plasma	56
Table 7.	Effect of centrifugation methods on kinin levels.....	79
Table 8.	Recommendations for preanalytical conditions for kinin assays.....	80
Table 9.	Results for the assessment of linearity of kinins in saline.....	96
Table 10.	Accuracy and precision results for all kinins in saline	97
Table 11.	Results of stability studies for kinins in saline	100
Table 12.	Characteristics of the healthy volunteers donating plasma and nasal fluids for kinin determination.....	111
Table 13.	Results of sampling of nasal lavage fluid.....	115

VIII. List of Figures

Figure 1.	Overview of the kallikrein-kinin system.....	2
Figure 2.	Postulated systemic effects of a dysregulated kallikrein-kinin system in COVID-19	7
Figure 3.	Illustration of the “one-factor-at-a-time” and the design of experiments approach.....	18
Figure 4.	Flow-diagram of the design of experiments approach for improving sensitivity of kinins.....	25
Figure 5.	Individual and interactive effect plots for bradykinin	31
Figure 6.	Response surface plots of predicted bradykinin peak area of the mobile phase optimisation.....	32
Figure 7.	Optimised design space for the mobile phase optimization for bradykinin	33
Figure 8.	Radar chart of the interaction effects of the injection solvent components with consumables for bradykinin	36
Figure 9.	Example chromatograms of the D-optimal optimisation of the injection solvent and sample collection materials.....	37
Figure 10.	Injection solvent compositions for bradykinin according to calculated robust and optimised setpoints	38
Figure 11.	Example chromatogram of bradykinin spiked plasma samples	40
Figure 12.	Example chromatograms of kinins in plasma	47
Figure 13.	Evaluation of protease inhibitors for generation of blank plasma	50
Figure 14.	Comparison of distinct protease inhibitor approaches for kinins in plasma	58
Figure 15.	Kininases involved in the degradation of bradykinin and kallidin	68
Figure 16.	Self-generation of bradykinin and formation of its metabolites after blood sampling	73
Figure 17.	Effects of distinct protease inhibitors on the generation of bradykinin in plasma	74
Figure 18.	Plasma stability of kinins in plasma and whole blood in the presence of various protease inhibitors	76
Figure 19.	Investigation of the impact of blood sampling conditions on kinin levels	78
Figure 20.	Box-whisker-plots of the kinin levels for inter-day and interindividual variability in healthy volunteers.....	81
Figure 21.	Contour plots of the D-optimal optimization for the response of bradykinin in distinct injection solvent compositions	94
Figure 22.	Recoveries of kinins in saline during evaluation of washing steps	95
Figure 23.	Example calibration curves for all investigated kinins in saline.....	96
Figure 24.	Example chromatograms for the kinin peptides in saline	98
Figure 25.	Recovery and absolute matrix effect of all analytes using saline matrix.....	99
Figure 26.	Box plots of kinin peptide concentrations of nine healthy volunteers in nasal lavage fluid.....	101

Figure 27. Kinin profiles in plasma of healthy individuals	112
Figure 28. Kinin profiles in nasal fluids of healthy volunteers	114
Figure 29. Distribution of the hydroxylated kinin to non-hydroxylated kinin ratio	115
Figure 30. Comparison of endogenous kinin profiles.....	116
Figure 31. The kallikrein-kinin system with its link to the contact activation system in COVID-19	121
Figure 32. Kinin levels measured in bronchoalveolar lavage fluid of COVID-19 patients (n=21) and controls (n=19)	124
Figure 33. Overview of the conducted work to establish reliable and sensitive bioanalytical mass spectrometric platforms	129

1. Introduction

1.1. The kallikrein-kinin system

The kallikrein-kinin system (KKS) is a complex endogenous cascade with multifunctional roles in health and disease. It is involved in blood pressure regulation, inflammation, renal, cardiac and neurological functions, nociception, cell proliferation, angiogenesis and mitigation [Costa-Neto et al. 2008]. It is closely related with other important metabolic cascades such as the renin-angiotensin-aldosterone system (RAAS), coagulation, or complement pathways [Moreau et al. 2005]. The discovery of the KKS began in 1909, when Abelous and Bardier found a hypotensive substance in human urine [Abelous & Bardier 1909]. This finding and further research elicited the fundamentals of the KKS until 1937, consisting of the interaction of kallikreins, kininogens, kinins, kinin receptors and kininases [Yarovaya & Neshkova 2015]. This basic principle has remained valid until today: kallikreins are the kinin-forming enzymes, kininogens the substrates, kinins the poly- or oligopeptides active on bradykinin receptors with their metabolites, and kininases the degrading enzymes of kinins. While kallidin was already discovered in 1937 [Werle et al. 1937], the exploration of bradykinin, the most prominent kinin, took until 1949 [Rocha e Silva et al. 1949]. A decisive step in research regarding the KKS, was then the unravelling of the structure of bradykinin and kallidin in the beginning of the 1960s, which allowed a better investigation of the KKS [Yarovaya & Neshkova 2015]. Further research in the following decades until now has resulted into the current picture of the KKS, which is summarized in Figure 1.

1.1.1. Metabolism of kinins

In plasma, the nonapeptide bradykinin is formed from high molecular weight kininogen (HMWK) by plasma kallikrein, while the decapeptide kallidin (Lys(0)-bradykinin) is cleaved by tissue kallikrein from low molecular weight kininogen (LMWK) or HMWK (Figure 1) [Campbell 2013]. Both kininogen precursors are glycoproteins synthesized in the liver and contain the kallidin/bradykinin sequence in their midportion between a heavy chain (362 amino acids) and a light chain, which size differs for HMWK and LMWK [Campbell 2013]. Whereas the light chain of LMWK (50-68 kDa) consist of 38 amino acids, HMWK is a larger protein with 255 amino acids in its light chain (88-120 kDa) [Campbell 2013]. The formation of bradykinin from HMWK by activity of plasma kallikrein is strongly related to the intrinsic coagulation cascade. Contact of blood to either pathophysiologic biological or artificial surfaces leads to relatively slow autoactivation of factor XII into factor XIIa. Factor XIIa subsequently cleaves prekallikrein into plasma kallikrein (Figure 1) [Schmaier 2016]. Plasma kallikrein in turn very rapidly amplifies the formation of factor XIIa in a positive feedback mechanism, and as a consequence,

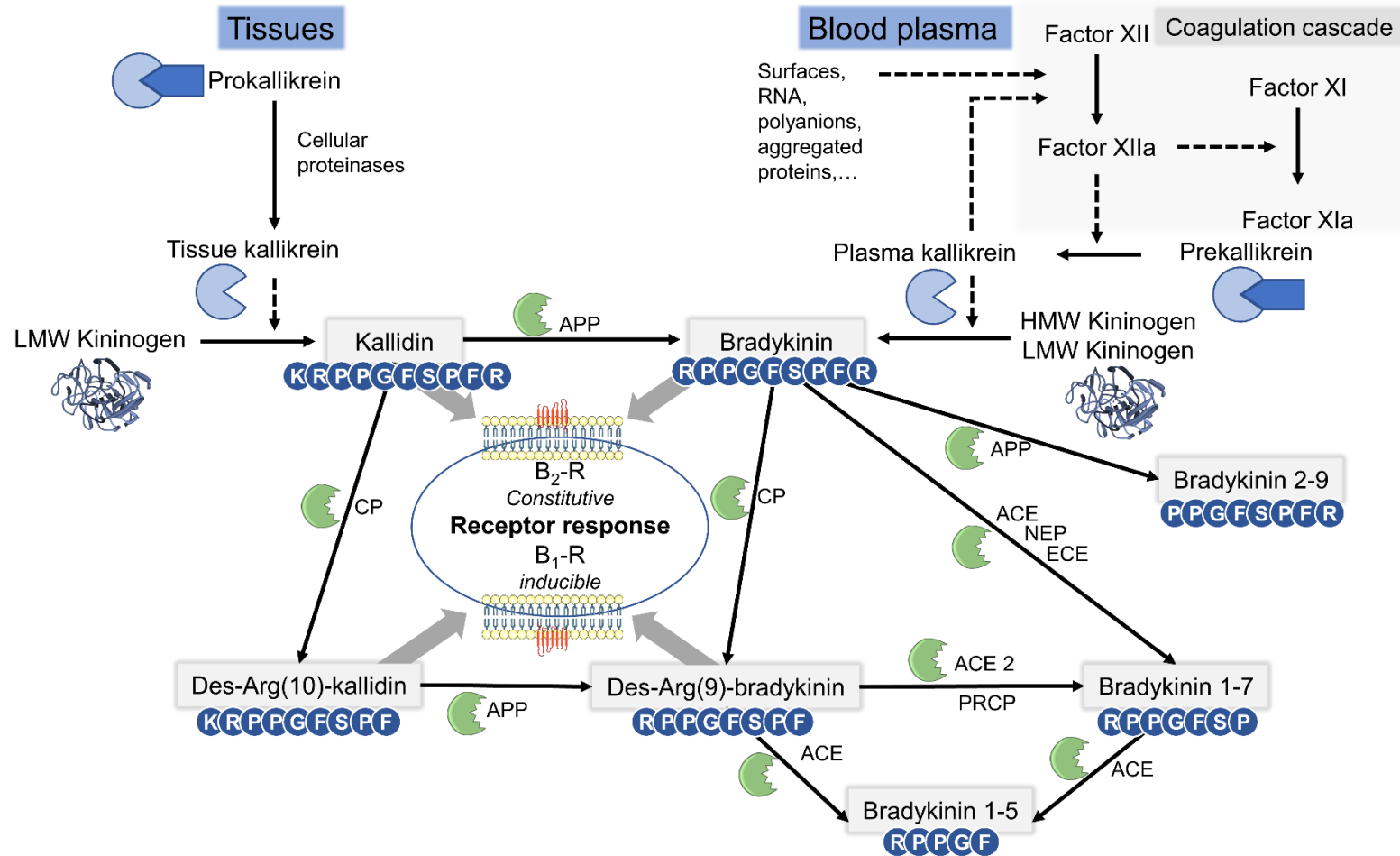


Figure 1. Overview of the kallikrein-kinin system. The kinins bradykinin and kallidin are formed by activity of plasma or tissue kallikrein before further metabolism. Whereas the four kinins bradykinin, kallidin, des-Arg(10)-kallidin and des-Arg(9)-bradykinin are active on bradykinin receptors, the other metabolites are inactive on these receptors. The kinin amino acid sequences are displayed in the one letter code. ACE: angiotensin-converting enzyme, APP: aminopeptidase P, B₁/B₂-R: bradykinin receptor type 1/2, CP: carboxypeptidase, DPP: dipeptidyl peptidase IV, ECE: endothelin-converting enzyme, HMW: high molecular weight, LMW: low molecular weight, NEP: neprilysin, PEP: prolyl endopeptidase, PRCP: prolylcarboxypeptidase, RNA: ribonucleic acid

more bradykinin is formed by increasingly available plasma kallikrein [Schmaier 2016]. Endogenously, this process is controlled by C1-esterase inhibitor (C1INH), which regulates factor XII and plasma kallikrein activation [Schmaier 2016]. Bradykinin as well as kallidin are rapidly degraded by kininases, and thus exhibit short half-lives of less than one minute [McCarthy et al. 1965; Marceau et al. 2020]. Aminopeptidase P converts kallidin, which differs from bradykinin by an additional N-terminal lysin, into bradykinin in plasma [Sheikh & Kaplan 1989; Kaplan & Ghebrehiwet 2021]. By action of carboxypeptidase N (in plasma) or M (in endothelium), kallidin and bradykinin are cleaved into their C-terminal des-Arg metabolites des-Arg(10)-kallidin and des-Arg(9)-bradykinin (Figure 1) [Sheikh & Kaplan 1989; Sheikh & Kaplan 1986]. Alternatively, bradykinin can also be degraded into its fragment bradykinin 1-7 by angiotensin-converting enzyme (ACE), neprilysin or endothelin converting enzyme, or into inactive bradykinin 2-9 by aminopeptidase P [Hoang & Turner 1997; Sheikh & Kaplan 1989]. Des-Arg(9)-bradykinin is either directly converted into bradykinin 1-5 by ACE or indirectly via bradykinin 1-7 by action of ACE 2 or prolylcarboxypeptidase and ACE (Figure 1) [Sheikh & Kaplan 1989; Donoghue et al. 2000; Chajkowski et al. 2011].

1.1.2. Pharmacology of kinins

Kinins mediate ambivalent pharmacological activities, which are either classified proinflammatory or protective for e.g. heart and kidney function [Moreau et al. 2005]. These are exerted by interaction with two subtypes of the G-protein coupled bradykinin receptors, the B₁ and B₂ receptor [Marceau et al. 2020]. Kallidin and bradykinin predominantly activate constitutive B₂ receptors, whereas des-Arg(10)-kallidin and des-Arg(9)-bradykinin interact with inducible B₁ receptors, which are upregulated during inflammation or tissue damage [Marceau et al. 2020]. Activation of the bradykinin receptors leads to increases in intracellular calcium, followed by protein kinase C activation [Yarovaya & Neshkova 2015]. This triggers intracellular signal transmission via second messengers like prostacyclin, nitric oxide, cyclic guanine monophosphate, and phosphoinositol [Yarovaya & Neshkova 2015; Maurer et al. 2011]. Formation of these messengers promotes physiological and pathophysiologic effects. For example antihypertensive, antithrombogenic, antiproliferative and antifibrinogenic effects are exerted [Maurer et al. 2011]. In addition, it stimulates proinflammatory effects, like vasodilation, hyperthermia, oedema and pain [Maurer et al. 2011]. As a consequence of these multifunctional roles, the KKS is supposed to be involved in several diseases like angioedema, sepsis, COVID-19, stroke, acute myocardial infarction, allergy, or cancer [Nicolau et al. 2020; Kashuba et al. 2013; Nokkari et al. 2018].

The elucidation of the exact role of the KKS in these disorders would be of great scientific, but also social value in terms of potential new therapeutic targets. As of now, only few drugs targeting the KKS are approved for clinical use, of which all are indicated for the treatment of

angioedema. Those either inhibit plasma kallikrein (ecallantide, berotralstat, lanadelumab), are C1-INH concentrates, or B₂ receptor antagonists (icatibant) [Nicola et al. 2019]. The significance of pharmacological interventions for other diseases is largely unresolved, as data on the involvement of the KKS in humans are often lacking [Bakhle 2020].

1.1.3. Current status of bioanalysis of kinins

Despite the important role of the KKS in health and disease, the reliable determination of endogenous kinin levels is currently greatly hindered. This is reasoned by several issues, which make accurate quantification of kinins challenging. First, low endogenous abundance of kinins demands for sensitive assays [Pellacani et al. 1994]. Second, peptides are very adsorptive and tend to stick on surfaces, thus affecting accuracy and precision, especially in low concentrations [Hoofnagle et al. 2016]. Third, structural similarities of kinins and their metabolites, which often differ only in one amino acid, require selective assays. Fourth, kinins exhibit short half-lives in biological fluids and therefore immediate stabilization by a tailored inhibitor cocktail is urgently required if meaningful results are to be obtained [Marceau et al. 2020; Pellacani et al. 1994]. Last but not least, bradykinin can be artificially generated in plasma by contact activation and potentially distort bradykinin and downstream metabolite levels [Schmaier 2016]. In addition, available methods are time-intensive, technically challenging and specimen quality is strongly dependent from the preanalytical handling [Kaplan & Maas 2017]. These issues are addressed in detail in section 1.4.

The variety of hurdles described also effects kinin levels published in the literature: particularly in plasma, levels diverging in multiple orders of magnitude from the low pg/mL (picomolar) up to the high ng/mL (nanomolar) range have been reported, even in the healthy [Duncan et al. 2000; Campbell 2000; van den Broek et al. 2010]. Namely, plasma bradykinin levels have been measured from 2.3 – 2.8 pg/mL [Nussberger et al. 1998; Cugno et al. 2000] up to approximately 106 ng/mL [van den Broek et al. 2010] in healthy volunteers. This currently impedes reliable data evaluation and comparison of study results. Plasma, serum or whole blood are the predominantly researched matrices with regard to kinin quantification. However, kinins are also present in other matrices, such as urine, saliva, respiratory lavage fluids, synovial fluid, or tears [Mann & Tighe 2012; Turner et al. 2000; Murphey et al. 2000; Vickers et al. 2002; Erdös & Skidgel 1997].

Traditionally, immunoassays have been applied for kinin determination. However, owing to cross-reactivities of immunoassays, differentiation of kinin peptides requires extensive sample preparation efforts including multiple sample purification steps before analysis [Duncan et al. 2000; Campbell et al. 1993]. The comprehensive determination of kinins is beneficial against the background of numerous pathways influencing the formation and degradation of kinins *in*

vivo. Disease and pharmacological agents may affect these pathways differently. Further, additionally to bradykinin, other active kinins, such as kallidin, des-Arg(9)-bradykinin, and des-Arg(10)-kallidin, act on different receptors, which in turn are assumed to be regulated in a disease-specific manner. Comparison of pathological alterations against physiological kinin profiles may help identify new therapeutic targets. To facilitate the comprehensive determination of kinins and overcome selectivity-related issues of immunoassays due to similar peptide structures, liquid-chromatography with tandem mass spectrometry (LC-MS/MS) represents a suitable tool. Quantification limits of published LC-MS/MS assays for bradykinin, however, are quite high in comparison to the sensitivity of immunoassays; respectively their quantification limits are between 100 pM [Lindström et al. 2019] and 10 nM [van den Broek et al. 2010; Lame et al. 2016]. Lortie et al. 2009 demonstrated the high potential of LC-MS/MS by quantification of several kinins simultaneously [Lortie et al. 2009]. However, demonstration of suitability of the assays by comprehensive method validation according to international regulatory bioanalytical guidelines and insufficient sensitivity remain currently still key barriers of available LC-MS/MS assays.

Altogether, reduced scientific progress regarding reliable determination of kinins was achieved in the past as compared to other related endogenous systems like the RAAS despite same advances in scientific methodologies [Bakhle 2020]. This hinders the advancement of scientific knowledge and should be addressed in view of the importance of the KKS for many diseases. Recently, understanding of disease-specific kinin alterations has become a subject of research focus during the COVID-19 pandemic, where a bradykinin storm was early implicated in the disease pathology, demonstrating the urgency for establishing reliable kinin quantification.

1.2. Coronavirus disease 2019

The newly emerging pandemic of coronavirus disease 2019 (COVID-19) aroused interest for the investigation of the KKS in connection. COVID-19 is caused by infection with the novel severe acute respiratory syndrome coronavirus 2 (SARS-CoV-2). It is transmitted via respiratory droplets and aerosols. After infection, the virus undergoes local replication and propagation in the nasal epithelial cells and further spreads along the ciliated cells in the conducting airways. During this stage, patients are asymptomatic with a low immune response, but highly infectious [Parasher 2020]. SARS-CoV-2 further invades the upper respiratory tract and the disease manifests itself with symptoms of fatigue, fever and dry cough. The immune response is triggered and in the majority of patients (mild to moderate course) the progress of disease is stopped by a sufficient immune response [Huang et al. 2020]. Less common, headache, sore throat, anosmia, malaise, nasal congestion, muscle aches and gastrointestinal issues appear in these patients. Thereby, the individual's symptomatology was suggested to be likely related to the specific tissue distribution of viral infection around the body [Garvin et al. 2020]. However, about 20% of patients progress to involvement of the lower respiratory tract infection (severe course) with dyspnoea, often in combination with hypoxemia [Wang et al. 2020; Parasher 2020]. In many cases progressive respiratory failure develops resulting in clinical pictures fulfilling the criteria of acute respiratory distress syndrome (ARDS) [Berlin et al. 2020]. Moreover, lymphopenia, thromboembolic complications, acute cardiac, kidney, and liver injury, as well as cardiac arrhythmias, rhabdomyolysis, coagulopathy and shock can occur. These symptoms were proposed to be associated to clinical and laboratory signs of inflammation (e.g. increased interleukine-1, interleukine-6, tumor necrosis factor α) [Moore & June 2020].

Therefore, it has further been postulated that observed COVID-19 symptoms are in connection with a dysregulated KKS (Figure 2) [Maat et al. 2020; Roche & Roche 2020; van de Veerdonk et al. 2020b; Nicolau et al. 2020]. The transmembrane enzyme ACE 2 has been identified as the receptor of SARS-CoV-2 enabling it to enter cells, which is highly expressed on respiratory endothelial cells. As it also degrades active des-Arg(9)-bradykinin, it has been hypothesized that an impaired degradation of inflammatory des-Arg(9)-bradykinin promotes symptoms of COVID-19. Further, increased kinin production via alternative cleavage of kinin precursors or induction of the bradykinin-forming enzyme kallikrein were hypothesized [Nicolau et al. 2020; van de Veerdonk et al. 2020b; Kaplan & Ghebrehiwet 2021; Garvin et al. 2020]. Increasingly available kinins and subsequent activation of bradykinin receptors results in vasodilation and release of proinflammatory interleukins and chemokines, which further trigger an upregulation of the inducible B₁ receptors [Couture et al. 2001]. The inflammation-related B₁ receptor upregulation then might further aggravate inflammation.

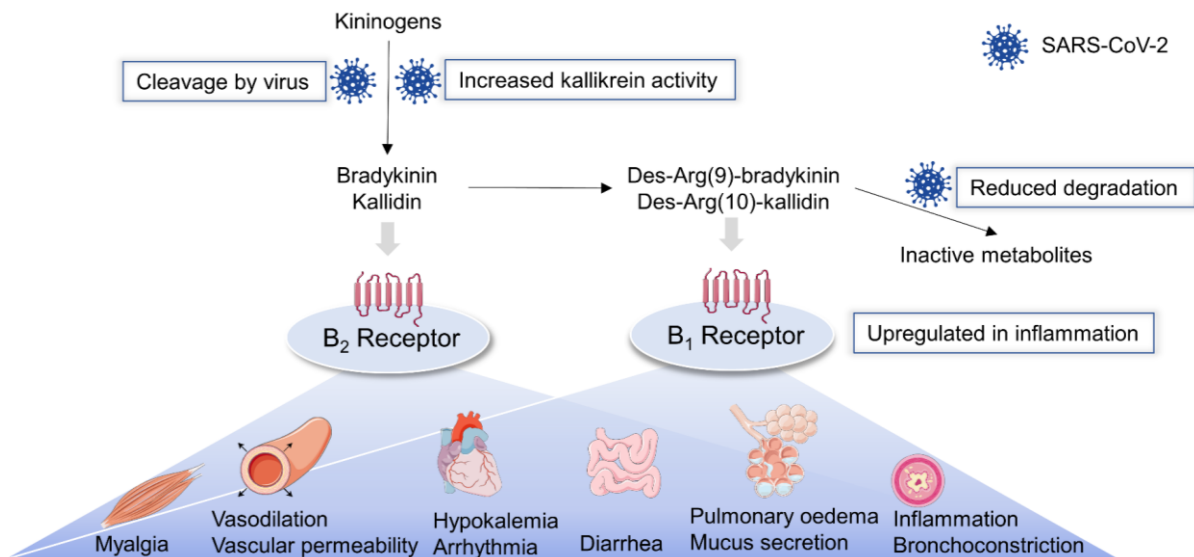


Figure 2. Postulated systemic effects of a dysregulated kallikrein-kinin system in COVID-19. The blue boxes show the postulated consequences on the kallikrein-kinin system by interaction with SARS-CoV-2. Following, increased kinin levels are supposed to mediate symptoms by bradykinin receptor activation. *B₁/B₂ receptor: bradykinin receptors type 1/2, SARS-CoV-2: severe acute respiratory syndrome coronavirus 2*

RNA expression analysis in human bronchoalveolar lavage fluid (BALF) samples has revealed increased expression of kallikrein, bradykinin receptors, and kininogen in COVID-19 positive versus controls [Garvin et al. 2020]. In addition, increased carboxypeptidase expression has been found, which degrades bradykinin into proinflammatory des-Arg(9)-bradykinin. These results were subsequently interpreted to mean that a 'bradykinin storm' might be responsible for the onset of COVID-19 symptoms. However, the impact of altered gene expression on the generation of active kinin peptides remains unclear yet.

Confirmation of a dysregulated KKS in COVID-19 patients would allow for the identification of new potential therapeutic targets. As of now, therapeutic options with significant success for the treatment of COVID-19 could not be established. The administration of oxygen in hypoxemic patients is undertaken non-invasively or by intubation depending on the amount of required oxygenation [Berlin et al. 2020]. Remdesivir and dexamethasone are currently the only drugs approved by the European Medicines Agency (EMA) for pharmacotherapeutic treatment. Both are, however, only recommended for severe COVID-19 courses [Malin & Spinner 2021]. In oxygenated patients, the glucocorticoid dexamethasone was shown to provide benefits regarding reduced mortality in a randomized controlled trial [Horby et al. 2020]. The virostatic remdesivir was authorized with a conditional market authorization and should be administered within one week after the onset of symptoms only in non-invasively oxygenated patients, whereby its benefit is more controversially discussed [Falcão et al. 2021]. Most pharmacotherapies under investigation are antiviral or immune-based therapies targeting the virus directly or supporting the immune response [Barkoff & Mousa 2020]. In addition, drugs

interacting with the KKS are currently examined in clinical trials targeting the hypothesized thromboinflammatory activation triggered by SARS-CoV-2. The B₂ receptor antagonist icatibant, which is approved for the treatment of hereditary angioedema, was investigated in an exploratory study with 9 cases and a reduction of oxygen supplementation was observed in comparison to controls [van de Veerdonk et al. 2020a]. Studies including larger collectives are currently ongoing [Mansour et al. 2021]. Moreover, the kallikrein inhibitors aprotinin or lanadelumab are studied in clinical trials [Vanassche et al. 2020; NCT04460105; NCT04422509]. Despite successful approval and application of vaccines, pharmacotherapeutic treatment options remain an important field of investigation, especially against the background of newly emerging virus mutations. Exploring the pathophysiology of SARS-CoV-2 might contribute to insights for the rationale of new potential therapeutic targets.

These treatment options are urgently needed for hospitalized patients, which are particularly at risk for severe COVID-19 progression. Hospitalized COVID-19 patients are more predominantly adults of middle age and older as well as adults with comorbidities [Wu & McGoogan 2020]. In addition, mortality increases with age [Wu & McGoogan 2020], with mortalities of 8.0 % in those aged 70 – 79 years and 14.8 % in those over 80 years, in contrast to an overall mortality of 2.3% in the whole population (n=44.672 cases). Their severe illness and high risk of mortality classifies them as vulnerable patients, which raises ethical considerations for bioanalytical research.

1.3. Ethical considerations regarding bioanalysis of kinins in the critically ill

As critically ill patients are a subgroup of vulnerable patients, ethical challenges have to be considered. The most commonly applied matrices for pharmacokinetic and pharmacodynamic bioanalysis are serum and plasma sampled from venous puncture [Mould & Upton 2013]. However, this matrix type has certain limitations in vulnerable patients. Only restricted blood volumes are available, as the blood drawn is limited owing to ethical reasons. While for example it is limited in paediatrics in dependence of the total body weight, in the seriously ill it is limited as the risk of iatrogenic anaemia increases [Ullman et al. 2016; Ad hoc group for the development of implementing guidelines for Directive 2001/20/EC 2008]. Blood for research is sampled in addition to routine blood analysis of established biomarkers, and consequently has to be posteriorized to routine blood sampling. On average, 40 mL of blood are drawn from a patient in the intensive care unit per day – this increases the risk of anaemia and the need for blood transfusions during a stay of several days to weeks [Ranasinghe & Freeman 2014]. Therefore, the additional burden of blood collections for research, some of which may involve repeated blood collections, should be minimized as much as possible.

Hence, drawn blood volumes should be reduced (e.g. development of low volume assays (<500 µL blood) and least invasive blood sampling techniques (e.g. capillary blood by finger prick) should be employed. Further, current international guidelines also call for the development of non-invasive detection methods with a view to patient welfare [Ad hoc group for the development of implementing guidelines for Directive 2001/20/EC 2008]. This becomes all the more important when - as in the context of KKS - the disease process to be investigated also takes place at locations that favour such sample collection. Measurement of biomarkers in blood usually provides more systemic information, whereas the informative value of biomarkers in alternative body fluids (e.g. respiratory lavage fluid, saliva) is often more locally limited [Stolina et al. 2009; Vujosevic & Simó 2017]. However, for diseases that occur first or mostly locally, measuring biomarkers at their site of action might be superior. For example, COVID-19 is a multiorgan disease, which initially affects the upper respiratory tract before further spread in the lower respiratory tract or other organs in more severe cases [Collange et al. 2020]. Changes in plasma biomarkers might therefore only be downstream of changes in respiratory lavage fluids like nasal lavage fluid (NLF). Further, such approaches are useful for short-lived and mainly tissue-based potential biomarkers like kinins to obtain additional information. Thus, biomarker determination from biological fluids of distinct body compartments might offer a more differentiated picture of the overall clinical condition. Ultimately, the biological fluid investigated should be chosen in dependence of the research question.

Also due to the low endogenous peptide levels and the limitation of blood volumes for ethical reasons, previous technological approaches for kinins often reached their limits in clinical application. Therefore, addressing these issues is necessary to contribute to increasing the knowledge of the role of the KKS in health and disease.

1.4. Issues and challenges in bioanalytical peptide quantification with focus on kinins

Bioanalysis is a subdiscipline of analytical chemistry and focuses on the quantitative measurement of drugs, metabolites and biomarkers for pharmacokinetic, toxicokinetic, pharmacodynamic, bioequivalence or bioavailability studies [Steve Unger et al. 2013]. Common matrices that are subject of interest include body fluids (e.g. plasma, whole blood, saliva, BALF, urine) or organ tissues (e.g. lung, kidney, heart). These biological samples commonly obtain high concentrations of undesired matrix (salts, lipids, large proteins) and rather low concentrations of the analyte of interest in the pg/mL to ng/mL range. The quantitative assessment of xenobiotics (e.g. drugs and metabolites) and biotics (e.g. peptides, proteins) in biological samples requires various techniques to deal with substances which potentially have an adverse impact on correct and precise determination on the analyte of interest.

Accurate bioanalytical quantification of peptides in particular represents a great challenge for bioanalysts, as the target analyte is present in an endogenous matrix with biochemically very similar proteins and peptides. Approximately 20.000 proteins alone are encoded by the human genome; but this number does not include post-translational modifications, single amino acid polymorphisms, splice variant isoforms, or protein products (e.g. peptide hormones) [Baker et al. 2017]. This high number of endogenous peptides and proteins is composed of only 21 amino acids [Schmidt & Simonović 2012], demonstrating the complexity, but also similarity of the matrix for peptide quantification. Hence, the development of robust and sensitive assays often requires increased effort in contrast to small molecules due to a variety of challenges during method development and validation. Most common sample purification techniques used for small molecules like liquid-liquid extraction or protein precipitation are not applicable due to insufficient recovery, sensitivity, specificity, and robustness of peptides [Ewles & Goodwin 2011]. Additional distortion of bioanalytical results can be affected by non-specific peptide adsorption, *ex vivo* stability issues, sampling conditions and sample handling. Moreover, challenges are faced during setup of the LC-MS/MS assay and bioanalytical method validation. These general issues affect particularly kinin peptides, which will be outlined in the following.

1.4.1. Sampling and biological sample handling

It is well known that preanalytical variables highly impact the sample quality and reliability of results in general, but particularly in peptide analysis [Debunne et al. 2020; Cao et al. 2019]. According to the literature, most errors occur during the preanalytical phase with rates between 32–75% [Carraro & Plebani 2007; Bonini et al. 2002]. Thereby, variations in sampling, processing, and storage of biological samples are important potential confounders. Use of

different anticoagulants in blood collection tubes, the presence of gel separators, needle gauge, or the site of blood collection are some of the factors influencing the proteome during blood sampling [Rai & Vitzthum 2006]. Untargeted proteomic approaches using whole blood and plasma have revealed that centrifugation speed, temperature, freeze-thaw cycles, and delayed processing impact the abundance of peptides and proteins [Daniels et al. 2019; Hassis et al. 2015]. Additionally, quantification of analytes related to the coagulation cascade are even more susceptible to preanalytical variabilities [Lawrence 2003].

Owing to the strong interrelationship of the KKS to the intrinsic coagulation cascade by factor XII and the rapid metabolism of kinins, kinin levels are prone to artificial *ex vivo* alterations. This has contributed to a high discrepancy of bradykinin levels diverging in several orders of magnitude [van den Broek et al. 2010; Campbell 2000]. Reporting on chosen preanalytical variables (e.g. blood collection device, technique) of kinin determination is highly limited [Nussberger et al. 1998; Duncan et al. 2000; van den Broek et al. 2010; Lindström et al. 2019]. Therefore, preanalytical variables affecting the robust quantification of kinins must be identified. On basis of these findings, standardized protocols for specimen sampling and handling should be set up and deviations be clearly documented [Lippi et al. 2020a].

1.4.2. Non-specific peptide adsorption

In contrast to small molecules, peptides and proteins tend to adsorb to vessel, tip or tubing walls during sample preparation [Hoofnagle et al. 2016]. This can impact linearity, accuracy, precision and repeatability of targeted quantification, as usually, the lower the analyte's concentration, the higher its tendency to stick to surfaces [Hoofnagle et al. 2016]. The extent of adsorption of peptides varies depending on the triangular relationship between the physicochemical properties of the peptide, the solvent and the container material [Hoofnagle et al. 2016]. While peptides with basic amino acids will rather form interactions with residual silanol groups of glass, peptides with nonpolar amino acids will rather interact with hydrophobic polypropylene containers [Goebel-Stengel et al. 2011]. The peptide bradykinin has two terminal basic amino acids (arginine) and several central hydrophobic amino acids (proline, phenylalanine) (Figure 1), and hence might adsorb to glass and/or polypropylene. Reduction of non-specific peptide adsorption might be achieved by addition of organic solvents, acids, or base [Hoofnagle et al. 2016]. In addition, protein low binding materials are getting increasingly available in recent years, which promise to reduce non-specific peptide adsorption in aqueous solutions.

The extent of non-specific adsorption of kinins has not been investigated as of now, despite the importance regarding their reliable quantification. Owing to the multiple factors affecting peptide adsorption, investigation of these variables in advance to further method development

is essential to understand how processing of kinins should be handled to achieve reliable and robust quantification.

1.4.3. *Ex vivo* stability

Similarly to small molecule drugs, peptides can show metabolic or chemical instabilities in biological fluids [Reed 2016]. While metabolic instability refers to enzymes cleaving peptides or their precursor proteins/peptides, chemical instabilities include hydrolysis, oxidation, or isomerization over time. In contrast to small molecule drugs or proteins, peptides are most susceptible to metabolic or chemical instability [Evans et al. 2020]. This potentially causes alterations from endogenous levels after sampling and during storage of the obtained sample [Baykan et al. 2017]. Ensuring stability in the analysed biological matrix is therefore essential and should be shown according to the limits defined by bioanalytical regulatory guidelines for biomarkers [US Food and Drug Administration 2018; International Council for Harmonisation 2019]. Commercially available protease inhibitor mixes might be a suitable choice for some applications, but do not provide adequate stability of peptides in the matrix in all cases [Debunne et al. 2020]. Rather simple approaches like organic precipitation or acidification can often sufficiently inactivate enzymes and stabilize peptide levels [Ewles & Goodwin 2011]. Otherwise, the customized combination of serine protease inhibitors (e.g. aprotinin, phenylmethylsulphonyl fluoride), metalloprotease inhibitors (e.g. ethylenediaminetetraacetic acid, phenanthroline), aspartate protease inhibitors (e.g. pepstatin A), or cysteine protease inhibitors (e.g. iodoacetamide) might be necessary depending on the generation and degradation pathways of the peptide of interest.

Kinin peptides are particularly prone to metabolic instabilities owing to the variety of metabolic pathways and thus comprehensive determination requires broad inhibition of proteases. For kinins, all of the outlined approaches have been applied for *ex vivo* stabilization. However, stability of kinins using the respective protease inhibitor approach was not adequately proven and limits ($\leq \pm 15\%$ at multiple levels within the investigated period) of the FDA guideline were exceeded [Lindström et al. 2019; Seip et al. 2014; Campbell et al. 1993; Hubers et al. 2018]. For the comprehensive determination of kinins, a complex cascade of multiple kininases (mainly metallo- and serine proteases (Figure 1)) has to be inhibited to prevent *ex vivo* kinin alterations by generation or degradation. The extent to which previous approaches need to be optimised in order to achieve sufficient stabilisation ($\leq \pm 15\%$) of all kinins in biological fluids must therefore be investigated.

1.4.4. Sample purification from biological fluids

Bioanalytical sample purification is a preanalytical separation step, by which isolation of the analyte from the matrix, enrichment of the analyte and minimization or depletion of matrix are reached. The purpose of sample purification is to facilitate the compatibility of the sample with subsequent quantification methods, e.g. LC-MS/MS [Henion et al. 1998]. For example, phospholipids must be removed from the matrix, as these surfactants act ion-suppressing in LC-MS/MS, and thus reduce sensitivity and reliability. Simultaneously to purification of the sample, recovery of the analyte of interest has to be maintained despite aiming to minimize the undesirable matrix fraction in order to maintain sensitivity. Owing to many factors affecting the intertwining between analyte and matrix, the optimal sample purification strategy is highly dependent from both, and has to be carefully assessed in order to achieve the above-mentioned goals [Zhou et al. 2017]. Thus, sample purification is considered to be the bottleneck in bioanalysis, and regarded as slow and the most labour-intensive step [Blomberg 2009].

Peptides are often more difficult to separate from other endogenous proteins and peptides as compared to small molecule drugs due to chemical similarity [Ewles & Goodwin 2011]. Typical challenges encountered are issues with maintaining solubility, increased matrix interferences, and effective disruption of protein binding besides the already discussed non-specific adsorption: these difficulties can result in reduced recovery, higher variability of assay performance, and the need to achieve higher specificity. Simple sample purification techniques like protein precipitation or liquid-liquid extraction are usually not applicable owing to coprecipitation, lower solubility of peptides in organic solvents due to zwitterionic forms, or insufficient protein binding disruption [Ewles & Goodwin 2011]. These issues can often be overcome by using SPE, which uses size exclusion to eliminate the most abundant proteins (e.g. albumin, immunoglobulins). Thereby, it has to be ensured that target peptides are effectively disrupted from the biomatrices in order to avoid loss of peptides due to size exclusion. The orthogonal combination of an ion exchanger and reversed phase leads to increased selectivity by improved separation of other matrix compounds, reduced matrix effects and increased recovery, thus improving sensitivity. However, the development of suitable SPE protocols for simultaneous analysis of multiple peptides is often time-intensive.

For kinins, SPE is usually applied for sample purification prior to LC-MS/MS or immunometric detection, if kinins are aimed to be distinguished [Duncan et al. 2000; Campbell et al. 1993; Lindström et al. 2019; Seip et al. 2014]. Particularly if several kinins are to be determined simultaneously, distinct recoveries are found owing to the distinct affinities of the analytes to the sorbent material (e.g. bradykinin 32% vs. 85% for bradykinin 1-7 [Duncan et al. 2000]).

This can hardly be avoided owing to the distinct physicochemical characteristics, but should be minimised as best as possible to allow sensitive analysis from biological matrices.

1.4.5. Liquid chromatography coupled with tandem mass spectrometry

Traditionally, peptides and proteins in biological samples have been quantified by immunoassays, which offer high sensitivity and high throughput. However, they often lack specificity, particularly for peptides, thus resulting in interferences from other structurally similar peptides, proteins or metabolites. These drawbacks can be overcome by LC-MS/MS analysis. Though, development of LC-MS/MS methods for peptides shows additional difficulties in comparison to small-molecule drugs.

Liquid chromatography coupled with mass spectrometry (LC-MS/MS) is grounded in a three step separation; i.e. retention time (LC); precursor ion mass-to-charge ratio (m/z) (MS) and the product ion m/z (MS) [Hoofnagle & Wener 2009]. In targeted LC-MS/MS analysis, the precursor ion and the product ion are usually identified using a synthesized standard during method development and chosen transitions are monitored to establish the identity in biological matrices. This allows for detection of low abundant analytes, while in untargeted analysis commonly only the most abundant ions can be detected. Such limitation makes the latter less suitable for analysing complex and dynamic samples such as biological fluids. The additional coupling with chromatographic separation leads to a high orthogonal resolving power, allowing to distinguish similar analyte structures. LC-MS/MS therefore supports analysis with high precision, accuracy, selectivity and sensitivity.

Most peptides can be analysed using reversed-phase separation (LC), but peptides frequently show poor peak shapes and separation as multiply charged molecules often exhibit poor retention and secondary interactions with the stationary phase [Ewles & Goodwin 2011]. Optimisation of the column material and addition of modifiers to the mobile phase are therefore often necessary. Usually C18 columns are best suited for peptides, but alternatively the use of other materials such as phenyl-hexyl or C8 may also be advantageous. [Ewles & Goodwin 2011]. Examples of commonly used modifiers in the mobile phase are acids, such as formic acid, which on the one hand neutralise the acidic groups, but also improve ionisation in the mass spectrometer. In contrast to small molecules, mass spectrometric fragmentation of peptides is rather inefficient owing to their larger size, multiple charge states and complex fragmentation [Kang et al. 2020]. Hence, the sensitivity of LC-MS/MS analysis of peptides is usually inferior to immunometric detection [Kang et al. 2020]. Sensitivity might be improved for peptides using supercharger like dimethyl sulfoxide (DMSO) or ethylene glycol (EG) [Yu et al. 2017]. These increase the average charge distribution of peptides and thus improve ionization efficiency [Miladinović et al. 2012].

In addition, for endogenous compounds, the availability of analyte-free biological matrices does not exist per definition [Thakare et al. 2016]. However, the bioanalytical guideline of the US Food and Drug Administration (FDA) states that the biological matrix used should be the same as used for study samples, but be free of measurable analyte and matrix effects in comparison to study samples [US Food and Drug Administration 2018]. Hence, the choice of a suitable quantification approach poses a challenging task in bioanalysis. Various approaches have been used in LC-MS/MS, including background subtraction, standard addition, surrogate matrices – such as neat solutions, artificial matrices of biological fluids, or stripped matrices – and surrogate analytes [Thakare et al. 2016]. The surrogate matrix approach is the most widely used, whereby simple surrogates like buffer or water are often unsuitable owing to divergency in matrix effects [Cabooter et al. 2019]. Altogether, quantification of low-abundant peptides requires more elaborated LC-MS/MS method optimization compared to small molecules.

While bradykinin immunoassays are featured with high sensitivities of 0.5 pg/mL – 1.4 pg/mL for bradykinin [Hilgenfeldt et al. 1995; Pellacani et al. 1994; Nielsen et al. 1982], quantification limits of available LC-MS/MS assays are substantially higher between 106 pg/mL and 106 ng/mL [Lindström et al. 2019; van den Broek et al. 2010]. An overview of the characteristics of available mass spectrometric assays for kinins is given in Table 1. The large discrepancy in sensitivity exemplifies the previously described issues in LC-MS/MS peptide quantification and demonstrates the need for sophisticated improvement of mass spectrometric sensitivity to allow for similar sensitivity as achieved for immunoassays.

Table 1. Overview of available liquid chromatography coupled to tandem mass spectrometry assays for kinins in plasma, serum or whole blood.

Authors	Kinins assessed	LLOQ	LoD	Blank matrix	Quantification
[Lindström et al. 2019]	Bradykinin	106.0 pg/mL	31.8 pg/mL	Water	Multipoint calibration
[Hubers et al. 2018]	Bradykinin Bradykinin 1-5	n.a. n.a.	0.5 pg/mL 1 pg/mL	Whole blood	One-point by surrogate analyte
[Ion et al. 2017]	Bradykinin Des-Arg(9)-bradykinin Bradykinin 1-7	10.0 ng/mL 2.0 ng/mL 1.0 ng/mL	n.a.	Acetonitrile/0.1 % formic acid 15/85 (v/v)	Multipoint calibration
[Lame et al. 2016]	Bradykinin	192.5 pg/mL	n.a.	Plasma	Standard addition
[Seip et al. 2014]	Bradykinin 1-5	151.9 pg/mL	20.2 pg/mL	Blank whole blood	Multipoint calibration
[Lame 2013]	Bradykinin	80.0 pg/mL	n.a.	Plasma	Standard addition
[van den Broek et al. 2010]	Bradykinin (Hyp3)-bradykinin Des-Arg(9)-bradykinin	10.0 ng/mL 4.0 ng/mL 2.0 ng/mL	n.a.	Bovine plasma	Multipoint calibration
[Murphey et al. 2001]	Bradykinin 1-5	n.a.	2.3 pg/mL	Plasma	One-point by surrogate analyte

LLOQ: lower limit of quantification, LoD: limit of detection, n.a.: not applicable

1.4.6. Method development and optimization

Method development in bioanalysis might be a time-consuming factor, owing to many critical steps, such as sample preparation, mass spectrometric sensitivity, or method robustness. Typically, these are investigated within classical approaches, such as ‘one-factor-at-a-time’ or ‘trial and error’, which pose a high workload and uncertain success, as factor interactions and potential synergisms remain unknown. This might lead to loss of precision, accuracy, or robustness of the assay.

Therefore, design of experiment (DoE) represents a novel tool in bioanalysis for elaborated method development, after being established in other areas such as agriculture or the pharmaceutical industry. It is now being embedded in analytical quality by design approaches, which help in the development of robust and cost-effective analytical methods throughout their whole lifecycle [Beg et al. 2021]. By implementing DoE, increased flexibility within a lean approach is provided, as a method operable design region is determined. In recent years, the benefits of DoE have increasingly gained attention in bioanalysis, lately also being considered in a recent draft (United States Pharmacopeia chapter 1220) by regulatory authorities [United States Pharmacopeia Validation and Verification Expert Panel 2017]. However, it is still rather seldomly used in combination with LC-MS/MS bioanalysis, despite being a powerful tool for optimizing methods for challenging analytes like peptides [Maes et al. 2014b; van Wanseele et al. 2017].

For illustration of the “one-factor-at-a-time” approach in contrast to DoE, a fictive and simplified example is given in Figure 3. To optimize the coffee taste (=result), one can – amongst others – vary the temperature of the water (factor 1) and the extraction time (factor 2). Application of the “one-factor-at-a-time” approach, one would start optimizing the water temperature from 80°C to 100°C and determine the best coffee taste at 95°C. Subsequently the extraction time would be evaluated based on the best water temperature (Figure 3A). However, this approach does not consider interactions of these factors, as in this example the best taste was developed by a lower water temperature in combination with a longer extraction temperature (Figure 3, red area). This becomes even more meaningful if several impacting factors are aimed to be examined. Applying a DoE plan, multiple factors at one time are varied simultaneously in the desired ranges. Since the experiments are distributed in a rectangular space, the direction of better results can be identified (Figure 3B).

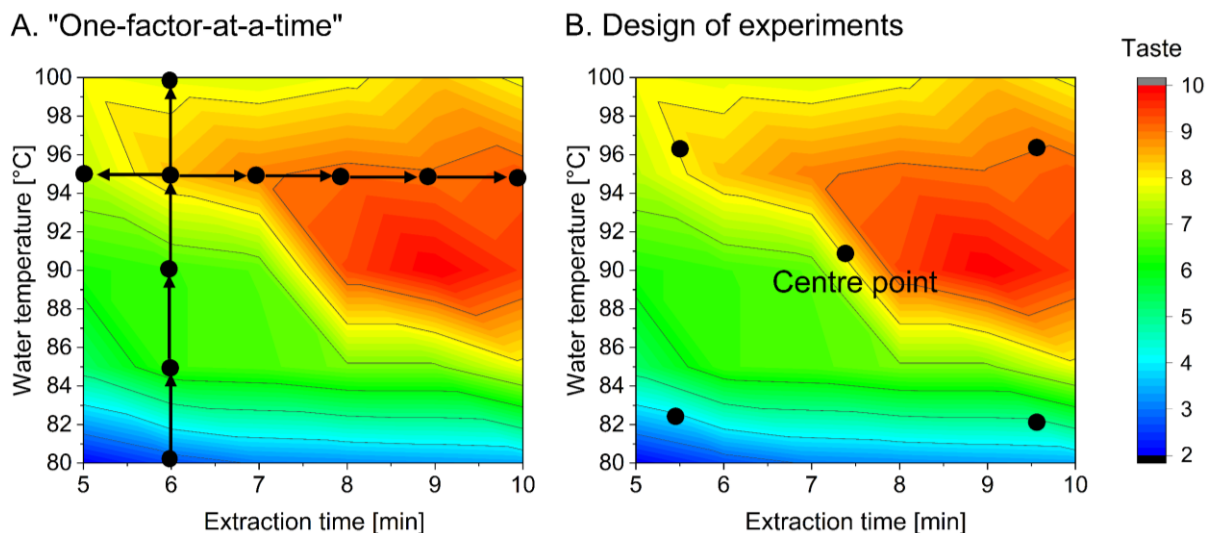


Figure 3. Illustration of the “one-factor-at-a-time” and the design of experiments approach. In A. the “one-factor-at-a-time” approach is shown, starting from one origin. In B. simultaneous changing of multiple factors around one centre point (the reference around which the other experiments are arranged) are investigated, which allows for better information of the optimal region. Dots represents the experiments conducted and a 10 on the colour scale is the optimal taste.

There are three main objectives of DoE: screening, optimization and robustness testing [Eriksson et al. 2008]. At the beginning of the experimental setup, generally screenings are used to identify factors with the highest influence on the result from a large set of factors. Further, the range of the factors can be indicated at this stage. Following, by optimization designs, the identified relevant factors are tested in distinct combinations in their expected ranges to find the optimum method operable design region. As optimization is more complex than screening, it requires more experiments per factor. In return, it also delivers more detailed information compared to screening. In a last step, robustness testing is applied to confirm the robustness of the chosen optimal setting in face of small variations around it within the design region. The aim of this phase is to ensure the reliability on the hand, or, on the other hand, to understand how a setting needs to be adapted within boundaries to reach the desired reliability.

In addition to saving time in method development, this approach also allows processes to be better understood and delivers multiple point solutions. Even if new insights are subsequently gained during analytical life cycle management, the investigated factors may be adapted and an alternative set point found that is more consistent with the new assay conditions. The application to the development of challenging peptide quantification is therefore a rationale choice and is assumed to allow for a more sophisticated assay development, which will result in more reliable, reproducible and optimized assays for the determination of kinin peptides.

1.4.7. Method validation

Validation of a developed method according to established regulatory guidelines should always be conducted before analysis of any clinical study samples to demonstrate the method suitability for its intended use [Hopfgartner 2020]. The most prominent guidelines are those of the EMA, the FDA and the International Council for Harmonisation (ICH) [US Food and Drug Administration 2018; International Council for Harmonisation 2019; European Medicines Agency 2011]. Key issues to be addressed are the specificity and selectivity of the assay, accuracy and precision, the measurement range, sensitivity, matrix effects, recovery, and sample storage. For example, the lower limit of quantification (LLOQ) is confirmed, referring to the lowest concentration, which can be accurately and precisely measured within specified limits (e.g. $\leq \pm 20\%$ for LC-MS/MS). Quantification below the LLOQ is not acceptable as it shows increased risk for biases, such that level data between the LLOQ and limit of detection (LoD) can only be qualitatively or semi-quantitatively assessed [Tiwari & Tiwari 2010]. Hence, validation is undertaken to ensure that the developed method is “fit-for-purpose” for the intended use and the reliability and reproducibility of the generated data is ensured. Otherwise, undetected measurement errors could result in biases and the utility of the predictive value of the biomarker would be limited. Recent advances allow peptide and protein quantification at higher throughputs, attracting attention and making them potential biomarkers for clinical trials. This is evidenced by the fact that not until the FDA's 2018 guideline or the ICH's 2019 draft, the validation of endogenous analytes/biomarkers was considered [US Food and Drug Administration 2018; International Council for Harmonisation 2019]. Both now set the same acceptance criteria for small drug molecules and endogenous compounds/biomarkers in LC-MS/MS. In light of the previously described issues regarding reliable peptide quantification in comparison to small molecules, this poses a challenge for bioanalysts making sophisticated method development prior to validation essential.

To the best of our knowledge, none of the available kinin assays has been validated as comprehensively and to such strict acceptance limits as those reflected in these guidelines. In comparison to these, applied in-house validations assessed some of the validation parameters only at single quality control levels [Lindström et al. 2019; Murphey et al. 2001], used too few quality control levels [Lindström et al. 2019; Ion et al. 2017; Seip et al. 2014], or neglected essential validation parameters [Ion et al. 2017; Lame 2013; Lame et al. 2016; Murphey et al. 2001; van den Broek et al. 2010]. Others did not report any validation results [Hubers et al. 2018]. Nevertheless, validation is inevitable to ensure reliable and robust data collection and evaluation as well as the credibility of study results.

2. Aim of the thesis

Kinins are considered potential biomarkers in disorders like COVID-19, sepsis, angioedema, stroke, or cancer. However, available studies report kinin levels in biological fluids diverging in several orders of magnitude hindering differentiation between levels in health and disease. The reliable and accurate determination of peptides of the KKS is currently impeded by their low abundance, non-specific adsorption, poor ionization efficiency in LC-MS/MS, structural similarity, artificial generation in plasma, and their short half-lives.

Therefore, the aim of this work is the development and application of reliable and guideline compliant bioanalytical mass spectrometric platforms for the simultaneous monitoring of kinin peptides in human fluids.

For this purpose, the following five main objectives are addressed within this scope:

1. Reduction of non-specific peptide adsorption and improvement of mass spectrometric sensitivity by using the powerful tool of design of experiments. The use of design of experiments within this thesis should empower refined understanding of the underlying issues and deliver higher quality results with multiple point solutions.
2. Development and validation of a novel LC-MS/MS platform assay for seven kinin peptides in plasma. Based on the sensitivity improvements during the method development using DoE, the ability of the assay to provide reliable data should be proven according to international regulatory guidelines.
3. Investigation and standardization of impactful preanalytical variables affecting the reliability and robustness of kinin quantification in plasma. Addressing the known confounding factors, the feasibility of collecting repeatable plasma kinin levels should be systematically and extensively investigated in healthy volunteers using an LC-MS/MS platform proven to deliver high-quality data.
4. Development and validation of an alternative, non-invasive quantification approach for seven kinins applying LC-MS/MS for respiratory lavage fluids. Similarly to plasma, a guideline-compliant LC-MS/MS platform, which is ready-to-use in context of clinical studies, was aimed to be implemented.
5. Application of the established LC-MS/MS platform within clinical trials. It was sought to demonstrate the potential of the assays in clinical settings and provide preliminary contributions to a more in-depth understanding of the *in vivo* role of kinins in healthy and COVID-19 diseased patients.

3. Improving sensitivity for the targeted mass spectrometric analysis of bradykinin using a design of experiments approach

3.1. Background

The nonapeptide bradykinin is involved in several physiological and pathophysiological processes in humans [Marceau & Regoli 2004; Taddei & Bortolotto 2016]. Current research on bradykinin is primarily focused on *in vitro* measurements in tissues and its pharmacological effects, whereas the relevance of endogenous plasma bradykinin levels still remains to be clarified [Anton et al. 2019; Qin et al. 2019]. This context is partially related to the fact that bradykinin has a short half-life of 30 seconds and is present in low picomolar plasma concentrations only [Campbell 2000]. Thus, its reliable determination requires a sensitive quantification method, which can be facilitated by LC-MS/MS. However, published methods lack the sensitivity to detect bradykinin by LC-MS/MS within the desired physiological range [Lindström et al. 2019; van den Broek et al. 2010; Ion et al. 2017]. Consequently, it is necessary to optimise the sensitivity of an LC-MS/MS method to enable the measurement of low bradykinin levels in human plasma.

Particularly in terms of quantitative peptide analysis, the phenomenon of non-specific peptide adsorption, which is especially pronounced in lower concentrations, is raising difficulties for reliable determination due to peptide losses during storage and sample preparation [John et al. 2004]. The triangular relationship between the physicochemical properties of the peptide, characteristics of the used storage materials and the injection solvent composition substantially influences non-specific adsorption [Maes et al. 2014a; Goebel-Stengel et al. 2011; Feickert & Burckhardt 2019]. Bradykinin can adsorb to glass, polystyrene (PS) and polypropylene (PP) due to its terminally positively charged and centrally hydrophobic amino acids [Kristensen et al. 2015; RübSam et al. 2018]. To reduce interactions with sample collection materials and increase the solubility of peptides, the addition of acids, DMSO or organic solvents have demonstrated beneficial effects for other peptides [Hoofnagle et al. 2016; van Midwoud et al. 2007].

Another possibility to enhance the sensitivity of an LC-MS/MS method is the investigation of suitable additives to the mobile phase to improve the ionisation of bradykinin. Modifiers such as DMSO, ethylene glycol (EG) or propionic acid (PA) have been described to boost the signal response in the untargeted LC-MS/MS analysis of peptides [Yu et al. 2017]. Varying signal intensity increases for several peptides were described, depending on the concentration and type of modifier added to the chromatographic mobile phase as well as on the LC-MS/MS

This work was published in a peer-reviewed journal:

Gangnus T, Burckhardt BB (2020) Improving sensitivity for the targeted LC-MS/MS analysis of the peptide bradykinin using a design of experiments approach. *Talanta*. 218:121134. doi: 10.1016/j.talanta.2020.121134

The author of this thesis was responsible for conceptualization, methodology, validation, investigation, writing - original draft, writing - review & editing, and visualization.

system used [Yu et al. 2017; Hahne et al. 2013]. The systematic investigation and optimisation of the aforementioned parameters would demand high experimental effort if traditional “one-factor-at-a-time” or “trial and error” methods are applied. Therefore, to reduce the number of experiments required for the optimisation of the LC-MS/MS method, the approach of DoE represents a rational choice [Hecht et al. 2016]. It offers the possibility to investigate different parameters within fewer experiments in comparison to the conventional bioanalytical method development process, while additionally providing the advantage of exploring multiple factor effects and complex interactions [Lee 2019].

In the present work, the DoE approach was applied to analyse and optimise the interactions between injection solvent composition and sample collection materials in order to minimise the adsorption of bradykinin to common container materials. With the aim of maximising the signal response of bradykinin in LC-MS/MS, the composition of the mobile phase by the inclusion of modifiers was further examined. The optimised results were then applied to determine endogenous bradykinin levels in human plasma.

3.2. Materials and Methods

3.2.1. Chemicals and reagents

Bradykinin (99%, High-performance liquid chromatography (HPLC)), formic acid (FA, $\geq 98\%$), trifluoroacetic acid (TFA, 100.3%) and EG ($\geq 99\%$) were purchased from Sigma Aldrich (St. Louis, MO, USA). [Phe⁸Ψ(CH-NH)-Arg⁹]-bradykinin (97.5%, HPLC); Tocris, Bristol, UK) was applied as the internal standard. HPLC-grade methanol, water and DMSO ($\geq 99.9\%$), as well as MS-grade methanol, were obtained from Fisher Scientific (Loughborough, UK). Furthermore, HPLC-grade acetonitrile (ACN; Applichem, Darmstadt, Germany), propionic acid ($\geq 99.5\%$) and MS-grade water (Honeywell Fluka, Seelze, Germany), as well as ammonia (30.9%) (VWR Chemicals, Radnor, PA, USA) were utilised.

Regarding consumables, pipette tips and protein low-binding tubes from Sarstedt (Nümbrecht, Germany) were used. Further, standard glass vial inserts (100 μ L, borosilicate type 1, VWR International GmbH, Darmstadt, Germany) and LC-MS certified glass vials (12*32 mm, conical bottom, borosilicate type 1, treated to reduce free surface ions, Waters, Eschborn, Germany) were applied. The following 96-well sample collection plates were utilized during the experiments: protein LoBind polypropylene (500 μ L, round bottom, LB-PP; Eppendorf, Hamburg, Germany), PS (1100 μ L, round bottom, Brand, Wertheim Germany) as well as polypropylene (PP; of the distinct suppliers: Waters (conical bottom, 700 μ L, Eschborn, Germany), Brand (round bottom, 500 μ L, Wertheim, Germany) and Corning (round bottom, 500 μ L, New York, USA)) were used.

Plasma purification was performed using 96-well Oasis weak cation exchange (WCX) μ -elution plates (Waters).

3.2.2. Preparation of kinin stock and working solutions

1 mg of bradykinin and [Phe⁸Ψ(CH-NH)-Arg⁹]-bradykinin as an internal standard were dissolved separately in 0.5 mL 0.1% FA in water (v/v) and subsequently diluted with 0.1% FA in water (v/v) to obtain stock solutions of 1 μ g/mL using protein low binding tubes. For the DoE experiments, aliquots of 5 mL working solution containing 6 ng/mL bradykinin and 12 ng/mL internal standard in 75/25 ACN/water with 1% TFA (v/v) were prepared. While the stock solutions were stored at -80 °C, the working solutions were stored at -20 °C. For all handling steps, pipette tips were pre-rinsed three times with the particular peptide solution being subsequently used. This procedure was applied to saturate the non-specific binding of the peptides

3.2.3. Sample preparation

For the analysis of materials and injection solvents, one aliquot of the working solution was thawed on the day of analysis and 50 μL were distributed into the cavities of the different sample collection materials. The solution was evaporated to dryness using a Thermomixer Comfort (Eppendorf, Hamburg, Germany) under a gentle nitrogen stream and shaking at 350 rpm and 40 °C. The residues were then reconstituted in the respective injection solvent in accordance with the DoE protocol and vortexed for one minute at 400 rpm before analysis.

For mobile phase optimisation, 50 μL of the working solution was dispensed into the sample collection plate (PP, supplier B). Then, 100 μL of water was added and vortexed at 400 rpm for one minute prior to measurement.

For the preparation of plasma samples, 150 μL of human plasma was extracted via SPE. As recommended by the vendor, an Oasis[®] 96-well WCX μ -elution plate was preconditioned with 200 μL methanol and 200 μL 5% aqueous ammonium hydroxide (v/v). Then, 150 μL of human plasma was loaded onto the cartridges, which were pre-filled with 150 μL of 5% aqueous ammonium hydroxide (v/v). All samples were then washed with 200 μL 5% aqueous ammonium hydroxide (v/v) and 200 μL 10% ACN in water (v/v). Elution was conducted twice with a mixture of 25 μL ACN/water/TFA 75/25/1 (v/v). Subsequently, samples were evaporated under a gentle nitrogen stream with shaking at 350 rpm and 40 °C. Dissolution was conducted with the optimised injection solvent or 0.1% FA in 90/10 water/methanol (v/v).

3.2.4. Design of experiments

DoE is a statistical tool for the systematic discovery of the influence of predefined factors on a desired response by building a computer model to reduce the experimental effort. This approach was employed to form a lean set of experiments for the examination of mobile phase composition as well as sample collection material and injection solvent composition. Different designs were developed for both parts, dependent on the DoE phase and the number and type of factors. For the first identification of the impact of determinants, a full-factorial interaction model was chosen. Throughout this manuscript this approach is defined as 'screening' with its primary purpose to identify significant main effectors and reduce eligible factors [Eriksson et al. 2008]. For the optimisation, D-optimal designs were selected. They are built by a computer-generated algorithm that chooses a reduced number of experiments which are regarded as the best set for analysis. A common reason for their selection is when qualitative and quantitative formulation factors are combined. The D-optimal design was also applied for the confirmation of injection solvent composition since it provided the leanest set of experiments to screen the design space. The G-efficiency was aimed to be higher than 0.6 for the D-optimal designs to ensure sufficient efficiency in comparison to designs with a higher number of

experiments. For the evaluation of the models, the peak area of bradykinin was used as a measure of sensitivity to assess the effects. An overview of all applied models and their factors are presented in Figure 4.

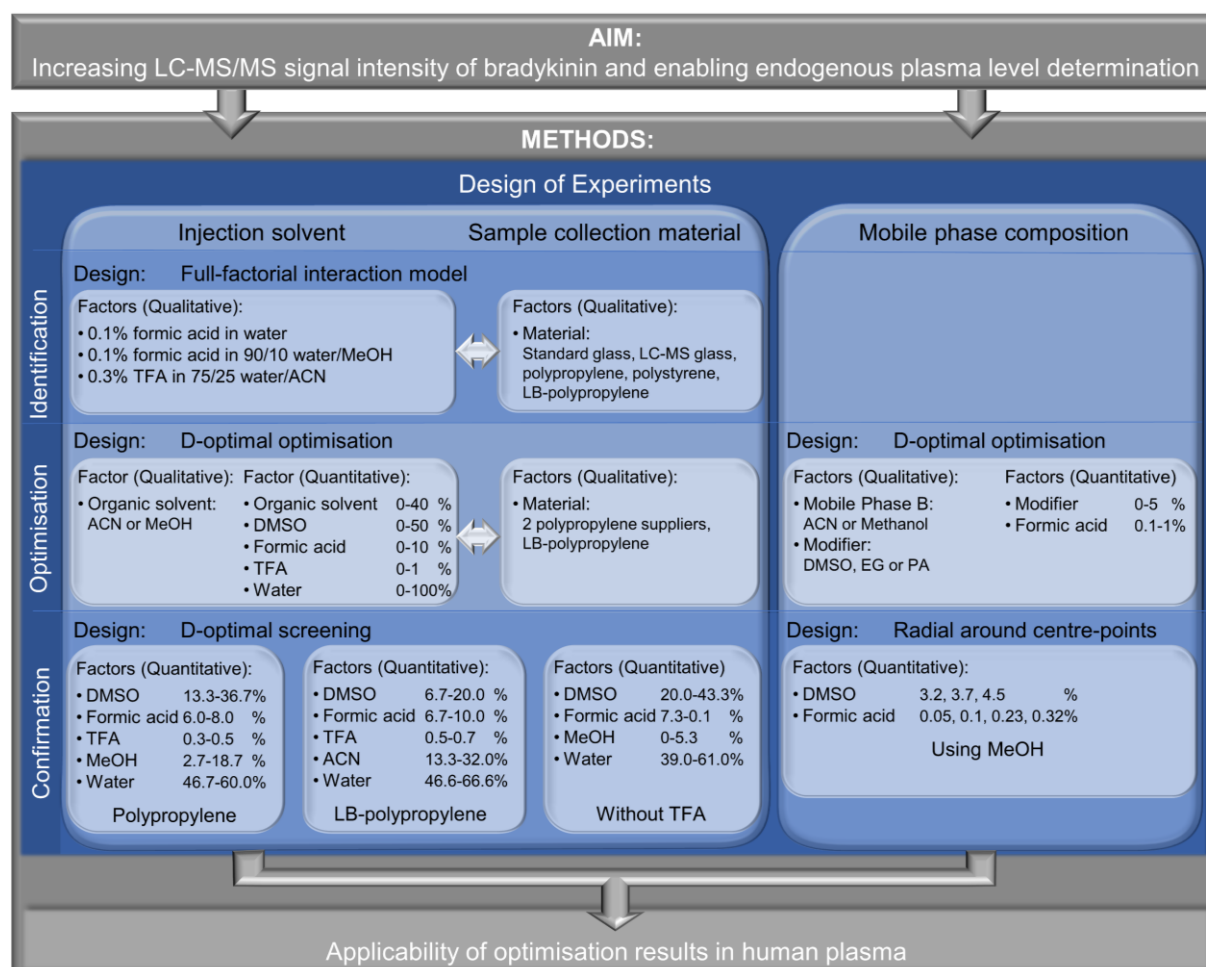


Figure 4. Flow-diagram of the design of experiments approach for improving sensitivity of kinins. The design of experiments encompassed the applied optimisation of the injection solvent, sample collection material and mobile phase composition. ACN: acetonitrile, DMSO: dimethyl sulfoxide, EG: ethylene glycol, LB: protein low-binding, LC-MS/MS: liquid chromatography coupled to mass spectrometry, MeOH: methanol, PA: propionic acid, TFA: trifluoroacetic acid

3.2.4.1. Mobile phase composition

The investigation of the optimal mobile phase composition was divided into optimisation and confirmation runs. For optimisation, a D-optimal optimisation design with 26 runs and one centre-point, all conducted in quintuplicate, was created. Two qualitative factors—the type of organic mobile phase B (methanol or ACN) and the type of added modifier (EG, PA or DMSO) utilised—were investigated. As quantitative factors, the modifier added to both mobile phases in a concentration range of 0–5% (v/v), while FA at a concentration of 0.1–1.0% (v/v) was examined. Higher amounts of modifiers were not applied to limit the contamination of the ion optics by DMSO. The constant addition of FA was utilised to ensure the availability of an ion-

pairing reagent since bradykinin is typically present as twice positively charged peptide. Higher FA concentrations were not applied due to the corrosive and background increasing characteristics of FA. In contrast to the common use of the term reproducibility, which refers to the variation of experimental data between different laboratories, in the here applied DoE approach, reproducibility was defined as the variation of the response at the centre-point compared to the overall variation of all responses (Equation 1). It was aimed to be higher than 0.5 with regard to 1 being excellent reproducibility.

$$\text{Reproducibility} = 1 - (\text{Mean square of the pure error} / \text{Mean square of total error})$$

Equation 1. Calculation of reproducibility in the design of experiments model.

Further, for a significant and reliable model, the goodness of fit (R^2) and of prediction (Q^2), were expected to be greater than 0.5 at minimum, with a maximal difference of 0.3. Robustness testing was conducted through a Monte Carlo simulation with one million iterations. Thereby, a robust setpoint in the design space was determined. The design space was calculated with the principal object to maximise the peak area, and was aspired to deviate by less than 15% of the maximum predicted peak area. The latter requirement was derived from bioanalytical recommendations [European Medicines Agency 2011].

To confirm the optimised results, a radial design in the low and high limits of the design space was created with seven runs and one centre point, which were measured in quintuplicate. Two centres were formed by the optimised setpoint, which reaches the maximised calculated response within factor limits and the robust setpoint. Additionally, lower and higher concentrations of DMSO and FA around the evaluated robust and optimised setpoints were tested.

The run order was chosen randomly, but all quintuplicate measurements were performed successively to save time and reduce solvent consumption since priming and rinsing of the LC-system were obligatory between different mobile phase compositions.

3.2.4.2. Injection solvent and sample collection material

The examination of injection solvent composition and sample collection material comprised the three steps screening, optimisation and confirmation. These stages were necessary to evaluate the broad factor and level range regarding different materials, injection solvent components and their interactions.

In the first step, a full-factorial screening with an interaction model was developed to primarily reduce eligible types of sample collection materials. This facilitated the rapid scanning and identification of appropriate sample collection materials and injection solvents, with the aim of minimising non-specific adsorption. The latter was considered to be the lowest when the signal response was highest. For the sample collection materials, standard glass, LC-MS glass, PS,

PP (Supplier A) and LB-PP were examined since they were assumed to show differences in the non-specific adsorption of bradykinin due to their distinct chemistry. Preliminary results had shown that silanization of standard glass did not improve signal responses compared to polypropylene. Moreover, the observed high batch to batch inconsistency of the silanized glass ware by the in-house method led to the exclusion of this approach within the DoE. Three classical approaches for an injection solvent were chosen, which included the mobile phase composition of the start gradient (90/10 water/methanol, 0.1% FA (v/v)), the SPE elution solvent (25/75 ACN/water, 0.3% TFA (v/v)) and the stock solution solvent (water, 0.1% FA (v/v)). These factors were analysed in 14 experiments in triplicate and one centre-point in nonaplicate. The nine replicates of the centre-point ran in random order throughout the whole measurement and subsequently enabled the evaluation of the within-day repeatability of the peptide determination.

In the second step, a D-optimal optimisation design with a quadratic model was developed on the basis of the screening results. The D-optimal design allowed for the optimisation of a wide range of quantitative formulations and qualitative factors with a reduced number of experiments. The three PP sample collection materials (PP supplier B and C, LB-PP) and the organic solvent type (ACN and methanol) were examined as qualitative factors. For the composition of the injection solvent, five formulation factors were investigated. The organic solvent (ACN or methanol) was studied at a range of 0–40% (v/v). The upper limit was set to 40% since an increased risk for breakthrough and peak distortion was observed in preliminary tests if the organic fraction exceeded 40%. Furthermore, DMSO was analysed at a concentration range of 0–50% (v/v). TFA (0–1% v/v) and FA (0–10% v/v) were also analysed. Lastly, water at a range of 0–100% (v/v) was added to fill up the mixture to the final end volume. These formulation components were chosen due to their abilities to increase solubility and decrease potential ionic interactions. The designed model consisted of 42 experiments measured in triplicate and one centre point measured in nonaplicate. The minimum requirements regarding model characteristics and the calculation of the robust setpoint and design space were set equivalently to the mobile phase optimisation.

In the third step, confirmation runs were performed in the design space hypercube of the D-optimal optimisation. The hypercube marks the ranges in which all factors can be simultaneously changed, provided that the specified aim will not fail. Since up to five quantitative formulation factors were analysed, a different approach had to be chosen compared to the mobile phase confirmation runs in order to reduce experimental effort. Therefore, a D-optimal screening was chosen by which various design points in the design space were tested for their deviation from the peak area of the optimised and robust setpoints. Three designs were created to study (1) the best performing PP material, (2) the LB-PP material and (3) the best performing setting without the use of TFA more closely. This enabled

the reliable comparison of standard PP to LB-PP and to evaluate the need for TFA in the injection solvent. Next to the robust setpoint, the respectively optimised setpoint was also included in the runs. This resulted in 14 runs for LB-PP (five factors), 16 runs for PP material (five factors) and 11 runs for the composition without TFA (four factors). All runs were performed and analysed in triplicate with one centre point in nonaplicate (respective formulation ranges are displayed in Figure 4).

All conducted experiments were performed in a random order with the spreading of centre points to ensure the comparability of the results over the analysis period.

3.2.5. Applicability of optimizations

First, human blank plasma samples spiked with the same concentrations of bradykinin and internal standard as used for the neat solutions were analysed to demonstrate the transferability of the optimisation results. Therefore, the optimised settings were compared to the laboratory standard settings in triplicate. 150 μL human blank plasma samples spiked with 2 ng/mL bradykinin and 4 ng/mL internal standard were extracted, evaporated to dryness and reconstituted in 150 μL of the optimised injection solvent (5.3/36.6/49.3/8.7 methanol/DMSO/water/FA (v/v), supplier B) or the initial one (10/90 methanol/water with 0.1% FA (v/v), supplier A). These samples were analysed with the primarily utilised mobile phase solvents (0.1% FA (v/v) in water (A) and methanol (B)) and subsequently with the optimised solvents (additionally 3.2% DMSO (v/v) to A and B).

Then, endogenous bradykinin levels were determined in a native plasma sample of a healthy female volunteer (26 years old) under the optimised conditions in triplicate. Bradykinin levels were quantified to demonstrate the applicability of the conducted optimisations using high concentrations also to determine low endogenous plasma levels.

3.2.6. Instrumentation

HPLC was performed on an Agilent 1200 series system (Agilent Technologies, Ratingen, Germany) consisting of a degasser, a binary solvent manager and a column oven. The applied CTC HTC PAL autosampler (CTC Analytics AG, Zwingen, Switzerland) was equipped with a 50 μL sample loop. This system was coupled to an API 4000 mass spectrometer (AB Sciex, Darmstadt, Germany) for detection.

3.2.6.1. Chromatographic conditions

HPLC separation was performed using a Waters XBridge™ C18 column (3.0 x 150 mm, 3.5 μm) with a Waters XBridge guard column (3.5 μm). A gradient separation with a flow of 0.7 mL/min using water (mobile phase A) and methanol or ACN (mobile phase B) was applied. Both mobile phases were acidified with FA (0.1–1% (v/v)) and mixed with different modifiers

(0–5% (v/v)), according to the DoE protocols. The LC gradient was set as follows for all conducted experiments: 0–1 min: 10% B; 1–2 min: 10–20% B; 2–4 min: 20–90% B; 4–5 min: 90–100% B; 5–6 min: 100% B; 6–7 min: 100–10% B. While the column oven temperature was set to 60 °C, the equilibration time was 4 minutes. Autosampler temperature was maintained at 19 °C. Before every injection, the injection syringe was pre-rinsed three times with the sample dissolved in the injection solvent and this volume discarded to minimise losses due to the non-specific adsorption of bradykinin via the injection system. After injecting 50 µL of a sample, the autosampler sample syringe was rinsed with 0.2% FA in 80/20 ACN/water (v/v).

3.2.6.2. Mass spectrometry

Bradykinin detection was performed in positive electrospray ionisation mode and quantification was executed in multiple reaction monitoring mode. The chosen transitions of bradykinin and the internal standard ([Phe⁸Ψ(CH-NH)-Arg⁹]-bradykinin) were 530.9 → 641.3 m/z and 524.0 → 274.1 m/z, measured with a dwell time of 100 ms. The declustering potential was set to 87 V and 80 V, the entrance potential to 11 V and 10 V, the collision energy to 41 V and 52 V and the collision cell exit potential to 20 V for bradykinin and the internal standard. The curtain gas was maintained at 25 psi, gas 1 at 55 psi, gas 2 at 80 psi and the collision gas at 9 psi. The ion spray voltage was settled at 5000 eV.

3.2.7. Software packages

All LC-MS/MS measurements were controlled by Analyst[®] 1.6.2 software (AB Sciex, Darmstadt, Germany) and raw data evaluation was executed using Multiquant[™] 3.0.2 (AB Sciex, Darmstadt, Germany). MODDE Pro 12.0 (MKS Instrument AB, Malmö, Sweden) was used to set up and evaluate the DoE. Figures were created using OriginPro[®] 2019 (OriginLab Corporation, Northhampton, MA, USA).

3.3. Results and Discussion

3.3.1. Optimisation of mobile phase composition

The mobile phase composition was investigated in two steps comprising optimisation and confirmation runs. This approach enabled a gain of intensity by a factor of 7.7 of bradykinin in neat solutions.

3.3.1.1. D-optimal optimisation design

For the evaluation of the D-optimal optimisation design of the mobile phase composition, statistical analysis was performed using multiple linear regression. The conducted D-optimal optimisation design was classified by $R^2 = 0.91$, $Q^2 = 0.88$ and reproducibility = 0.98. This fulfilled the predefined criteria and proved the model to fit well as well as featuring good prediction and reproducibility. A logarithmic transformation was applied to obtain the best mathematical fit of the model.

Additional information regarding experiments, peak intensity and shape are provided in Appendix 1 and Appendix 2.

Analysis of influencing factors

To evaluate the impact of the individual effects, as well as the interactive effects within this study, the normalised coefficient plot was used. While positive normalized coefficients indicate a beneficial impact on bradykinin area, negative ones imply worsening effects. It clearly demonstrated that methanol (individual effect) is the more suitable organic solvent for the determination of bradykinin when compared to ACN (Figure 5A, Appendix 3). A predicted increase of factor 2.1 was calculated for the use of methanol. A higher FA concentration of 1% (v/v) was preferable in ACN, whereas 0.1% FA (v/v) provided an 18.7% higher intensity in methanol compared to the addition of 1% FA (v/v). The inclusion of modifiers had a significant positive effect on the signal intensity (Figure 5A, Figure 6). Thereby, DMSO and EG were the more suitable modifiers for bradykinin when compared to PA. Namely, by adding the optimised modifier concentration to the acidified mobile phase in methanol, signal response increases by factors of 1.9 for 3.7% DMSO, 1.8 for 4.0% EG, 1.6 for 3.9% PA were revealed; in ACN, these values were 2.9 for 4.8% DMSO, 3.3 for 5.0% EG and 2.3 for 4.2% PA. These findings are in accordance with the literature, where Hahne et al. observed a 2–4-fold increase of digested proteins in HeLa cells by the addition of 5% DMSO [Hahne et al. 2013]. Moreover, Yu et al. 2017 found that EG at a concentration of 1–3% represents a good alternative to 5% DMSO for digested proteins [Yu et al. 2017]. The beneficial effects of EG on the determination of bradykinin as an equivalent alternative were confirmed in the here presented study, if EG was added in similar concentrations to DMSO (3.7% DMSO and 4.0% EG) [Yu et al. 2017]. The

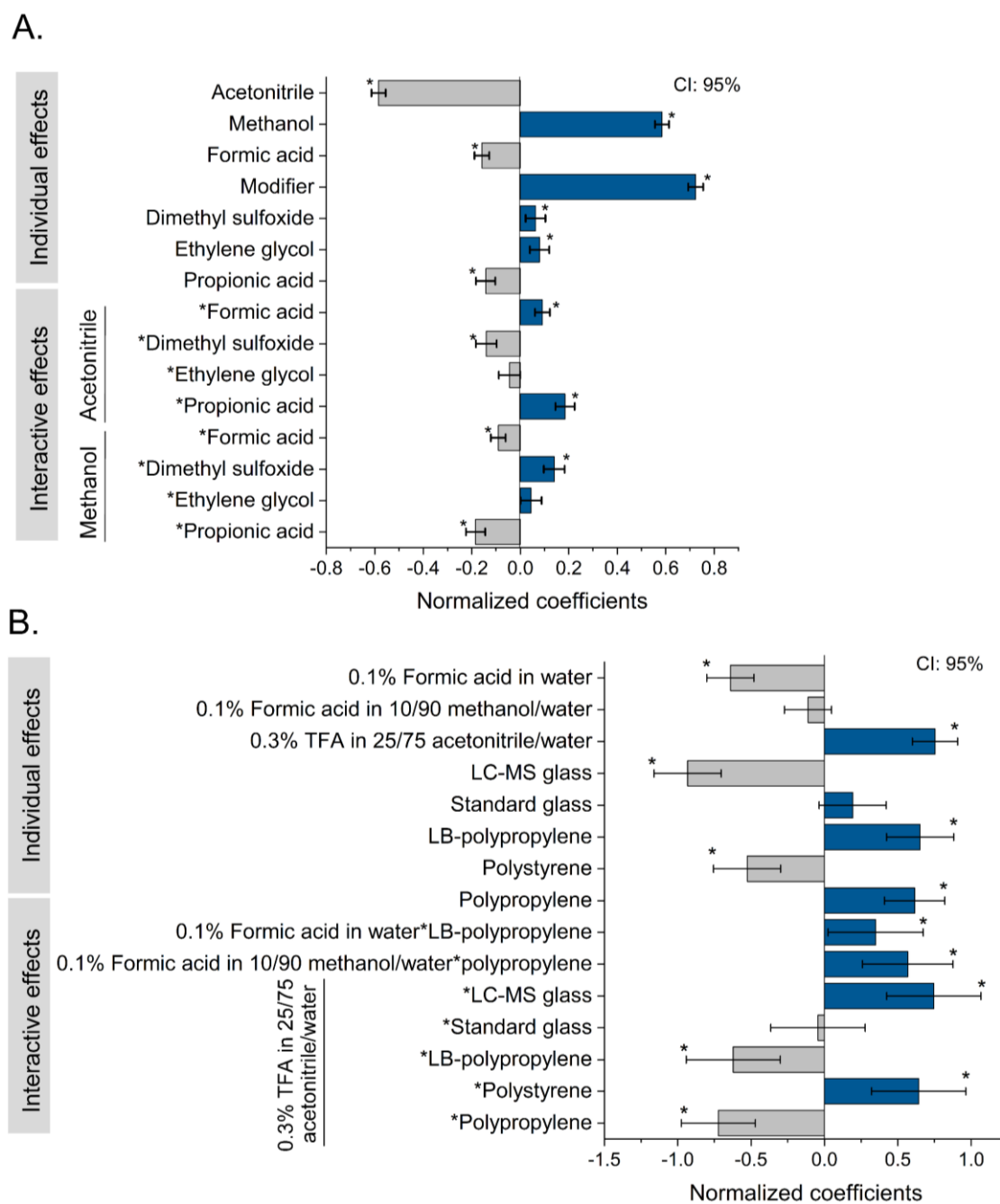


Figure 5. Individual and interactive effect plots for bradykinin. Normalised coefficient plots of (A) the optimisation by a D-optimal design of the mobile phase composition and (B) the full-factorial screening of injection solvents and sample collection material showing individual and interactive effects. Positive normalized coefficients of the factors indicate an increase of peak area. CI: confidence interval, LB: protein low-binding, LC-MS: liquid chromatography coupled to mass spectrometry, TFA: trifluoroacetic acid, *: $p < 0.05$ (Student's *t*-test)

modifier PA was selected for investigation as the injection solvent contained TFA, which is known for its ion-suppressing effects in electrospray ionisation. An approach to reduce its ion suppression is the addition of the weaker acid PA to the mobile phase, which results in the protonation of TFA and thus increased volatility [Feickert & Burckhardt 2019]. Using the so-called “TFA-fix” method, a signal-to-noise ratio increase by a factor of 10–100 for several

peptides was observed. However, these findings could not be confirmed for the present investigation of the peptide bradykinin since no substantial gain in the sensitivity of the TFA/PA combination was detected.

Based on these results, methanol and DMSO were chosen from the qualitative factors for further experiments. Apart from its supercharging effects, DMSO has also been shown to reduce carry-over in LC-MS/MS [Hahne et al. 2013]. Owing to the stronger elution force of DMSO, the solvent can cause earlier peptide elution [Yu et al. 2017]. Nevertheless, for bradykinin, only a slight forward-shift of 0.1 minutes was identified when increasing its concentration from 0 to 5% (v/v) using methanol as the organic mobile phase.

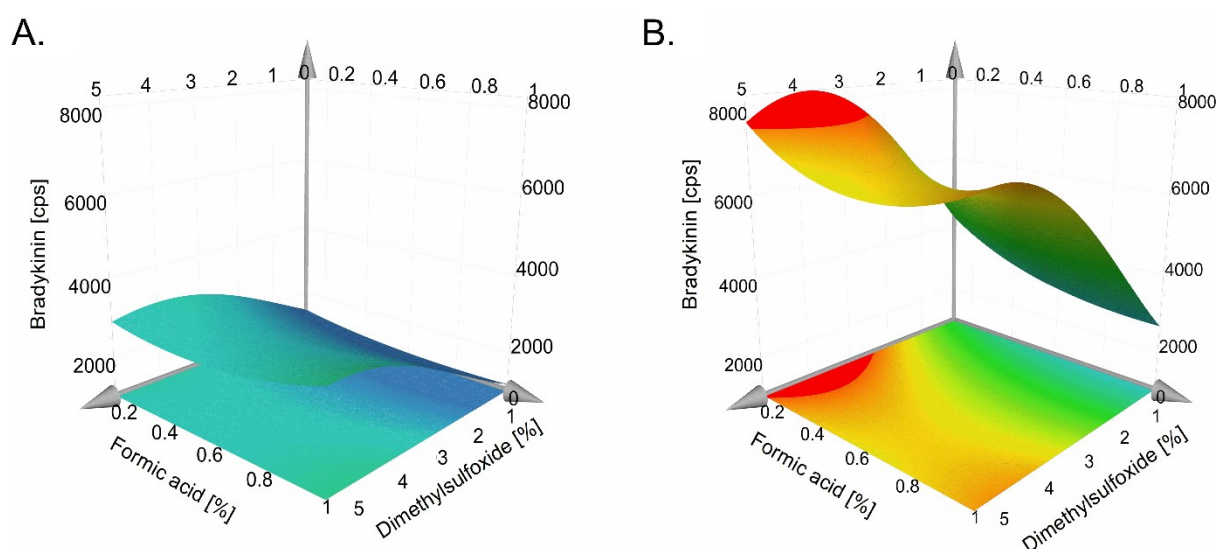


Figure 6. Response surface plots of predicted bradykinin peak area of the mobile phase optimisation. The plots represent the predicted peak areas using the modifier dimethylsulfoxide and formic acid in A. acetonitrile and B. methanol. Cps: counts per second.

Calculated setpoints

The setpoint reaching the highest predicted intensity (optimised setpoint) was calculated to consist of 3.7% DMSO and 0.1% FA using methanol (v/v) and showed a normalised distance to target (log D) of -10. Since a log D < 0 indicates that all results are within the set limits, the observed log D of -10 represented an optimal fit of all predictions to the target value.

A robust setpoint could only be calculated for a deviation of 20% of the maximised peak area and was found to be 3.7% DMSO and 0.23% FA (v/v) with a log D of -1.28. For the robust setpoint, the distance to the design space boundaries is maximised and simultaneously aims for a high log D (Figure 7A). In this case a higher FA concentration and a higher log D resulted as 0.1% FA displayed the lower limit of the applied FA concentration. The higher than aspired deviation required to calculate the robust setpoint was further evaluated within the confirmation runs. The optimised setpoint was predicted to be more intense by a factor of 1.1 when compared to the robust one.

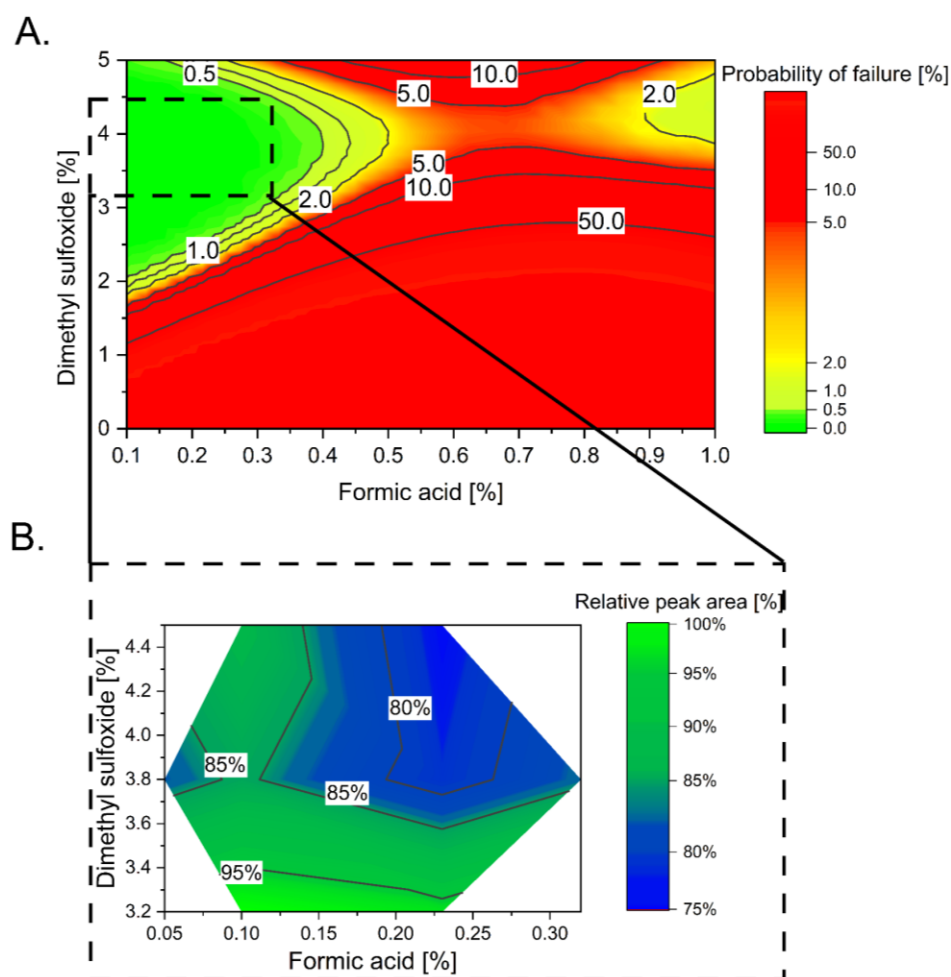


Figure 7. Optimised design space for the mobile phase optimization for bradykinin. A. The contour plot was created by a Monte Carlo simulation (one million iterations) for the addition of dimethyl sulfoxide (0–5% v/v) and formic acid (0.1–1% v/v) in methanol. The green colour indicates the design space with a probability of failure < 0.5% to reach a deviation of less than 20%. B. The contour plot shows the measured relative peak areas within the confirmation runs, where the maximum aspired deviation is marked by the 85% line (green area), which is in line with bioanalytical recommendations. The white colour marks the area that was not investigated.

3.3.1.2. Confirmation runs

To clarify the distinct findings of FA concentrations calculated for the optimised versus the robust setpoint as well as to identify the area within the design space showing the aspired 15% deviation, confirmation runs were applied. Therefore, a radial design around the setpoints in the design space limits was performed similarly to the conduction of confirmation runs recommended by Stevens et al. 2019 [Stevens & Anderson-Cook 2019]. Since the optimised setpoint with an FA concentration of 0.1% (v/v) lay at the boundary of the design space, an additional lower FA concentration (0.05% v/v) was included to verify whether even lower FA concentrations remained beneficial for the mobile phase composition.

Compared to the calculated robust setpoint, all mobile phase compositions were equal or performed even better. The highest mean signal response was observed using 3.2% DMSO and 0.1% FA (v/v) (Figure 7B), which corresponds to a lower DMSO concentration than calculated for the setpoints and resulted in an increase of about 10% of intensity compared to the optimised setpoint. The difference in FA concentrations of 0.23% (v/v) (robust setpoint) versus 0.1% (v/v) (optimised setpoint) showed negligibly higher intensities for 0.1% FA (v/v) of 1.2%. Since the optimisation design failed to calculate a robust setpoint for the aspired deviation of 15%, the confirmation runs enabled the determination of areas in which the latter was reached (Figure 7B, green area, marked by the 85% line). The confirmation runs facilitated a slight adaptation of the optimisation design, which helped to further increase the signal intensity by determining a shifted setpoint. Although the newly found DMSO concentration was at the lower limit of the confirmation runs, it was decided to not further examine lower DMSO concentrations since 5% DMSO was advantageous to 2.5% DMSO during the D-optimal approach. Altogether, a DMSO concentration of 3.2% with 0.1% FA using methanol (v/v) for the mobile phase B was found to provide the highest signal intensities for the LC-MS/MS determination of bradykinin and was subsequently applied for plasma samples.

Further details are provided in Appendix 4.

3.3.2. Optimisation of injection solvent and sample collection material

The investigation of the injection solvent composition and the sample collection material was successfully performed by conducting screening, optimisation and confirmation runs.

3.3.2.1. Full-factorial screening design

The full-factorial screening design of the three distinct injection solvents (SPE elution solvent, stock solution and the mobile phase composition of the start gradient) and five sample collection materials revealed an improvement by a factor increase of 12.0 when comparing the highest signal response (observed in PP (Supplier A)) to the lowest (observed in LC-MS glass). The LB-PP material performed similarly to PP regarding the signal response but was less affected by the use of the investigated solutions and showed lower CVs within the triplicate measurements. In particular, LC-MS glass and PS showed very high CVs of up to 88% when using 0.1% FA in 10/90 methanol/water (v/v) [mobile phase composition of the start gradient] or 0.1% FA (v/v) [stock solution]. High CVs can indicate adsorption or instabilities in the injection solvents, since triplicate measurements were analysed in a randomly chosen order, potentially resulting in time influencing the results. Upon using 0.1% FA (v/v) or 0.1% FA in 10/90 methanol/water (v/v) in standard glass, a tendency towards decreasing areas over time within the triplicate measurements was noted. The observation that the combination of glass and the use of the strong acid TFA increases signal intensity can be reasoned by the fact that,

below a pH of 3, free silanol groups are rather protonated; therefore, the interaction with positively charged bradykinin (isoelectric point: 12.0) is reduced [Mathé et al. 2013]. PS was further affected by the high ACN concentrations during evaporation to dryness and showed traces of damage. More information is presented in Appendix 5 and Appendix 6.

Based on the screening results, it was decided to choose PP and LB-PP for the subsequent optimisation as these were the only materials within the normalised coefficient plot showing a significant positive effect on predicted peak area (Figure 5B). Moreover, TFA was also included in the optimisation experiments, since its use as the 'SPE elution solvent' resulted in all materials performing equally with CV being reduced. Within intermediate experiments, a change from the PP of supplier A was decided since it was preferable to work with a conical bottom instead of a round one due to less residual volume. Within these experiments no substantial difference on signal intensity could be observed by comparing conical versus round bottom. These findings were confirmed also by the low overall variability of the optimised setpoints in different container materials during the D-optimal optimisation design.

3.3.2.2. D-optimal optimisation design

Partial least squares regression was performed to statistically analyse the D-optimal optimisation design of the injection solvent and sample collection material. The model showed a reproducibility of 0.91, $R^2 = 0.83$ and $Q^2 = 0.66$, thus fulfilling the predefined criteria for a good and predictive model. The maximum calculated improvement between the optimised and worst-performing setting differed by a factor of 26.6.

Analysis of influencing factors

The evaluation of individual effects revealed that TFA, closely followed by FA and water, had the highest positive effect on the intensity of bradykinin. The addition of either DMSO or organic solvent alone negatively influenced the intensity. The type of material (-0.1% for supplier B and -3.4% for supplier C to LB-PP) or organic solvent (-0.1% using ACN instead of methanol) had no major impact on signal intensity. However, when also regarding two-way interactions between the organic solvent and material, methanol had a positive influence using the PP of supplier B (+18.3%), whereas it was ACN in the LB-PP (+9.2%) and PP of supplier C (+8.2%) (Figure 8). Compared to the reference mixture, which consisted of 27.7/22.1/0.5/5.5/44.2 DMSO/methanol/TFA/FA/water in PP, a higher DMSO and FA fraction was preferable in the PP of supplier B (Figure 8). In the PP of supplier C, increased TFA and water fractions were more suitable. For LB-PP, the addition of organic solvent had the greatest further improvement. The assumption that different manufacturing processes regarding one type of material can influence non-specific adsorption was hereby confirmed. Notably, when comparing the signal intensities of bradykinin in 100% water between PP and LB-PP material, an increase of factor

12.8 was observed (mean area \pm standard deviation: 883.7 ± 63.7 vs. $11\,275.0 \pm 1\,525.0$ cps). However, adding an organic fraction or acid reduced these differences and improved signal intensities for all materials (predicted maximum peak areas: LB-PP: 23,286.8 cps, PP supplier B: 22,367.9 cps, PP supplier C: 21,264.2 cps).

Additional data is provided in Appendix 7 and Figure 9.

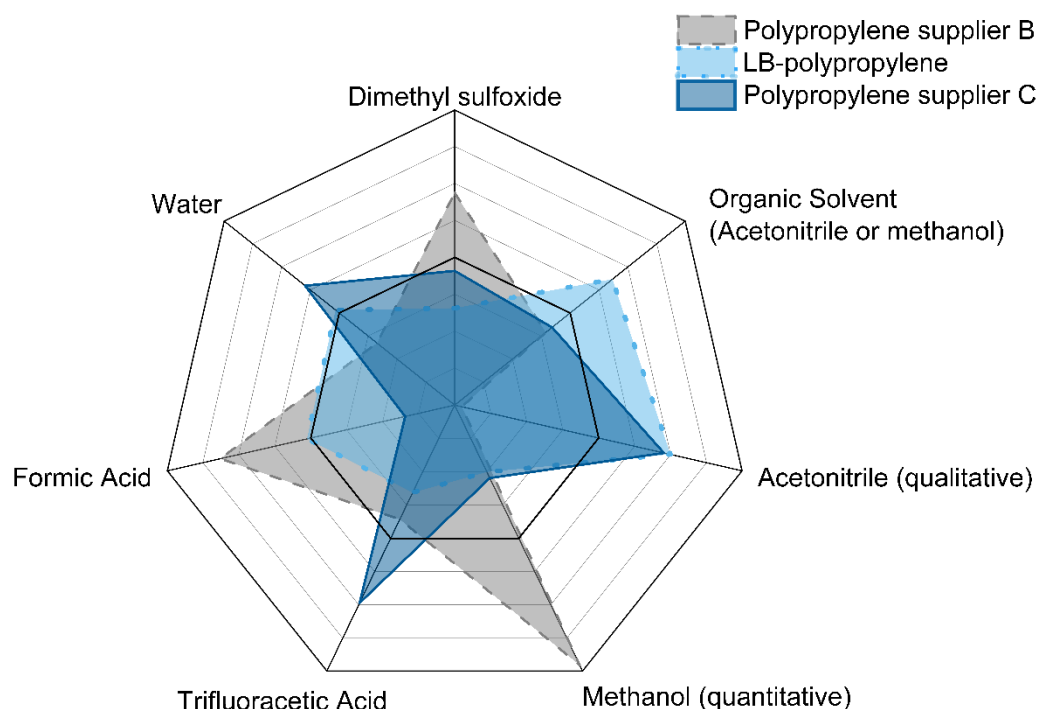
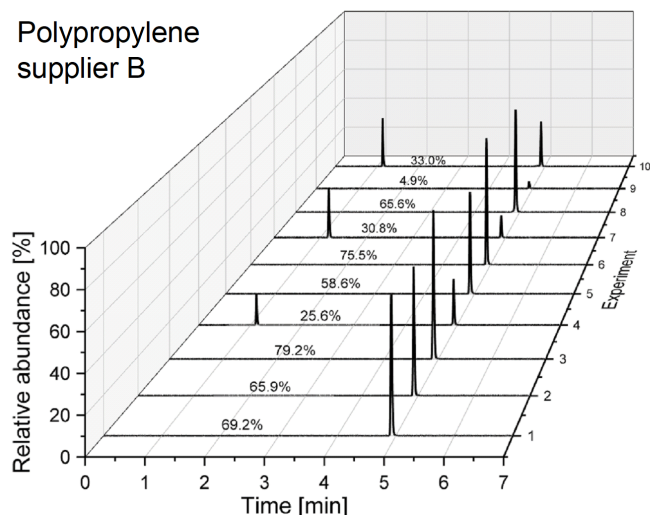


Figure 8. Radar chart of the interaction effects of the injection solvent components with consumables for bradykinin. The effects of the injection solvent with polypropylene of supplier B (dark grey, dashed), protein low-binding (LB) polypropylene (light blue, dotted) and polypropylene of supplier C (darker blue, solid line) based on the coefficient effects are depicted. The data were normalised to the coefficient effect of methanol (outer black line). The inner black line represents the reference mixture, consisting of 27.7% dimethyl sulfoxide, 22.2% methanol, 0.5% trifluoroacetic acid, 5.5% formic acid and 44.1% water in polypropylene. With the exception of acetonitrile and methanol (qualitative), all factors are quantitative.

Calculated setpoints

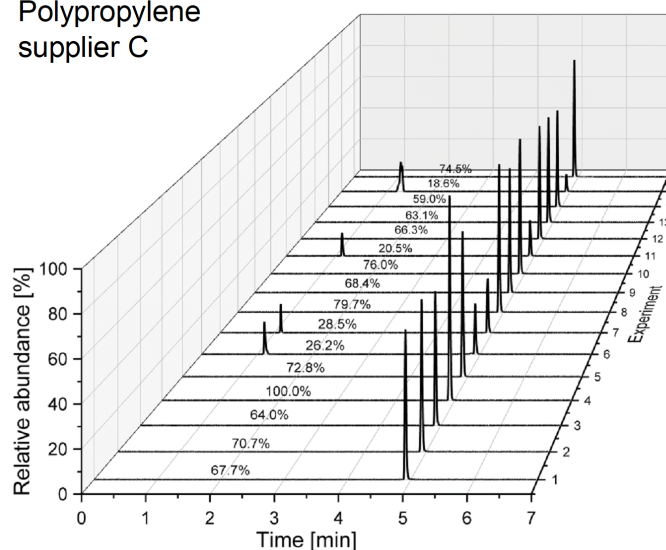
Optimised and robust setpoints were calculated for the three different settings in order to compare LB-PP to standard PP and to evaluate the need for TFA. Figure 10 provides detailed information on the six different injection solvent compositions (e.g. the robust setpoint for the injection solvent using polypropylene consisted of 13.3% methanol, 26.6% DMSO, 53.0% water, 0.4% TFA and 6.7% FA). All predicted injection solvent compositions consisted of a high amount of acid (7–10% (v/v)), approximately 50–60% water (v/v) and 33.6–51.9% combined DMSO and ACN or methanol (v/v). Every calculated setpoints fulfilled the requirements of a log D < 0. Since the same supplier was used for the setting of the best PP and the one without TFA, the mixtures differed primarily in the amount of FA, which was

Polypropylene supplier B



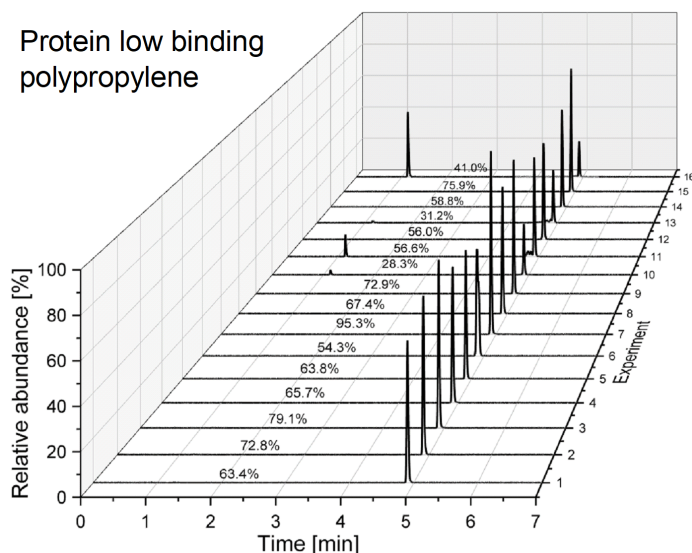
Experiment	Tailing factor	Peak width at 50%
10 40% ACN, 1% TFA, 10% FA, 49% Water	1.07 (n=3)	0.03
9 100% Water	1.25 (n=3)	0.03
8 50% DMSO, 50% Water	1.04 (n=3)	0.03
7 50% DMSO, 40% ACN, 10% Water	1.33 (n=3)	0.03
6 50% DMSO, 10% FA, 40% Water	1.20 (n=3)	0.03
5 50% DMSO, 1% TFA, 49% Water	1.25 (n=3)	0.03
4 49% DMSO, 40% MeOH, 1% TFA, 10% FA	1.25 (n=3)	0.03
3 40% MeOH, 10% FA, 50% Water	1.19 (n=3)	0.03
2 1% TFA, 10% FA, 89% Water	1.22 (n=3)	0.03
1 40% MeOH, 1% TFA, 59% Water	1.26 (n=3)	0.03

Polypropylene supplier C



Experiment	Tailing factor	Peak width at 50%
16 40% MeOH, 5% FA, 55% Water	1.29 (n=3)	0.03
15 40% ACN, 60% Water	1.21 (n=3)	0.03
14 20% MeOH, 80% Water	1.29 (n=3)	0.03
13 0.5% TFA, 99.5% Water	1.26 (n=3)	0.03
12 50% DMSO, 50% Water	1.08 (n=3)	0.03
11 50% DMSO, 40% ACN, 10% FA	1.16 (n=3)	0.03
10 27.7% DMSO, 22.2% MeOH, 0.6% TFA, 5.5% FA, 44.2% Water	1.25 (n=12)	0.03
9 50% DMSO, 1% TFA, 5% FA, 44% Water	1.34 (n=3)	0.03
8 50% DMSO, 1% TFA, 10% FA, 39% Water	1.17 (n=3)	0.03
7 50% DMSO, 40% MeOH, 0.5% TFA, 9.5% water	1.32 (n=3)	0.03
6 50% DMSO, 20% MeOH, 10% FA, 20% Water	1.27 (n=3)	0.03
5 40% MeOH, 1% TFA, 10% FA, 49% Water	1.23 (n=3)	0.03
4 25% DMSO, 40% ACN, 1% TFA, 34% Water	1.06 (n=3)	0.03
3 25% DMSO, 10% FA, 65% Water	1.29 (n=3)	0.03
2 10% FA, 90% Water	1.22 (n=3)	0.03
1 1% TFA, 99% Water	1.32 (n=3)	0.03

Protein low binding polypropylene



Experiment	Tailing factor	Peak width at 50%
16 25% DMSO, 40% MeOH, 35% Water	1.21 (n=3)	0.03
15 40% MeOH, 1% TFA, 10% FA, 49% Water	1.20 (n=3)	0.03
14 100% Water	1.26 (n=3)	0.03
13 50% DMSO, 40% ACN, 1% TFA, 9% Water	1.21 (n=3)	0.03
12 50% DMSO, 50% Water	1.07 (n=3)	0.03
11 50% DMSO, 40% MeOH, 5% FA, 5% Water	1.37 (n=3)	0.03
10 50% DMSO, 39% ACN, 1% TFA, 5% FA	1.20 (n=3)	0.03
9 50% DMSO, 20% MeOH, 1% TFA, 29% Water	1.16 (n=3)	0.03
8 50% DMSO, 0.5% TFA, 10% FA, 39.5% Water	1.24 (n=3)	0.03
7 40% ACN, 0.5% TFA, 59.5% Water	1.13 (n=3)	0.03
6 25% DMSO, 40% ACN, 10% FA, 25% Water	1.15 (n=3)	0.03
5 25% DMSO, 1% TFA, 74% Water	1.28 (n=3)	0.03
4 25% DMSO, 1% TFA, 10% FA, 64% Water	1.26 (n=3)	0.03
3 20% ACN, 10% FA, 70% Water	1.23 (n=3)	0.03
2 10% FA, 90% Water	1.23 (n=3)	0.03
1 1% TFA, 5% FA, 94% Water	1.33 (n=3)	0.03

Figure 9. Example chromatograms of the D-optimal optimisation of the injection solvent and sample collection materials. ACN: acetonitrile, DMSO: dimethyl sulfoxide, FA: formic acid, MeOH: methanol, TFA: trifluoroacetic acid

increased by the exclusion of TFA. The predicted intensities of the optimised and robust setpoints were similar at a range of -4% to +6% of their overall mean. Altogether, high concentrations of FA (6.7–10.0% (v/v)) seemed to be preferable for bradykinin to reduce non-specific adsorption, which exceeded literature recommendations of 0.1–1% (v/v) [Hoofnagle et al. 2016; Stejskal et al. 2013; Chen 2013]. It is rather unlikely that an increasing amount of acid has an influence on improved ionisation in the ion source of the mass spectrometer, as it was shown in the mobile phase optimisation that low FA concentrations are preferable. Consequently, this high FA amount might be related to either the reduction of non-specific adsorption of bradykinin to the sample collection material or to chromatographic system parts before dilution by the mobile phase.

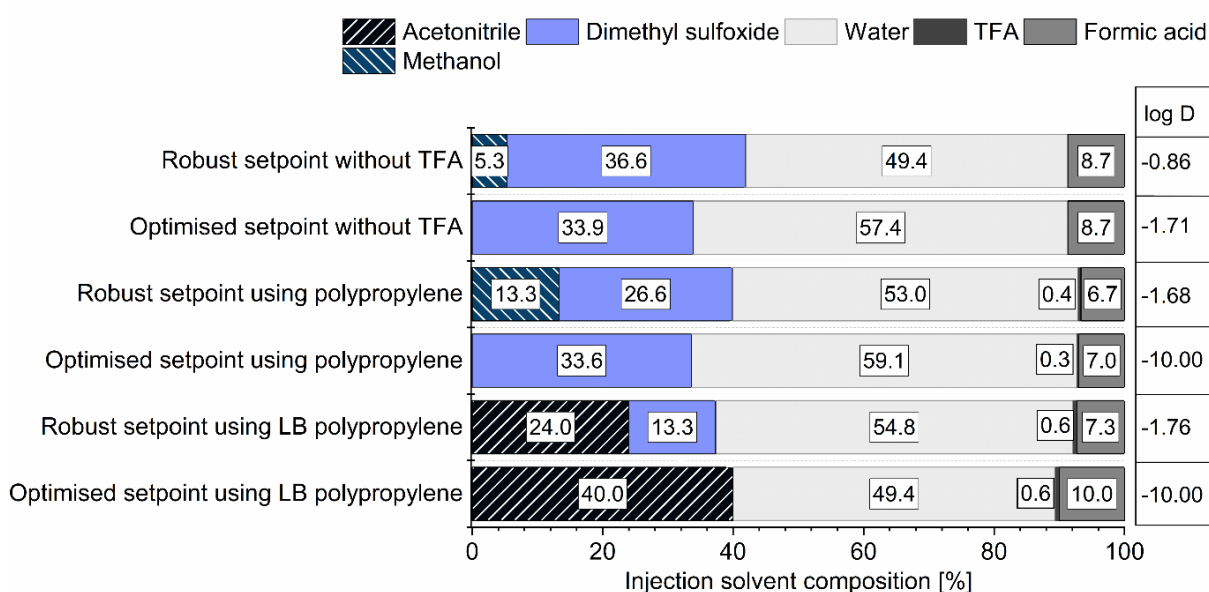


Figure 10. Injection solvent compositions for bradykinin according to calculated robust and optimised setpoints. Setpoints were computed using polypropylene, protein low-binding (LB) polypropylene and no trifluoroacetic acid (TFA). The normalised distance to target is given next to the solvent composition by the normalised distance to target ($\log D$). The optimised setpoint yields the predicted highest response, whereas the robust one is created by Monte Carlo simulations within the acceptance boundaries.

3.3.2.3. Confirmation runs

The design space optimisation revealed no major differences between the six different injection solvent compositions at the setpoints (Figure 10) and confirmed the conducted optimisation. Precision over all experiments was 7.8% (CV) for the formulations without TFA, 10.1% in the PP of supplier B and 7.8% in the LB-PP; therefore, consistent results within the design space were measured. The observed mean peak area differences between the best setpoint and the worst performing composition were 14.3% without TFA, 15.2% in the PP of supplier B and 19.2% in the LB-PP. Furthermore, it was confirmed that a solvent composition without the use of TFA (calculated robust setpoint) was possible to use and resulted in similar signal intensities

in comparison to those using TFA (+5.6% to the PP of supplier B and +1.2% to the LB-PP). More detailed information is provided in Appendix 8. Consequently, the DoE approach enabled the discovery of an alternative setpoint by which the use of TFA was avoided despite its indicated usefulness during the screening. This finding is useful given the fact that, when measuring other peptides on the same LC-MS/MS system, those might exhibit ion suppression caused by TFA.

Within the screening, it was observed that protein low-binding material offered the option to use different solutions with similar signal responses of bradykinin, which is especially favourable when using high amounts of water. However, with the help of the DoE, it was shown that using more expensive protein low-binding material is not necessary if it is possible to optimise the injection solvents since comparable signal responses were observed after the optimisations.

Although substantial improvements in peak intensity could be achieved as part of these experiments, it is advisable to evaluate the effect of blocking agents during dissolution of the lyophilizate for future measurements [26]. This was not conducted within this work, but it is conceivable that it could be used to further control adsorption effects.

3.3.3. Applicability

First, the optimisation results were confirmed by their application to spiked plasma samples. Through optimising the mobile phase composition, the intensity was doubled when comparing the initial conditions (0.1% FA using methanol (v/v)) against the new ones (0.1% FA and 3.2% DMSO using methanol (v/v)). This finding complies with predictions given by the mobile phase D-optimal optimisation design, which calculated a factor increase of 1.9 for the addition of 3.2% DMSO (v/v) in a neat solution. The optimisation of the injection solvent led to an improvement through a factor increase of 1.3 when comparing the best screening design setting of 0.1% FA in 90/10 water/methanol (v/v) in the PP of supplier A to the optimised one consisting of 8.7% FA in 49.5/5.3/36.6 water/methanol/DMSO (v/v) in the PP of supplier B. When combining the optimisation results of the mobile phase composition with the injection solvent and sample collection material, a total improvement by a factor increase of 2.8 was revealed for bradykinin (Figure 11). For the internal standard, which was not regarded in deciding the best setting, a factor increase of 4.0 was observed, which was also mainly achieved by the mobile phase optimisation. Overall, the observed increases in plasma were not as high as suggested by the outcome obtained in neat solution during the DoE phase. This might be explained by the fact that initial conditions for bradykinin evaluation in plasma were already carefully chosen on preliminary screening results. For example, only PP was selected for plasma evaluation instead of glass vials due to identified adsorption processes.

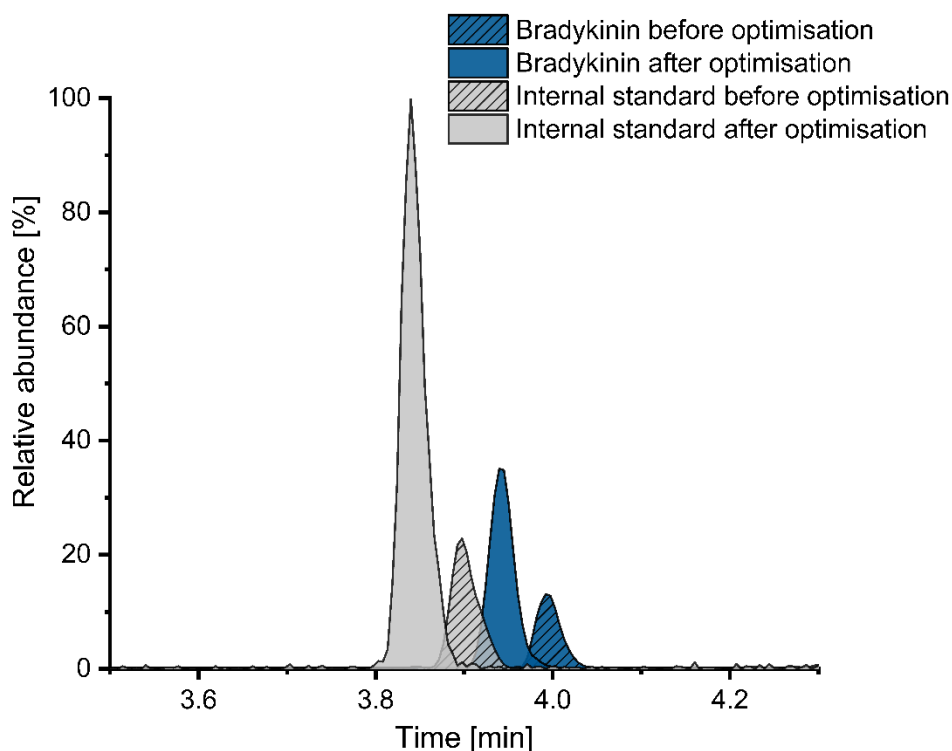


Figure 11. Example chromatogram of bradykinin spiked plasma samples. Peak results with 2 ng/mL bradykinin (blue) and 4 ng/mL of its internal standard (grey) before the optimisation are indicated by the dashed pattern.

On the basis of these improvements, the applicability of the method developed here to determine endogenous plasma levels was successfully proven. Linearity of the developed method was shown in a range of 1000 pg/mL to 7.81 pg/mL ($r = 0.998$, linear weighting $1/x$) with a LLOQ of 7.81 pg/mL. Bradykinin concentrations of 16.0 pg/mL were detected in a native plasma sample of a healthy woman. This result is in line with Ceconi et al., who noted a mean of 18.3 pg/mL bradykinin by radioimmunoassay and SPE in 45 healthy subjects [Ceconi et al. 2007]. LC-MS/MS methods published by van den Broek et al. [van den Broek et al. 2010] and Ion et al. [Ion et al. 2017] featured a quantification limit of 10 ng/mL [van den Broek et al. 2010]. Their ability to anyway quantify bradykinin was due to insufficient prevention of the *ex vivo* generation of bradykinin [Campbell 2000]. Recently, an improved method was published that presented a quantification limit of 100 pg/mL; however, bradykinin could not be quantified in 59% of the patient samples due to a lack of sensitivity [Lindström et al. 2019]. This demonstrates the importance of a sensitive LC-MS/MS method and emphasises the value of the developed optimisations in order to enable the quantification of endogenous plasma bradykinin.

3.4. Conclusion

The presented DoE approach was used to systematically investigate and successfully optimise factors and interactions reducing the non-specific adsorption of bradykinin and increase its signal intensity in LC-MS/MS. The conducted approach contributed to revealing optimal settings for the LC-MS/MS determination of bradykinin and could further be used to avoid the addition of TFA in the injection solvent. The optimisation results were successfully applied to the determination of endogenous human plasma bradykinin levels and can contribute to enabling future reliable LC-MS/MS detection of the low-abundance peptide bradykinin.

4. Targeted mass spectrometric platform for the comprehensive determination of peptides in the kallikrein-kinin system in plasma

4.1. Background

The KKS is involved in many physiological and pathophysiological processes, including regulation of blood pressure, cardiac function, renal function, inflammation, pain, and cough [Kashuba et al. 2013; Duncan et al. 2000]. Clinical conditions to which kinins are connected comprise angioedema and ACE-inhibitor-induced cough, in which elevated levels of the kinin bradykinin are postulated [Hubers et al. 2018; Chung & Pavord 2008]. Further, the so-called 'bradykinin storm' has been implicated in the ongoing COVID-19 pandemic, as it has been proposed to lead to severe COVID-19 pathologies [Garvin et al. 2020]. The active kinins bradykinin and kallidin are produced by proteolytic cleavage from kininogen through the action of plasma and tissue kallikrein, respectively (Figure 1) [Campbell 2000]. Moreover, bradykinin can be generated by aminopeptidase P- mediated cleavage of kallidin. Bradykinin and kallidin, along with their des-Arg metabolites, des-Arg(9)-bradykinin and des-Arg(10)-kallidin, contribute to the biological activity of kinins in humans. These active kinins are degraded by distinct enzymes (e.g. ACE, ACE 2, carboxypeptidase N or aminopeptidase P) into inactive metabolites (e.g. bradykinin 1-7, bradykinin 1-5) in plasma (Figure 1) [McLean et al. 2005; Blais et al. 1999]. During COVID-19, a dysregulated KKS is hypothesized to be caused by reduced des-Arg(9)-bradykinin degradation through virus-associated ACE 2 inhibition on the one hand and increased bradykinin production via alternative cleavage of bradykinin precursors or induction of the bradykinin-forming enzyme kallikrein on the other hand [Nicolau et al. 2020; van de Veerdonk et al. 2020b; Kaplan & Ghebrehiwet 2021; Garvin et al. 2020]. Confirmation of these postulated alterations requires a comprehensive quantitative determination of the KKS peptide levels.

However, despite its important physiological and pathophysiological roles, the current *in vivo* knowledge about the KKS remains limited, as the reliable and accurate determination of peptides of the KKS in plasma is a major hurdle. Artefactual changes of endogenous levels owing to rapid enzymatic degradation or artificial generation of bradykinin through contact with surfaces need to be prevented by an adequate protease inhibitor [Cyr et al. 2001; Eddleston et al. 2006; Björkqvist et al. 2013]. Further, their low endogenous concentrations of few pg/mL and the structural similarity of kinins with their precursors and metabolites call for sensitive and specific assays [Duncan et al. 2000]. These confounding factors have contributed to diverging reported ranges of kinin levels. Immunometric detection-based assays claim low detection

This work was published in a peer-reviewed journal:

Gangnus T, Burckhardt BB (2021) Targeted LC-MS/MS platform for the comprehensive determination of peptides in the kallikrein-kinin system. *Analytical and Bioanalytical Chemistry*. 413(11):2971–2984. <https://doi.org/10.1007/s00216-021-03231-9>

The author of this thesis was responsible for conceptualization, methodology, validation, writing—original draft, review and editing, and visualization.

limits of 0.5 pg/mL – 1.4 pg/mL for bradykinin [Hilgenfeldt et al. 1995; Pellacani et al. 1994; Nielsen et al. 1982]. Using these assays, reported endogenous levels ranged between 1.7 pg/mL and 15.8 pg/mL for bradykinin in healthy volunteers. However, the disadvantage of immunoassays is that they commonly suffer from cross-reactivities with related kinins. LC-MS/MS can overcome these specificity issues. Approaches towards quantification of several kinins simultaneously by nano LC-MS/MS indicated the high potential of this technique [Lortie et al. 2009]. Nevertheless, reported levels of bradykinin applying available LC-MS/MS assays still vary from 200 pg/mL [Lindström et al. 2019; Lame et al. 2016] up to 160 ng/mL [van den Broek et al. 2010] in healthy volunteers. Consequently, other studies have focused on the determination of only the more stable metabolite bradykinin 1-5, whose levels are unaffected by the artificial generation of bradykinin if the degradation of bradykinin is sufficiently inhibited [Seip et al. 2014; Murphey et al. 2001]. However, this approach only delivers limited information as the alterations in the KKS cascade are dominated by different concomitant metabolic pathways leading to the formation of bradykinin 1-5. Moreover, LC-MS/MS offers a tool for the determination of multiple peptides simultaneously, representing an advantage over immunoassays. Measurement of all active kinin peptides and their major metabolites in one method would allow for the collection of more information and a more comprehensive picture of the status of the KKS than the measurement of single kinins (e.g. bradykinin 1-5). For this purpose, a platform technology is required to facilitate the thorough monitoring of the KKS peptides, as well as their comprehensive investigation in patient groups in which the KKS has been implicated.

Thus, this study aimed to develop, validate and establish a targeted LC-MS/MS platform and demonstrate its applicability for the determination of plasma levels in healthy volunteers for the following kinin peptides: bradykinin, kallidin, des-Arg(9)-bradykinin, des-Arg(10)-kallidin, bradykinin 1-7, bradykinin 1-5 and bradykinin 2-9. The comprehensive investigation of the entire kinin peptide cascade was aspired at facilitating a better understanding of the impact of altered enzyme activities on the presence of active kinins within the KKS in disease.

4.2. Materials and Methods

4.2.1. Preparation of kinin stock and working solutions

Kallidin TFA salt (96.9%, HPLC; Tocris, Bristol, UK), bradykinin acetate (99.0%, HPLC; Sigma-Aldrich, St. Louis, MO, USA) and their metabolites des-Arg(9)-bradykinin acetate (98.7%, HPLC; Santa Cruz Biotechnology, Dallas, TX, USA), bradykinin 1-7 TFA salt ($\geq 95.0\%$, HPLC; GenScript, Piscataway Township, NJ, USA), bradykinin 1-5 TFA salt ($\geq 95.0\%$, HPLC; GenScript), bradykinin 2-9 TFA salt ($\geq 95.0\%$, HPLC; GenScript) and des-Arg(10)-kallidin TFA salt (95.9%, HPLC; Tocris) were dissolved and diluted separately in 0.3% TFA in 25/75 ACN/water (v/v/v) prior to the preparation of a combined working solution containing 400 ng/mL of each peptide (free base). All peptide concentrations given within this study were corrected for salt content and peptide purity referring to the conducted amino acid analysis. [Phe⁸Ψ(CH-NH)-Arg⁹]-bradykinin TFA salt (97.5%, HPLC; Tocris), the internal standard, was dissolved in 0.1% FA in water (v/v) and subsequently diluted to achieve a working solution of 500 ng/mL in 0.3% TFA in 25/75 ACN/water (v/v/v). All peptide solutions were prepared using low protein binding tubes (Sarstedt, Nümbrecht, Germany).

4.2.2. Human blood samples

Blood samples were donated by healthy volunteers and sampled in S-Monovettes[®] (Sarstedt, Nümbrecht, Germany) containing 1.6 mg/mL EDTA or 0.106 mol/L trisodium citrate. All participants gave written informed consent prior to their enrolment. The study was conducted in accordance with the Declaration of Helsinki and approved by the ethics committee of the medical faculty at the Heinrich Heine University (study number: 6112).

4.2.3. Sample preparation

In this study, human blank plasma was generated by sampling blood into trisodium citrate S-Monovettes[®] spiked with hexadimethrine bromide and nafamostat mesylate to prevent the artificial generation of bradykinin. After centrifugation at 2000 × g for 10 min at room temperature, the plasma was left at room temperature for 4 h to enable degradation of short-lived kinins. The blank plasma generated was stored at -20 °C until use.

Before preparation of QC or calibration curve samples, a protease inhibitor was added to blank plasma samples, consisting of a mixture of 19.8 μM nafamostat mesylate, 3 mg/mL hexadimethrine bromide (both already added for blank plasma generation), 1% FA, 16.1 mg/mL EDTA, 20 mM trisodium citrate, 1 μM omapatrilat and 1 mM chloroquine. SPE was performed using 96-well Oasis WCX μ-elution plates (Waters, Milford, MA, USA). The wells were conditioned with 200 μL methanol, followed by 200 μL water. Subsequently, all cartridges were prefilled with 150 μL of 3 ng/mL internal standard in 8% phosphoric acid (v/v) before

loading 150 μL of plasma sample. Washing was performed using 300 μL of 25 mM phosphate buffer, followed by 300 μL water and 300 μL 10% methanol in water (v/v). Elution was conducted three times with 50 μL 1% TFA in 75/25 ACN/water (v/v/v). The resulting eluate was evaporated to dryness under a gentle stream of nitrogen at 60°C while shaking at 300 rpm. The residue was dissolved in 75 μL of 10/10/80 FA/methanol/water (v/v/v).

4.2.4. Liquid chromatography coupled with tandem mass spectrometry

An Agilent 1200 SL series system (Agilent Technologies, Ratingen, Germany) equipped with a degasser (G1379B), a binary pump SL (G1379B) and a column oven TCC SL (G1316B) was used. For chromatographic separation, a Phenomenex Synergi™ 2.5 μm Hydro-RP 100 Å column (100 x 2.0 mm; Torrance, CA, USA) with an AQ C18 (4.0 x 2.0 mm) security cartridge was applied. The mobile phases consisted of water and methanol (B), both containing 3.2% DMSO and 0.1% FA (v/v). A 7.5 min binary gradient at a flow rate of 0.4 mL/min and a column oven temperature of 60°C was applied as follows: 0–1.5 min: 5% B, 1.5–2.2 min: 5%–20% B, 2.2–2.7 min: 20%–27% B, 2.7–3.1 min: 27%–35% B, 3.1–6.2 min: 35%–95% B, 6.2–6.7 min: 95% B, 6.7–7.5 min: 95%–5% B. Thereafter, the column was re-equilibrated for 3 min. The injection volume of 50 μL was applied with a PAL HTC-xt autosampler (CTC Analytics AG, Zwingen, Switzerland), and samples were stored at 18°C.

Table 2. Kinin-specific transitions and voltage parameters for mass spectrometric detection.

Analyte	Transition [m/z]	Dwell time [ms]	Declustering potential [V]	Entrance potential [V]	Collision energy [V]	Collision cell exit potential [V]
Kallidin	396.9→506.3	65	95	9	23	14
Bradykinin	530.9→522.4	65	120	10	31	14
Des-Arg(9)-bradykinin	452.8→263.2	75	85	10	22	15
Des-Arg(10)-kallidin	516.8→752.5	65	100	10	29	11
Bradykinin 2-9	452.8→404.3	50	120	9	24	11
Bradykinin 1-7	379.3→642.4	75	63	10	16	10
Bradykinin 1-5	287.2→108.3	50	61	8	15	11
[Phe ⁸ Ψ(CH-NH)-Arg ⁹]-bradykinin	523.9→274.3	75	100	12	48	18

ms: milliseconds, m/z: mass-to-charge ratio, V: Volt

The LC system was coupled to an API 4000 mass spectrometer (AB Sciex, Darmstadt, Germany) equipped with a Turbo V source for detection. The electrospray ionisation source was operated in positive mode with multiple reaction monitoring mode. The curtain gas was maintained at 31 psi, the collision gas at 8 psi, the nebuliser gas at 45 psi and the heater gas at 65 psi. The ion spray voltage was set at 5500 V, while the source temperature was 350°C. Peptide-specific parameters are displayed in Table 2 and the respective product ion spectra of each kinin are shown in Figure 12. The most intense transition per peptide was used for quantification to allow for highest achievable sensitivity. Since only one transition was used for

the quantification, the specificity was ensured by the relative retention time to the internal standard. Controlling and data acquisition were conducted using Analyst® 1.6.2 software (AB Sciex), and data evaluation was performed using MultiQuant™ 3.0.2 (AB Sciex).

4.2.5. Method development for kinin quantitation in plasma

4.2.5.1. Blank plasma generation

Due to the endogenous presence of kinins in human plasma, it was aimed to develop a surrogate matrix mimicking human biological samples at best. Therefore, distinct serine protease inhibitors were evaluated for their ability to prevent the artificial generation of bradykinin after blood sampling. These inhibitors scarcely affect the mainly metalloprotease-mediated degradation of bradykinin; thus, the protocol takes advantage of the enzymatic degradation of kinins in plasma. Therefore, plasma was drawn into prespiked S-Monovettes® and aliquots of the plasma stored at 21 °C were analysed after 30 min, 1.5 h and 4.5 h. The following inhibitors were investigated and compared to plasma without inhibitor (each n=3): 4-(2-aminoethyl)benzolsulfonylfluoride (AEBSF), hexadimethrine bromide, aprotinin, nafamostat mesylate and leupeptin. Additionally, the final blank generation protocol was evaluated for six human sources, whose generated blanks were analysed in triplicate to ensure the depletion of endogenous peptides across multiple sources.

4.2.5.2. Determination of the calibration curve range in plasma

Prior to the validation, LLOQ and upper limit of quantification (ULOQ) for each analyte were assessed. To improve the LLOQ, various plasma sample volumes between 100 µL to 300 µL were concentrated after SPE by reconstitution in only 75 µL of the injection solvent. Quantification limits from 0.78 pg/mL up to 3,000 pg/mL using 13 calibrators were investigated for the predefinition of the calibrators and the quality control (QC) levels.

4.2.6. Validation of kinin quantitation in plasma

Kinins are potential biomarkers as their role has been described in diverse health and disease states (e.g. angioedema, sepsis). The context of use is to describe the KKS quantitatively in healthy versus diseased populations to record data on the alterations of the peptides and evaluate the potential of the kinins as biomarkers. Following the successful validation, the assay is intended to be applied within clinical studies regarding COVID-19. Validation was carried out according to an in-house validation plan that encompasses the bioanalytical guideline of the FDA [US Food and Drug Administration 2018]. Linearity, accuracy, precision, sensitivity, carry-over, recovery, dilution integrity, parallelism and stability were assessed. Additionally, absolute matrix effects and the CV of the internal standard normalised matrix factor were evaluated according to the bioanalytical guideline of the EMA [European Medicines Agency 2011].

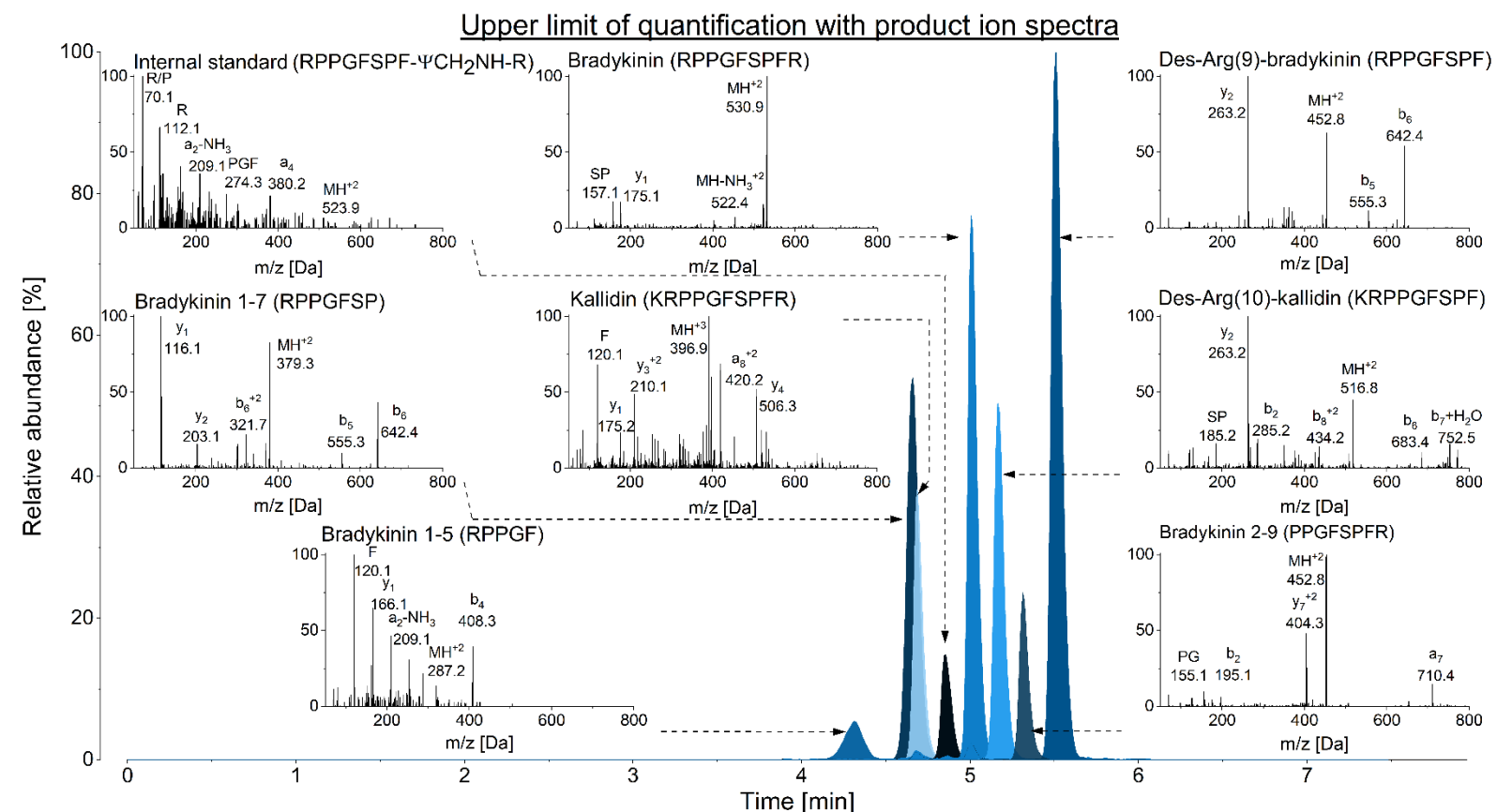
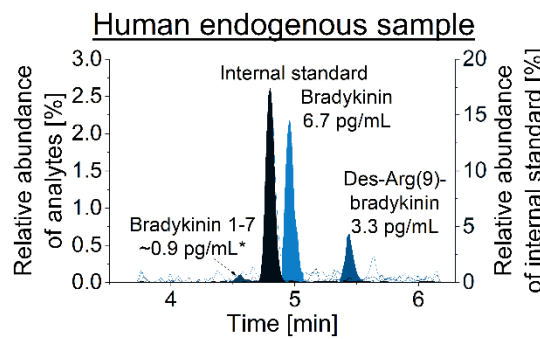
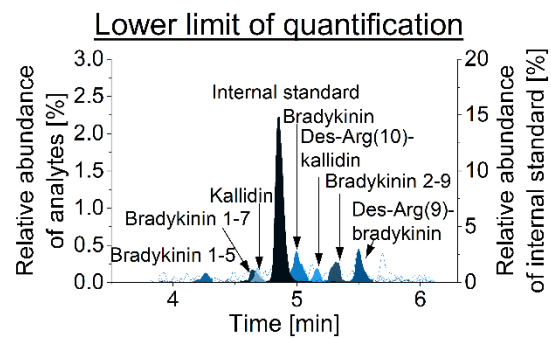
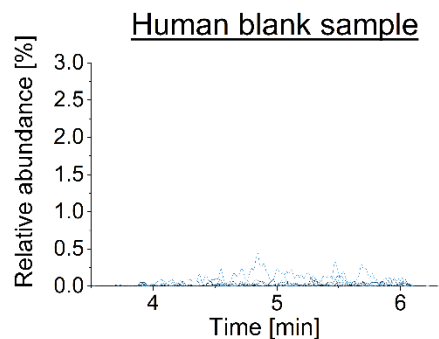


Figure 12. Example chromatograms of kinins in plasma. A blank, the lower and upper limit of quantification and one endogenous sample of a male volunteer are shown. In the presentation of the upper limit of quantification, the product ion scans of all analytes and the internal standard are additionally displayed with the main ion fragments. The corresponding amino acid code for each peptide is given in the top right of each scan. *extrapolated level below the quantification limit, IS: internal standard



Linearity of the method was determined by measuring the peak area ratio response (analyte area/internal standard area) for three calibration curves in a range from 2.0 pg/mL (LLOQ) to 1,000.0 pg/mL (ULOQ). The calibration curve ranges were analysed for each analyte separately. The deviation of the calculated concentration from the nominal concentration (RE) was not allowed to exceed $\pm 15\%$, with the exception of the LLOQ, for which deviations of $\pm 20\%$ were tolerated. A minimum of 6 calibration curve points and $\geq 75\%$ had to fulfil this criterion, and the RE was recalculated for all remaining calibration curve points if a value had to be excluded.

Accuracy and precision were established using five replicates from each QC level ($n=4$) in three independent runs on three distinct days. Therefore, a QC high (750.0 pg/mL), a QC mid (125.0 pg/mL) and several QC lows/LLOQs (31.1 pg/mL, 15.6 pg/mL, 7.8 pg/mL, 3.9 pg/mL and 2.0 pg/mL) were analysed. Different QC low/LLOQ levels were used, depending on the calibration curve range. Using one-way analysis of variance (ANOVA), intermediate precision (within-run) and the day-different precision (between-run) were calculated and had to be $\leq 15\%$ (CV) at the distinct QC levels, with the exception of the LLOQ, for which CVs of $\leq 20\%$ were permitted. Between-run accuracy was calculated as the mean RE of three runs. Accuracy was confirmed if the mean calculated concentrations from the nominal concentrations deviated by $\leq 15\%$ (RE) at the QC levels and $\leq 20\%$ at the LLOQ. Additionally, the analyte response had to exceed 5 at the LLOQ. The analyte response was determined by the signal-to-noise ratio calculated by the SignalFinder™ integration algorithm using Multiquant™ 3.0.2.

To check for possible carry-over, six ULOQ and six blank samples were consecutively injected. The response of the analytes in the blank samples was not allowed to exceed 20% of the response at the LLOQ and 5% of the response of the internal standard.

Recovery of the analytes was calculated by comparing the mean area response of plasma samples spiked before SPE to blank plasma samples spiked with the analytes after SPE. The following QC levels were assessed using this method: the QC high (750.0 pg/mL), the QC mid (125.0 pg/mL), and two QC lows (31.1 pg/mL and 7.8 pg/mL). The same QC levels were used for the calculation of the absolute matrix effect, which was determined by analysis of the mean area response of blank matrix spiked with analytes after SPE compared to the mean analyte response of a neat solution using the same analyte concentrations. Further, the CV of the internal standard normalised matrix factor was assessed using blank plasma samples from six healthy volunteers. The matrix factor was calculated for each source after comparing the mean area ratio of blank samples spiked with analytes after SPE to the mean area ratio of a neat solution of analytes at two QC levels (high [750.0 pg/mL] and low [31.1 pg/mL]). The CV was determined for all calculated internal standard normalised matrix factors and was restricted to $\leq 15\%$ to ensure that the internal standard corrects for individual-dependent matrix effects.

Further, dilution integrity was evaluated for a 1:10 dilution of a 6 ng/mL spiked plasma sample in a fivefold approach. A maximum deviation of 15% (CV and RE) was allowed. Additionally, parallelism was assessed by four serial dilutions of endogenous samples within the calibration range of the assay. As no samples of diseased patients were available, blood was sampled from three healthy volunteers without the addition of the protease inhibitor to allow for the artificial generation of bradykinin and its metabolites. The protease inhibitor was added after 30 minutes to plasma. Kallidin and des-Arg(10)-kallidin were spiked at a mid-concentration within the calibration range, as these peptides are not artificially generated after blood sampling. Stock samples and dilutions were analysed in triplicates and back-calculated values of the diluted values were compared to undiluted samples, whereby the CV had to be $\leq 15\%$.

Finally, stability was examined using three replicates of four QC levels (high [750.0 pg/mL], mid [125.0 pg/mL] and low [31.1 pg/mL and 7.8 pg/mL]). To assess benchtop stability, plasma samples were placed at room temperature for 1.5 h and 3 h before further processing and analysis. Freeze-thaw stability was determined after one, two and four cycles of complete thawing and refreezing of samples at -80°C . Further, long-term stability of the plasma samples was analysed after 1, 2 and 4 weeks. For all stability investigations, the maximum deviation of the calculated concentration to the nominal concentration compared to a freshly prepared calibration curve was $\leq 15\%$ (RE).

4.2.7. Applicability of kinin quantitation in plasma

Endogenous plasma levels of the kinin peptides were determined in three healthy volunteers (2 men, 1 woman). Lower kinin concentrations are expected in healthy volunteers than in patients with kinin-mediated diseases (e.g. angioedema), thus making this investigation serve as an especially stringent measure of the ability of the platform to detect low kinin levels. Blood was sampled under aspiration into EDTA-containing S-Monovettes® prespiked with and without the protease inhibitor. Blood sampling was conducted in the sitting position between 10:30 a.m. and 12:30 p.m. Repeated blood sampling on two distinct days was conducted in two volunteers. Additionally, plasma of healthy volunteers was sampled into BD™ P100 and P800 blood collection tubes (BD, Heidelberg, Germany) to facilitate comparison to previously published kinin levels. Subsequent to blood sampling, samples were centrifuged at $2000 \times g$ for 10 min at room temperature and plasma was transferred into low protein binding tubes before further processing.

4.3. Results

4.3.1. Method development for kinin quantitation in plasma

4.3.1.1. Blank plasma generation

AEBSF and aprotinin alone did not sufficiently prevent the artificial generation of bradykinin (Figure 13). Additionally, a high CV was observed for AEBSF, caused by one replicate exceeding the other bradykinin values by factor 10, indicating variable inhibition despite same storage and handling conditions of the replicates. Even after the exclusion of outliers, AEBSF performed inferior to nafamostat and hexadimethrine bromide. While nafamostat and leupeptin only decreased the formation of bradykinin at the 0.5 and 1.5 h timepoints, the lowest levels of bradykinin were detected with the use of hexadimethrine bromide. Nafamostat and hexadimethrine bromide seemed to be the most promising regarding reproducibility of a blank matrix, as lowest bradykinin levels and CV were observed. Both were applied in combination and their combined use was found to result in blank plasma after 4.5 h (Figure 13). Further storage at room temperature for 24 h confirmed that the plasma remained blank using this inhibitor combination. The consistency of the results was evaluated in six sources, and blank plasma was successfully generated for each source.

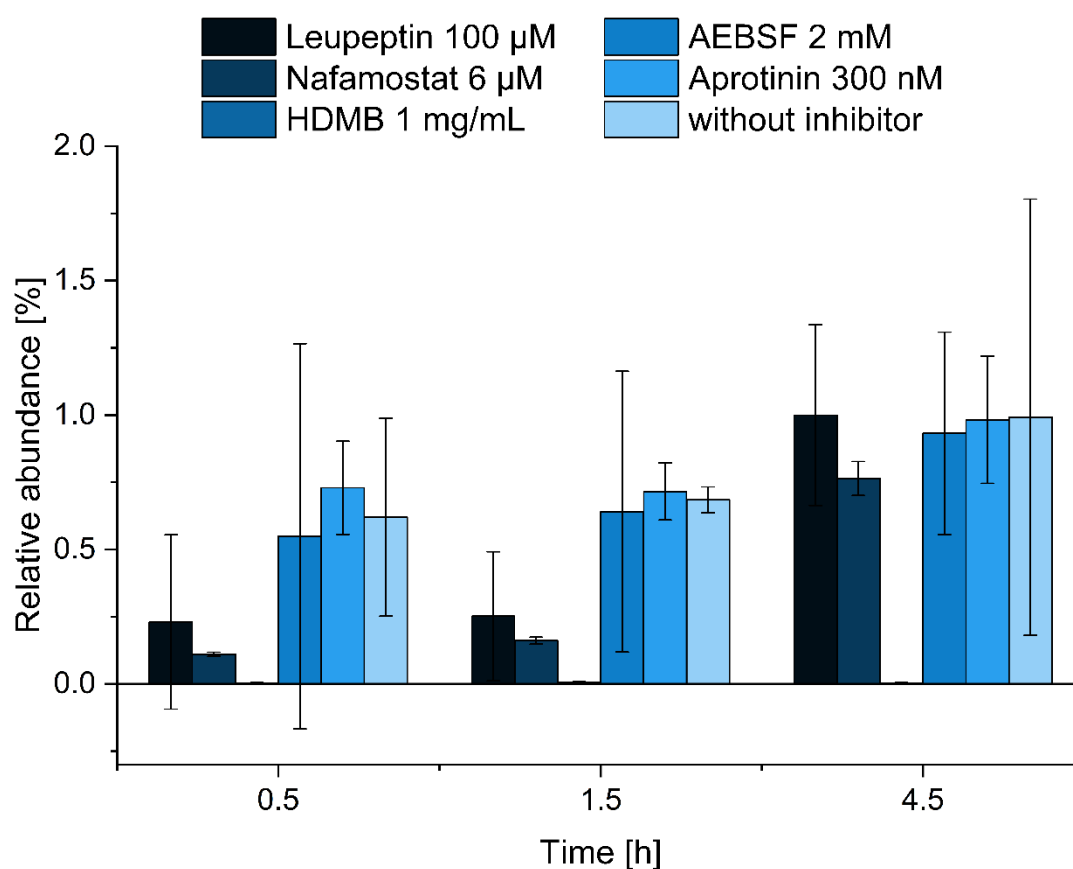


Figure 13. Evaluation of protease inhibitors for generation of blank plasma. All experiments were conducted in triplicates (mean \pm standard deviation). AEBSF: 4-(2-aminoethyl)benzolsulfonylfluorid, HDMB: hexadimethrine bromide

4.3.1.2. Determination of the calibration curve range in plasma

By increasing the plasma sample volume loaded on the SPE cavity from 100 μL to 150 μL , an improvement by the same factor was observed for the LLOQ. Further increasing the sample volume to 300 μL resulted in an equal intensity of bradykinin 1-5, which may have been affected by ion suppression due to increased matrix presence. A calibration curve applying 150 μL of plasma resulted in linear ranges between an LLOQ of 1.3–5.0 pg/mL (depending on the kinin) and an ULOQ of 3,000 pg/mL (for all kinins). Repetition of this range and evaluation of precision and accuracy revealed that power or Wagner regression was necessary to include all calibrator levels in a valid run. In addition to matrix effects, non-linearity can result from SPE column overloading and detector saturation due to co-eluting matrix compounds. Hence, to enable more common regression methods, the calibration curve range was reduced to 10 calibrator levels ranging from 2.0 to 1,000 pg/mL.

4.3.2. Validation of kinin quantitation in plasma

4.3.2.1. Linearity

All analytes showed good linearities (mean $r \geq 0.998$, $n=3$) through the studied concentration range. Best fits were achieved using $1/x^2$ weighting and quadratic regression. The four analytes bradykinin, des-Arg(10)-kallidin, des-Arg(9)-bradykinin and bradykinin 1-7 were linear within a range of 2.0 to 1000.0 pg/mL (10-point calibration line). For the other analytes, the same ULOQs were used, but higher LLOQs were set as follows: bradykinin 1-5: 15.6 pg/mL (7 points), bradykinin 2-9: 7.8 pg/mL (8 points) and kallidin: 3.9 pg/mL (9 points). In molar units, these LLOQs were 1.9 pM for bradykinin, 2.2 pM for des-Arg(9)-bradykinin, 2.6 pM for bradykinin 1-7, 27.2 pM for bradykinin 1-5, 3.4 pM for kallidin, 8.6 pM for bradykinin 2-9 and 1.9 pM for des-Arg(10)-kallidin. Example chromatograms of the LLOQ and ULOQ are presented in Figure 12.

4.3.2.2. Accuracy, precision and sensitivity

All RE values were $\leq \pm 14.6\%$ at all QC levels except for the LLOQ, at which the values were $\leq \pm 17.1\%$, thus fulfilling the guideline criteria of the FDA of $\leq \pm 15\%$ (RE) at the QC levels and $\leq \pm 20\%$ (RE) at the LLOQ, respectively [US Food and Drug Administration 2018]. Between-run accuracy at the QC high (750.0 pg/mL) and mid (125.0 pg/mL) levels was between -3.5% and 1.8% (RE). Between-run variation, used to measure precision, was below 6.9% (CV) at these levels. All precision results for the QC low (7.5–14.7% (CV)) and the LLOQ (10.9–19.8% (CV)) similarly complied with the regulatory guideline of the FDA ($\leq 15\%$ at the QC levels and $\leq 20\%$ at the LLOQ) [US Food and Drug Administration 2018]. Detailed results for within- and between-run accuracy as well as precision are displayed in Table 3. The signal-to-noise ratios at the respective LLOQs were 89:1 for bradykinin 1-5, 144:1 for bradykinin 1-7, 134:1 for

kallidin, 214:1 for bradykinin, 93:1 for des-Arg(10)-kallidin, 67:1 for bradykinin 2-9 and 333:1 for des-Arg(9)-bradykinin.

4.3.2.3. Carry-over

The carry-over in a blank following an ULOQ sample was below 20% for all analytes: 0.0% for bradykinin 1-5, 5.4% for kallidin, 3.2% for bradykinin 1-7, 5.4% for bradykinin, 1.7% for des-Arg(10)-kallidin, 5.1% for bradykinin 2-9 and 10.8% for des-Arg(9)-bradykinin. For the internal standard, no carry-over was observed.

Table 3. Accuracy and precision results for kinins in plasma.

Analyte	Nominal concentration [pg/mL]	Accuracy				Precision		
		Day 1 RE [%]	Day 2 RE [%]	Day 3 RE [%]	Between-run RE [%]	Within-run CV [%]	Between-run CV [%]	
Kallidin	QC high	750.0	1.1	-1.5	-2.1	-0.8	3.1	3.2
	QC mid	125.0	-0.9	-4.6	-1.6	-2.4	3.3	3.6
	QC low	7.8	-8.0	-8.5	-11.1	-9.2	8.9	8.9
	LLOQ	3.9	-14.6	-9.0	-12.7	-12.1	10.9	10.9
Bradykinin	QC high	750.0	1.9	-1.5	-1.9	-0.5	3.4	3.7
	QC mid	125.0	-7.0	-0.2	-3.1	-3.4	2.0	3.9
	QC low	3.9	13.2	2.4	-5.4	3.4	10.5	13.0
	LLOQ	2.0	8.0	-4.4	-9.0	-1.8	15.2	16.3
Des-Arg(10)-kallidin	QC high	750.0	2.2	1.9	1.4	1.8	3.0	3.0
	QC mid	125.0	-5.7	0.8	2.8	-0.7	2.7	5.1
	QC low	3.9	2.7	-11.6	9.7	0.3	11.2	14.7
	LLOQ	2.0	5.4	-5.7	3.8	1.2	18.4	18.4
Des-Arg(9)-bradykinin	QC high	750.0	2.7	-4.5	-0.5	-0.8	2.5	4.3
	QC mid	125.0	3.2	-5.6	5.5	1.1	2.4	6.2
	QC low	3.9	1.6	14.5	-5.9	3.4	7.7	12.1
	LLOQ	2.0	-1.6	11.9	-17.1	-2.3	14.7	19.8
Bradykinin 2-9	QC high	750.0	4.7	-0.3	-0.2	1.4	2.3	3.5
	QC mid	125.0	2.4	-4.3	6.5	1.5	4.8	6.9
	QC low	15.6	13.8	-0.2	9.9	7.8	9.8	11.0
	LLOQ	7.8	13.5	-3.9	-4.2	1.8	15.4	17.0
Bradykinin 1-7	QC high	750.0	1.1	1.9	-1.9	0.4	2.3	2.8
	QC mid	125.0	-1.6	-1.6	0.2	-1.0	3.0	3.0
	QC low	3.9	-4.5	-2.7	-6.5	-4.6	7.5	7.5
	LLOQ	1.9	-4.5	-3.5	-16.9	-8.3	13.6	14.6
Bradykinin 1-5	QC high	750.0	-2.9	-1.0	-5.2	-3.0	2.7	3.2
	QC mid	125.0	0.1	-4.4	-0.4	-1.6	5.3	5.4
	QC low	31.1	9.5	-5.7	-4.6	-0.2	12.3	13.9
	LLOQ	15.6	-6.8	1.9	-8.6	-4.5	11.9	12.2

CV: coefficient of variation, LLOQ: lower limit of quantification, QC: quality control, RE: relative error

4.3.2.4. Recovery and matrix effects

The mean recovery at all distinct QC levels investigated (n=4 levels, n=3 replicates) was above 90% for the four rather lipophilic peptides bradykinin (91.1%), des-Arg(10)-kallidin (95.5%), bradykinin 2-9 (92.0%) and des-Arg(9)-bradykinin (97.2%). Mean recovery was 69.5% for bradykinin 1-5, 88.2% for kallidin and 78.7% for bradykinin 1-7 (Table 4). Lower recoveries

were observed for the more hydrophilic peptides (bradykinin 1-5, bradykinin 1-7, kallidin) with fewer basic functional groups (bradykinin 1-7, bradykinin 1-5), presumably because of less reversed phase retention and ion exchange with the acidic carboxyl groups of the WCX SPE material. The mean absolute matrix effect for all distinct QC levels (n=4 levels, n=3 replicates) was -54.0% for bradykinin 1-5, -26.6% for kallidin, -27.3% for bradykinin 1-7, -13.8% for bradykinin, -17.3% for des-Arg(10)-kallidin, -27.3% for bradykinin 2-9 and -16.1% for des-Arg(9)-bradykinin (Table 4).

Table 4. Absolute matrix effect, coefficient of variation of internal standard normalized matrix factor and recovery for all kinin peptides in plasma.

Analyte	Absolute matrix effect			
	QC high (750.0 pg/mL)	QC mid (125.0 pg/mL)	QC low (31.1 pg/mL)	QC low (7.8 pg/mL)
Bradykinin 1-5	-54.3%	-54.9%	-52.9%	-
Kallidin	-25.5%	-27.6%	-27.5%	-25.6%
Bradykinin 1-7	-27.1%	-30.7%	-29.5%	-22.0%
Bradykinin	-19.0%	-11.4%	-13.4%	-11.2%
Des-Arg(10)-kallidin	-20.7%	-16.9%	-14.2%	-17.3%
Bradykinin 2-9	-31.3%	-24.8%	-25.7%	-
Des-Arg(9)-bradykinin	-26.3%	-28.0%	-27.3%	-16.1%

Analyte	Internal standard normalized matrix factor (CV [%], n=6)	
	QC high (750.0 pg/mL)	QC low (31.1 pg/mL)
Bradykinin 1-5	11.2%	10.3%
Kallidin	1.9%	3.6%
Bradykinin 1-7	0.8%	3.5%
Bradykinin	2.1%	4.8%
Des-Arg(10)-kallidin	2.0%	2.5%
Bradykinin 2-9	1.5%	6.6%
Des-Arg(9)-bradykinin	1.0%	2.7%

Analyte	Recovery			
	QC high (750.0 pg/mL)	QC mid (125.0 pg/mL)	QC low (31.1 pg/mL)	QC low (7.8 pg/mL)
Bradykinin 1-5	73.3%	60.9%	74.3%	-
Kallidin	90.8%	87.0%	79.4%	95.7%
Bradykinin 1-7	80.2%	74.6%	82.0%	78.0%
Bradykinin	93.2%	87.9%	91.0%	92.1%
Des-Arg(10)-kallidin	93.8%	91.7%	91.4%	105.2%
Bradykinin 2-9	95.5%	88.3%	92.4%	-
Des-Arg(9)-bradykinin	97.7%	98.8%	93.9%	98.5%

CV: coefficient of variation, QC: quality control

The CV of the internal standard normalised matrix factor was below 15% at the investigated QC levels using plasma from six volunteers and thus confirmed no inter-source variability (Table 4). At the QC high level (750.0 pg/mL), the CV of the internal standard normalised matrix factors was 2.1% for bradykinin, 1.9% for kallidin, 1.0% for des-Arg(9)-bradykinin, 2.0% for des-Arg(10)-kallidin, 0.8% for bradykinin 1-7, 1.5% for bradykinin 2-9 and 11.2% for bradykinin 1-5. At the QC low level (31.1 pg/mL), the CV was 4.8% for bradykinin, 3.6% for kallidin, 2.7% for des-Arg(9)-bradykinin, 2.5% for des-Arg(10)-kallidin, 3.5% for bradykinin 1-7, 6.6% for bradykinin 2-9 and 10.3% for bradykinin 1-5. Haemolyzed and lipemic samples were not assessed as part of specificity investigations.

4.3.2.5. Dilution integrity and parallelism

Dilution integrity was confirmed for a 1:10 dilution of a 6 ng/mL plasma sample. Accuracy (RE) and precision (CV) were as follows for the kinin peptides: -13.0% (RE)/4.9% (CV) for bradykinin 1-5, -2.2%/0.2% for kallidin, -5.5%/2.5% for bradykinin 1-7, -1.7%/2.5% for bradykinin, -2.0%/2.0% for des-Arg(10)-kallidin, -10.1%/3.2% for bradykinin 2-9 and -4.7%/2.7% for des-Arg(9)-bradykinin.

Endogenously generated plasma levels for the assessment of parallelism varied interindividually for each kinin throughout the whole calibration curve range. The CV of the back-calculated concentrations of the dilutions was between 1.7% and 12.8% for all kinins and the three sources and therefore guideline-compliant. Depending on the observed low concentrations in undiluted samples, levels could not be determined for all dilution steps. Details are provided in Table 5.

Table 5. Parallelism of the kinins in plasma. Values of endogenous/spiked plasma samples as stock concentration and back-calculated values of diluted samples are given.

Analyte		Source 1	Source 2	Source 3
Kallidin	Undiluted concentration	161.9 pg/mL	139.1 pg/mL	155.6 pg/mL
	Dilution factor	Back-calculated concentration [pg/mL]		
	2	162.2	129.5	164.9
	4	157.0	134.2	163.5
	8	157.5	157.7	171.1
	16	137.9	174.9	151.9
	CV [%]	6.5	12.8	3.9
Bradykinin	Undiluted concentration	733.7 pg/mL	63.9 pg/mL	294.7 pg/mL
	Dilution factor	Back-calculated concentration [pg/mL]		
	2	712.9	59.7	305.5
	4	697.9	72.2	315.3
	8	691.0	75.0	325.8
	16	700.9	85.9	323.8
	CV [%]	2.4	14.3	4.0

Analyte		Source 1	Source 2	Source 3
Des-Arg(10)-kallidin	Undiluted concentration	230.4 pg/mL	214.9 pg/mL	208.4 pg/mL
	Dilution factor	Back-calculated concentration [pg/mL]		
	2	229.1	199.6	229.6
	4	228.1	201.8	212.1
	8	225.8	238.7	222.9
	16	220.5	204.3	236.6
	CV [%]	1.7	7.6	6.1
Des-Arg(9)-bradykinin	Undiluted concentration	812.2 pg/mL	39.5 pg/mL	138.2 pg/mL
	Dilution factor	Back-calculated concentration [pg/mL]		
	2	852.1	39.5	137.6
	4	829.7	44.5	138.3
	8	849.9	47.8	130.6
	16	892.5	< LLOQ	118.7
	CV [%]	3.5	9.5	7.3
Bradykinin2-9	Undiluted concentration	114.9 pg/mL	9.4 pg/mL	66.7 pg/mL
	Dilution factor	Back-calculated concentration [pg/mL]		
	2	103.4	< LLOQ	58.0
	4	130.4	< LLOQ	71.2
	8	119.1	< LLOQ	53.3
	16	104.8	< LLOQ	< LLOQ
	CV [%]	9.7	n.a.	10.8
Bradykinin 1-7	Undiluted concentration	196.9 pg/mL	7.3 pg/mL	69.6 pg/mL
	Dilution factor	Back-calculated concentration [pg/mL]		
	2	190.0	3.8	72.2
	4	185.3	2.0	67.6
	8	177.8	< LLOQ	69.9
	16	176.1	< LLOQ	74.8
	CV [%]	4.6	4.8	4.4
Bradykinin 1-5	Undiluted concentration	28.8 pg/mL	< LLOQ	25.4 pg/mL
	Dilution factor	Back-calculated concentration [pg/mL]		
	2	34.1	< LLOQ	< LLOQ
	4	< LLOQ	< LLOQ	< LLOQ
	8	< LLOQ	< LLOQ	< LLOQ
	16	< LLOQ	< LLOQ	< LLOQ
	CV [%]	12.0	n.a.	n.a.

CV: coefficient of variation, LLOQ: lower limit of quantification, n.a.: not available

4.3.2.6. Stability

All analytes were stable for 1.5 h on the benchtop. After 3 h, low concentrations of bradykinin and bradykinin 1-7 and high and mid concentrations of des-Arg(9)-bradykinin were outside the set limit of $\leq \pm 15\%$. Freeze-thaw stability was confirmed for one and two freeze-thaw cycles for every kinin peptide. In contrast to the other analytes, which were also stable for four freeze-thaw cycles, bradykinin 1-7 and bradykinin 1-5 trended towards a decrease. Long-term stability at -80°C was confirmed for a period of four weeks for all peptides (maximum period of investigation). Detailed results are provided in Table 6.

Table 6. Results of the kinin stability assessments in plasma.

Analyte	Nominal concentration [pg/mL]		Benchtop stability		Freeze-Thaw Stability			Long-term stability
			1.5 h at 21 °C RE [%]	3 h at 21 °C RE [%]	1 cycle RE [%]	2 cycles RE [%]	4 cycles RE [%]	4 weeks RE [%]
Kallidin	QC high	750.0	-3.3	-9.6	1.1	-7.2	-10.3	-6.7
	QC mid	125.0	-1.7	-10.8	-9.5	-2.1	-2.7	8.6
	QC low	31.1	-4.4	-0.7*	-4.4	1.4	-5.3	6.6
	QC low	7.8	0.0	-0.8	12.4	-14.9	-6.5	14.9
Bradykinin	QC high	750.0	-1.4	-7.4	0.4	-7.8	-8.3	-3.0
	QC mid	125.0	-1.2	1.2	-3.2	-6.2	-10.8	5.9
	QC low	31.1	1.4	8.4*	-1.5	-6.2	-9.8	10.0
	QC low	7.8	4.9	138.0	-1.5	1.6	-7.3	4.5
Des-Arg(10)-kallidin	QC high	750.0	-0.9	-11.2	6.1	-8.4	-7.9	-2.1
	QC mid	125.0	6.9	-2.4	-0.8	-7.7	-7.7	0.9
	QC low	31.1	13.1	-7.9*	-1.2	0.4	-8.6	13.8
	QC low	7.8	9.7	9.4	-11.8	0.8	3.5	10.6
Des-Arg(9)-bradykinin	QC high	750.0	-4.6	-21.8	-0.3	-8.4	-7.9	0.5
	QC mid	125.0	1.1	-16.1	2.1	-7.7	-7.7	3.3
	QC low	31.1	3.4	-5.2*	5.4	0.4	-8.6	12.3
	QC low	7.8	-10.2	11.8	-11.7	0.8	3.5	8.2
Bradykinin 2-9	QC high	750.0	-3.3	-9.1	-1.1	-7.2	-10.6	-0.6
	QC mid	125.0	-2.4	-8.0	-0.5	-12.2	-11.7	1.7
	QC low	31.1	4.7	3.8*	11.8	-4.7	-0.5	9.0
Bradykinin 1-7	QC high	750.0	1.7	2.1	2.0	-6.6	-7.0	-2.6
	QC mid	125.0	9.0	3.6	-1.3	-2.6	-6.1	6.0
	QC low	31.1	3.1	10.7*	4.0	-6.3	-15.3	7.5
	QC low	7.8	11.8	16.0	-7.3	0.3	-12.3	13.6
Bradykinin 1-5	QC high	750.0	-0.6	-7.6	4.0	-8.0	-20.3	-11.0
	QC mid	125.0	-1.1	-2.6	-8.3	-5.8	-14.1	11.3
	QC low	31.1	-8.7	-5.3*	-5.4	-2.8	-30.6	13.9

* n=1, QC: quality control, RE: relative error

4.3.3. Applicability of kinin quantitation in plasma

Endogenous plasma levels of three healthy volunteers ranged between 2.3 pg/mL and 6.8 pg/mL (median 4.7 pg/mL) for bradykinin. Des-Arg(9)-bradykinin was detected in one male source at a concentration of 3.2 pg/mL, whereas the other sources showed levels below the LLOQ (2 pg/mL). Similarly, des-Arg(10)-kallidin was quantified in one female source, at a concentration of 3.2 pg/mL. Bradykinin 1-7, bradykinin 2-9, bradykinin 1-5 and kallidin were below the quantification limit. An example chromatogram is shown in Figure 12. The reproducibility of measured kinin levels was confirmed on two distinct days in two human sources (median 5.8 pg/mL bradykinin). The ready-to-use BD™ P100 and P800 tubes also reduced the artificial generation/degradation of bradykinin. However, the inhibitory power was less than the one of prespiked Monovettes® and subsequently, the generation was less controlled being reflected by higher levels of detected bradykinin levels (median 74.4 pg/mL using P100 and 157.5 pg/mL using P800) (Figure 14). In contrast, substantially higher levels of bradykinin and its metabolites were observed using collection devices without any inhibitor (Figure 14). Increases of determined levels of factor 62 up to 800 were observed. The experiments using non-inhibited samples were conducted as fast as possible **at room temperature**, whereby the time period from blood collection, transport, 10 minutes centrifugation until loading of plasma on the SPE at the bench took about 20 minutes.

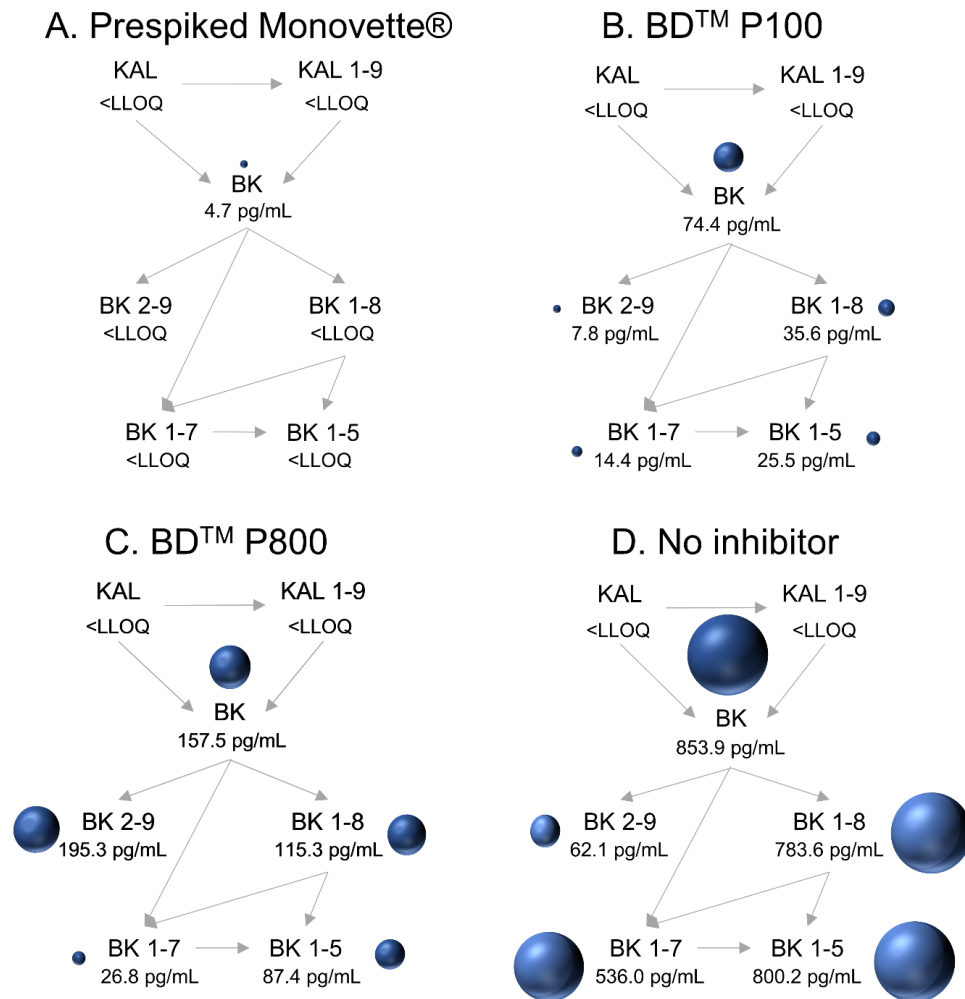


Figure 14. Comparison of distinct protease inhibitor approaches for kinins in plasma. Kinin levels were determined in prespiked Monovettes® (A), in BD™ P100 tubes (B), in BD™ P800 tubes (C) and without the use of inhibitors (D). Measured endogenous median levels of kinin peptides (n=3) are displayed. The bullet size reflects the amount of kinin peptides measured. BK: bradykinin, KAL: kallidin

4.4. Discussion

A sensitive and targeted LC-MS/MS platform for the comprehensive determination of the active kinins with their major metabolites was successfully validated according to the regulatory bioanalytical guideline of the FDA [US Food and Drug Administration 2018]. A broad calibration curve range covering expected concentrations of kinins in disease, with LLOQs in the low pg/mL range, was established. No source-dependent matrix effects were identified, and suitable stability of the analytes in plasma was observed.

The validated kinin peptide platform represents a novel tool that enables the determination of kinins in plasma with clearly improved sensitivity and with a comprehensiveness that has not been previously published. While low detection limits (0.4–11.7 pg/mL) have been claimed for immunoassays [Hilgenfeldt et al. 1995; Duncan et al. 2000; Enzo Life Sciences, Inc.], these lack specificity due to cross-reactions owing to structural similarities (Figure 1). This leads to the requirement for extensive sample clean-up, including chromatographic separation and multiple SPEs, prior to quantification by immunoassay [Duncan et al. 2000; Campbell et al. 1993]. However, to date, reported quantification limits for bradykinin by LC-MS/MS are quite high – namely, between 94 pg/mL [Lindström et al. 2019] up to 10 ng/mL in plasma or serum [van den Broek et al. 2010; van Winden et al. 2010; Lame et al. 2016]. The presented assay shows a far more sensitive quantification limit of 2 pg/mL for bradykinin. Preceding investigations using a design of experiments approach identified non-specific peptide adsorption and the usefulness of modifiers (3.2% DMSO and 0.1% FA) in the mobile phase as highly impacting factors concerning the assay's sensitivity (section 3 [Gangnus & Burckhardt 2020]). Despite the distinct physicochemical properties of the peptides, an adjustment within the design space allowed for the identification of an injection solvent (10/10/80 FA/methanol/water [v/v/v]) reducing non-specific adsorption for all kinins (section 6 [Gangnus & Burckhardt 2021a]). For example, quantification limits of 2 ng/mL were achieved for des-Arg(9)-bradykinin by van den Broek et al. in 2010 [van den Broek et al. 2010]; thus, the presented assay marks an improvement by a factor of 1000. Further, current LC-MS/MS assays or immunoassays require at least 500 µL of plasma/1 mL of blood to establish these (low) quantification limits, whereas the presented assay requires only 150 µL of plasma [Lindström et al. 2019; van den Broek et al. 2010; van Winden et al. 2010; Duncan et al. 2000; Campbell et al. 1993]. This reduction enables repeated blood sampling in severely ill patients without increasing the risk of anaemia. Additionally, to the best of our knowledge, validated LC-MS/MS assays are not yet on hand for bradykinin 1-7, bradykinin 2-9, kallidin and des-Arg(10)-kallidin in plasma. Thus, with this study, the sensitive, comprehensive and simultaneous determination of all active kinin peptides with their major metabolites is facilitated for the first time in plasma.

An ideal surrogate matrix should closely resemble the study samples and be analyte-free [Wakamatsu et al. 2018]. Previous LC-MS/MS assays for bradykinin used water [Lindström et al. 2019] or bovine plasma as a surrogate matrix due to the endogenous presence of kinins in human matrix [van den Broek et al. 2010]. However, different compositions of a surrogate matrix in comparison to study samples might lead to matrix effects affecting the accuracy of the results [Wakamatsu et al. 2018]. Therefore, a better approach is provided by the use of standard addition for bradykinin [Lame et al. 2016]. However, the principle of standard addition becomes labour-intensive if multiple samples are to be analysed, and it requires a large volume of the patient sample due to the preparation of calibration curves for each study sample. A special feature of the established platform is the use of human blank plasma for calibration curves and QC samples. The use of blood from a volunteer with endogenous levels of bradykinin 1-5 below the detection limit as blank matrix [Seip et al. 2014], resembles the approach used within this study. However, in this study, blank plasma was actively generated and depletion of kinins by the applied procedure was successfully confirmed in six volunteers. This enables cost-effective blank generation regardless of the availability of a particular source.

All analytes were stable for 1.5 h on the benchtop, for four weeks at -80°C (indicating long-term stability) and for at least two freeze-thaw cycles at the distinct QC levels. This confirms the suitability of the preanalytical conditions and the prevention of artificial generation or degradation of peptides throughout distinct concentration ranges. Stability experiments for kinin peptides in plasma are rare. Lindström et al. reported long-term stability of a 106 ng/mL sample for one year, but freeze-thaw stability was not observed, as indicated by a 19% decrease of the nominal concentration after one freeze-thaw cycle and a 45% decrease after a second cycle (FDA limit: $\leq\pm 15\%$) [Lindström et al. 2019; US Food and Drug Administration 2018]. Van den Broek et al. 2010 found bradykinin (114 ng/mL) and des-Arg(9)-bradykinin (8 ng/mL) to be stable for one hour on ice, for five months at -80°C and for three freeze-thaw cycles [van den Broek et al. 2010]. Lower concentrations, as assessed in this study, have not yet been investigated. However, at these concentrations, instability due to insufficient inhibition of degrading enzymes becomes obvious. For example, generation of bradykinin has been observed after 3 h on the benchtop at the lowest QC level, whereas at higher concentrations, it was not identifiable. Insufficient suppression of artificial generation due to instability of the protease inhibitor at room temperature may be causative. These results reveal that stability investigations covering the entire calibration curve range are essential.

The endogenous kinin concentrations measured (in the low pg/mL range) were in the range of levels determined by immunometric detection. Campbell et al. 1993 reported levels of 2.0 pg/mL for bradykinin, <0.8 pg/mL for des-Arg(9)-bradykinin ($<$ LLOQ), and <1 pg/mL for bradykinin 1-7 ($<$ LLOQ) in healthy volunteers ($n=12$) [Campbell et al. 1993]. Duncan et al. 2000 reported levels of <0.4 pg/mL for bradykinin ($<$ LLOQ), 0.6 pg/mL for des-Arg(9)-bradykinin,

1.8 pg/mL for bradykinin 1-7, and < 0.5 pg/mL for kallidin and des-Arg(10)-kallidin (< LLOQ) (n=8-11) [Duncan et al. 2000]. In contrast, much higher values were determined by Lindström et al., who reported plasma bradykinin levels between 530 and 1,166 pg/mL by LC-MS/MS [Lindström et al. 2019]. In addition, van den Broek et al. reported concentrations of 57 – 162 ng/mL of bradykinin and 50 – 151 ng/mL of des-Arg(9)-bradykinin in serum from healthy controls in [van den Broek et al. 2010]. Lame et al. 2013 and 2016, compared distinct commercially available inhibitors and found reduced plasma levels of 90.0 pg/mL [Lame 2013] and 186.0 pg/mL [Lame et al. 2016] of bradykinin using BD™ P100 tubes as compared to the use of no inhibitors (810.7 pg/mL [Lame et al. 2016]). Levels in BD™ P800 plasma could not be determined owing to degradation of the internal standard (des-Arg(10)-kallidin) in these samples [Lame et al. 2016]. Similarly, in this study median levels of 74.4 pg/mL of bradykinin using BD™ P100 tubes were observed, which were substantially lower compared to the use of no inhibitor, where levels of 853.9 pg/mL were determined. However, elevated levels of bradykinin and its metabolites in comparison to the prespiked Monovettes® indicate incomplete inhibition of kinin metabolism by the protease inhibitor in BD™ P100/P800 tubes. Insufficient prevention of factor XII-mediated artificial bradykinin generation might be causative for the observed varying kinin levels; especially if no protease inhibitor was added. This makes careful stability assessments, as discussed above, essential for reliable quantification results.

While concentrations of kinins are low in healthy individuals, in patients with kinin-mediated diseases, they are expected to be increased; thus, the established platform is capable of quantifying clinically relevant concentrations. The developed platform is especially useful for extending the knowledge about diseases in which the KKS in plasma plays a substantial role in their pathophysiology. This includes, for example, sepsis and angioedema, in which activation of the KKS is assumed to be causative for vasodilation, inflammation and oedema formation [Nicola 2017; Cugno et al. 2003]. Despite strong evidence in animal models for a link between coagulopathy, the KKS and septic shock, evidence in humans is limited and needs further investigation [Nicola 2017]. In severe COVID-19, elevated D-dimers, in conjunction with a strong decrease in platelet count, indicate an increased activation of the coagulation system [Zhou et al. 2020; Lippi et al. 2020b]. Due to the strong correlation of the KKS to the intrinsic coagulation system via the activation of plasma kallikrein by factor XII, subsequently elevated active kinin levels might explain symptoms like inflammation, cough, diarrhoea, anosmia and capillary leakage [Nicolau et al. 2020; Kinsey & Machin 1989]. Additionally, alternative bradykinin-forming pathways might develop, and des-Arg(9)-bradykinin degradation by ACE2 might be impaired [Nicolau et al. 2020; Roche & Roche 2020]. RNA sequence analysis has shown that plasma kallikrein and bradykinin precursors are expressed at increased levels and that degrading enzymes (e.g. ACE) are substantially downregulated in patients with COVID-19 [Garvin et al. 2020]. The simultaneous analysis of bradykinin and kallidin in conjunction with

their metabolites is facilitated for the first time by the developed LC-MS/MS platform, making it possible to shed light on the consequences of the detected alterations at the RNA level on the active kinin peptides, as well as their potentially altered degradation. If exploratory investigations confirm the usefulness of kinins as biomarkers, further steps towards a full validation will be undertaken using patient samples (e.g. extensive investigation of matrix effects, selectivity, parallelism, stability, relative accuracy) [Piccoli et al. 2019; International Council for Harmonisation 2019].

4.5. Conclusion

A sensitive and targeted LC-MS/MS platform was established and validated according to bioanalytical guideline of the FDA for bradykinin 1-5, bradykinin 1-7, bradykinin 2-9, des-Arg(9)-bradykinin, kallidin, bradykinin and des-Arg(10)-kallidin. Quantification limits in the low pg/mL range in conjunction with a broad calibration curve range were established. The platform was successfully applied to determine endogenous levels of kinin peptides in plasma of healthy volunteers. It facilitates the simultaneous determination of the major kinins and allows the generation of a more complete picture of the KKS in diseases in which it plays a role, such as angioedema and COVID-19.

5. Tackling reliable determination of peptides of the kallikrein-kinin system in human plasma

5.1. Background

The KKS is an endogenous cascade of several bioactive kinin peptides that promote vasodilation, diuresis, inflammation, vascular permeability, and angiogenesis [Campbell 2013]. Kinins are considered potential biomarkers in disorders like COVID-19, cancer, sepsis, or angioedema; bradykinin receptors represent already approved or promising pharmacotherapeutic targets [Garvin et al. 2020; Kashuba et al. 2013; Nicola 2017]. However, bioanalysis of endogenous kinin levels is highly sensitive to artificial alterations hindering their reliable quantification and interpretation of study results. The KKS is closely intertwined with the intrinsic coagulation cascade by the factor XII-driven plasma contact system (Figure 1). Contact between blood and either pathophysiological (e.g. neutrophil extracellular traps (NET)) or artificial (e.g. glass) surfaces initiates autoactivation of factor XII [Hofman et al. 2016]. Activated factor XII triggers liberation of bradykinin from its precursor by augmenting plasma kallikrein activity, which in turn amplifies factor XII activation. This cascade induces a pathophysiological or artificial rise in bradykinin and its metabolites.

It is well known that preanalytical variables highly impact the sample quality and reliability of results with most errors occurring during the preanalytical phase with rates between 32–75% [Carraro & Plebani 2007; Bonini et al. 2002]. Bioanalytical assays related to the coagulation system or particularly peptide analysis are most prone to variations caused by inadequate specimen handling [Lawrence 2003; Debunne et al. 2020]. Insufficient control of contact activation during blood sampling and processing provides a potential source of error in kinin quantitation [Hofman et al. 2016]. Additionally, bradykinin and kallidin have short half-lives (<1 min) [Decarie, A. 1996]. Thus, inadequate blood sampling conditions and downstream processes alter kinin levels artificially, impeding reliable kinin quantification.

Published approaches vary regarding the used protease inhibitor and reporting on preanalytical variables is limited [Seip et al. 2014; Duncan et al. 2000; Nussberger et al. 1998; Lindström et al. 2019]. Consequently, communicated bradykinin levels disclosed large discrepancies in multiple orders of magnitude, ranging from low pg/mL to high ng/mL levels in healthy volunteers [Duncan et al. 2000; van den Broek et al. 2010; Wheelock et al. 2017; Pellacani et al. 1992; Nussberger et al. 1998]. This large variability, even in healthy individuals,

This work was published in peer-reviewed journals:

Gangnus T and Burckhardt BB (2021) Stabilization of short-lived peptides of the kallikrein-kinin system in human plasma to facilitate use as promising biomarkers. *Clinical chemistry* 67(9):1287-1289. <https://doi.org/10.1093/clinchem/hvab129>

Gangnus T and Burckhardt BB (2022) Reliable measurement of plasma kinin peptides: Importance of preanalytical variables. *Research and Practice in Thrombosis and Haemostasis* 6(1): e12646 <https://doi.org/10.1002/rth2.1246>

The author of this thesis was responsible for the concept, performance of experiments, data analysis, visualization, writing – draft and approval.

hinders clinical comparison and interpretation of levels among laboratories [Blais et al. 1997].

This work was published in peer-reviewed journals:

Gangnus T and Burckhardt BB (2021) Stabilization of short-lived peptides of the kallikrein-kinin system in human plasma to facilitate use as promising biomarkers. *Clinical chemistry* 67(9):1287-1289. <https://doi.org/10.1093/clinchem/hvab129>

Gangnus T and Burckhardt BB (2022) Reliable measurement of plasma kinin peptides: Importance of preanalytical variables. *Research and Practice in Thrombosis and Haemostasis* 6(1): e12646 <https://doi.org/10.1002/rth2.1246>

The author of this thesis was responsible for the concept, performance of experiments, data analysis, visualization, writing – draft and approval.

Some research groups have therefore focused on determining the more stable, inactive metabolite bradykinin 1-5 only, which has a prolonged half-life (~90 minutes) and is less prone to artificial changes [Murphey et al. 2001]. However, a comprehensive picture of alterations within the KKS for pathophysiological processes remains insufficient, with the recording of only single kinin levels despite the versatility of metabolic processes within the KKS (Figure 1).

Since differentiation between health and disease and comparability between studies are currently impeded by the lack of standardized preanalytical procedures, it was aimed to implement robust kinin quantitation in plasma by identifying key variables. Plasma levels of the kinins bradykinin, kallidin, des-Arg(9)-bradykinin, des-Arg(10)-kallidin, bradykinin 1-7, bradykinin 2-9, and bradykinin 1-5 were monitored with the goals of facilitating the control of contact activation, enabling *ex vivo* stabilization and developing a standardized protocol, thereby achieving accuracy and reliability of collected kinin levels.

5.2. Materials and Methods

5.2.1. Human samples

Blood samples were donated by healthy adult volunteers. The study was conducted in accordance with the Declaration of Helsinki and was approved by the Ethics Committee of the Medical Faculty at the Heinrich-Heine University (study number: 6112). All participants gave written informed consent prior to enrolment.

5.2.2. Investigations on extent and time-course of artificial kinin alterations

Initially, the extent of artificial kinin formation by contact activation in a routine blood collection without protease inhibition was assessed (n=4). Blood was collected freshly into EDTA S-Monovettes® (Sarstedt, Nümbrecht, Germany), was centrifuged within 15–20 min, and immediately analysed.

Additionally, *ex vivo* formation and degradation of bradykinin and its metabolites in freshly collected blood samples were monitored over time to investigate the latency of this process. At predefined time-points after blood sampling, customized protease inhibitor [Gangnus & Burckhardt 2021b] was added to whole blood aliquots to stop reactions (15, 30, 45, 60, 90, 120, 180, 240, 300 s, 10, 15 and 30 min). Subsequently, whole blood was centrifuged and plasma was immediately analysed.

5.2.3. Impact of protease inhibitors on *ex vivo* kinin stability

To investigate suitable protease inhibitors, blood was drawn freshly in inhibitor pre-spiked tubes as listed below. Subsequently, one aliquot of plasma was immediately analysed (reference value), while the other aliquot was stored on the benchtop (21°C) for a predefined time until further analysis. All experiments were conducted in triplicate.

5.2.3.1. Control of artificial bradykinin generation

To extend previous studies (section 4 [Gangnus & Burckhardt 2021c]), it was aimed to examine in greater detail the effective prevention of artificial bradykinin generation. Bradykinin, the first kinin released during contact activation mediated by the serine proteases factor XII and plasma kallikrein, was monitored in the presence of several serine protease inhibitors. Best inhibition of generation was assumed in samples with the lowest bradykinin levels; due to its short half-life ($t_{1/2}$ ~20 seconds [Decarie, A. 1996]) and lacking inhibition of main degrading enzymes, bradykinin should degrade rapidly. Blood was sampled into S-Monovettes® (Sarstedt, Nümbrecht, Germany) pre-spiked with one of the following inhibitors: 2 µg/mL aprotinin (Sigma-Aldrich, St. Louis, MO, USA), 1 mg/mL hexadimethrine bromide ([≥94%] Sigma-Aldrich, St. Louis, MO, USA), 3.5 µg/mL nafamostat mesylate ([≥98%] Sigma-Aldrich, St.

Louis, MO, USA), 43 µg/mL leupeptin hemisulfate ([>90%] Sigma-Aldrich, St. Louis, MO, USA), 200 µg/mL chicken-egg trypsin-inhibitor (Sigma-Aldrich, St. Louis, MO, USA), 17.4 µg/mL phenylmethanesulfonyl fluoride (PMSF, DRG Instruments GmbH, Marburg, Germany), and 479 µg/mL 4-(2-Aminoethyl)benzenesulfonyl fluoride (AEBSF [≥97.0%]; Sigma-Aldrich, St. Louis, MO, USA). Bradykinin levels were measured immediately (reference value), 1.5 hr and 4.5 hr after sampling to rate the inhibition of artificial generation. Then, additional concentrations and combinations of the best performing single inhibitors were evaluated. As a reference, uninhibited plasma was evaluated.

5.2.3.2. Control of kinin degradation

Subsequently, the inhibition of degradation of the seven kinins was examined. Kinin metabolism is mainly characterized by serine- and metalloprotease-catalysed degradation (Figure 15). Thus, the suitability of inhibitors described to hinder the corresponding proteases was investigated. Blood was sampled into EDTA S-Monovettes® pre-spiked with 3 mg/mL hexadimethrine bromide and 10.8 µg/mL nafamostat to prevent bradykinin generation. Kinins were spiked in a concentration of 1 ng/mL before blood sampling to monitor their degradation/formation.

Bradykinin:

Arg¹–Pro²–Pro³–Gly⁴–Phe⁵–Ser⁶–Pro⁷–Phe⁸–Arg⁹

Kallidin:

(Lys)⁰–Arg¹–Pro²–Pro³–Gly⁴–Phe⁵–Ser⁶–Pro⁷–Phe⁸–Arg⁹

Abbreviation	Full kininase name	Catalytic type	Cleavage site
ACE	Angiotensin-converting enzyme	Metallo	7-8, 5-6
ACE 2	Angiotensin-converting enzyme 2	Metallo	7-8
APP	Aminopeptidase P	Metallo	0-1, 1-2
CP	Carboxypeptidase	Metallo	8-9
DPP IV	Dipeptidylpeptidase IV	Serine	4-5
ECE	Endothelin-converting enzyme	Metallo	7-8
EP 24.15	Endopeptidase 24.15	Metallo	5-6
NEP	Nepriylsin	Metallo	7-8, 4-5
PEP	Prolylendopeptidase	Serine	7-8, 2-3, 3-4
PRCP	Prolylcarboxypeptidase	Serine	7-8

Figure 15. Kininases involved in the degradation of bradykinin and kallidin. These are shown with their catalytic type and cleavage site for kallidin/bradykinin in the Table [Campbell 2013; Vickers et al. 2002; Harbeck & Mentlein 1991; Barrett et al. 2004].

The following protease inhibitors were added (catalytic type in parentheses): 16–31 mg/mL EDTA disodium dihydrate (metallo; [≥99%] Carl Roth GmbH+Co.KG, Karlsruhe, Germany), 2.9–5.9 mg/mL tri-sodium citrate dihydrate (metallo; [>99.5%] Fisher Scientific, Loughborough,

UK), 0.1–1% FA (unspecific, Merck KGaA, Darmstadt, Germany), 1% ammonia (unspecific, VWR Chemicals, Radnor, PA, USA), 77 ng/mL enalaprilat dihydrate (ACE-specific [100%]; European Directorate for the Quality of Medicines & HealthCare, Strasbourg, France), 0.03% sodium hydroxide (unspecific, VWR Chemicals, Radnor, PA, USA), 0.9–9 mg/mL 1,10-phenanthroline (metallo [$\geq 99\%$]; Sigma-Aldrich, St. Louis, MO, USA), 4–409 ng/mL omapatrilat (ACE & neprilysin-specific [$\geq 98\%$]; Sigma-Aldrich, St. Louis, MO, USA), 515 $\mu\text{g/mL}$ chloroquine diphosphate (prolylcarboxypeptidase-specific [$\geq 98\%$]; Sigma-Aldrich, St. Louis, MO, USA), and 17.4–174 $\mu\text{g/mL}$ PMSF (serine). Plasma aliquots of each inhibitor combination were analysed after one and three hr ($n=3$). A difference of $\leq 15\%$ (RE) between the two time-points ($(\text{area analyte/area internal standard [3 hours]}) / (\text{area analyte/area internal standard [1 hour]}) - 1$) with a coefficient of variation (CV) $\leq 15\%$ was allowed to ensure stability over the time course in line with bioanalytical regulatory guidelines of the FDA [US Food and Drug Administration 2018].

5.2.3.3. Comparison to previous approaches

Next, previously published protease inhibitor approaches were evaluated: blood was directly sampled into ice-cold ethanol (1:3, precipitation; [$\geq 99.8\%$]; Sigma-Aldrich, St. Louis, MO, USA) or a mixture of 4 M guanidine thiocyanate (GTC [99%]; BLDpharm, Kaiserslautern, Germany) with 1% trifluoroacetic acid (TFA [1:5, chaotropic]; Applichem GmbH, Darmstadt, Germany), as well as commercially available protease inhibitor-coated BD™ P100 and P800 tubes (BD, Heidelberg, Germany). These approaches were compared to the customized protease inhibitor and to blood sampled without protease inhibitors. All tubes were spiked with 1 ng/mL of kinins to monitor degradation/formation, and plasma aliquots were analysed after 1 and 3 hr ($n=3$).

5.2.4. Effect of blood sampling and handling on kinin quantification

Owing to the contact activation-mediated artificial rises of kinin levels during storage, it was investigated whether blood sampling already had an impact on measured kinin levels. Blood was sampled into EDTA tubes pre-spiked with the customized protease inhibitor in the upright position. The tubing was pre-filled to avoid insufficient filling by air volume. Three tubes were drawn sequentially per setting and per volunteer to better assess the consistency of kinin levels, which might be compromised by contact activation. To compare blood collection systems, a distinct peripheral arm vein (left/right median cubital, cephalic, or basilic) was used to avoid impacts of venipuncture or time delays. An inter-experimental control was drawn in triplicate using 21G Safety Multifly® with 200 mm tubing (0.8x19 mm) (Sarstedt, Nümbrecht, Germany) and 1.2 mL S-Monovettes®.

5.2.4.1. Blood collection system

Seven different collection devices were examined: conventional straight 21G needles, 0.8x25.4 mm (S-Monovette® Safety needle, Sarstedt, Nümbrecht, Germany) and 0.8x32 mm (BD Eclipse™, BD, Heidelberg, Germany); butterfly winged 21G Safety Multifly® needles with 200 mm tubing (0.8x19 mm) and 80 mm tubing (0.8x19 mm, Sarstedt, Nümbrecht, Germany); 25G Safety Multifly® needles with 200 mm tubing (0.5x19 mm, Sarstedt, Nümbrecht, Germany); 18G Vasofix® Safety peripheral intravenous catheters (13x45 mm, B. Braun, Melsungen, Germany) and Micro-Needles 21G (0.8x19 mm, Sarstedt, Nümbrecht, Germany). Using the Micro-Needle, blood was sampled without the adapter/tubing by directly dripping the blood in the opened S-Monovette®.

5.2.4.2. Blood collection tube

Four distinct blood collection devices were assessed: EDTA S-Monovettes® (with three diameters: 1.2 mL (with mixing ball), 2.7 mL and 9 mL; Sarstedt, Nümbrecht, Germany) and EDTA Vacutainers® 2 mL (BD, Heidelberg, Germany). All were compared using 21G Safety Multifly® needles with 200 mm tubing (Sarstedt, Nümbrecht, Germany). Glass tubes were excluded due to increased factor XII autoactivation on negatively charged surfaces [Schmaier 2016] and non-specific adsorption of bradykinin (section 3 [Gangnus & Burckhardt 2020]).

5.2.4.3. Blood collection technique

First, the effects of time-delays were assessed, when the blood flow was stopped for a two minute rest in the butterfly tubing, and a five minute rest in the peripheral catheter. Second, blood collection via aspiration in comparison to the vacuum technique was evaluated. Third, the venipunctures were conducted in an antegrade and retrograde direction to analyse potential differences in shear forces. Fourth, the influence of a tourniquet application was examined. All approaches were investigated applying 21 G Safety Multifly® needles with 200 mm tubing into 1.2 mL S-Monovettes® under aspiration, except otherwise stated.

5.2.5. Effect of specimen handling on kinin quantification

5.2.5.1. Time until centrifugation

In clinical blood collection settings, blood can often not be processed and centrifuged immediately (e.g. non-availability of centrifuges on ward). During this dwell-time altered peptide metabolism might influence the reliability of results. In contrast to plasma, whole blood retains increased metabolic activities via additional proteolytic enzymes located on cells [O'Leary et al. 2013; Rutkowska-Zapała et al. 2015; Hendriks et al. 1991]; therefore, kinin stability might be compromised differently when compared with plasma. Sampled whole blood containing

customized protease inhibitor was centrifuged as soon as possible (30 min; reference), 75 min and 110 min after blood sampling and benchtop stability was analysed (n=3).

5.2.5.2. Centrifugation method

For each centrifugation protocol, spiked kinin peptides in a concentration of 150 pg/mL (n=3) were evaluated. Three different centrifugation methods were applied at 21°C. First, we used the laboratory's standard protocol of a single centrifugation at 2000 x g for 10 min; second, a single centrifugation at 2000 x g for 20 min; and third, a two-step centrifugation at 2000 x g for 10 min followed by 16.100 x g for 10 min. Additionally, we assessed temperature influence, whereby whole blood was sampled on ice and centrifuged at 2000 x g for 10 min at 4°C.

5.2.6. Validation and applicability of the standardized protocol

Based on identification of impactful preanalytical variables, a standardized protocol for kinin quantification was developed. To determine the reliability of the optimized preanalytical conditions, the repeatability of sampling was assessed. The following standardized protocol was applied: venous blood was collected in an antegrade fashion into three consecutive 1.2 mL EDTA S-Monovettes® pre-spiked with customized protease inhibitor using 21 G Safety Multifly® needles with 200 mm tubing (Sarstedt) under aspiration. Phlebotomy was conducted in the upright position between 11 am and 1 pm using a tourniquet. Samples were centrifuged at 2000 x g for 10 min at 21 °C. Kinin levels were determined in one female volunteer on five different days (inter-day variability). In addition, venous blood was collected from seven healthy volunteers (interindividual variability). A deviation of ± 2 pg/mL of the individual kinin levels from the mean value (n=3) for each volunteer/time-point was considered acceptable.

5.2.7. Liquid chromatography coupled to tandem mass spectrometry monitoring of kinins

Kinins were measured by a previously established in-house LC-MS/MS platform, which had been validated according to the bioanalytical guideline of the FDA [US Food and Drug Administration 2018] using the customized protease inhibitor (section 4, [Gangnus & Burckhardt 2021c]).

5.2.8. Quality control system

To prove the validity and collection of high-quality data, all measurements were handled within a quality control system. Based on established in-house bioanalytical quality control systems [Suessenbach et al. 2020] and regulatory guidelines [US Food and Drug Administration 2018], this included that validation and applicability runs were processed with calibration standards and quality control samples. A system suitability test was performed prior to each analysis to ensure accurate and reproducible LC-MS/MS performance. Additionally, an inter-experimental

control was drawn in triplicate (section 2.3) to ensure that variabilities were affected by the blood collection setting but not biological variability.

5.2.9. Statistical analysis

Descriptive statistics (mean \pm standard deviation (SD) or median [interquartile range (IQR)]) and box-whisker-plots were used to describe kinin level data. Outcomes were analysed using the Mann-Whitney U-test or Levene test for equality of variance. Statistical analyses were performed with the two-sided alternative hypothesis at the 5% significance level. Calculations and graphics were made using OriginPro 2021 (9.8.0.200).

5.3. Results

5.3.1. Investigations on extent and time-course of artificial kinin alterations

Levels of bradykinin and its metabolites (mean \pm SD) sampled without protease inhibitor were in the high pg/mL–ng/mL range with high interindividual variation (n=4): 3,130.8 \pm 2,921 pg/mL for bradykinin, 2,318.5 \pm 1,951.6 pg/mL for des-Arg(9)-bradykinin, 1,356.8 \pm 834.3 pg/mL for bradykinin 1-7, 753.80 \pm 943.9 pg/mL for bradykinin 2-9, and 779.0 \pm 53.3 pg/mL for bradykinin 1-5. Kallidin and des-Arg(10)-kallidin, unaffected by contact activation, fell below the LLOQ.

Monitoring of artificial kinin generation revealed increased bradykinin levels 30 s after blood sampling, continuously rising over the observed 30 min period (Figure 16). Bradykinin metabolites emerged between 30 s to 3 min. After 30 min, des-Arg(9)-bradykinin was the main metabolite detected. An equilibrium between generation and degradation occurred for bradykinin 1-7 and bradykinin 2-9 (40% and 20% of bradykinin generation), but not for bradykinin 1-5 or des-Arg(9)-bradykinin. The rapid artificial changes highlighted the need for direct sampling into protease inhibitors and the urgency for investigating blood sampling conditions.

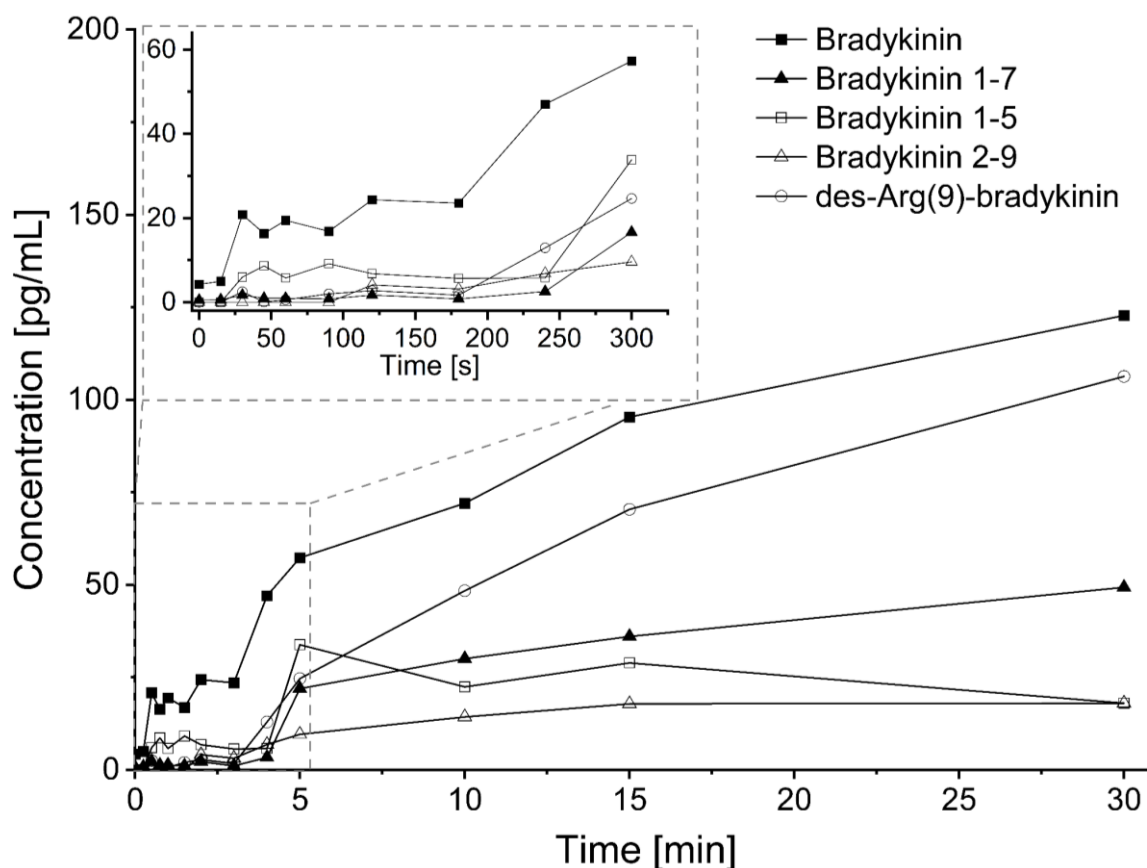


Figure 16. Self-generation of bradykinin and formation of its metabolites after blood sampling. Spontaneous contact activation without *in vitro* activation in the absence of inhibitors in healthy volunteer in EDTA S-Monovettes® was monitored.

5.3.2. Impact of protease inhibitor on *ex vivo* kinin stability

5.3.2.1. Control of artificial bradykinin generation

Similar or higher bradykinin levels were detected using the serine protease inhibitors aprotinin, PMSF, or AEBSF compared with uninhibited plasma (Figure 17); hence, artificial generation of bradykinin was not adequately limited. In comparison, nafamostat, leupeptin (0.5/1.5 hr) and chicken-egg trypsin-inhibitor (0.5 hr) reduced bradykinin generation; however, increased bradykinin levels were observed after 4.5 hr. Lowest levels of bradykinin (0.4% compared with uninhibited) were found using hexadimethrine bromide, which prevented bradykinin generation most effectively. Higher concentrations of nafamostat and hexadimethrine bromide correlated positively with prevention of bradykinin formation (Figure 17). The combination of 10.8 µg/mL nafamostat and 3 mg/mL hexadimethrine bromide rendered bradykinin undetectable, indicating control of artificial bradykinin generation.

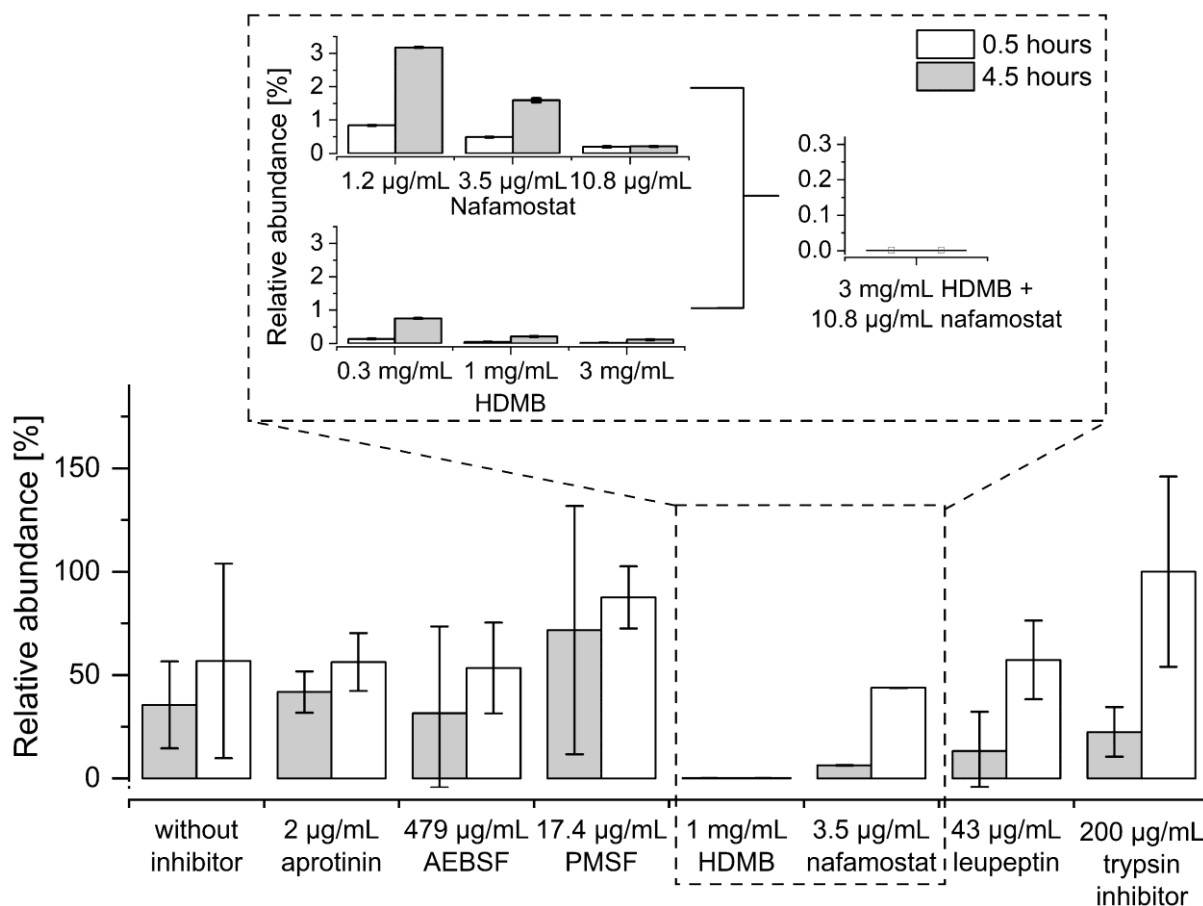


Figure 17. Effects of distinct protease inhibitors on the generation of bradykinin in plasma. The relative abundance of bradykinin 0.5 and 4.5 hours after blood sampling is shown. In the inset, the evaluation of distinct concentrations of the best performing inhibitors HDMB and nafamostat and their combination are depicted. Mean values with standard deviation ($n=3$). AEBSF: 4-(2-Aminoethyl)benzenesulfonyl fluoride hydrochloride, HDMB: hexadimethrine bromide, PMSF: phenylmethanesulfonyl fluoride

5.3.2.2. Control of kinin degradation

Use of hexadimethrine bromide and nafamostat (preventing the generation of bradykinin) resulted in degradation of all kinins, ranging from -15.1% (des-Arg(9)-bradykinin) to -78.0% (kallidin) (Figure 18A1). Phenanthroline led to complete loss of the more hydrophilic peptides bradykinin 1-5 and bradykinin 1-7 via interaction with the solid-phase extraction (SPE) sorbent. Reduced degradation of <27% was observed when adding the metalloprotease inhibitors EDTA (31 mg/mL) and citrate (5.9 mg/mL) with the exception of bradykinin 2-9, which was completely degraded. Unspecific protease inhibition via basification using ammonia or sodium hydroxide did not improve stability of bradykinin 2-9 (-88/-96%). The systematic evaluation rendered the effect of individual inhibitors visible, when acidification reduced bradykinin 2-9 degradation to 32% (1% FA) and to 61% (0.1% FA), respectively. Addition of omapatrilat limited between-sample variability (CV) and stabilized kinin levels to $\leq 15\%$ relative error (RE), with the exception of des-Arg(9)-bradykinin and bradykinin 1-5. To improve their stability, the addition of serine protease inhibitors (benzamidine, PMSF and chloroquine) was screened, and the prolylcarboxypeptidase inhibitor chloroquine was identified to stabilize all kinins (RE and CV $\leq 15\%$). Thus, the final customized protease inhibitor consisted of 3 mg/mL hexadimethrine bromide, 10.8 $\mu\text{g/mL}$ nafamostat, 31 mg/mL EDTA, 5.9 mg/mL citrate, 1% FA, 409 ng/mL omapatrilat and 515 $\mu\text{g/mL}$ chloroquine.

5.3.2.3. Comparison to previous protease inhibitors

Investigation of the previously applied protease inhibitor GTC/TFA led to repeated clogging of the μ elution SPE cavities despite re-centrifugation at 16.100 x g and was infeasible using the established LC-MS/MS platform. Precipitation by ethanol delivered stable levels of kinins over the investigated timeframe with the exception of des-Arg(9)-bradykinin (-17.4% decrease) (Figure 18A2). Moreover, recovery in comparison to customized protease inhibitor-spiked plasma samples was reduced up to a factor of five (kallidin), compromising sensitivity and hampering determination of low endogenous levels (<LLOQ: 2 pg/mL for bradykinin). The use of commercially available BD™ P100 or P800 tubes was similarly unsuitable for the determination of kinins as indicated by losses of -41% (bradykinin 2-9) to -100% (kallidin, des-Arg(10)-kallidin) (Figure 18A2).

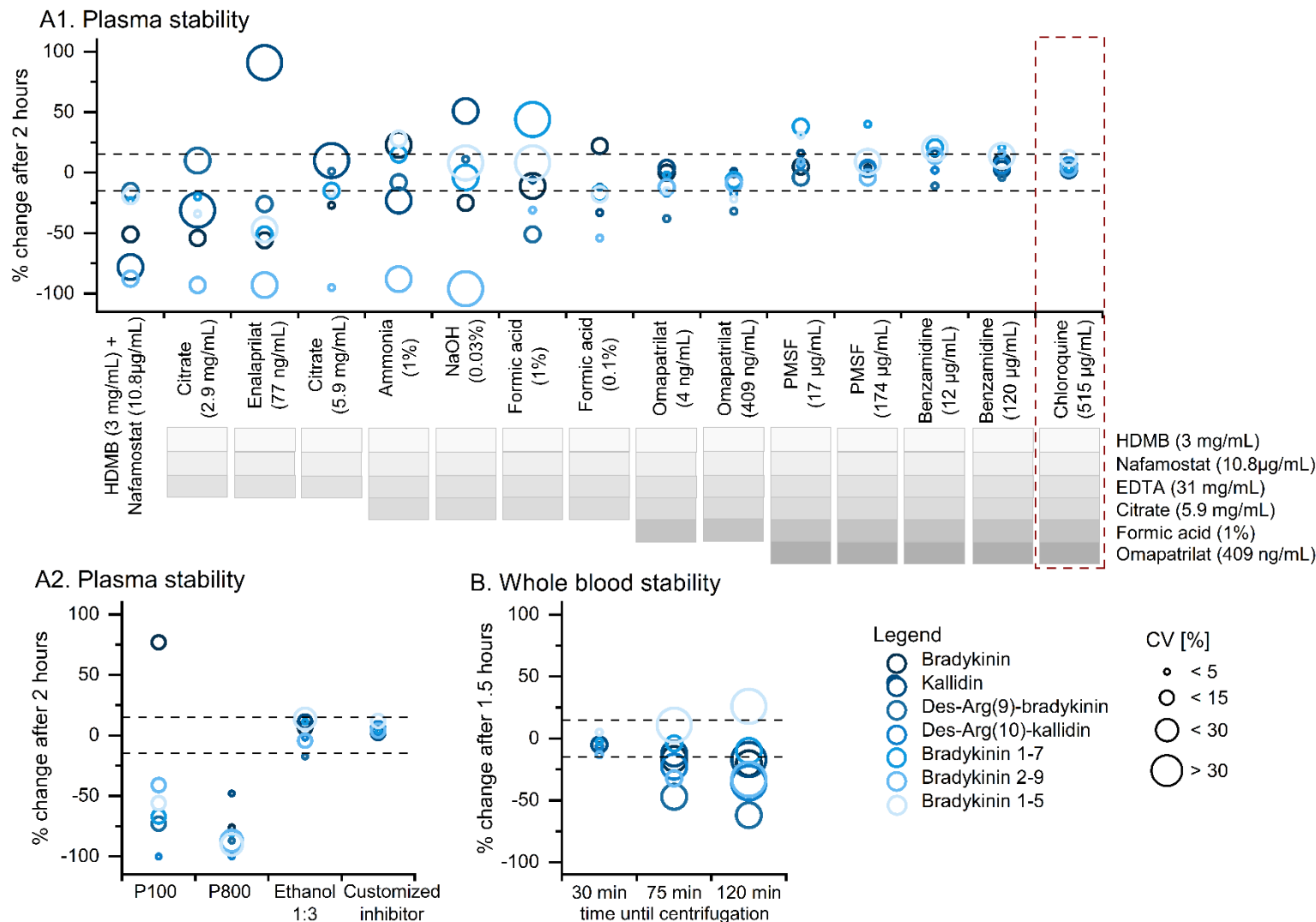


Figure 18. Plasma stability of kinins in plasma and whole blood in the presence of various protease inhibitors. A1/2 depicts the percentage change of plasma kinin levels within 2 hours. B shows the percentage change of kinins during whole blood storage. The components/performance of the final customized protease inhibitor improving stepwise kinin stability are highlighted in grey/dotted red. Dotted lines indicates maximum relative error of $\pm 15\%$ according to the FDA guideline [US Food and Drug Administration 2018]. Circle size represents coefficient of variation (CV) [%] ($n=3$). EDTA: ethylenediamine-tetraacetic acid, HDMB: hexadimethrine bromide, NaOH: sodium hydroxide, PMSF: phenylmethane-sulfonyl fluoride

5.3.3. Effect of blood sampling and handling on kinin quantification

5.3.3.1. Blood collection devices

When comparing blood collection systems, no significant difference was found between the 21G butterfly-winged systems with 80 mm or 200 mm tubing (Figure 19A). However, collection with 21G straight needles varied significantly (Eclipse: $p=0.009$, S-Monovette® Safety: $p=0.029$). Undetectably in the control, des-Arg(9)-bradykinin (median 8.4 pg/mL and 4.2 pg/mL, respectively) and bradykinin 1-7 (median 2.8 pg/mL, only S-Monovette® Safety) were partially detectable in these samples, indicating artificial generation of kinins. When sampling with the 21G Micro Needle, bradykinin levels (median 32.0 [13.0–67.7] pg/mL) were detected besides an artificial generation of des-Arg(9)-bradykinin (median 3.7 [1.4–6.4] pg/mL).

In comparing needle sizes, a significant negative impact of the smaller needle size (25G) on bradykinin levels was detected ($p=0.013$). In addition, des-Arg(9)-bradykinin and bradykinin 1-7 were only detectable using the smaller needle size. Use of the peripheral catheter resulted in highest bradykinin levels (19.2 [18.6–47.0] pg/mL, $p<0.001$) and increased levels of des-Arg(9)-bradykinin (16.4 [10.6–46.4] pg/mL), bradykinin 1-7 (14.7 [9.8–47.9] pg/mL), and bradykinin 1-5 (57.4 [28.1–216.0] pg/mL).

5.3.3.2. Blood collection tube

The altered blood-to-surface ratio due to distinct diameters of S-Monovettes® did not compromise kinin levels, when sampled under aspiration (Figure 19B). Interestingly, differences were found between S-Monovettes® and Vacutainer® tubes; the latter showed higher variability in kinin levels ($p=0.042$, Figure 19D). Blood sampling technique may explain these differences.

5.3.3.3. Blood collection technique

Time delays must be avoided, as significant increases in kinin levels for both butterfly (8-fold) and peripheral catheter (25-fold) sampling were observed ($p<0.001$ and $p=0.003$; Figure 19C). Metabolites of bradykinin were increasingly detectable in the samples drawn with a time delay (up to median 238.3 pg/mL for bradykinin 1-5).

Comparison between Vacutainers® and S-Monovettes® indicated, blood should be collected using the aspiration technique. Significant differences in bradykinin levels were found for vacuum collection using Vacutainers ($p=0.042$). This tendency was also detectable for vacuum collection using S-Monovettes® ($p=0.051$) (Figure 19D). The evaluation of potential shear forces affected by antegrade or retrograde cannulation showed significantly elevated levels of bradykinin when inserted in a retrograde fashion ($p=0.028$). The use of a tourniquet for less than 2 min did not impact kinin levels.

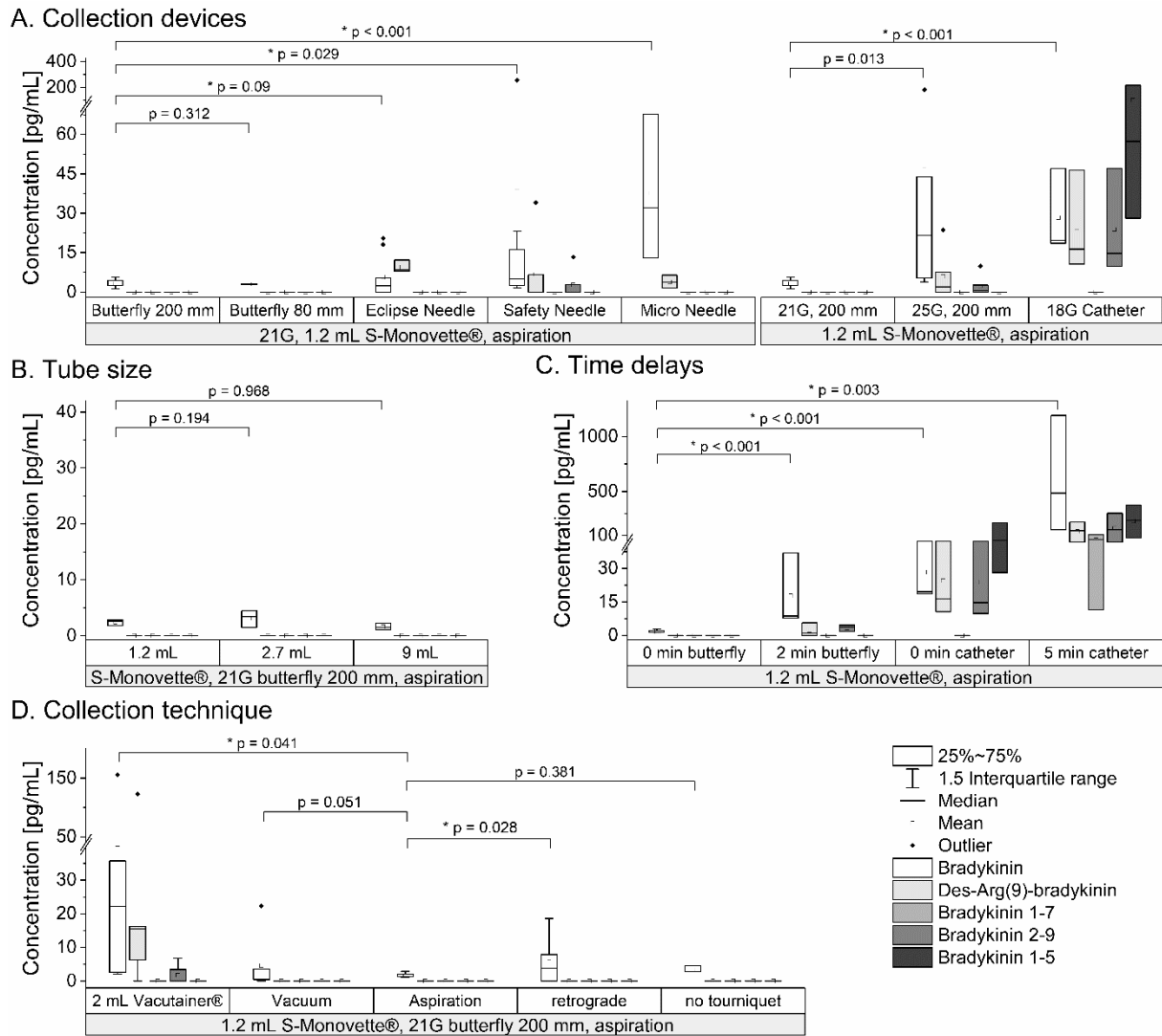


Figure 19. Investigation of the impact of blood sampling conditions on kinin levels. Box-whisker-plots show the impact of distinct blood collection devices (A), the tube size (B), time delays (C) and the collection technique (D); $n \geq 3$. An interexperimental control using Safety Multifly® needles 21G with 200 mm tubing into 1.2 mL S-Monovettes® under aspiration was run for each experiment. * $p < 0.05$, Levene test for equality of variance

5.3.4. Effect of specimen handling on kinin quantification

5.3.4.1. Time until centrifugation

Kinins were subject to increased degradation in whole blood despite use of the customized protease inhibitor (Figure 18C). In comparing times until centrifugation, centrifugation within 30 minutes resulted in relative errors $\leq 15\%$ compared to a fresh standard for all kinins. Delayed centrifugation after 75 and 120 min caused a decline of kinin levels (up to -62% for des-Arg(9)-bradykinin). An exception was bradykinin 1-5; levels increased up to 26% (120 min), demonstrating accumulation of the most stable kinin. Additionally, increased variability between the tubes was observed over time (Figure 18C).

5.3.4.2. Centrifugation method

Comparison of centrifugation methods did not yield significant differences ($p > 0.38$) in kinin levels (Table 7). Kinin levels were up to 13.6% higher when processed on ice and centrifuged at 4°C . In addition, lowest variability between the tubes was found using double centrifugation for spiked plasma.

Table 7. Effect of centrifugation methods on kinin levels. Concentrations are reported as mean \pm standard deviation ($n=3$) with corresponding p -value ($p < 0.05$, Mann-Whitney U-test).

Analyte	Speed Time Temperature	2000 x g	2000 x g	2000 + 16.1000 x g	2000 x g
		10 min 21 °C	20 min 21 °C	10 min + 10 min 21 °C	10 min 4°C
Bradykinin	Concentration [pg/mL]	158.4 \pm 17.0	155.0 \pm 22.1	156.9 \pm 9.6	168.1 \pm 9.2
	p-value		1	1	0.6625
Kallidin	Concentration [pg/mL]	151.0 \pm 10.1	138.2 \pm 5.1	143.8 \pm 18.5	155.3 \pm 19.0
	p-value		0.3827	0.6625	1
Des-Arg(9)-bradykinin	Concentration [pg/mL]	135.5 \pm 11.0	121.6 \pm 5.0	131.2 \pm 8.5	151.9 \pm 11.2
	p-value		0.0809	1	0.3827
Des-Arg(10)-kallidin	Concentration [pg/mL]	155.3 \pm 22.4	140.4 \pm 6.9	152.8 \pm 14.8	162.5 \pm 17.6
	p-value		0.5066	1	1
Bradykinin 1-7	Concentration [pg/mL]	161.4 \pm 15.5	153.3 \pm 10.8	159.2 \pm 16.5	169.0 \pm 12.4
	p-value		0.6625	0.6625	0.3827
Bradykinin 2-9	Concentration [pg/mL]	144.6 \pm 11.6	144.3 \pm 4.0	141.4 \pm 17.1	155.2 \pm 8.4
	p-value		1	1	0.3827
Bradykinin 1-5	Concentration [pg/mL]	132.9 \pm 29.8	141.7 \pm 57.8	136.1 \pm 14.0	151.0 \pm 27.5
	p-value		1	1	1

5.3.5. Validation and applicability of the standardized protocol

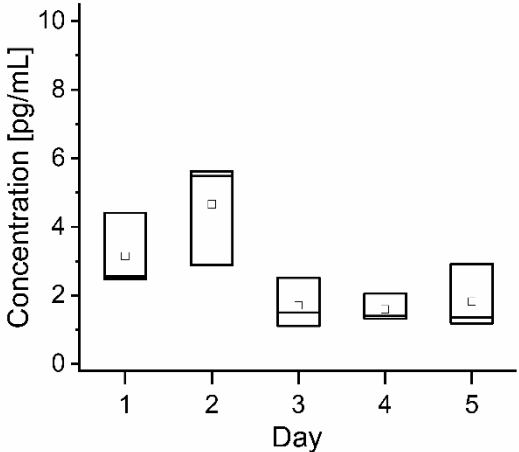
A standardized blood sampling and handling protocol was developed from the findings and is presented in Table 8. Using this protocol, the evaluated preanalytical conditions were successfully validated and applied. Mean \pm SD values of 2.5 ± 1.5 pg/mL bradykinin were found in one healthy volunteer (27 years) on five distinct days and an inter-tube variation <1.7 pg/mL from the mean ($n=3$) per day was detected (Figure 20). Consecutive sampling of three tubes in seven healthy subjects (29 [27-54] years) also revealed kinin levels in a similar range (mean levels for subjects 0–4.3 pg/mL) and the inter-tube variation was <1.2 pg/mL from the mean. Levels of 2.4 ± 0.4 pg/mL for des-Arg(10)-kallidin were found in one female volunteer, whereas all other kinin levels were below the LLOQ. More detailed results can be found in Figure 20.

Table 8. Recommendations for preanalytical conditions for kinin assays.

Preanalytical variable	Guidance
Protease inhibitor	<ul style="list-style-type: none"> - Protease inhibitor pre-spiked tubes are essential - A mixture of 3 mg/mL hexadimethrine bromide, 10.8 μg/mL nafamostat, 31 mg/mL EDTA, 5.9 mg/mL citrate, 1% FA, 409 ng/mL omapatrilat and 515 μg/mL chloroquine complied with regulatory demands
Blood collection system	<ul style="list-style-type: none"> - Use butterfly-winged needles with a needle size of 21 G
Blood collection tube	<ul style="list-style-type: none"> - Use polypropylene tubes, avoid glass - Use of tube size from 1.2 mL up to 9 mL possible
Blood collection technique	<ul style="list-style-type: none"> - Use aspiration technique applying a constant move - Rapidly perform sampling of blood and avoid any time delays after venipuncture
Whole blood storage	<ul style="list-style-type: none"> - Centrifuge within 30 minutes after blood sampling
Centrifugation method	<ul style="list-style-type: none"> - Apply 2000 x g for 10 minutes at 21 °C
Plasma storage	<ul style="list-style-type: none"> - 1.5 hours on the benchtop at 21 °C - at least 4 weeks at -80 °C - 2 freeze-thaw cycles (-80 °C) <p>using the developed protease inhibitor (section 4 [Gangnus & Burckhardt 2021c])</p>

EDTA: ethylenediaminetetraacetic acid, FA: formic acid

A. Inter-day variability



B. Interindividual variability

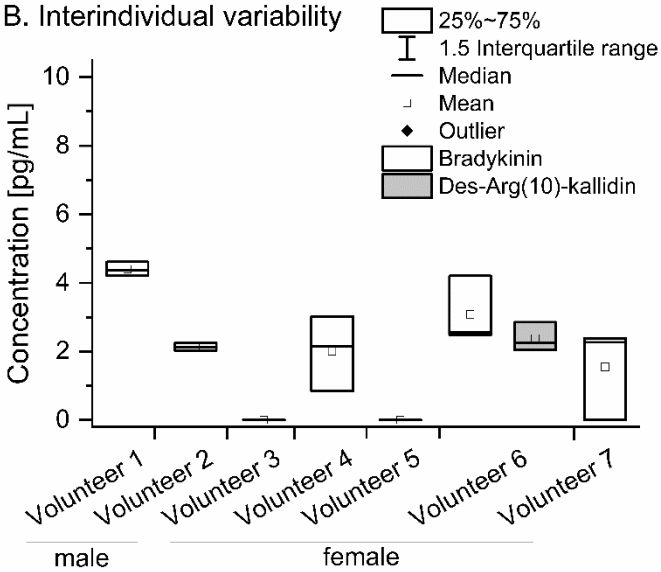


Figure 20. Box-whisker-plots of the kinin levels for inter-day and interindividual variability in healthy volunteers. The developed standardized protocol was used. Only kinin levels above the lower limit of quantification were shown (n=3).

5.4. Discussion

This study identified impactful preanalytical variables (e.g. sampling technique, blood collection devices, protease inhibitor) on plasma kinin levels. Control of kinin generation, degradation and stability by protease inhibitors, blood sampling conditions and sample handling was addressed by the development of a standardized protocol. Applying this protocol, coupled with a validated LC-MS/MS platform, proved its applicability for robust and reliable kinin determination in human plasma.

Strong dependence of the sample collection have hindered reliable and accurate kinin quantification [Kaplan & Maas 2017; Hofman et al. 2016]. This obstacle contributed to great differences in previous research, with kinin levels ranging from 0.4 pg/mL to 162 ng/mL bradykinin in healthy volunteers [Duncan et al. 2000; van den Broek et al. 2010; Wheelock et al. 2017; Pellacani et al. 1992] rendering the identification of dysregulated KKS difficult to identify in disease. This study demonstrated high interindividual variability and rapid artificial generation of bradykinin and its metabolites in uninhibited plasma without *in vitro* activation. Amongst the evaluated stabilization approaches, the customized protease inhibitor showed most efficient stabilization of *ex vivo* kinin levels. This inhibitor was shown to be advantageous for the comprehensive monitoring of kinins in regard to previously used protease inhibitors. Finally, by using the implemented standardized protocol, repeatability of measured kinin levels was demonstrated. The limitation of inter-day and interindividual variability was exemplified in this study (<1.7 pg/mL). The postulated conduct and extent of sample collection and on-ward preparation according to the standardized protocol allow for implementation into clinical routine for further investigation of kinins in diseases, such as angioedema, or sepsis.

Nevertheless, controlling only the artificial generation is insufficient to reliably describe, understand, and target the KKS due to short half-lives. Further, the comprehensive monitoring of kinins other than bradykinin, especially active ones known to interact with bradykinin receptors, is particularly important when considering possible therapeutic targets. Protease inhibitors used so far showed their potential, but did not sufficiently stabilize all kinins investigated within this study. Moreover, previously published approaches failed to show comprehensive proof of stability or disclosed deviations exceeding the limits of the regulatory FDA guidance [Seip et al. 2014; Campbell et al. 1993; Lindström et al. 2019]. Using ethanol in a ratio of 3:1 initially appeared suitable [Murphey et al. 2001], but caused up to five-fold lower recovery, and therefore was classified less suitable for endogenous determination due to reduced sensitivity. The here presented systematic evaluation of inhibitors interfering with kininases resulted in a customized protease inhibitor, which itself proved FDA-conforming benchtop stability for 1.5 hr, freeze-thaw stability for two cycles and at least four weeks long-term stability in plasma (section 4 [Gangnus & Burckhardt 2021c]).

The phlebotomy setting severely impacted the reliability and accuracy of kinin levels. For coagulation assays, conventional straight needles were suggested as superior to butterfly needles or peripheral catheters due to reduced haemostatic alteration and decreased surface area for contact activation [Spronk et al. 2009]. Others found no differences between these three collections systems [Loeffen et al. 2012; Lippi et al. 2005]. In this study, consistent kinin levels were only obtained using butterfly tubing. This might be explained by more handling space due to the tubing and thus avoidance of needle pressure on the vessel wall during exchange of blood sampling tubes. The measurement of kinin levels using catheters is not reasonable, as the highest kinin levels were measured with this setting. The time until the catheter is positioned probably plays a significant role in kinin generation, but kinin levels also rose sharply during time-delays while the catheter was in the vein. Therefore, it is advisable to always puncture anew when taking repeated blood samples for the determination of kinin values and, in addition, to use veins that have not been punctured so far. For haemostatic investigations it is further recommended to minimize trauma during blood draws, to avoid producing bubbles or foam, and to reduce shear stress [Magnette et al. 2016]. In line, blood sampling in Vacutainers® or S-Monovettes® under vacuum produced more variable results compared with blood sampling under aspiration. Consequently, reduction of shear forces and stress on the vessel in addition to rapid sampling, facilitated the most consistent kinin level measurements.

The protease inhibitor and sample collection settings were identified as most crucial for control of kinin generation, whereas sample handling was predominantly decisive regarding loss of kinins. Increased availability of degrading enzymes on blood cells, e.g. aminopeptidases or ACE2, presumably limited the stability of kinins in whole blood (30 min) in comparison to plasma (1.5 hr) [O'Leary et al. 2013; Rutkowska-Zapała et al. 2015; Hendriks et al. 1991; Gangnus & Burckhardt 2021c]. Hence, time until centrifugation proved to be an additional factor for variable kinin levels. Additionally, non-specific peptide adsorption during sample handling must be reduced to further minimize variability of recovery, particularly in extracted samples due to reduced saturation of protein-binding surfaces [Hoofnagle et al. 2016]. Besides the use of protein low-binding tubes, high acidic amounts and organic solvents using polypropylene materials were shown to reduce adsorption of kinins and contribute to the improvement of accuracy and precision (section 3 [Gangnus & Burckhardt 2020]).

5.5. Conclusion

The developed protocol in combination with the LC-MS/MS platform (section 4 [Gangnus & Burckhardt 2021c]) enable improved studies of diseases related to the KKS, such as COVID-19, angioedema, sepsis, Alzheimer's disease, epilepsy, cancer or stroke. The reliable quantification of kinins facilitates investigation of kinin profile alterations between health and disease and therefore might help identifying promising new therapeutic targets.

6. Sensitive mass spectrometric determination of kinins in respiratory saline lavage fluid in light of COVID-19

6.1. Background

In March 2020 the World Health Organization declared a pandemic of COVID-19 due to alarming levels of spread and severity. COVID-19 is caused by infection with the novel SARS-CoV-2. Hospitalized patients commonly present with symptoms of fever, cough, and dyspnoea and can develop pulmonary oedema in early disease [Wang et al. 2020]. It has been postulated that these symptoms are in connection with a dysregulated KKS [Maat et al. 2020; Roche & Roche 2020; van de Veerdonk et al. 2020b; Nicolau et al. 2020]. As yet, concentrations of peptides within the KKS have not been reported in COVID-19 patients and their role remains unclear.

Activation of the KKS, i.e. by tissue and plasma kallikrein, leads to the formation of the kinins bradykinin and kallidin (lys-bradykinin), both potent activators of B₂ receptors on endothelial cells [Marceau et al. 2020]. The activation of these receptors promotes vasodilation, inflammation, and capillary leakage leading to oedema [Ellis & Fozard 2002; Magerl et al. 2014]. Bradykinin and kallidin are cleaved by carboxypeptidase N and M into des-Arg(9)-bradykinin and des-Arg(10)-kallidin, respectively, which are ligands for the B₁ receptor, as demonstrated in *in vitro* experiments using human tissues [Blais et al. 1997; Ellis & Fozard 2002]. The *in vivo* activation of B₁ receptors in animals was shown to mediate inflammation, bronchoconstriction, and extravasation, which causes (pulmonary) oedema [McLean et al. 2005; Gobeil et al. 1997]. The B₁ receptor is furthermore upregulated during inflammation, thus providing increased receptor binding sites for des-Arg(9)-bradykinin and des-Arg(10)-kallidin [Ellis & Fozard 2002; Magerl et al. 2014; Broadley et al. 2010]. While des-Arg(10)-kallidin is further cleaved into des-Arg(9)-bradykinin, the latter is mainly degraded by the ACE 2 [Sodhi et al. 2018; Vickers et al. 2002]. ACE 2 has been identified as the binding site of SARS-CoV-2, enabling it to enter cells [van de Veerdonk et al. 2020b; Hoffmann et al. 2020]. It is thus assumed that cleavage of active des-Arg(9)-bradykinin into the inactive bradykinin 1-7 is considerably reduced during SARS-CoV-2 infection. In this context, viral attenuation of ACE 2 activity contributed to the pathogenesis of lung inflammation that was concomitant with increased B₁ receptor expression [Sodhi et al. 2018]. Therefore, the KKS is suggested to be involved in the pathogenesis of COVID-19 via the viral blockade of ACE 2, leading to elevated active des-Arg(9)-bradykinin levels [van de Veerdonk et al. 2020b; Tolouian et al. 2020]. Monitoring of seven kinin peptides (bradykinin, kallidin, des-Arg(9)-bradykinin, des-Arg(10)-kallidin, bradykinin 1-7, bradykinin 1-5 and bradykinin 2-9) may provide insights

This work was published in a peer-reviewed journal:

Gangnus T, Burckhardt BB (2021) Sensitive mass spectrometric determination of kinin-kallikrein system peptides in light of COVID-19. *Scientific Reports*. 11, 3061. <https://doi.org/10.1038/s41598-021-82191-7>

The author of this thesis was responsible for conceptualization, methodology, validation, writing—original draft, review and editing, and visualization.

into the hypothetically altered kinin metabolism during SARS-CoV-2 infection.

Because ACE 2 is highly expressed in the nasal epithelium, the nose is presumed to represent the main entry point of SARS-CoV-2 prior to further spread within the host [Sungnak et al. 2020]. Therefore, saline lavage fluids from the respiratory tract would likely be the most suitable matrix to investigate alterations in the KKS peptide levels, as these fluids originate from the main area of viral infection and clinical symptoms in mild to severe courses (e.g. cough, nasal congestion, pulmonary inflammation and oedema) [Nicolau et al. 2020]. While sampling of epithelial lining fluid in the lower airways by bronchoalveolar lavage is limited by its invasiveness requiring anaesthesia, the use of NLF offers the advantage of non-invasive, cheap and easy sampling [Pitrez et al. 2005]. In the NLF of healthy volunteers, kinin levels were reported to be typically less than 100 pg/mL by immunometric detection, however, no quantitative differentiation of the kinins was possible due to the underlying analytical technique applied [Proud et al. 1983; Turner et al. 2000]. The susceptibility to cross-reactivity with similar structures—which is the case for kinin peptides (Figure 1)—represents the main disadvantage of immunoassays. Nevertheless, highly sensitive immunoassay-based quantification methods that can distinguish kinin peptides have been developed using plasma or tissues, but they require extensive effort for sample purification, including (multiple) SPEs, liquid–liquid extraction, and chromatographic separation prior to immunoassay [Campbell et al. 1993; Duncan et al. 2000].

LC-MS/MS represents a rational choice to overcome immunoassay-related limitations. Nevertheless, to date, no LC-MS/MS method has been reported that can comprehensively determine kinin peptides in respiratory saline lavage fluids. Validated LC-MS/MS methods are available for the determination of single kinin peptides (bradykinin, des-Arg-(9)-bradykinin and bradykinin 1-5) from plasma, serum, or whole blood and lack sensitivity in the desired low pg/mL range [Lindström et al. 2019; Baralla et al. 2011; van den Broek et al. 2010]. Owing to the substantial dilution of epithelial lining fluid by a factor of 60–120 during lavage, a suitable assay must be highly sensitive [Franciosi et al. 2011]. The reliable analysis of low levels of endogenous peptides in diluted matrix, whereby the peptides are often characterized by non-specific peptide adsorption, requires extensive method development [John et al. 2004; Goebel-Stengel et al. 2011]. For that, DoE has proven its usefulness as a lean tool for method development of multifactor-dependent settings and contributes to signal increase in LC-MS/MS (section 3 [Feickert & Burckhardt 2019; Gangnus & Burckhardt 2020]).

Therefore, this study aimed to develop and validate a novel LC-MS/MS method characterized by a broad calibration curve range to comprehensively and sensitively determine KKS peptides (bradykinin, kallidin, des-Arg(9)-bradykinin, des-Arg(10)-kallidin, bradykinin 1-7, bradykinin 1-5 and bradykinin 2-9) to enable reliable insights into their alterations in COVID-19 – or other disease states (e.g. allergies or lung cancer) – in comparison to controls. Information regarding

these alterations will contribute to the understanding of the pathophysiology related to these peptides and may help to identify new therapeutic targets.

6.2. Materials and Methods

6.2.1. Chemicals and reagents

Kallidin TFA salt (96.9%, HPLC; Tocris, Bristol, UK), bradykinin acetate (99.0%, HPLC; Sigma-Aldrich, St. Louis, MO, USA), and their metabolites des-Arg(9)-bradykinin acetate (98.7%, HPLC; Santa Cruz Biotechnology, Dallas, TX, USA), bradykinin 1-7 TFA salt ($\geq 95.0\%$, HPLC; GenScript, Piscataway Township, NJ, USA), bradykinin 1-5 TFA salt ($\geq 95.0\%$, HPLC; GenScript), bradykinin 2-9 TFA salt ($\geq 95.0\%$, HPLC; GenScript), and des-Arg(10)-kallidin TFA salt (95.9%, HPLC) were used in this study. [Phe⁸Ψ(CH-NH)-Arg⁹]-bradykinin TFA salt (97.5%, HPLC) was applied as the internal standard. FA ($\geq 98\%$) and TFA (100.3%) were supplied by Sigma Aldrich. HPLC-grade methanol, water, and DMSO ($\geq 99.9\%$), and MS-grade methanol and ammonium acetate (99.5%) were obtained from Fisher Scientific (Loughborough, UK). Furthermore, HPLC-grade ACN (Applichem, Darmstadt, Germany), MS-grade water (Honeywell Fluka, Seelze, Germany), and ammonia (30.9%) (VWR Chemicals, Radnor, PA, USA) were utilized. Isotonic saline solution 0.9% was provided by B. Braun (Melsungen, Germany).

Sampling of NLF in healthy volunteers was performed in compliance with the ethical principles of the Declaration of Helsinki and was approved by the ethics committee of the medical faculty at the Heinrich-Heine University of Duesseldorf in October 2017 (study number: 6112). Written informed consent was obtained from all participants before enrolment. Bioanalysis was conducted in accordance with Good Clinical Laboratory Practice.

6.2.2. Preparation of kinin stock and working solutions

Lyophilized kinin peptides were dissolved and diluted separately in 0.3% TFA in 25/75 ACN/water (v/v/v) prior to the preparation of a combined working solution containing 500 ng/mL of each peptide salt. [Phe⁸Ψ(CH-NH)-Arg⁹]-bradykinin as an internal standard was dissolved in 0.1% FA in water (v/v) and subsequently diluted to achieve a working solution of 500 ng/mL in 0.3% TFA in 25/75 ACN/water(v/v/v). All peptide solutions were prepared using low protein-binding tubes (Sarstedt, Nümbrecht, Germany).

6.2.3. Sample preparation

A 0.9% isotonic saline solution was used as blank surrogate matrix for the respiratory saline lavage fluids. Owing to the endogenous presence of kinins and the long half-life of bradykinin 1-5, no reliable kinin-free human blank matrix could be generated. Optimized inhibitors were applied to effectively prevent the generation and degradation of the kinin peptides. A mixture of 19.8 μM nafamostat mesylate, 3 mg/mL hexadimethrine bromide, 1% FA, 16.1 mg/mL ethylenediaminetetraacetic acid (EDTA) and 20 mM trisodium citrate was therefore spiked to

the samples. SPE was performed by applying 96-well Oasis WCX μ -elution plates (Waters, Milford, MA, USA). All cartridges were conditioned with 200 μ L of methanol, followed by 200 μ L of 5% aqueous ammonium hydroxide (v/v). Subsequently, the wells were prefilled with 150 μ L of 3 ng/mL internal standard in 5% aqueous ammonium hydroxide (v/v), and 100 μ L of sample was then loaded. Washing was performed with 300 μ L of 5% aqueous ammonium hydroxide (v/v) and 300 μ L of 10% methanol in water (v/v). Elution was conducted three times with 50 μ L of 1% TFA in 75/25 ACN/water (v/v/v). The resulting eluates were evaporated to dryness under a gentle stream of nitrogen at 60 °C while shaking at 300 rpm. The residues were dissolved in 75 μ L of 10/10/80 FA/methanol/water (v/v/v).

6.2.4. Liquid chromatography coupled with tandem mass spectrometry

Chromatography was performed on an Agilent 1200 SL series system (Agilent Technologies, Ratingen, Germany) consisting of a degasser (G1379B), a binary pump SL (G1379B) and a column oven TCC SL (G1316B). A Phenomenex Synergi™ 2.5 μ m Hydro-RP 100 Å column (100x2.0 mm; Torrance, CA, USA) was used for the chromatographic separation. The mobile phases were composed of water and methanol (B) both containing 3.2% DMSO and 0.1% FA (v/v). A 7.5 min binary gradient was applied, maintaining the amount of mobile phase B at 5% for 1.5 min, increasing it to 20% until 2.2 min, to 27% until 2.7 min, to 35% until 3.1 min, and finally to 95% after 6.2 min. Mobile phase B was kept constant at 95% until 6.7 min before decreasing it to 5% and column re-equilibration for 3 min. The flow rate was set to 400 μ L/min, and the injection volume of 50 μ L was applied with an HTC PAL autosampler (CTC Analytics AG, Zwingen, Switzerland). After every injection, the autosampler syringe was rinsed twice with 0.2% FA in 80/20 ACN/water (v/v/v). Samples were stored at 18 °C in the autosampler.

The LC system was coupled to an API 4000 (AB Sciex, Darmstadt, Germany) mass spectrometer equipped with a Turbo V source for detection. The electrospray interface was operated in positive mode with multiple reaction monitoring mode. The curtain gas was maintained at 31 psi, the collision gas at 8 psi, the nebulizer gas at 45 psi, the heater gas at 65 psi, the ion spray voltage at 5500 V, and the source temperature at 350 °C. Peptide-specific parameters are displayed in Table 2.

Data acquisition was conducted using Analyst® 1.6.2 software (AB Sciex, Darmstadt, Germany), and raw data evaluation was performed using Multiquant™ 3.0.2 (AB Sciex, Darmstadt, Germany).

6.2.5. Method development for kinin quantitation in saline lavage fluids

6.2.5.1. Adaption of optimized injection solvent

A previously conducted DoE approach to optimize the injection solvent conjointly with the sample collection material to reduce non-specific adsorption of bradykinin and thus increase sensitivity (section 3 [Gangnus & Burckhardt 2020]), had to be adapted to avoid peak broadening or breakthrough of the more hydrophilic kinin peptides. By using the D-optimal optimization model, an amount of 5–20% organic fraction in the injection solvent was investigated. This range correlated with the binary gradient, as no breakthrough of the kinins was expected. Furthermore, the calculations included a maximum intensity loss of 15% of the predicted intensity of the optimized injection solvent, based on current bioanalytical guidelines for the accuracy limits [US Food and Drug Administration 2018]. Six injection solvent compositions were calculated with distinct organic fractions and analysed in triplicates by LC-MS/MS measurement, and responses and peak shapes were compared to the original injection solvent for bradykinin only (8.7% FA in 5.3/36.6/49.4 methanol/DMSO/water (v/v/v)).

6.2.5.2. Improvement of solid-phase extraction recovery

The method development focused on maximizing recovery to reduce peptide loss during washing steps and to enable the detection of endogenous concentrations in the low pg/mL range. A previously developed SPE protocol for bradykinin only (section 3 [Gangnus & Burckhardt 2020]) had to be adapted, since the kinin peptides differ in their amounts of hydrophobic and positively charged amino acids (Figure 1). Mixed-mode strong cation exchange (MCX) and WCX μ elution SPE were considered to evaluate which material would fit best to all analytes. All experiments evaluating the washing and elution solvents were conducted using neat solution in duplicate.

6.2.6. Validation of kinin quantitation in saline

Bioanalytical method validation was conducted considering the regulatory bioanalytical guidelines of the FDA [US Food and Drug Administration 2018]. Linearity, accuracy, precision, sensitivity, recovery, matrix effect, carry-over, and stability were considered during the validation process.

6.2.6.1. Linearity

Linearity was determined in six runs using nine to eleven distinct calibrator levels (depending on the LLOQ of the individual peptide), which were analysed in single determinations. In compliance with bio-analytical guidelines, the actual concentration of 75% of all calibration

curve standards had to deviate less than $\pm 15\%$ ($\pm 20\%$ at the LLOQ) from their nominal concentration (RE) [US Food and Drug Administration 2018].

6.2.6.2. Accuracy, precision and sensitivity

Accuracy and precision were assessed using up to seven QC levels covering the whole calibration range on three distinct days. The number of QCs depended on the magnitude of the calibration range per peptide. Five replicates per QC level were analysed each day. Accuracies were determined as the deviation of the actual concentration from the nominal concentration (RE) for within-run and for between-run accuracy. Using one-way ANOVA, within-run precision was calculated as repeatability and between-run precision as day-different intermediate precision (CV). In line with regulatory guidelines, accuracy and precision were not allowed to exceed $\pm 15\%$ ($\pm 20\%$ at the LLOQ) [US Food and Drug Administration 2018]. The signal-to-noise ratio (S/N) had to be higher than 5:1 at the LLOQ. The limit of detection (LoD) was further calculated as follows using the results from six calibration curves (Equation 2) [International Council for Harmonisation 1995]:

$$\text{Limit of detection} = \frac{3.3\sigma}{S}$$

Equation 2. Calculation of limit of detection. σ : standard deviation of the y-intercept, S : mean slope of the calibration curves

6.2.6.3. Carry-over

Carry-over was evaluated by alternatingly injecting blank samples and ULOQ calibration curve standards six times. According to regulatory bioanalytical guidelines, carry-over in the blank sample following the ULOQ was not allowed to exceed 20% of the LLOQ signal and 5% of the internal standard signal [US Food and Drug Administration 2018].

6.2.6.4. Recovery and absolute matrix effect

Recovery was determined at four distinct QC levels covering the calibration curve range (high, middle, low and around the LLOQ) in triplicate. Pre-spiked extracted samples were compared to processed blank samples spiked with the same concentrations after μ elution SPE. Matrix effects of the peptides were analysed at the same four distinct QC levels by comparison of post-spiked samples to neat solutions (n=3).

6.2.6.5. Stability

Stability studies were conducted at four QC levels (high, middle, low and around the LLOQ) under different storage conditions. Benchtop stability was investigated by placing the prepared QC samples at room temperature for one and three hours (n=5). Freeze-thaw stability (room temperature to $-80\text{ }^{\circ}\text{C}$) was evaluated by analysing the QC levels after one and three cycles

(n=5). Between each cycle, samples were frozen for at least 12 hours. The autosampler stability was assessed by keeping QC samples in the autosampler at 18 °C for 18 hours and then repeating the QC sample measurement. Finally, short-term stability of processed and evaporated samples was analysed after storage for 24 hours at +4 °C (n=5). Stability at the specific conditions was proven if the mean concentration at each level did not exceed $\pm 15\%$. To evaluate the stability of the analyte working solution, peak areas of the kinin peptides on 15 distinct days after 15 freeze-thaw cycles, measured routinely during method performance qualification (1 ng/mL, neat solution), were analysed for their CV (acceptable: $\leq 15\%$).

6.2.7. Applicability of kinin quantitation in nasal lavage fluid

Nasal lavage with 10 mL of 0.9% isotonic saline (5 mL per nostril) was performed in nine healthy volunteers (6 female/3 male). Volunteers were healthy adults above the age of 18 years without any signs of a respiratory infection or allergy. The volunteers were asked to tip their head backwards, hold the breath, and refrain from swallowing. The obtained fluid was collected directly into the inhibitor cocktail and was immediately vortexed after completing the sampling. The recovered volume was documented to enable the non-invasive normalization of kinin levels. At least 30% of the instilled volume had to be recovered during the lavage in line with the American Thoracic Society guideline for bronchoalveolar lavage [Meyer et al. 2012]. The samples were centrifuged at 4 °C for 15 min at 500 ×g to remove cells, mucus, and debris. A 100 µL aliquot of the supernatant was analysed.

6.3. Results

6.3.1. Method development for kinin quantitation in saline lavage fluids

6.3.1.1. Improvement of kinin sensitivity

Analysing the contour plots of the D-optimal optimization model for the original injection solvent composition and the contour plots with restricted organic amount, showed clearly that high acidic amounts were necessary for the injection solvent, as well as the highest organic amount that would be compatible with peak shapes of the hydrophilic peptides (Figure 21). Of the six investigated injection solvent compositions, 10/10/80 FA/methanol/water (v/v/v) gave best peak shapes for bradykinin 1-5, by maintaining good signal intensity for bradykinin with 98.8 ± 2.3 % of the optimized injection solvent composition (predicted: 91.4% with a log(D) of 0.49 and probability of failure of 0.12%).

6.3.1.2. Improvement of kinin recovery

Using MCX SPE, the more hydrophobic or charged peptides (bradykinin, des-Arg(10)-kallidin, kallidin, and the internal standard) could not be satisfactorily eluted, when applying two 100 μ L elutions of 5% of ammonium hydroxide in ACN, as indicated by low recoveries of 0–3%. Increasing the elution volume or adding ammonium acetate to the elution solvent to produce a salting-out effect did not substantially improve recoveries. Therefore, a customized protocol using WCX with modified washing steps was developed. In particular, the more hydrophilic kinins and those containing fewer amino functional groups (bradykinin 1-5 and bradykinin 1-7) were not robust regarding the recovery, as they were washed out when using an organic amount exceeding 10% methanol, subsequently affecting sensitivity and precision (Figure 21). An increased amount of washing solvent (300 μ L of 10% methanol) did not affect peptide recoveries but resulted in more precise values and was subsequently applied as described in the sample preparation section.

6.3.2. Validation of kinin quantitation in saline

The results for linearity measurements gave best fits using quadratic regression except for bradykinin 1-5, where linear regression was applied (mean $r \geq 0.9960$ for all analytes). The broad dynamic calibration curve ranges were (depending on the analyte) between 4.4–22.8 pg/mL for the LLOQ and between 4,505.9–8,255.5 pg/mL for the ULOQ. More detailed results for the linearity and the respective calibration curve ranges are presented in Table 9 and an example in Figure 23.

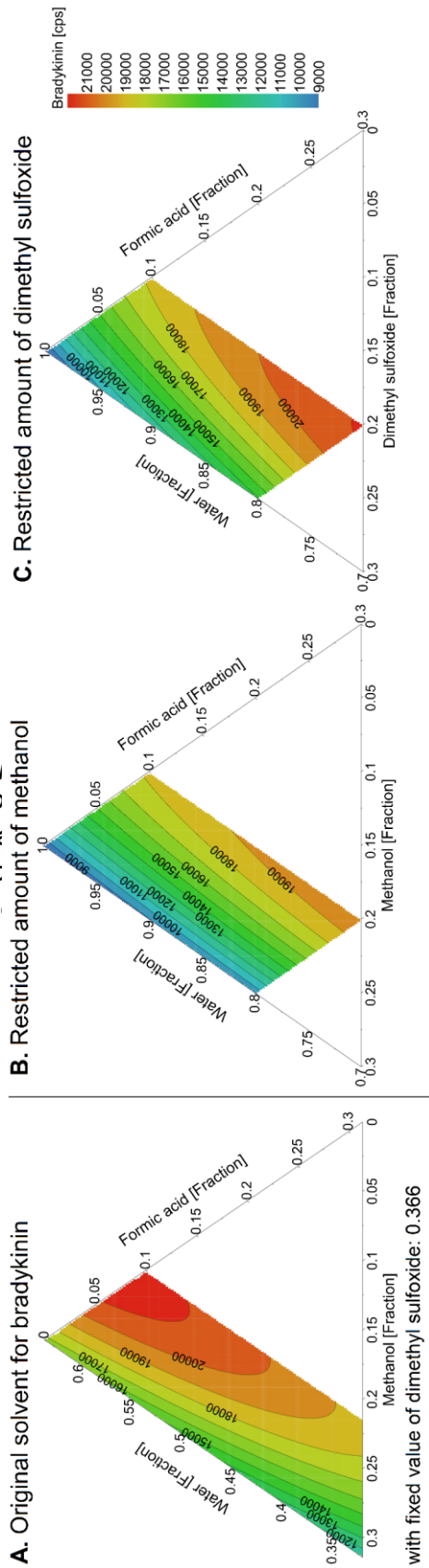
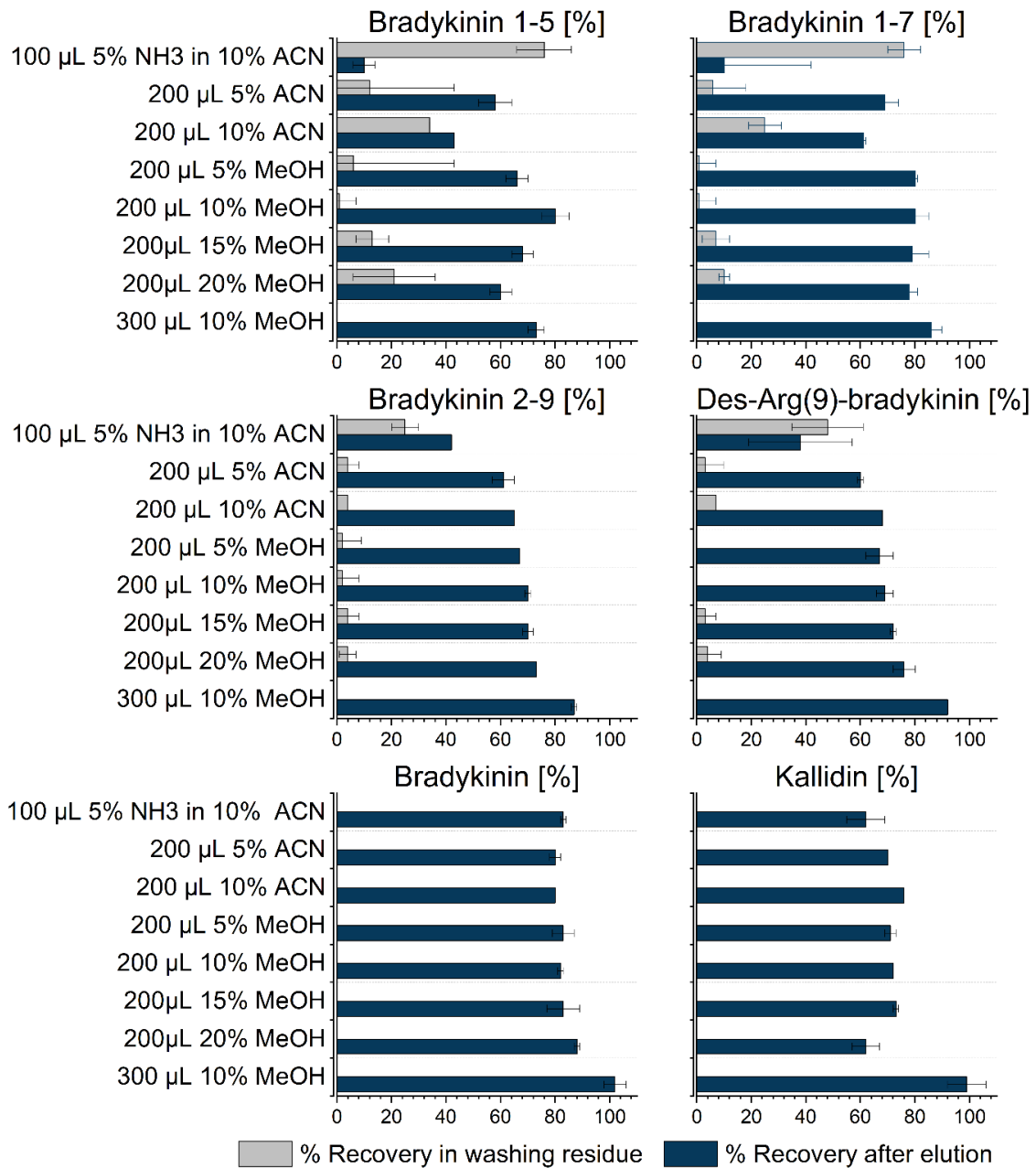


Figure 21. Contour plots showing the response of bradykinin in distinct injection solvent compositions. The color scale indicates the response in cps (counts per second). The white areas indicate the regions, that were not investigated or were not compatible with the hydrophilic peptides.

The within-run and between-run precision as well as accuracy results for all investigated QC levels are presented in Table 10. Guideline-compliant results were obtained for all kinin peptides [US Food and Drug Administration 2018]. In line with the maximally allowed deviation of 20% for accuracy and precision at the LLOQ, the LLOQ was set to 4.4 pg/mL for kallidin (S/N: 94), to 6.7 pg/mL for bradykinin (S/N: 96), to 10.6 pg/mL for des-Arg(10)-kallidin (S/N: 199), to 7.3 pg/mL for (des-Arg(9)-bradykinin (S/N: 403), to 6.5 pg/mL for bradykinin 1-7 (S/N: 155), to 8.1 pg/mL for bradykinin 2-9 (S/N: 65) and to 22.8 pg/mL for bradykinin 1-5 (S/N: 39). Example chromatograms for the comprehensive determination of seven kinin peptides (b and c) lead to a standard deviation of 1.5 cps for hydrophilic peptides. White areas indicate the regions, that were not investigated or were not compatible with the hydrophilic peptides.

respective LLOQ, and the high QC are displayed in Figure 24. The LoD was calculated as 3.5 pg/mL for kallidin, 2.5 pg/mL for bradykinin, 2.5 pg/mL for des-Arg(10)-kallidin, 3.0 pg/mL for des-Arg(9)-bradykinin, 4.4 pg/mL for bradykinin 1-7, 5.6 pg/mL for bradykinin 2-9 and 13.6 pg/mL for bradykinin 1-5.



	Number of amino acids	Maximum positive charges	Isoelectric point	GRAVY
Bradykinin 1-5	5	2	9.75	-1.060
Bradykinin 1-7	7	2	9.75	-1.100
Bradykinin 2-9	8	2	10.18	-0.613
Des-Arg(9)-bradykinin	8	2	9.75	-0.613
Bradykinin	9	3	12.00	-1.044
Kallidin	10	4	12.01	-1.330

Figure 22. Recoveries of kinins in saline during evaluation of washing steps using neat solutions and applying weak cation exchange μ elution solid-phase extraction ($n=2$). Peptide characteristics were calculated using ProtParam [Gasteiger et al. 2005]. ACN: acetonitrile, GRAVY: grand average of hydropathicity index, MeOH: methanol, NH₃: ammonia

Table 9. Results for the assessment of linearity of kinins in saline. Corresponding peptide-specific nominal concentrations of the LLOQ and ULOQ are given. (n=6).

Analyte	Linearity			Dynamic range	
	Mean r	Regression	Weighting	LLOQ [pg/mL]	ULOQ [pg mL]
Kallidin	0.9998	Quadratic	1/x	4.4	4505.9
Bradykinin	0.9987	Quadratic	1/x ²	6.7	6861.3
Des-Arg(9)-bradykinin	0.9981	Quadratic	1/x ²	7.3	7419.1
Des-Arg(10)-kallidin	0.9987	Quadratic	1/x ²	10.6	5348.9
Bradykinin 2-9	0.9977	Quadratic	1/x ²	8.1	8255.5
Bradykinin 1-7	0.9980	Quadratic	1/x ²	6.5	6669.0
Bradykinin 1-5	0.9960	Linear	1/x ²	22.8	5757.0

LLOQ: lower limit of quantification, ULOQ: upper limit of quantification

The carry-over following the injection of an ULOQ sample was below 20% of the signal of the LLOQ for all analytes (kallidin: 19.0%, bradykinin: 17.0%, des-Arg(10)-kallidin: 16.8%, des-Arg(9)-kallidin: 19.1%, bradykinin 1-7: 11.9%, bradykinin 2-9: 18.9%, bradykinin 1-5: 4.4%). No carry-over was observed for the internal standard.

At the distinct QC levels, recoveries did not vary substantially, as indicated by the low CVs of ≤ 5% between the different levels. The more hydrophilic analytes bradykinin 1-5 (mean 34.1%) and bradykinin 1-7 (mean 45.8%) presented lower recoveries compared to the peptides with more lipophilic or additional amine functional groups (mean 74.1% to 88.4%) (Figure 25). Mean ion suppression of the four levels ranged from -16.8% (bradykinin 1-5) to -4.3% (des-Arg(10)-kallidin) (Figure 25).

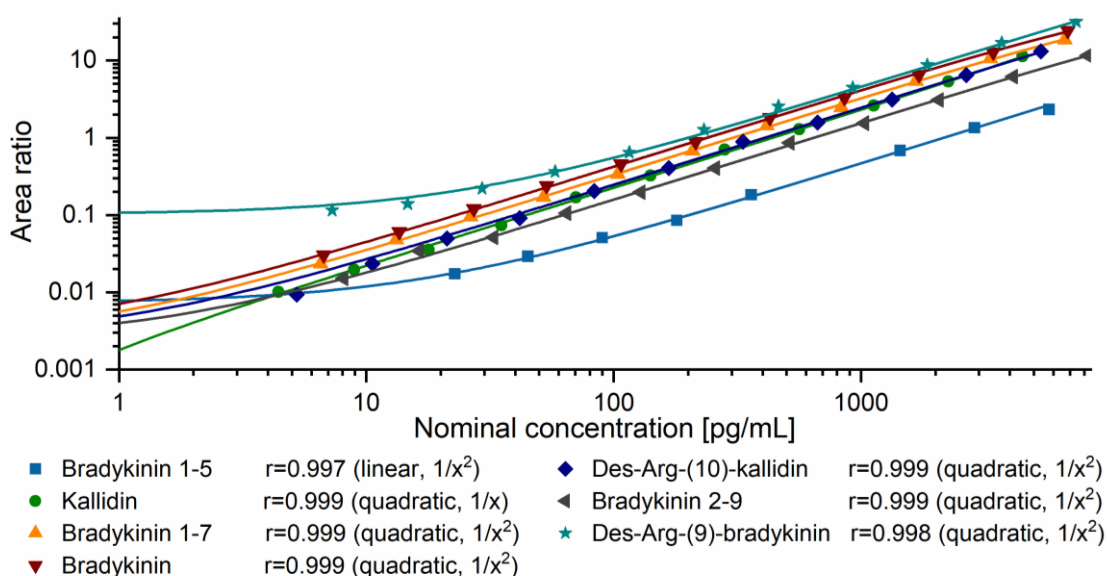


Figure 23. Example calibration curves for all investigated kinins in saline.

Table 10. Accuracy and precision results for all kinins in saline. Using one-way ANOVA, within-run precision was calculated as repeatability and between-run precision as the day-different intermediate precision.

Analyte	Nominal concentration [pg/mL]	Accuracy				Precision		
		Day 1 RE [%]	Day 2 RE [%]	Day 3 RE [%]	Between-run RE [%]	Within-run CV [%]	Between-run CV [%]	
Kallidin	QC high	3379.4	3.56	-0.78	2.67	1.81	2.85	3.40
	QC mid	281.6	4.88	10.00	3.96	6.28	4.56	5.10
	QC low 4	70.4	-2.52	5.28	-7.64	-1.63	4.56	7.77
	QC low 3	35.2	-8.37	5.33	-5.18	-2.74	6.87	9.60
	QC low 2	17.8	-3.79	5.86	-3.42	-0.45	7.55	8.70
	QC low 1	8.9	-0.33	5.34	-9.53	-1.51	9.98	11.74
	LLOQ	4.4	8.29	16.40	-2.99	7.23	13.50	15.11
Bradykinin	QC high	5145.9	1.09	3.57	2.89	2.52	4.16	4.16
	QC mid	428.8	4.30	5.01	4.28	4.53	5.05	5.05
	QC low 4	107.2	2.50	3.31	-2.75	1.02	4.13	4.92
	QC low 3	53.6	-1.30	4.28	-6.91	-1.31	3.82	6.62
	QC low 2	27.2	-1.23	4.31	-10.03	-2.32	6.28	9.29
	QC low 1	13.6	-0.39	2.29	-8.99	-2.36	9.10	10.13
	LLOQ	6.7	11.70	2.40	-4.48	3.21	9.10	11.33
Des-Arg(10)-kallidin		4011.						
	QC high	7	5.29	2.22	3.88	3.79	3.76	3.76
	QC mid	334.3	9.72	3.24	6.15	6.37	3.81	4.58
	QC low 4	83.6	2.25	-1.47	-0.37	0.14	6.45	6.45
	QC low 3	41.8	1.25	-1.48	-4.57	-1.60	4.46	4.97
	QC low 2	21.2	5.61	2.30	-6.55	0.45	7.23	9.00
	LLOQ	10.6	7.09	10.40	-7.32	3.39	10.11	12.84
Des-Arg(9)-bradykinin	QC high	5564.3	-0.79	2.54	0.27	0.67	4.14	4.14
	QC mid	463.7	7.82	8.80	12.01	9.54	5.07	5.07
	QC low 4	116.0	0.96	7.96	7.22	5.38	3.99	5.11
	QC low 3	57.9	-0.45	3.95	1.55	1.68	3.02	3.46
	QC low 2	29.4	0.69	3.21	-6.48	-0.86	8.58	9.20
	QC low 1	14.7	-0.02	0.04	-13.40	-4.46	9.83	11.96
	LLOQ	7.3	11.29	9.25	-7.27	4.42	7.59	11.88
Bradykinin 2-9	QC high	6191.6	2.37	1.51	4.25	2.71	4.77	4.77
	QC mid	516.0	7.05	5.54	10.58	7.72	4.80	4.92
	QC low 4	129.0	6.91	5.60	0.61	4.38	5.46	5.83
	QC low 3	64.5	7.02	3.24	-3.07	2.40	8.25	8.90
	QC low 2	32.7	10.37	6.87	-12.36	1.63	9.64	14.81
	QC low 1	16.3	11.11	1.17	-3.97	2.77	11.28	12.55
	LLOQ	8.1	15.14	15.50	-8.02	7.54	12.97	17.08
Bradykinin 1-7	QC high	5001.8	3.06	14.11	0.18	5.78	7.31	9.54
	QC mid	416.8	10.80	10.66	8.45	9.97	8.01	8.01
	QC low 4	104.2	5.22	8.32	14.89	9.48	4.16	5.85
	QC low 3	52.1	7.78	6.04	2.81	5.54	7.47	7.47
	QC low 2	26.4	6.46	6.98	-7.74	1.90	8.77	11.35
	QC low 1	13.2	8.43	1.98	0.12	3.51	6.53	7.20
	LLOQ	6.5	16.57	3.21	0.27	6.68	12.92	14.14
Bradykinin 1-5	QC high	4317.8	0.22	7.46	-0.19	2.50	9.71	9.71
	QC mid	359.8	10.15	14.57	-0.95	7.92	9.01	10.95
	QC low 4	90.0	2.10	12.37	7.64	7.37	10.37	10.44
	QC low 3	45.0	9.55	13.09	11.80	11.48	12.38	12.38
	LLOQ	22.8	6.65	12.08	13.82	10.85	14.92	14.92

CV: coefficient of variation, LLOQ: lower limit of quantification, QC: quality control, RE: relative error

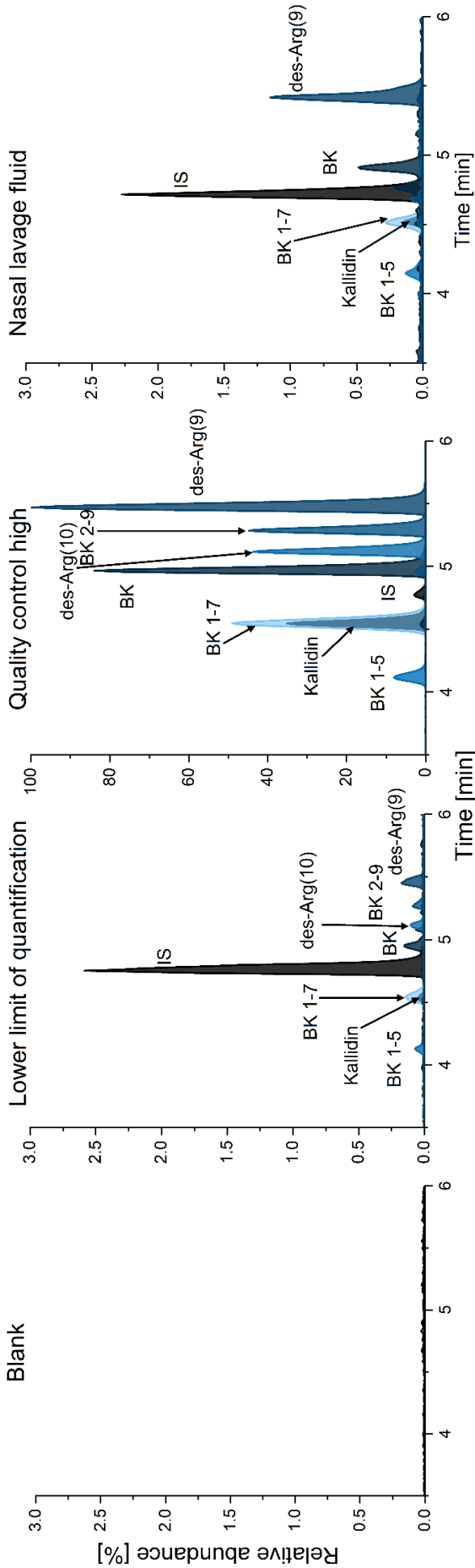


Figure 24. Example chromatogram of des-Arg(9): des-Arg(9) (IS: internal standard)

Figure 25. The nasal lavage fluid was obtained in a healthy volunteer. IS: internal standard, BK: bradykinin 1-5, Kallidin, IS: internal standard

All kinin peptides were stable during autosampler storage for 18 hours at 18 °C and throughout the short-term stability test for 24 hours at 4 °C (Table 11). With the exception of bradykinin 1-5, all other peptides were further stable for three freeze-thaw cycles and on the benchtop for 3 hours. Bradykinin 1-5 was only stable for one hour on the benchtop, whereas after 3 hours a mean decrease of -31.0% was observed. Additionally, bradykinin 1-5 showed a tendency to degrade during freeze-thaw cycles, with increased degradation after three cycles compared to one (mean decrease: -24.3% (1 hour) vs. -31.3% (3 hours)). However, bradykinin 1-5, as well as the other kinin peptides, were stable for 15 freeze-thaw cycles measured over the course of one month (CV: 13.8%) in the analyte working solution. Since enzyme-free matrix was applied, the degradation was not related to insufficient inhibition of enzyme activity. Therefore, degradation might be caused by ionic interactions known to potentially affect instability. Thus, patient samples should be exposed to as few as feasible freeze-thaw cycles and be prepared freshly whenever possible.

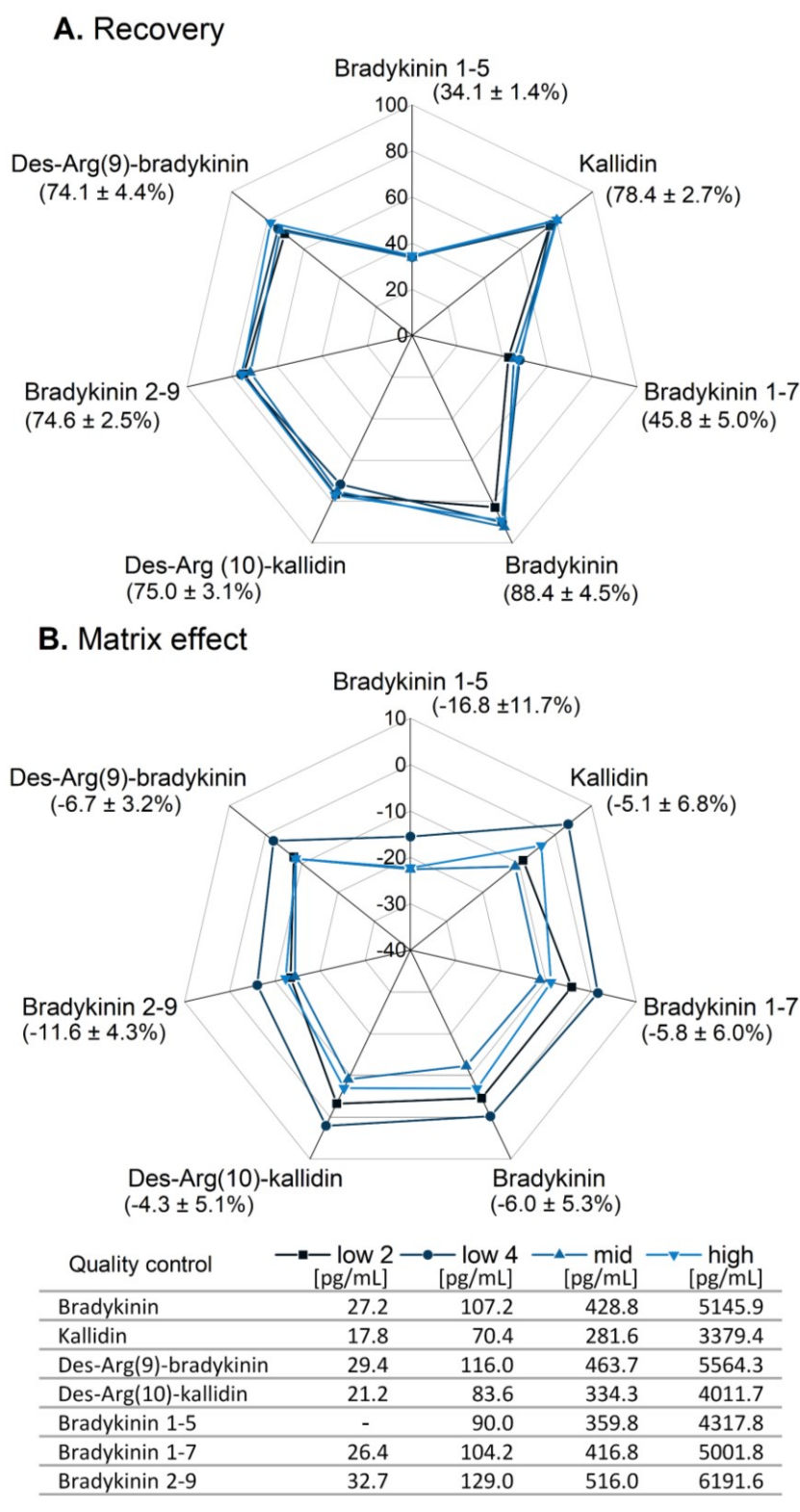


Figure 25. Recovery and absolute matrix effect of all analytes using saline matrix. Mean values and their coefficients of variation for recovery (A) and matrix effect (B) are presented in round brackets. Nominal concentrations of the quality control levels are depicted in the amended table.

Table 11. Results of stability studies for kinins in saline.

Stability:	Analyte	Nominal concentration [pg/mL]	Benchtop		Autosampler	Freeze-thaw		Short-term	
			3 hours		18 hours	3 cycles		24 hours	
			RE [%]	CV [%]	RE [%]	RE [%]	CV [%]	RE [%]	CV [%]
Kallidin	QC low 2	17.8	-6.3	4.3	4.9	-0.9	10.9	3.0	6.4
	QC low 4	70.4	-7.6	2.2	7.1	-1.3	7.3	1.9	3.6
	QC mid	281.6	-8.1	2.6	5.0	-1.2	2.9	2.7	1.4
	QC high	3379.4	-9.0	3.0	13.1	0.3	2.7	7.8	2.0
Bradykinin	QC low 2	27.2	-6.4	8.9	13.8	5.9	5.7	8.7	7.8
	QC low 4	107.2	-10.7	5.5	9.4	2.6	6.2	13.4	1.9
	QC mid	428.8	-9.0	3.3	3.0	0.8	2.2	12.8	1.3
	QC high	5145.9	-7.3	3.8	7.7	3.2	2.8	14.7	2.0
Des-Arg(10)-kallidin	QC low 2	21.2	-6.2	6.5	9.1	4.4	10.5	14.0	10.2
	QC low 4	83.6	-9.4	3.2	8.3	0.5	7.0	11.6	4.4
	QC mid	334.3	-7.1	3.3	6.4	1.1	2.8	10.5	2.3
	QC high	4011.7	-4.9	3.5	7.7	-1.0	2.7	07.0	1.0
Des-Arg(9)-bradykinin	QC low 2	29.4	-14.8	11.4	-8.3	0.6	5.4	9.3	3.8
	QC low 4	116.0	-14.2	2.9	6.8	-1.6	5.4	10.4	2.6
	QC mid	463.7	-7.9	3.4	-0.2	-0.8	2.5	10.8	2.8
	QC high	5564.3	-13.3	2.5	4.6	-0.9	2.8	14.0	2.6
Bradykinin 2-9	QC low 2	32.7	-10.9	9.2	-6.3	9.0	3.9	13.7	7.7
	QC low 4	129.0	-13.5	7.9	10.5	1.5	4.4	12.2	4.7
	QC mid	516.0	-11.8	4.3	8.3	-3.8	1.6	4.1	2.4
	QC high	6191.6	-14.0	5.4	13.6	0.7	1.4	14.2	1.4
Bradykinin 1-7	QC low 2	26.4	-5.4	6.6	7.6	13.5	13.2	8.1	5.5
	QC low 4	104.2	-12.9	4.8	13.8	2.0	3.4	8.6	3.9
	QC mid	416.8	-9.1	4.3	9.1	-0.4	5.3	5.9	7.1
	QC high	5001.8	-10.3	3.5	8.3	-6.0	5.6	4.5	5.7
Bradykinin 1-5	QC low 4	90.0	-13.3 ⁺	13.4 ⁺	14.2	-34.1 [*]	24.9 [*]	-0.3	7.7
	QC mid	359.8	-13.0 ⁺	17.7 ⁺	-1.8	-16.0 [*]	9.0 [*]	7.9	3.9
	QC high	4317.8	1.2 ⁺	13.3 ⁺	9.8	-22.7 [*]	9.8 [*]	5.2	13.1

+ 1h on benchtop, * 1 freeze-thaw cycle, CV: coefficient of variation, QC: quality control, RE: relative error

6.3.3. Applicability of kinin quantitation in nasal lavage fluid

Endogenous levels of the kinin peptides in nine healthy volunteers were comprehensively determined in NLF and confirmed the method applicability. The recovery of instilled lavage volumes ranged from 33% to 89% in the healthy volunteers. Normalized mean levels for all kinin peptides were in the low pg/mL range; namely, 8.2 pg/mL for kallidin, 2.9 pg/mL for des-Arg(10)-kallidin, 22.5 pg/mL for bradykinin, 40.3 pg/mL for des-Arg(9)-bradykinin, 36.4 pg/mL for bradykinin 1-7 and 27.5 pg/mL for bradykinin 1-5 were measured. Bradykinin 2-9 was below the LoD (< 5.6 pg/mL) in all volunteer samples. Box plots of the level data are presented in Figure 26 and a representative example chromatogram is shown in Figure 24. Unnormalized data is shown in Appendix 9.

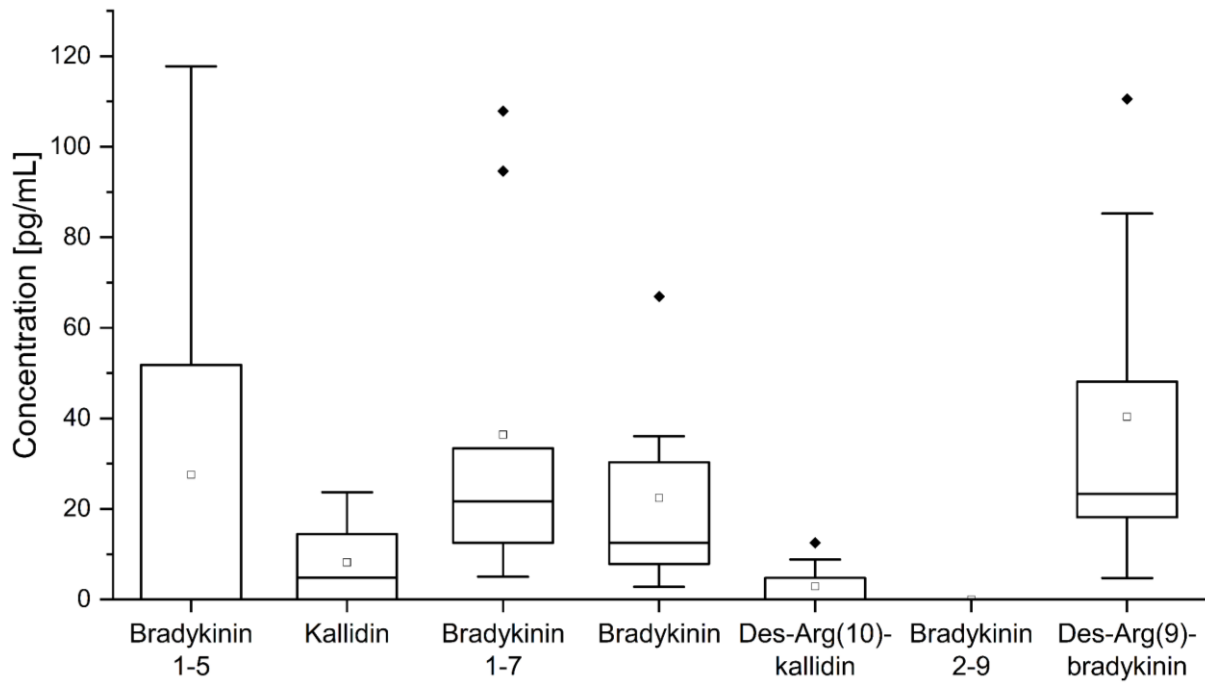


Figure 26. Box plots of kinin peptide concentrations of nine healthy volunteers in nasal lavage fluid. Data were normalized to the recovered volume of nasal instillation with 10 mL saline. ■: interquartile range, T: 1.5 interquartile range, -: median, □: mean, ◆: outlier.

6.4. Discussion

The presented novel LC-MS/MS assay enabled the comprehensive and accurate determination of bradykinin, kallidin, des-Arg(9)-bradykinin, des-Arg(10)-kallidin, bradykinin 2-9, bradykinin 1-7, and bradykinin 1-5 in NLF. Characterized by a high sensitivity (4.4–22.8 pg/mL depending on the kinin) despite the use of low volumes, the applicability of this method was successfully proven by determining low-abundance kinin peptides in NLF. Full validation according to regulatory bioanalytical guidelines was achieved [US Food and Drug Administration 2018].

To the best of our knowledge, this study is the first report of the comprehensive determination of kinin peptides in respiratory saline lavage fluid. Previous determinations of kinins in NLF by immunometric approaches did not quantitatively differentiate between the kinins and were limited to bradykinin and kallidin [Proud et al. 1983; Turner et al. 2000]. Immunoassays are prone to cross-reactivity with structurally similar peptides, which impacts the accuracy and reliability of the results. Further, these methods do not allow the simultaneous investigation and differentiation of kinin peptides from one sample aliquot. Thus, disease-related alterations in the KKS cascade by inhibition or inducement of enzyme activities that affect the generation or degradation of kinin peptides cannot be comprehensively assessed. Furthermore, data obtained from available LC-MS/MS methods is limited and provides a narrow scope of information. The restricted determination of not more than two kinin peptides simultaneously and the generally inadequate sensitivity to detect endogenous peptides in the low pg/mL range by LC-MS/MS has not yet allowed for a comprehensive assessment of the KKS.

Therefore, in advance of this method validation, extensive and systematic investigation was conducted to improve the sensitivity by optimizing the mobile phase and reducing nonspecific peptide adsorption of bradykinin (section 3 [Gangnus & Burckhardt 2020]). By means of the DoE approach, substantial signal intensity increases for bradykinin—by a factor of 7.7 for the mobile phase optimization and by a factor of 26.6 for the injection solvent optimization—were achieved (section 3 [Gangnus & Burckhardt 2020]). Following this approach, the intensity of the other peptides could now be improved through DoE and formed the basis to facilitate the low detection limits of 6.7 pg/mL for bradykinin and the range of 4.4 to 22.8 pg/mL for the other six kinin peptides using saline matrix. As suitable assays in saline solution are lacking, the performance of the developed assay can only be discussed in relation to other human matrices. For bradykinin 1-5, Seip et al. 2014 obtained a similar LLOQ of 20.3 pg/mL (vs. 22.8 pg/mL in the here presented study), but applied larger sample volumes (1 mL blood) [Seip et al. 2014]. The measurement of des-Arg(9)-bradykinin by LC-MS/MS was marked by a quantification limit of 2 ng/mL [van den Broek et al. 2010]. The LC-MS/MS assay of Lindström

et al. 2019, established a LLOQ of 106.2 pg/mL for bradykinin using 500 μ L of plasma [Lindström et al. 2019], which was already a factor of 100 below previously published LC-MS/MS methods with detection limits of 10 ng/mL [Baralla et al. 2011; van den Broek et al. 2010]. However, this sensitivity was not sufficient to determine endogenous levels of bradykinin throughout all their plasma samples [Lindström et al. 2019].

In the current study, for the first time in NLF, concentrations of endogenous levels of specific kinin peptides were detectable in saline matrix and allowed for their comprehensive determination. Proud et al. 1983, measured kinin peptides in eight controls by immunometric detection, seven had levels below the LLOQ (< 20 pg/mL) and one had a level of 100 pg/mL. As mentioned above, a quantitative breakdown of the total kinin concentration compared to the respective peptides could not be made [Proud et al. 1983]. Turner et al. 2000, determined kinin levels of 68 (43–183) pg/mL (combined bradykinin and kallidin without distinction) (median (80% central range), $n=8$) [Turner et al. 2000]. This is in line with the measured levels of healthy volunteers in NLF, where distinguished mean levels of 22.5 pg/mL for bradykinin and 8.2 pg/mL for kallidin were obtained. Levels for bradykinin 1-7, des-Arg(9)-bradykinin, des-Arg(10)-kallidin and bradykinin 1-5 were also in the low pg/mL range, as expected. Whereas bradykinin, bradykinin 1-7 and des-Arg(9)-bradykinin were detectable in all samples, presence of the other kinins in NLF varied individually and bradykinin 2-9 was below the quantification limit in all samples. Because levels of the cleaved peptides are not published elsewhere, a reliable classification of the concentrations is only possible to a limited extent, and it is rather necessary to ascertain these endogenous levels in larger healthy and diseased cohorts in future studies. Levels in patients are expected to exceed those in healthy volunteers if the hypothesis of a dysregulated KKS in COVID-19 can be confirmed. Therefore, the broad calibration curve range of the developed assay, covering a span of a factor of 250–1000 depending on the analyte, is expected to be suitable because it allows measuring endogenous levels in healthy controls, as well as detecting possible elevations. Further, application of the assay can easily be extended to other diseases in which alterations within the KKS are to be expected and provides the advantage of non-invasive and easy-to-handle sampling. Thus, it allows to investigate e.g. lung cancer, respiratory allergic reactions, and bradykinin-mediated side effects of ACE inhibitors [Hicks et al. 2018; Borghi & Veronesi 2018; Golias et al. 2007].

The developed LC-MS/MS assay further outmatched previously published immunoassay methods separating kinin peptides (bradykinin 1-7, des-Arg(9)-bradykinin, and bradykinin) in the low-abundant endogenous range regarding sample preparation effort, as it makes the final results available within 2 hours of sampling. Campbell et al. 1993 applied a combination of C18 SPE followed by liquid-liquid extraction and chromatographic separation prior to immunoradiometric detection [Campbell et al. 1993]. Duncan et al. 2000 purified their samples through five rounds of SPE followed by chromatographic separation before the fractions were

analysed by immunoassay [Duncan et al. 2000]. Lower limits of quantification (0.3–0.4 pg/mL) were reached using these approaches; however, also 1 mL of blood was applied, which subsequently shows a sensitivity nearly equal to the presented LC-MS assay (100 μ L sample volume). Advantages of the LC-MS assay are that falsification due to cross-reactivity can be excluded, and the obtained values are attributed to single peptides. Further, the significantly reduced sample preparation effort achieved in combination with a fast analysis time (~2 hours vs. ~1 day), provides the opportunity to reduce the time working with potentially infectious patient samples.

Isotonic saline was chosen as the surrogate matrix for preparation of calibration curve and quality control samples to obtain blank matrix and avoid any interference with endogenous kinin peptides in respiratory lavage fluids. This was presumed to be an adequate approach, as NLF is mostly made up of saline owing to instillation with saline during lavage, with a reported dilution of factor 60–120 [Franciosi et al. 2011]. Further, mucus, debris, and cells are separated by centrifugation. An important issue in quantitative lavage analysis is that the volume infused during saline lavage is not always equal to the volume sampled [Bowen & Licea-Perez 2013]. Therefore, when comparing data sets of determined peptide levels, e.g. at different time points or in different patients, normalizing against an endogenous dilution marker, such as albumin, total protein abundance, or urea has been proposed [Rennard et al. 1986]. However, results might be influenced by capillary leakage in many respiratory disorders and an additional blood sampling is required to calculate the dilution [Rennard et al. 1986; Blic et al. 2000]. Currently, no standardization regarding normalization of lavage fluids is available as stated in a consensus statement of the International Society for Heart and Lung Transplantation in 2020 [Martinu et al. 2020]. To maintain the non-invasive manner of the assay, in this study the recovered volume was used for normalization, which is the most commonly applied normalization strategy [Martinu et al. 2020]. Because saline is used as surrogate matrix, the assay is not limited to the investigation of respiratory saline lavage fluids in humans, but can also be used in animal models. Thereby, the innovative assay allows to investigate the pathophysiology of COVID-19 but might also support the identification of possible new therapeutic targets if the hypothesis of an altered KKS can be confirmed in COVID-19.

6.5. Conclusion

In conclusion, the novel LC-MS assay facilitates the comprehensive determination of kallidin, bradykinin, des-Arg(10)-kallidin, des-Arg(9)-bradykinin, bradykinin 1-7, bradykinin 2-9 and bradykinin 1-5 for the first time in saline. The method is well-suited for research purposes considering its high sensitivity and broad calibration curve range in combination with low applied volumes. The successfully validated method will contribute to elucidate the pathophysiology of SARS-CoV-2 by facilitating the investigation of the postulated connection between a dysregulated KKS and other clinical syndromes (e.g. COVID-19).

7. Mass spectrometric study of variation in kinin peptide profiles in nasal fluids and plasma of adult healthy individuals

7.1. Background

The KKS is a complex cascade of proteins, proteases, and active and inactive kinin peptides. The KKS is involved in physiological and pathophysiological processes and is thoroughly intertwined with the RAAS; both systems acting counterregulatory to maintain physiological haemostasis [Schmaier 2003]. Kinins are inflammatory mediators implicated in the pathological development of cardinal signs of inflammation [Marceau et al. 2020]. Kinins exert their action by activating the G-protein coupled bradykinin receptors type 1 and 2, whereby type 1 is particularly upregulated during inflammation (Figure 1) [Broadley et al. 2010]. Despite the KKS's proposed involvement in many diseases, such as sepsis, COVID-19, stroke, Alzheimer's disease, and allergic reactions, hereditary angioedema currently remains the sole therapeutic application of targeting this system [Nicola 2017; Kaplan & Ghebrehiwet 2021; Marceau et al. 2020; Nokkari et al. 2018].

Lack of data establishing kinins as biomarkers has limited their clinical use. Scientific progress regarding robust kinin quantification has lagged behind comparable systems like the RAAS despite similar advances in scientific methodologies over the past decades [Bakhle 2020]. Determination of immunoreactive kinins does not differentiate the bradykinin type 2 receptor agonists bradykinin and kallidin, which are released through different pathways (Figure 1). Furthermore and particularly in plasma, bradykinin levels varying by several orders of magnitude (low pM to high nM) have been published, hindering distinction between health and disease as well as interstudy comparisons [van den Broek et al. 2010; Duncan et al. 2000; Lindström et al. 2019]. This variability is attributed to the high sensitivity of kinin level results to specimen handling during the pre-analytical and analytical phase; the short half-lives of kinin peptides and artificial generation of the kinin bradykinin in plasma via contact activation of factor XII render specimen handling technique essential (Figure 1) [Kaplan & Maas 2017; Schmaier 2016]. Moreover, existing data are often restricted on reporting levels of single kinin levels, thus neglecting the distinct effects of multiple active kinins on the two bradykinin receptor types and diverse metabolic pathways (Figure 1).

Recently, reliable and robust kinin determination has been investigated extensively using modern bioanalytical techniques. Improvement of the sensitivity of mass spectrometric assays established validated LC-MS/MS platforms for the comprehensive determination of active and inactive kinins in human plasma and respiratory lavage fluids (section 4, 5 and 6

This work is currently under review in a peer-reviewed journal:

Gangnus T, Burckhardt BB. Mass spectrometric study of variation in kinin peptide profiles in nasal fluids and plasma of adult healthy individuals. *Journal of Translational Medicine*

The author of this thesis was responsible for conceptualization, performance of experiments, data analysis, writing – draft & approval, visualization.

[Gangnus & Burckhardt 2021a; Gangnus & Burckhardt 2021c; Gangnus & Burckhardt 2020]). This technique facilitated the investigation and subsequent standardization of pre-analytical variables, contributing to a substantial reduction in inter-day and interindividual variability of plasma kinin levels (section 5 [Gangnus & Burckhardt 2022]). However, there is biological variation among healthy individuals, which might be additionally confounded by artificial kinin changes. Thus, a better understanding of kinin profiles in healthy individuals is essential for exploring and distinguishing disease-specific kinin profiles, as it has already become achievable for the RAAS [Kutz et al. 2021; Arendse et al. 2019]. Understanding disease-specific kinin profiles has become a subject of focus during the COVID-19 pandemic, where increased des-Arg(9)-bradykinin levels secondary to decreased ACE 2 activity after binding of SARS-CoV-2 have been implicated [van de Veerdonk et al. 2020b; Maat et al. 2020]. Considering the paucity of kinin level data for respiratory lavage fluids and diverging plasma levels, determining endogenous profiles in healthy individuals is indispensable to allow the identification of altered kinin levels in COVID-19 and other diseases.

Therefore, it was aimed to comprehensively study biological levels and variations in kinin peptide profiles (bradykinin, Hyp(3)-bradykinin, kallidin, Hyp(4)-kallidin des-Arg(9)-bradykinin, des-Arg(10)-kallidin, bradykinin 1-7, bradykinin 2-9, and bradykinin 1-5) in nasal fluids and plasma within a population of healthy volunteers using the above-mentioned LC-MS/MS platforms.

7.2. Materials and methods

7.2.1. Study design

This study was conducted per the principles expressed in the Declaration of Helsinki and approved by the ethics committee of the medical faculty at the Heinrich Heine University (study number: 6112). All participants provided written informed consent before their enrolment. Bioanalysis was conducted in compliance with Good Clinical Laboratory Practice. Healthy volunteers above the age of 18 years without any signs of respiratory infection or acute allergy were recruited (Appendix 11). Volunteers taking drugs interfering with the KKS were excluded. Participants were tested for COVID-19 (Panbio™ COVID-19 Ag Rapid, Abbott Laboratories, IL, US) to rule out asymptomatic SARS-CoV-2 infection before biological fluid sampling. Venous blood, NLF and demographic data were collected from the volunteers.

7.2.2. Blood sampling

A standardized protocol, proven to significantly limit inter-day and interindividual variability of kinin levels in plasma was employed for the collection of venous blood [16]. Blood was collected in the upright position into 2.7 mL K3 EDTA S-Monovettes® (Sarstedt, Nümbrecht, Germany) prespiked with customized protease inhibitor under aspiration (section 5 [Gangnus & Burckhardt 2021b]). Sampling into three consecutive tubes was performed to confirm adequate blood sampling by assessing inter-tube variability of bradykinin, which was aimed to be <2 pM. In addition, a fourth tube was drawn in the absence of inhibitors to monitor the impact of lack of inhibitors and inappropriate sampling on the artificial generation of plasma kinin levels. Therefore, protease inhibitor was added to the fourth tube 15 min after venipuncture.

Additionally, it was investigated whether kinin levels were subject to circadian rhythms. Blood was taken from a male and a female subject at the following time-points: 6 a.m., 9 a.m., 12 p.m., 3 p.m. and 6 p.m.

Blood was sampled using 21 G Safety Multifly® needles with 200 mm tubing (Sarstedt, Nümbrecht, Germany) from the left or right median cubital, cephalic, or basilic vein with the needle inserted in an antegrade fashion. Blood samples were immediately centrifuged at 2000 x g for 10 minutes at room temperature. Plasma was stored at -80 °C until analysis.

7.2.3. Sampling of nasal lavage fluid

Nasal lavage was performed with 10 mL of 0.9% normal saline (B. Braun, Melsungen, Germany) using 5 mL pre-filled syringes for each nostril and a Schnozzle® Nasal Irrigation Adapter (Splash Medical Devices, LLC, GA, US). The volunteers were asked to tip their heads

backwards, hold the breath, and refrain from swallowing. The fluid obtained was collected directly into the protease inhibitor and was vortexed after completing the sampling. At least 30% of the instilled volume had to be recovered during the lavage in line with the American Thoracic Society guideline for bronchoalveolar lavage [Meyer et al. 2012]. The samples were centrifuged at 4 °C for 15 min at 500 × g to remove cells, mucus, and debris. NLF samples were stored at -80 °C until analysis.

7.2.4. Estimating endogenous kinin levels in nasal epithelial lining fluid

Kinin levels in NLF are diluted by lavage fluid and therefore do not represent endogenous kinin levels. To allow for the estimation of kinin levels in endogenous nasal epithelial lining fluid (NELF), the dilution of urea in NLF compared to plasma was determined. Therefore, urea nitrogen was measured by an enzyme immunoassay (EIABUN, Invitrogen™, Carlsbad, CA, USA) in NLF (undiluted) and plasma (1:20 dilution) of healthy volunteers. The urea nitrogen assay performance was confirmed to be linear (mean $R^2 = 1$ [n = 4]), accurate (within- and between accuracy between -1.9% and 2.2% at three QC levels [low, mid, high]) and precise (within-run and between-run precision <3.6% at three QC levels [low, mid, high]), applying the customized protease inhibitor.

The dilution factor was then calculated by Equation 3 [Kaulbach et al. 1993]:

$$Dilution\ factor = \frac{[Urea_{plasma}(mg/dl)]}{[Urea_{NLF}(mg/dl)]}$$

Equation 3. Calculation of the dilution factor by nasal lavage. NLF: nasal lavage fluid

Using the determined individual-dependent dilution factor, kinin levels were corrected for the dilution by nasal lavage as follows (Equation 4 [Kaulbach et al. 1993]):

$$Kinin\ concentration_{NELF} = Kinin\ concentration_{NLF} * Dilution\ factor$$

Equation 4. Calculation of the kinin concentration in NELF. NELF: nasal epithelial lining fluid, NLF: nasal lavage fluid

In addition, the volume of sampled NELF by lavage was calculated using Equation 5 [Kaulbach et al. 1993]:

$$Volume_{NELF\ sampled} = \frac{Collected\ volume}{Dilution\ factor} * \frac{Lavage\ volume}{Collected\ volume - (Collected\ volume / Dilution\ factor)}$$

Equation 5. Calculation of the nasal epithelial lining fluid (NELF) volume sampled.

7.2.5. Mass spectrometric kinin quantification

The following kinins were quantitatively assessed: kallidin (TFA salt, 96.9%, HPLC; Tocris, Bristol, UK), bradykinin (acetate salt, 99.0%, HPLC; Sigma-Aldrich, St. Louis, MO, USA), and their metabolites des-Arg(9)-bradykinin (acetate salt, 98.7%, HPLC; Santa Cruz Biotechnology, Dallas, TX, USA), bradykinin 1-7 (TFA salt, $\geq 95.0\%$, HPLC; GenScript, Piscataway Township, NJ, USA), bradykinin 1-5 (TFA salt, $\geq 95.0\%$, HPLC; GenScript), bradykinin 2-9 (TFA salt, $\geq 95.0\%$, HPLC; GenScript), and des-Arg(10)-kallidin (TFA salt, 95.9%, HPLC). In addition, hydroxylated bradykinin and kallidin were determined: Hyp(4)-kallidin ($\geq 99\%$, HPLC, Peptanova, Sandhausen, Germany) and Hyp(3)-bradykinin ($\geq 99\%$, HPLC, Peptanova). [Phe⁸Ψ(CH-NH)-Arg⁹]-bradykinin (TFA salt, 97.5%, HPLC, Tocris) was applied as the internal standard. LC-MS/MS platforms in plasma and respiratory lavage fluids had been successfully validated according to regulatory bioanalytical guidelines of the FDA [US Food and Drug Administration 2018] regarding precision, accuracy, sensitivity, linearity, matrix effects, recovery and stability. Both platforms are characterized by LLOQs down to 1.9 pM (depending on the kinin). Details on the assay characteristics have been published elsewhere (section 4, 6 [Gangnus & Burckhardt 2021a; Gangnus & Burckhardt 2021c]). All stated peptide concentrations were corrected for salt content and peptide purity, referring to the conducted amino acid analysis. Picomolar concentrations were calculated from measured pg/mL levels considering the molecular weight by the conversion factors shown in Appendix 11.

7.2.6. Data analysis

LC-MS/MS data acquisition was conducted using Analyst® 1.6.2 software (AB Sciex, Darmstadt, Germany) and raw data evaluation was executed using MultiQuant™ 3.0.2 (AB Sciex, Darmstadt, Germany). Statistical analysis and graphics were generated using OriginPro 2021 (9.8.0.200). Descriptive statistics (mean \pm SD or median [IQR]) and box-whisker-plots were used to describe kinin level data. Outcomes were analysed using the Mann-Whitney U-test or the t-test. Statistical analyses were performed with the two-sided alternative hypothesis at the 5% significance level.

7.3. Results

7.3.1. Study population

In total, 28 volunteers were enrolled. These were white with a median of 26.5 [25 – 28] years. Of those, 11 were female and 17 were male. Plasma was successfully sampled from 24 subjects and NLF samples with a recovered volume of more than 30% were collected from 24 subjects. COVID-19 antigen tests were negative for all volunteers. Detailed demographics can be found in Table 12.

Table 12. Characteristics of the healthy volunteers donating plasma and nasal fluids for kinin determination. Data are expressed as median [interquartile range] or number (n (%)).

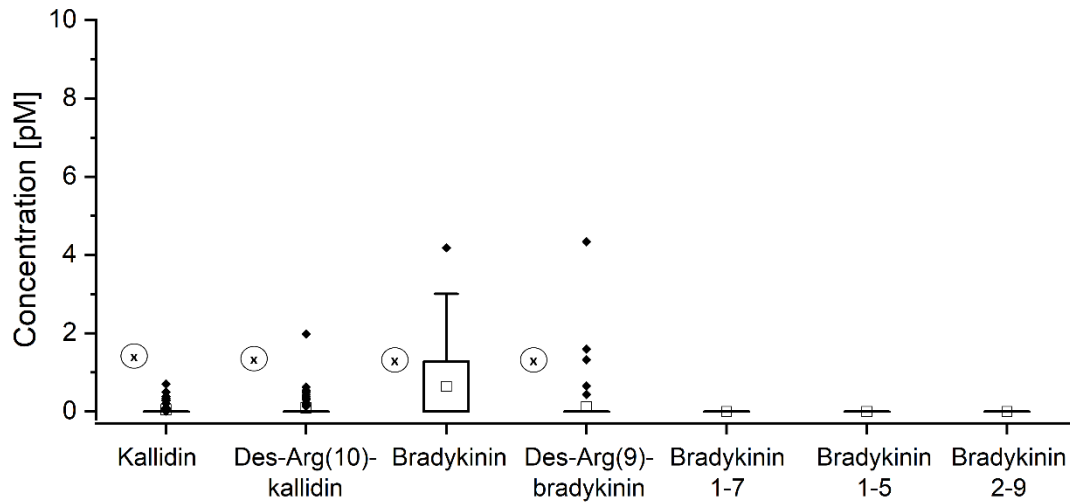
Demographics	Volunteers		
	all (n = 28)	male (n = 17)	female (n = 11)
Age [years]	26.5 [25-28]	27 [25-30]	26 [24-27]
Caucasians (n (%))	28 (100.0)	17 (100.0)	11 (100.0)
Medication (n (%))	7 (25.0)	2 (11.8) - insulin – 1 (5.9) - metoprolol – 1 (5.9)	4 (36.4) - hormonal contraception – 4 (36.4)
Reported allergies (n (%)) (all inactive)	10 (35.7)	8 (47.1) - dust mite – 3 (17.6) - pollen – 4 (23.5) - insect sting – 1 (5.9) - nuts – 1 (5.9)	2 (18.2) - pollen – 1 (9.1) - penicillin – 1 (9.1)

7.3.2. Endogenous kinin profiles in plasma

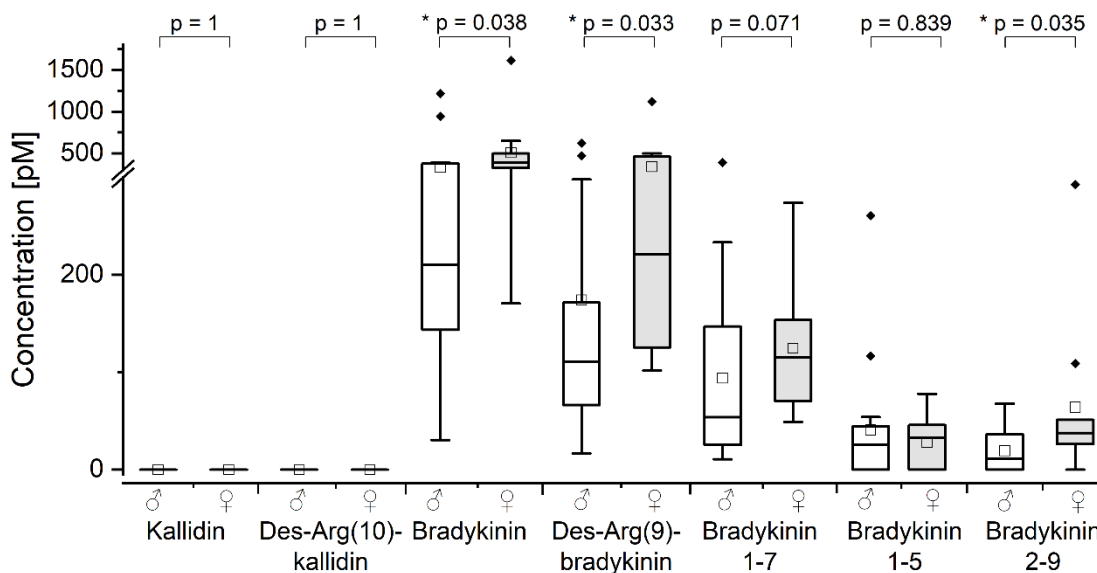
For 24 subjects, endogenous levels of kinins fell in the very low pM range, with inter-tube variations below 1.7 pM (median 0.0 [-0.2 – 0.3] pM). Median bradykinin levels were 0.0 [0.0 – 1.3] pM, with maximum level of 4.2 pM. Detected kinin levels below the validated LLOQ of the LC-MS/MS platform were set as 0. Other kinin levels were still lower and to a large extent below the LLOQ; therefore, values between the detection limit and LLOQ were recorded semi-quantitatively. For des-Arg(10)-kallidin, we measured levels from 0.2 pM (minimum) to 2 pM (maximum; n = 10), for des-Arg(9)-bradykinin 0.4 (minimum) to 4.3 pM (maximum; n = 5), and for kallidin 0.2 (minimum) to 0.7 pM (maximum; n = 9) (Figure 27). No gender-related differences in kinin concentrations were observed.

Furthermore, these low endogenous levels were confirmed throughout the day (6 a.m. to 6 p.m.) in one male and one female subject. No association between circadian rhythms and kinin levels was found.

A. Endogenous plasma levels



B. Plasma levels with delayed addition of inhibitor



C. Kinin levels (median [IQR])

Kinin	Endogenous (n = 24)	Delayed inhibition (n = 25)	LLOQ of assay
Kallidin [pM]	< LLOQ	< LLOQ	3.4
Bradykinin [pM]	0.0 [0.0 – 1.3]	322.2 [171.2 – 425.8]	1.9
Des-Arg(10)-kallidin [pM]	0.0 [0.0 – 0.0]	< LLOQ	1.9
Des-Arg(9)-bradykinin [pM]	0.0 [0.0 – 0.0]	160.8 [100.7 – 298.1]	2.2
Bradykinin 1-7 [pM]	< LLOQ	70.4 [48.9 – 147.0]	2.6
Bradykinin 1-5 [pM]	< LLOQ	26.0 [0 – 44.6]	27.2
Bradykinin 2-9 [pM]	< LLOQ	25.7 [0.0 – 46.5]	8.6

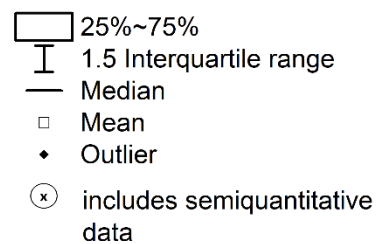


Figure 27. Kinin profiles in plasma of healthy individuals. Box plots of endogenous levels are displayed in A (n=24). Box plots of artificially altered kinin levels are presented in B (n=25). An overview of median [interquartile range (IQR)] levels is shown in C. * $p < 0.05$, Mann-Whitney U-test, LLOQ: lower limit of quantification

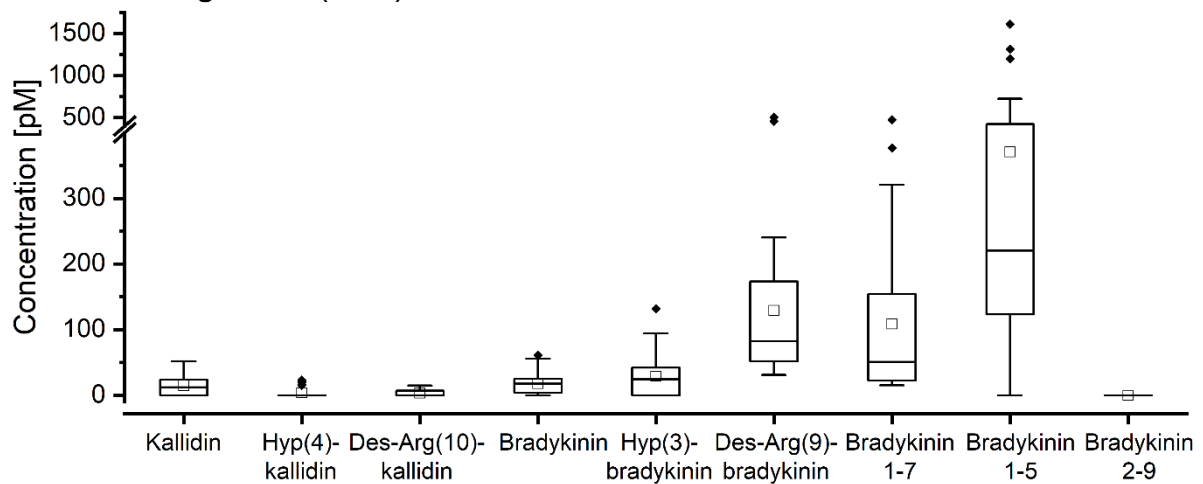
7.3.3. Kinin profiles applying inappropriate sampling conditions in plasma

Kinin levels in samples artificially altered by delayed addition of inhibitor after 15 minutes substantially increased compared with endogenous levels for bradykinin (median 322.2 [171.2 – 425.8] pM) and its metabolites des-Arg(9)-bradykinin (median 160.8 [100.7 – 298.1] pM), bradykinin 1-7 (median 70.4 [48.9 – 147.0] pM), bradykinin 2-9 (median 25.7 [0.0 – 46.5] pM), and bradykinin 1-5 (median 26.0 [0 – 44.6] pM) (Figure 27B). Kallidin and des-Arg(10)-kallidin resulted below their LLOQ. Artificial generation affected bradykinin most, and des-Arg(9)-bradykinin was the main detectable metabolite with a percentage metabolite/bradykinin ratio of 47.6% (median) after 15 minutes. Lower rates were found for bradykinin 1-7 (median 17.6%), bradykinin 2-9 (median 5.7%), and bradykinin 1-5 (median 3.8%). While no significant differences were observed between men and women regarding the relative formation of bradykinin metabolites, certain absolute kinin levels differed significantly (Figure 27). A more pronounced formation of bradykinin was found in female individuals (female: 410.9 [317.5 – 570.1] pM, male: 223 [152.2 – 401.3] pM, $p = 0.038$). While levels of bradykinin 1-5 and bradykinin 1-7 did not vary by gender, significant gender-specific differences in the generation of bradykinin metabolites were detected for des-Arg(9)-bradykinin (female: 221.4 [125.2 – 470.3] pM, male: 111.1 [66.5 – 171.5] pM, $p = 0.033$) and bradykinin 2-9 (female: 65.6 [37.5 – 292.6], male: 36.3 [11.6 – 67.7] pM, $p = 0.035$).

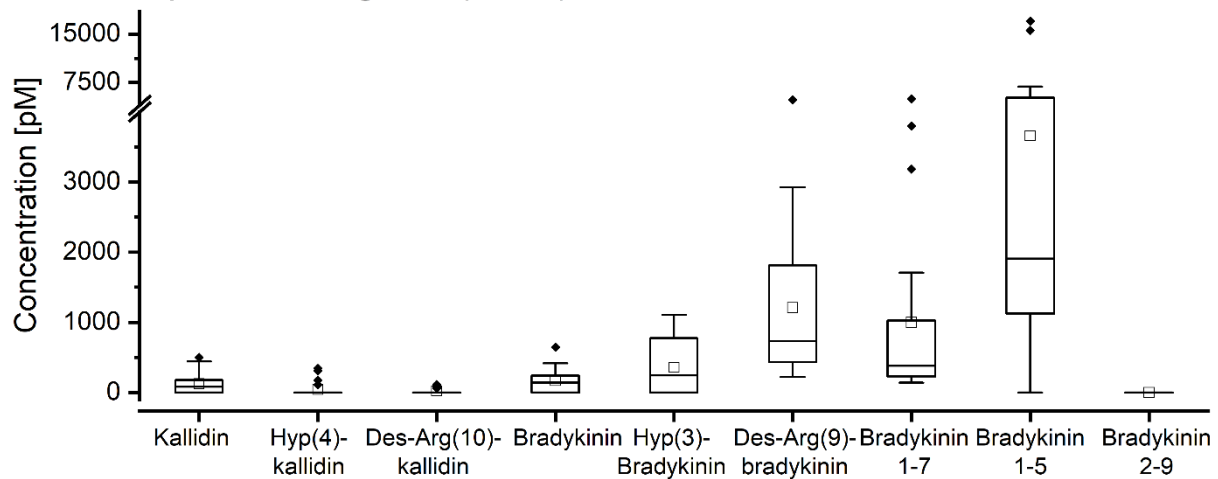
7.3.4. Kinin profiles in nasal lavage fluids of healthy volunteers

The mean percentage return volume of nasal lavage with 10 mL of saline was $73.1 \pm 11.5\%$ (Table 13). Kinin levels in NLF normalized to the return volumes were low for kallidin (12.0 [0.0 – 23.4] pM) and bradykinin (17.7 [3.9 – 25.3] pM) (Figure 28). For bradykinin, the hydroxylated form approximated the non-hydroxylated form with a mean ratio of 1.6 ± 1.0 (Figure 29A). Levels of hydroxylated kallidin were lower than non-hydroxylated kallidin with a mean ratio of 0.37 ± 0.33 (Figure 29B). Low levels of the kallidin metabolite des-Arg(10)-kallidin were only detectable in seven volunteers, resulting in median levels of 0.0 [0.0 – 6.8] pM. Higher concentrations were found for des-Arg(9)-bradykinin (82.1 [51.7 – 173.4] pM), bradykinin 1-7 (50.8 [22.1 – 153.9] pM) and bradykinin 1-5 (220.4 [123.1 – 422.2] pM). Levels of bradykinin 2-9 fell below the limit of detection. The percentage metabolite/bradykinin ratio was 604.6% (median) for des-Arg(9)-bradykinin, 568.1% for bradykinin 1-7, 1,396.3% for bradykinin 1-5 and 0% for bradykinin 2-9. No significant gender-specific differences for any kinin assessed were found in NLF.

A. Nasal lavage fluid (NLF)



B. Nasal epithelial lining fluid (NELF)



C. Kinin levels (median [IQR])

Kinin	NLF (n = 24)	NELF (n = 22)	LLOQ of assay
Kallidin [pM]	12.0 [0.0 – 23.4]	80.0 [0.0 – 177.8]	3.7
Hyp(4)-kallidin [pM]	0.0 [0.0 – 0.0]	0.0 [0.0 – 0.0]	8.1
Des-Arg(10)-kallidin [pM]	0.0 [0.0 – 6.8]	0.0 [0.0 – 0.0]	10.3
Bradykinin [pM]	17.7 [3.9 – 25.3]	139.1 [0.0 – 240.3]	6.3
Hyp(3)-bradykinin [pM]	24.4 [0.0 – 41.9]	241.5 [0.0 – 773.5]	18.5
Des-Arg(9)-bradykinin [pM]	82.1 [51.7 – 173.4]	729.6 [433.1 – 1812.3]	8.1
Bradykinin 1-7 [pM]	50.8 [22.1 – 153.9]	378.1 [230.0-1024.9]	8.6
Bradykinin 1-5 [pM]	220.4 [123.1 – 422.2]	1905.4 [1123.3 – 5138.5]	39.7
Bradykinin 2-9 [pM]	< LLOQ	< LLOQ	17.9

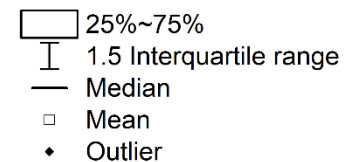


Figure 28. Kinin profiles in nasal fluids of healthy volunteers. In A. levels in nasal lavage fluid (NLF) normalized to the return volume (n=24) are shown and in B. levels in nasal epithelial lining fluid (NELF, n=22) are depicted. An overview of median [interquartile range (IQR)] levels is shown in C. LLOQ: lower limit of quantification

Table 13. Results of sampling of nasal lavage fluid. Data are expressed as mean \pm standard deviation or median [interquartile range].

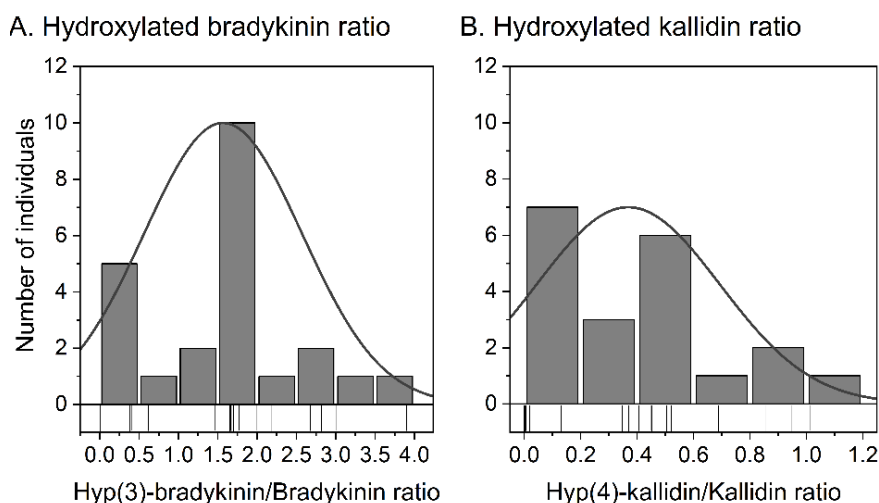
Nasal lavage	Volunteers		
	all (n = 28)	male (n = 17)	female (n = 11)
Recovered volume [%]	73.1 \pm 11.5	73.8 \pm 13.0	72.0 \pm 9.6
Plasma urea [mg/dL]	12.3 \pm 3.5	13.8 \pm 3.3	10.1 \pm 2.6
NLF urea [mg/dL]	1.0 \pm 0.6	1.1 \pm 0.4	0.9 \pm 0.7
Dilution factor	12.3 [10.0-19.0]	12.0 [10.4-16.9]	17.0 [10.0-21.6]
Volume NELF sampled [μ L]	883.6 [555.6-1,112.0]	910.4 [628.5-1,061.7]	623.5 [484.8-1,112.0]

NLF: nasal lavage fluid, NELF: nasal epithelial lining fluid

7.3.5. Estimating endogenous kinin levels in nasal epithelial lining fluid

The amount of NELF sampled was estimated by correlation of plasma and NLF urea. The median dilution factor in NLF was calculated to be median 12.3 [10.0 – 19.0] and the determined median NELF volume sampled was median 883.6 [555.6 – 1,112.0] μ L (Table 13). Estimated endogenous kinin levels in NELF were 80.0 [0.0 – 177.8] pM for kallidin, 0.0 [0.0 – 0.0] pM for Hyp(4)-kallidin, 139.1 [0.0 – 240.3] pM for bradykinin, 241.5 [0.0 – 773.5] pM for Hyp(3)-bradykinin, 378.1 [230.0 – 1,024.9] pM for bradykinin 1-7, 729.6 [433.1 – 1,812.3] pM for des-Arg(9)-bradykinin, and 1,905.4 [1,123.3 – 5,138.5] pM for bradykinin 1-5 (Figure 28). Des-Arg(10)-kallidin was quantifiable in five healthy volunteers (80.1 [75.5 – 109.0] pM, n=5), but below the LLOQ in most subjects, resulting in median levels of 0.0 [0.0 – 0.0] pM. Higher levels of des-Arg(10)-kallidin in these five individuals did not correlate with higher levels of other kinins. NELF levels for bradykinin 2-9 were not estimated, as these fell below the limit of detection in NLF. The percentage metabolite/bradykinin ratio was median 581.2% for des-Arg(9)-bradykinin, 731.2% for bradykinin 1-7, 1,533.4% for bradykinin 1-5 and 0% for bradykinin 2-9. No significant gender-specific differences were found.

Figure 29. Distribution of the hydroxylated kinin to non-hydroxylated kinin ratio for bradykinin (A) and kallidin (B). Individual data points are shown as thin lines on the x-axis.



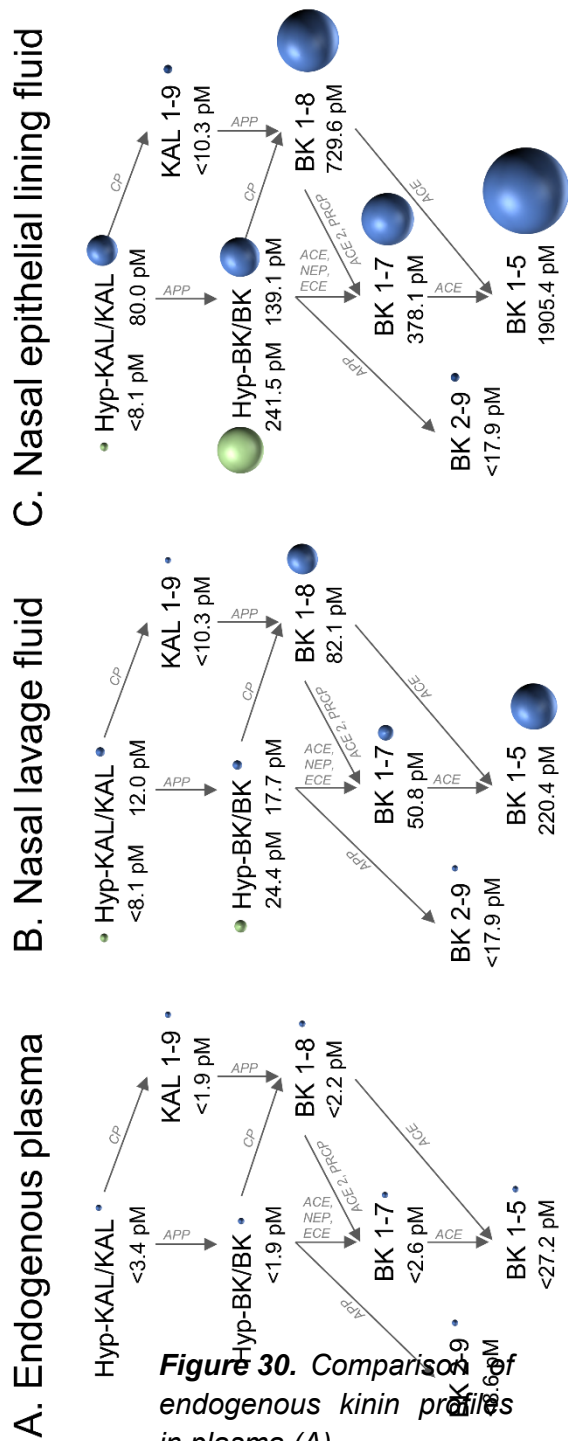


Figure 30. Comparison of endogenous kinin profiles in plasma (A), fluid (B) and nasal lining fluid (C). The ball size correlates with kinin concentration. ACE: angiotensin-converting enzyme, APP: aminopeptidase P, ECE: endothelin-converting enzyme, BK: bradykinin, CP: carboxypeptidase, Hyp: hydroxylated proline position 3 (BK) or 4 (KAL), KAL: kallidin, NEP: neprilysin, PRCP: prolyl

7.3.6. Comparison of kinin profiles in plasma and nasal fluids

Endogenous plasma levels of kinins were substantially lower compared to endogenous levels in NELF (Figure 30). In plasma, only bradykinin levels were detectable, while other metabolites fell below the quantification limit in most volunteers. In NLF and NELF, higher levels of bradykinin compared to plasma were found by a factor of 13.6 (NLF) and 107.0 (NELF). In addition, kallidin and des-Arg(10)-kallidin were quantifiable in NLF and NELF, whereas in plasma, these were only rarely detectable in samples. In contrast to plasma, endogenous metabolites of bradykinin were detectable in NLF and NELF, with bradykinin 1-5 representing the most abundant kinin.

7.4. Discussion

Within this study, kinin profiles in nasal fluids and plasma were assessed in healthy adult volunteers, a population commonly used as control groups in studies exploring biomarkers. This study presented the first comprehensive determination of nine kinin peptides and allowed the compilation of kinin profiles in 24 healthy adult individuals. While endogenous plasma levels were in the very low picomolar range, endogenous NELF levels were in the high picomolar to low nanomolar range. We found no significant gender-specific differences of endogenous kinin levels in plasma, NLF, or NELF.

Plasma kinin levels diverging in several orders of magnitude have been published thus far. For example, while Nussberger et al. measured bradykinin levels of 2.2 pM (n=22), van den Broek et al. found levels of 100.7 nM (n=6), a difference by a factor of approximately 50,000 in healthy volunteers [Nussberger et al. 1998; van den Broek et al. 2010]. These conflicting data hinder the comparison of data collected in this study with previously published data on kinins. Reliable research on endogenous kinin levels requires stabilization of short-lived kinins with a suitable inhibitor and control of the artificial generation of bradykinin by factor XII-mediated contact activation during sample collection and handling (section 5 [Gangnus & Burckhardt 2022; Gangnus & Burckhardt 2021b]). A standardized protocol was used in this study to measure reliable kinin levels, which allowed to confirm the blood sampling and handling process by evaluating the inter-tube variability (< 1.7 pM). The so collected bradykinin level data in healthy volunteers confirmed low levels of circulating bradykinin in plasma [Duncan et al. 2000; Nussberger et al. 1998; Nielsen et al. 1982; Campbell 2000]. Moreover, comprehensive data for six kinins in plasma were assessed and enhanced available data for bradykinin metabolites in plasma [Duncan et al. 2000; Seip et al. 2014; Campbell et al. 2005].

To date, only two studies have published data on kinin levels in NLF. These studies detected immunoreactive bradykinin levels between <18.9 – 141.5 pM [Proud et al. 1983] and median 64.2 pM [Turner et al. 2000] in eight volunteers, respectively. Assessment of immunoreactive bradykinin does not differentiate bradykinin from kallidin or their hydroxylated forms. In contrast, within this study kinins were selectively measured in 24 volunteers, whereby the sum of collected bradykinin and kallidin levels and their hydroxylated forms matched previous determinations of immunoreactive bradykinin [sum of medians: 54.1 pM]. However, NLF concentrations do not represent endogenous levels in NELF. Adjusting for differences in plasma and NLF urea, endogenous human NELF kinin levels were estimated for the first time and these levels were found to be higher than in NLF by a median factor of 12.3 using a lavage volume 10 mL. Altogether, higher levels of kinins were demonstrated in nasal fluids than in plasma, reflecting that KKS is primarily a tissue-based system [Campbell 2000].

Moreover, this study was not restricted on determining only the immunoreactive kinin fraction, but nine kinins were assessed differentiated. This is advantageous for several reasons. First, numerous pathways influence the formation and degradation of kinins *in vivo*, and disease and pharmacological agents may affect these pathways differently. Such effects can now be comprehensively studied using the collected kinin profiles in the present healthy cohort. Second, in addition to bradykinin, other active kinins, such as kallidin, des-Arg(9)-bradykinin, and des-Arg(10)-kallidin, act on different receptors, which in turn are regulated in a disease-specific manner. Comparison of pathological alterations against physiological kinin profiles may help identify new therapeutic targets. Third, kinins exist in both hydroxylated and non-hydroxylated forms [Campbell 2013; Campbell 2000]. The kinins bradykinin and kallidin and their respective hydroxylated forms exhibit similar biological activities but may be altered in a disease-specific manner [Dengler et al. 1990; Regoli et al. 1989]. The collection of kinin profiles in healthy volunteers, who frequently serve as control groups in clinical studies, facilitates the investigation of disease-related alterations in kinin profiles. For example, it was found that hypoxia increases bradykinin hydroxylation via increased activity of prolyl-4-hydroxylase- α 1 [Liu et al. 2020], and diseases such as COVID-19 may induce hydroxylation of kinins. Clinical investigation of this and similar hypotheses is now enabled by evaluating reference kinin profiles in healthy individuals.

With advancing scientific methodology, kinins may evolve into promising biomarkers in the future. For example, in COVID-19, an increase in bradykinin formation and a decrease in degradation of proinflammatory des-Arg(9)-bradykinin is thought to be responsible for symptoms [van de Veerdonk et al. 2020b; Nicolau et al. 2020]. The clinical picture of sepsis represents another promising field; the significance of kinins in humans remains unclear, but therapeutic benefits have been shown in *in vivo* animal models by administering bradykinin receptor type 1 antagonists [Nicola 2017]. Moreover, the KKS is known to be involved in the development of asthma, allergy, angioedema, epilepsy, stroke, and Alzheimer's disease [Ricciardolo et al. 2018; Kaplan & Maas 2017; Nokkari et al. 2018]. The evaluation of kinin profiles in these pathological processes using physiological profiles as a baseline for comparison may establish a better understanding of the pathophysiology, provide evidence for new therapeutic targets, and improve monitoring of the disease course.

7.5. Conclusion

In this study, comprehensive profiles of endogenous kinin profiles were collected in nasal fluids and plasma of healthy adult volunteers, which may serve as control groups in clinical studies exploring the value of kinins as biomarkers. While circulating plasma kinin levels were below 4.2 pM in our subjects, levels in NELF were in the high picomolar to low nanomolar range, depending on the kinin. We found no gender-specific differences in the fluids studied. The knowledge of comprehensive kinin profiles in healthy volunteers now forms the basis for evaluating disease-specific diagnostic or prognostic information of kinin profile alterations in diseases such as angioedema, sepsis, COVID-19, epilepsy, and Alzheimer's disease.

8. Investigation of kinin peptides in biological fluids of COVID-19 patients

8.1. Background

Shortly after the onset of the pandemic COVID-19, the first hypothetical publications appeared linking the symptoms of COVID-19 to the KKS (Figure 31). Symptoms were proposed to be associated to clinical and laboratory signs of inflammation (e.g. increased interleukine-1, interleukine-6, TNF α) [Moore & June 2020], which might be triggered by bradykinin receptor activation. In April 2020, van de Veerdonk et al proposed reduced inactivation of des-Arg(9)-bradykinin by ACE 2 due to SARS-CoV-2 binding [van de Veerdonk et al. 2020b]. As a consequence, activation of B₁ receptors was hypothesized to induce local vascular leakage in the lungs during ARDS. Hence, pharmacotherapeutic blockade of the KKS was suggested as a treatment strategy to prevent ARDS. This hypothesis was followed by many researchers and supplemented regarding proposed mechanisms. An increased kallikrein activity or alternative cleavage of HMWK by virus proteases was suggested, resulting in increased bradykinin levels [Nicolau et al. 2020]. The combined investigation of the KKS with the plasma contact system was further suggested to uncover the role of kinins on COVID-19 pathology due to potential linkage regarding bradykinin production in COVID-19 [Maat et al. 2020; Kaplan & Ghebrehiwet 2021; Meini et al. 2020]. In July 2020, Garvin et al. suggested a 'bradykinin storm' might be responsible for more severe symptoms observed during COVID-19 based on their findings after gene expression analysis. The research group found RNA upregulation of the B₁ receptor (2956-fold), the B₂ receptor (207-fold), the bradykinin precursor HMWK (2366-fold) and carboxypeptidase N (671-fold), which turns bradykinin into des-Arg(9)-bradykinin. In contrast, other bradykinin degrading enzymes like ACE (-8-fold) were downregulated. Further, the gene coding for C1-esterase inhibitor, which prevents activation of Factor XII was downregulated (-33-fold), thus opening the way for increased bradykinin formation. However, all insights were based on RNA analysis and impacts on protease activities and active peptide levels remained unresolved. In February 2021, further evidence to a dysregulated KKS was added, when Lipcsey et al. reported very low concentrations of Factor XII, prekallikrein and HMWK in comparison to controls [Lipcsey et al. 2021]. Low levels of these markers indicate an upregulation of the KKS, as these precursors are consumed. In addition, significant correlation of lower levels of these markers with mortality and organ failure were found. Due to these correlations, activation of the KKS along with the complement system was suggested to have a main role in driving inflammation.

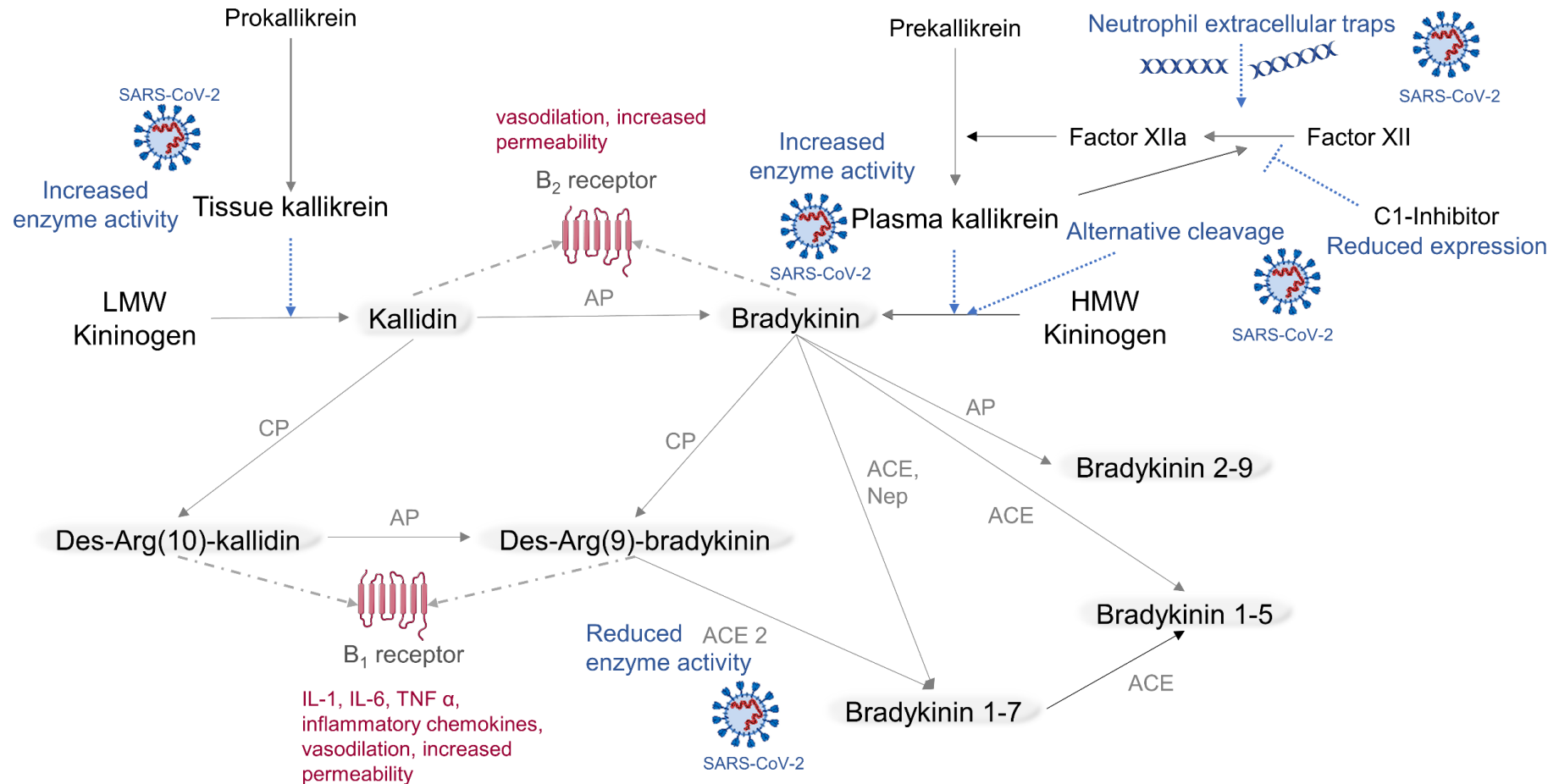


Figure 31. The kallikrein-kinin system with its link to the contact activation system in COVID-19. Reduced inhibition of Factor XII activation with increased stimulation of its activation by neutrophil extracellular traps might result in increased plasma kallikrein activity. In addition, tissue kallikrein activity was proposed to be increased, as well as SARS-CoV-2 mediated cleavage of HMW Kininogen was suggested. ACE 2 activity was hypothesized to be reduced due to virus binding, thus causing des-Arg(9)-bradykinin accumulation. Bradykinin receptor stimulation effects hyperpermeability, vasodilatory, and inflammatory effects. ACE: angiotensin-converting enzyme, AP: aminopeptidase, CP: carboxypeptidase, HMW: high molecular weight, LMW: low molecular weight, Nep: neprilysin, SARS-CoV-2: severe acute respiratory coronavirus 2

Despite increasing evidence for a role of the KKS in COVID-19 pathology, investigation of kinin peptides is still of particular interest. These peptides are the active mediators on bradykinin receptors and supposed to promote some of the most severe symptoms observed in COVID-19 like lung oedema, cardiovascular dysfunction, or thromboembolism. Only their investigation in addition to previous studies might allow for a more complete understanding of the pathology of COVID-19 and the interference of SARS-CoV-2 with the KKS.

8.2. A dysregulated kallikrein-kinin system in COVID-19 patients

In cooperation with the Katholieke Universiteit (KU) Leuven, Belgium (Peter Verhamme, Thomas Vanassche), the KKS was studied in BALF of COVID-19 patients. The following is a short summary of the joint publication [Martens et al. 2021].

In the study at the University Hospital Leuven, 21 patients hospitalized for COVID-19 and 19 patients hospitalized without COVID-19 were enrolled. While measurement of Myeloperoxidase-DNA (MPO-DNA), a marker for NETs, kallikrein and hydrolytic activity were measured at the Rega institute for medical research / KU Leuven, kinin levels were determined after ultraviolet virus inactivation at the Institute of Clinical Pharmacy (HHU) in Düsseldorf. The LC-MS/MS assay for the determination of kinins in respiratory lavage fluid, established in the course of this work (Section 6), contributed to enabling kinin quantitation in the highly diluted BALF. Whereas endogenous levels could not be determined by immunometric detection, the sensitive LC-MS/MS assay allowed for their quantification. This highlighted the value and importance of the here presented established LC-MS/MS platforms for clinical studies.

Levels of kallidin, des-Arg(10)-kallidin and bradykinin did not significantly differ between controls and COVID-19 patients (Figure 32 and Appendix 12 with pg/mL and pM levels). For des-Arg(9)-bradykinin and bradykinin 1-7 a trend towards increased levels in COVID-19 patients was detected (des-Arg(9)-bradykinin (median with [IQR]) 0.0 [0.0 – 40.3] pM in controls and 19.6 [4.0 – 62.8] pM in COVID-19 with $p = 0.062$; bradykinin 1-7 37.6 [14.9 – 121.6] pM in controls and 128.6 [39.7 – 259.3] pM in COVID-19 with $p = 0.056$). A significant difference was found for the most stable kinin bradykinin 1-5, with levels of 0.0 [0.0 – 88.8] pM in controls and 156.6 [57.3 – 368.9] pM in COVID-19 ($p = 0.001$). In comparison to non-COVID-19 patients, significant differences were found for tissue kallikrein, which activity was up to fourfold increased (median of 18.2 pM with IQR [4.9-756.6] vs median of 3.8 pM with IQR [1.4-12.7], respectively, $p = 0.030$). Plasma kallikrein activity was lower compared to tissue kallikrein activity and did not differ significantly between COVID-19 and non-COVID-19 patients (2.1 pM with IQR [0.0-4.5] vs 0.3 pM with IQR [0.0 – 0.8], $p = 0.183$). MPO-DNA complexes were also substantially increased in COVID-19 patients ($p < 0.001$).

It was supposed that the observed increased kallikrein activity and kinin levels in BALF from COVID-19 patients support the hypothesis of a dysregulated KKS in COVID-19 [Martens et al. 2021]. Proposed expression of kallikrein and kininogen genes in BALF of COVID-19 patients [Garvin et al. 2020] was hence also confirmed to have an effect on the formation of peptides or activity of enzymes. In addition, NETs, which can trigger the intrinsic coagulation by pathophysiologic activation of factor XII, were found to be elevated, and might provide the link between the KKS and observed thromboinflammatory symptoms in COVID-19.

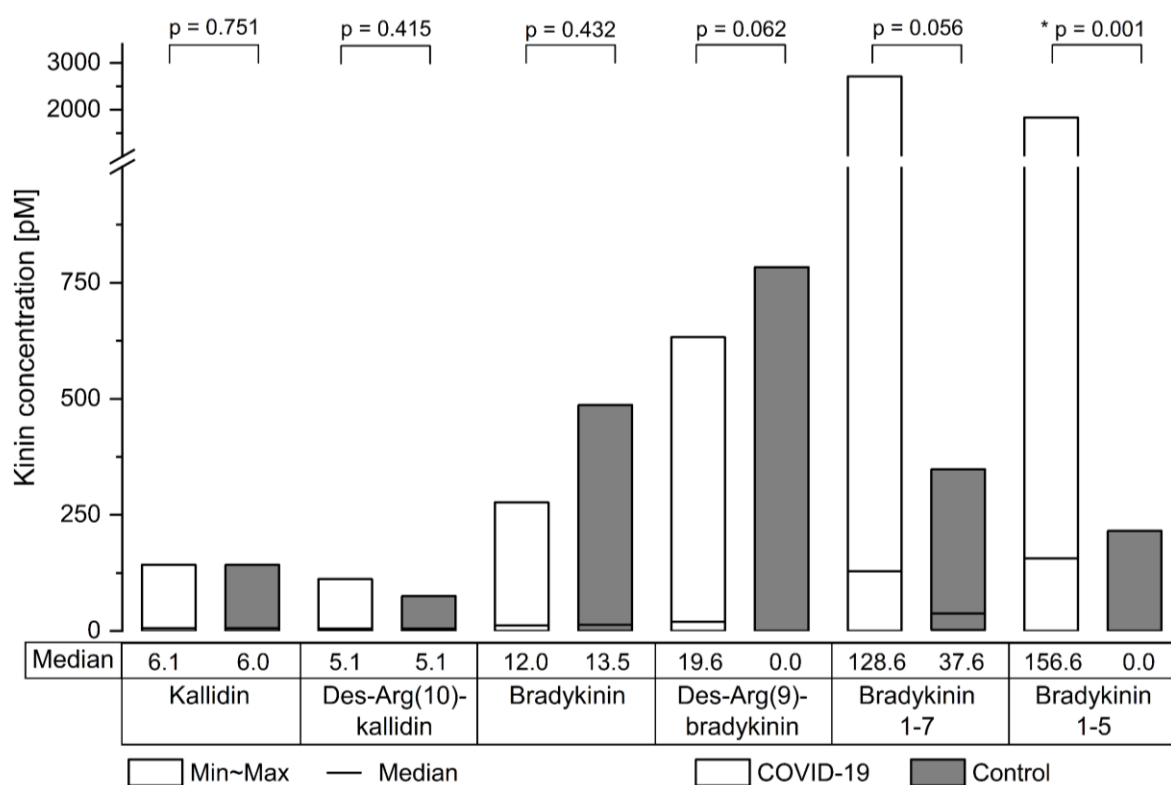


Figure 32. Kinin levels measured in bronchoalveolar lavage fluid of COVID-19 patients ($n=21$) and controls ($n=19$). Levels are expressed as median with [min-max] range [Martens et al. 2021].

However, logistical difficulties owing to the highly infectious sample material delayed the addition of the protease inhibitor. Due to the short half-life of bradykinin and kallidin in particular, the difference in kinin concentrations may therefore have become apparent only for the more stable peptides, such as bradykinin 1-5. Therefore, the effect of binding of SARS-CoV-2 to ACE2 on des-Arg(9)-bradykinin levels remains unknown for the time being.

Still, the insights gained from the studies conducted encourage the evaluation of drugs that interfere with the KKS as treatment options for COVID-19. Examples are the kallikrein inhibitor aprotinin, the B₂ receptor blocker icatibant, or the kallikrein inhibitory antibody lanadelumab. However, further research is still required to elucidate the complex interactions between the coagulation system, the fibrinolytic system, the KKS, the complement system, and the RAAS in COVID-19.

For this purpose, further studies are currently in progress or under evaluation. In collaboration with Radboud University medical centrum (Frank van de Veerdonk, Job Engels, Coen Maas) plasma of COVID-19 patients was recently analysed and is currently being evaluated. In addition, a cooperation with the University Hospital Düsseldorf (UKD) is being planned. These studies are sought to further contribute to a better understanding of the pathophysiology of SARS-CoV-2 and provide evidence for new pharmacotherapeutic targets.

9. Overall conclusion and perspective

In final summary, this thesis presents modern bioanalytical platforms for the reliable mass spectrometric quantitation of peptides in the kallikrein-kinin system from human biological fluids (Figure 33). Known issues, like their low abundance, poor mass spectrometric ionization efficiency, non-specific peptide adsorption, structural similarity, artificial generation in plasma, and their short half-lives, were systematically approached and advanced. The successfully established LC-MS/MS platforms were demonstrated to facilitate the reliable and accurate quantification of a complex endogenous peptide cascade. In this context, reliable quantification was meaningfully extended to sample collection and preparation by a tailored preanalytical protocol proven to significantly limit inter-day and interindividual variability. Finally, these sophisticated bioanalytical settings were applied within clinical trials and contributed to collect comprehensive kinin profiles in healthy and to confirm the hypothesis of a dysregulated KKS in COVID-19.

In order to achieve the basis for a reliable and accurate determination of the kinin peptides, systematic investigations were first carried out by means of DoE during method development. A critical determinant in LC-MS/MS quantification regarding peptides is sensitivity; the latter was substantially increased with regard to low abundant endogenous kinin levels. By mobile phase optimization, improvements by a factor of 7.7 through boosting electrospray ionization were achieved. Similarly, non-specific peptide adsorption to container materials or autosampler parts, which is more pronounced in lower concentrations, was successfully reduced by a striking factor of 26.6 when comparing the optimised injection solvent to water as the injection solvent and storage in polypropylene. Thereby, a high acidic fraction (up to 10%) was seen to be beneficial in order to reduce non-specific adsorption of kinins in polypropylene. The investigations carried out provided a refined understanding of key influencing factors and enabled multiple-point solutions for extending the findings to the incorporation of the remaining kinin peptides. Further, these optimizations were indispensable to achieve sensitive quantification limits appropriate for endogenous levels and to improve accuracy and precision of subsequently established bioanalytical assays.

Following, a comprehensive LC-MS/MS platform for seven kinins was developed using 96-well µelution SPE to promote a high sample throughput that meets the current requirements for analytical procedures in the context of clinical studies. Comprehensive validation of the developed LC-MS/MS assays according to current international bioanalytical regulatory guidelines confirmed the reliability for kinin determination in plasma. Linearity, accuracy, precision, sensitivity, carry-over, recovery, parallelism, matrix effects and stability were assessed in plasma of healthy volunteers. High sensitivity was achieved with LLOQs of 2

pg/mL – 15.2 pg/mL (depending on the kinin) using only 150 μ L of plasma. This represents an exceptional sensitivity in comparison to previously published LC-MS/MS assays for kinin peptides and confirmed the advantageous effects of DoE optimization during method development. No source-dependent matrix effects were identified, and suitable stability of the analytes in plasma was observed. In addition, the level of validation and the number of kinins concurrently recorded exceeds by far previously published assays. The confirmation of the fit-for-purpose suitability of the analytics by successful guideline-conform validation of the LC-MS/MS platforms, built the prerequisite for further investigation of preanalytical variables.

So far, heterogeneous concentrations of kinins had been reported in healthy humans and thus highlighted the urgency for investigation of impacting preanalytical variables beyond ensuring reliable analytical performance. Artificial *ex vivo* rise of bradykinin in plasma was found to already occur 30 s after blood sampling with high interindividual variation but was successfully prevented by a customized protease inhibitor. The reliability of kinin levels was substantially jeopardized by prolonged storage as whole blood, blood collection methodology (e.g. straight needles, catheters), the vacuum sampling technique or any time delays during venipuncture. The proposed standardized protocol was applied to healthy volunteers within a proof-of-concept and proven to significantly limit inter-day and interindividual variability of kinin levels. Thus, it was indicated, that by using a standardized protocol artificial rise of kinins via contact activation was controllable and reproducible kinin levels were measurable.

In a next step, the LC-MS/MS platform was then extended to alternative, non-invasive determination of kinins from respiratory lavage fluids. The fit-for-purpose suitability of this platform was also successfully confirmed according to regulatory guidelines of the FDA regarding linearity, accuracy, precision, sensitivity, carry-over, recovery, matrix effects and stability. Sensitive LLOQs in the range from 4.4 pg/mL to 22.8 pg/mL (depending on the kinin) were achieved using only 100 μ L of lavage fluid, despite considerable dilution of the respiratory epithelial lining fluid. Accurate mass spectrometric quantitation of multiple kinins in respiratory lavage fluids was achieved for the first time by this method.

Owing to the proven suitability of the developed LC-MS/MS platforms in combination with the tailored sample collection procedure, kinin profiles in healthy volunteers were established in plasma and NLF within a clinical trial. Such comprehensive investigations of peptides in the kallikrein-kinin system was not achieved before. Circulating plasma kinin levels were confirmed in the very low picomolar range with levels below 4.2 pM for bradykinin and even lower levels for the other kinins. Endogenous kinin levels in nasal epithelial lining fluids were substantially higher, including median levels of 80.0 pM for kallidin and 139.1 pM for bradykinin. Hydroxylated levels equalled mean bradykinin concentrations (Hyp(3)-bradykinin/bradykinin = 1.1), but hydroxylated kallidin levels were substantially lower than kallidin (Hyp(4)-

kallidin/kallidin = 0.16). No gender-specific differences on endogenous kinin levels were found. This well-characterized healthy cohort enables investigation of the potential of kinins as biomarkers and would provide a valid control group to study alterations of kinin profiles in diseases, such as angioedema, sepsis, stroke, Alzheimer's disease, and COVID-19.

Finally, the established mass spectrometric platforms were applied to determine kinin levels in COVID-19 diseased patients within international collaborations. In contrast to commercially available immunometric assays, the established LC-MS/MS assays with their broad calibration curve range were capable of quantifying low abundant endogenous levels of kinins in both, controls (n=19) and COVID-19 patients (n=31) in plasma and BALF. Besides an upregulation of kallikrein activity, kinins were significantly increased in COVID-19 as compared to the control collective. This supported the hypothesis of a dysregulated KKS put forward by scientists, and reinforced the investigation of drugs targeting the KKS in COVID-19. The prompt application of the developed methods provided a valuable contribution to the currently socially highly relevant field of corona research.

Due to the thoughtful method development, the LC-MS/MS platforms might be transferred to other biological samples after adaption of sample preparation. For example, LC-MS/MS assays for kinin quantification from saliva, urine or tissues are conceivable. The establishment of such additional assays enables more extensive studies in different body fluids or tissues, in humans or animals. Study of the status quo in multiple biological fluids of distinct body compartments may contribute to increase the knowledge regarding the *in vivo* regulation of the KKS. This opens up new horizons for the investigation of diseases and new therapeutic drug targets. Such assays are at present prepared for lung tissue, saliva and urine.

Similarly, additional kinins may be incorporated into the LC-MS/MS platforms. The chosen bioanalytical LC-MS/MS approach enables measurement of several kinins simultaneously insofar as they differ in their m/z or chromatographic retention time. The investigation of additional kinins, for example hydroxylated kinins or metabolites from subordinate degradation pathways, might offer further new insights, as they have been measured very rarely.

The sophisticated assays can be applied for a wide range of applications to support pharmacodynamic, preclinical or clinical studies. Studies may be extended in the future to investigation of diseases like sepsis, angioedema, allergy, multiple sclerosis, urticaria, diabetes or cancer. In these, the KKS was described to be associated with the disease development or progression. Despite often strong evidence from animal models, the *in vivo* links in humans are less clear. Reliable and accurate investigation of disease-specific alterations in kinin profiles in comparison to healthy volunteers might contribute to new insights into the disease pathologies. As a consequence, new therapeutic targets might be identified

and, pharmacotherapy can be improved. The low-volumes necessary for the quantification allow for repeated sampling even in severely ill patients when observing pharmacodynamic or pathophysiological responses without increasing the risk of anaemias by recurrent blood sampling. Due to successful validation according to international regulatory bioanalytical guidelines, kinins might also be used as biomarkers supporting regulatory decision making in drug development if the context of use of the LC-MS/MS platforms is enlarged. The approval of drugs targeting the KKS (kallikrein inhibitors, bradykinin receptor blockers), might be widened in this way. Just as well, the approval of promising new therapeutic drugs might be assisted. All these concepts empower to advance patient care with regard to the treatment of diverse diseases, in which the KKS is involved.

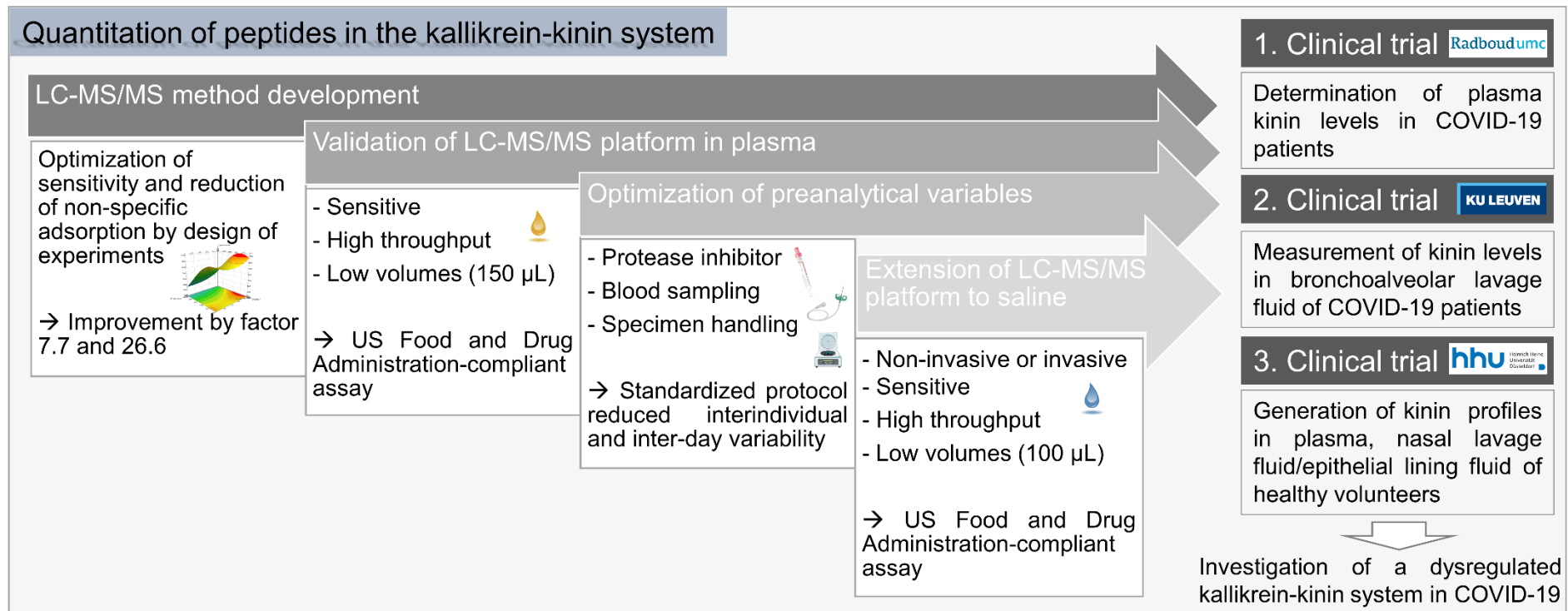


Figure 33. Overview of the conducted work to establish reliable and sensitive bioanalytical mass spectrometric platforms. All established bioanalytical platforms proved their fit-for-purpose suitability within (inter)national clinical trials (Radboud University Medical Centre [NL], Katholieke Universiteit Leuven [BE], Heinrich-Heine University Düsseldorf [GER]). COVID-19: coronavirus disease 2019, LC-MS/MS: liquid-chromatography coupled with tandem mass spectrometry

10. Acknowledgement and funding

Funding:

The work regarding the investigation of the kallikrein-kinin system in saline and bronchoalveolar lavage samples of COVID-19 patients was financed by Life Sciences Research Partners (formerly called D Collen Research Foundation), Leuven, Belgium.

The work regarding the analysis of blood samples of COVID-19 patients in plasma was financed by Radboud University, Nijmegen, Netherlands.

The work regarding the pharmacokinetic investigation of carvedilol and enalapril was supported by a combined grant of The Netherlands Heart Foundation (Grant number 2013T087) & the Foundation “Hartedroom”, The Netherlands.

Acknowledgement:

Participation in two conferences was supported by the Heine Research Academies and the Division of Analytical Chemistry of the German Chemical Society (GDCh) with congress grants.

The collaboration with Caroline P. Martens, Pierre Van Mol, Joost Wauters, Els Wauters, Bernard Noppen, Hanne Callewaert, Jean H. M. Feyen, Laurens Liesenborghs, Elisabeth Heylen, Sander Jansen, Carolina Velásquez Pereira, Sirima Kraisin, Ipek Guler, Matthias M. Engelen, Anna Ockerman, Anke Van Herck, Robin Vos, Christophe Vandembrielle, Philippe Meersseman, Greet Hermans, Alexander Wilmer, Kimberly Martinod, Marc Vanhove, Peter Verhamme, Johan Neyts, and Thomas Vanassche was greatly appreciated as it allowed to apply the developed kinin platforms to bronchoalveolar lavage samples of COVID-19 patients.

Similarly, the collaboration with Frank van de Veerdonk and Job Engel from Radboud University regarding the analysis of plasma samples of COVID-10 patients within the COVID_LAN trial was deeply appreciated

Finally, the cooperation with Michiel Dalinghaus, Marijke H. van der Meulen, Gideon J. du Marchie Sarvaas, Nico A. Blom, Arend D. J. ten Harkel, Hans M. P. J. Breur, Lukas A. J. Rammeloo, Ronald Tanke regarding the analysis of paediatric study samples (CARS II) was highly acknowledged.

11. References

- Abelous J, Bardier E (1909)** Les substance hypotensie de lúrine humaine normale. *Comptes rendus de la société de biologie* 66:511–512.
- Ad hoc group for the development of implementing guidelines for Directive 2001/20/EC (2008)** Ethical considerations for the clinical trials on medicinal products conducted with the paediatric population: Recommendations of the ad hoc group for the development of implementing guidelines for Directive 2001/20/EC relating to good clinical practice in the conduct of clinical trials on medicinal products for human use. *EudraLex*(10):Chapter V.
- Anton EL, Fernandes D, Assreuy J, da Silva-Santos JE (2019)** Bradykinin increases BP in endotoxemic rat: Functional and biochemical evidence of angiotensin II AT1 /bradykinin B2 receptor heterodimerization. *British journal of pharmacology* 176(14):2608–2626. <https://doi.org/10.1111/bph.14685>.
- Arendse LB, Danser AHJ, Poglitsch M, Touyz RM, Burnett JC, Llorens-Cortes C, et al. (2019)** Novel therapeutic approaches targeting the renin-angiotensin system and associated peptides in hypertension and heart failure. *Pharmacological Reviews* 71(4):539–570. <https://doi.org/10.1124/pr.118.017129>.
- Baker MS, Ahn SB, Mohamedali A, Islam MT, Cantor D, Verhaert PD, et al. (2017)** Accelerating the search for the missing proteins in the human proteome. *Nature communications* 8:14271. <https://doi.org/10.1038/ncomms14271>.
- Bakhle YS (2020)** How ACE inhibitors transformed the renin-angiotensin system. *British journal of pharmacology* 177(12):2657–2665. <https://doi.org/10.1111/bph.15045>.
- Baralla E, Nieddu M, Boatto G, Varoni MV, Palomba D, Demontis MP, et al. (2011)** Quantitative assay for bradykinin in rat plasma by liquid chromatography coupled to tandem mass spectrometry. *Journal of pharmaceutical and biomedical analysis* 54(3):557–561. <https://doi.org/10.1016/j.jpba.2010.09.041>.
- Barkoff CM, Mousa SA (2020)** Pharmacotherapy in COVID 19: Potential Impact of Targeting the Complement System. *Biomedicines* 9(1):11. <https://doi.org/10.3390/biomedicines9010011>.
- Barrett AJ, Rawlings ND, Woessner JF (2004)** Aspartic and metallo peptidases. 2nd ed.: Academic Press. London.
- Baykan O, Yaman A, Gerin F, Sirikci O, Haklar G (2017)** The effect of different protease inhibitors on stability of parathyroid hormone, insulin, and prolactin levels under different

- lag times and storage conditions until analysis. *Journal of clinical laboratory analysis* 31(6):e22144. <https://doi.org/10.1002/jcla.22144>.
- Beg S, Haneef J, Rahman M, Peraman R, Taleuzzaman M, Almalki WH (2021)** Introduction to analytical quality by design. In: Beg S, Hasnain MS, Rahman M, Almalki WH, editors. Handbook of analytical quality by design. Amsterdam: Academic Press, p 1–14.
- Berlin DA, Gulick RM, Martinez FJ (2020)** Severe Covid-19. *The New England journal of medicine* 383(25):2451–2460. <https://doi.org/10.1056/NEJMcp2009575>.
- Björkqvist J, Jämsä A, Renné T (2013)** Plasma kallikrein: The bradykinin-producing enzyme. *Thrombosis and haemostasis* 110(3):399–407. <https://doi.org/10.1160/TH13-03-0258>.
- Blais C, Drapeau G, Raymond P, Lamontagne D, Venneman I, Adam A (1997)** Contribution of angiotensin-converting enzyme to the cardiac metabolism of bradykinin: an interspecies study. *The American Physiology Society* 273(5):2263-2271.
- Blais C, Rouleau J-L, Brown NJ, Lepage Y, Spence D, Munoz C, et al. (1999)** Serum metabolism of bradykinin and des-Arg9-bradykinin in patients with angiotensin-converting enzyme inhibitor-associated angioedema. *Immunopharmacology* 43(2-3):293–302.
- Blic J de, Midulla F, Barbato A, Clement A, Dab I, Eber E, et al. (2000)** Bronchoalveolar lavage in children. ERS Task Force on bronchoalveolar lavage in children. European Respiratory Society. *European Respiratory Journal* 15(1):217–231.
- Blomberg LG (2009)** Two new techniques for sample preparation in bioanalysis: microextraction in packed sorbent (MEPS) and use of a bonded monolith as sorbent for sample preparation in polypropylene tips for 96-well plates. *Analytical and bioanalytical chemistry* 393(3):797–807. <https://doi.org/10.1007/s00216-008-2305-4>.
- Bonini P, Plebani M, Ceriotti F, Rubboli F (2002)** Errors in Laboratory Medicine. *Clinical chemistry* 48(5):691–698. <https://doi.org/10.1093/clinchem/48.5.691>.
- Borghi C, Veronesi M (2018)** Cough and ACE inhibitors: The truth beyond placebo. *Clinical pharmacology and therapeutics* 105(3):550–552. <https://doi.org/10.1002/cpt.1040>.
- Bowen CL, Licea-Perez H (2013)** Development of a sensitive and selective LC–MS/MS method for the determination of urea in human epithelial lining fluid. *Journal of Chromatography B* 917-918:24-29. <https://doi.org/10.1016/j.jchromb.2012.11.035>.
- Broadley KJ, Blair AE, Kidd EJ, Bugert JJ, Ford WR (2010)** Bradykinin-induced lung inflammation and bronchoconstriction: Role in parainfluenza-3 virus-induced inflammation

- and airway hyperreactivity. *The Journal of pharmacology and experimental therapeutics* 335(3):681–692. <https://doi.org/10.1124/jpet.110.171876>.
- Cabooter D, Augustijns P, Nelis M (2019)** Strategies for the quantification of endogenously present small molecules in biological samples. *LCGC Asia Pacific* 22(3):354–363.
- Campbell DJ (2000)** Towards understanding the kallikrein-kinin system: Insights from measurements of kinin peptides. *Brazilian Journal of Medical and Biological Research* 33(6):665–677. <https://doi.org/10.1590/s0100-879x2000000600008>.
- Campbell DJ (2013)** Bradykinin peptides. In: Kastin AJ, editor. *Handbook of biologically active peptides*, 2e: Elsevier, p 1386–1393.
- Campbell DJ, Kladis A, Duncan AM (1993)** Bradykinin peptides in kidney, blood, and other tissues of the rat. *Hypertension* 21(2):155–165. <https://doi.org/10.1161/01.HYP.21.2.155>.
- Campbell DJ, Krum H, Esler MD (2005)** Losartan increases bradykinin levels in hypertensive humans. *Circulation* 111(3):315–320. <https://doi.org/10.1161/01.CIR.0000153269.07762.3B>.
- Cao Z, Kamlage B, Wagner-Golbs A, Maisha M, Sun J, Schnackenberg LK, et al. (2019)** An integrated analysis of metabolites, peptides, and inflammation biomarkers for assessment of preanalytical variability of human plasma. *Journal of proteome research* 18(6):2411–2421. <https://doi.org/10.1021/acs.jproteome.8b00903>.
- Carraro P, Plebani M (2007)** Errors in a stat laboratory: types and frequencies 10 years later. *Clinical chemistry* 53(7):1338–1342. <https://doi.org/10.1373/clinchem.2007.088344>.
- Ceconi C, Fox KM, Remme WJ, Simoons ML, Bertrand M, Parrinello G, et al. (2007)** ACE inhibition with perindopril and endothelial function. Results of a substudy of the EUROPA study: PERTINENT. *Cardiovascular research* 73(1):237–246. <https://doi.org/10.1016/j.cardiores.2006.10.021>.
- Chajkowski SM, Mallela J, Watson DE, Wang J, McCurdy CR, Rimoldi JM, et al. (2011)** Highly selective hydrolysis of kinins by recombinant prolylcarboxypeptidase. *Biochemical and biophysical research communications* 405(3):338–343. <https://doi.org/10.1016/j.bbrc.2010.12.036>.
- Chen G (2013)** *Characterization of protein therapeutics using mass spectrometry*: Springer. Boston, MA.
- Chung KF, Pavord ID (2008)** Prevalence, pathogenesis, and causes of chronic cough. *The Lancet* 371(9621):1364–1374. [https://doi.org/10.1016/S0140-6736\(08\)60595-4](https://doi.org/10.1016/S0140-6736(08)60595-4).

- Collange O, Tacquard C, Delabranche X, Leonard-Lorant I, Ohana M, Onea M, et al. (2020)** Coronavirus disease 2019: Associated multiple organ damage. *Open forum infectious diseases* 7(7):ofaa249. <https://doi.org/10.1093/ofid/ofaa249>.
- Costa-Neto CM, Dillenburg-Pilla P, Heinrich TA, Parreiras-e-Silva LT, Pereira MGAG, Reis RI, et al. (2008)** Participation of kallikrein-kinin system in different pathologies. *International Immunopharmacology* 8(2):135–142. <https://doi.org/10.1016/j.intimp.2007.08.003>.
- Couture R, Harrisson M, Vianna RM, Cloutier F (2001)** Kinin receptors in pain and inflammation. *European Journal of Pharmacology* 429(1-3):161–176. [https://doi.org/10.1016/S0014-2999\(01\)01318-8](https://doi.org/10.1016/S0014-2999(01)01318-8).
- Cugno M, Agostini P, Brunner HR, Gardinali M, Agostoni A, Nussberger J (2000)** Plasma bradykinin levels in human chronic congestive heart failure. *Clinical Science* 99(5):461–466. <https://doi.org/10.1042/CS20000095>.
- Cugno M, Nussberger J, Cicardi M, Agostoni A (2003)** Bradykinin and the pathophysiology of angioedema. *International Immunopharmacology* 3(3):311–317. [https://doi.org/10.1016/S1567-5769\(02\)00162-5](https://doi.org/10.1016/S1567-5769(02)00162-5).
- Cyr M, Lepage Y, Blais C, Gervais N, Cugno M, Rouleau J-L, et al. (2001)** Bradykinin and des-Arg(9)-bradykinin metabolic pathways and kinetics of activation of human plasma. *American journal of physiology. Heart and circulatory physiology* 281(1):H275-283. <https://doi.org/10.1152/ajpheart.2001.281.1.H275>.
- Daniels JR, Cao Z, Maisha M, Schnackenberg LK, Sun J, Pence L, et al. (2019)** Stability of the human plasma proteome to pre-analytical variability as assessed by an aptamer-based approach. *Journal of proteome research* 18(10):3661–3670. <https://doi.org/10.1021/acs.jproteome.9b00320>.
- Debunne N, Spiegeleer A de, Depuydt D, Janssens Y, Descamps A, Wynendaele E, et al. (2020)** Influence of blood collection methods and long-term plasma storage on quorum-sensing peptide stability. *ACS omega* 5(26):16120–16127. <https://doi.org/10.1021/acsomega.0c01723>.
- Decarie, A. (1996)** Serum interspecies differences in metabolic pathways of bradykinin and [des-Arg9]BK: influence of enalaprilat. *American Physiological Society* 271(4 Pt 2):H1340–1347. <https://doi.org/10.1152/ajpheart.1996.271.4.H1340>.
- Dengler R, Faußner A, Müller-Esterl W, Roscher AA (1990)** [Hyp3]-bradykinin and [Hyp]-Lys-bradykinin interact with B2-bradykinin receptors and stimulate inositol phosphate

production in cultured human fibroblasts. *FEBS Letters* 262(1):111–114.
[https://doi.org/10.1016/0014-5793\(90\)80166-G](https://doi.org/10.1016/0014-5793(90)80166-G).

Donoghue M, Hsieh F, Baronas E, Godbout K, Gosselin M, Stagliano N, et al. (2000) A novel angiotensin-converting enzyme-related carboxypeptidase (ACE2) converts angiotensin I to angiotensin 1-9. *Circulation research* 87(5):E1-9.
<https://doi.org/10.1161/01.res.87.5.e1>.

Duncan AM, Kladis A, Jennings, Garry L., Dart, Anthony M., Murray Esler, Campbell DJ (2000) Kinins in humans. *American journal of physiology* 278(4):R897-R904.
<https://doi.org/10.1152/ajpregu.2000.278.4.R897>.

Eddleston J, Christiansen SC, Zuraw BL (2006) Kinins and neuropeptides | Bradykinin. In: Laurent GJ, Shapiro SD, editors. *Encyclopedia of respiratory medicine*. Amsterdam: Boston; Elsevier, p 502–506.

Ellis KM, Fozard JR (2002) Species differences in bradykinin receptor-mediated responses of the airways. *Autonomic and Autacoid Pharmacology* 22(1):3–16.
<https://doi.org/10.1046/j.1474-8673.2002.00230.x>.

Enzo Life Sciences, Inc. Bradykinin ELISA kit, ADI-900-206.
<https://www.enzolifesciences.com/ADI-900-206/bradykinin-elisa-kit/>, last check: 03.04.2021.

Erdös EG, Skidgel RA (1997) Metabolism of Bradykinin by Peptidases in Health and Disease. In: Farmer SG, editor. *The Kinin system*. San Diego: Academic Press, p 111–141.

Eriksson L, Johansson E, Kettaneh-Wold N, Wikström C, Wold S (2008) Design of experiments: Principles and applications. Third revised and enlarged edition: Umetrics Academy. Umeå.

European Medicines Agency (2011) Guideline Bioanalytical method validation.
https://www.ema.europa.eu/en/documents/scientific-guideline/guideline-bioanalytical-method-validation_en.pdf, last check: 07.04.2021.

Evans BJ, King AT, Katsifis A, Matesic L, Jamie JF (2020) Methods to enhance the metabolic stability of peptide-based PET radiopharmaceuticals. *Molecules* 25(10):2314.
<https://doi.org/10.3390/molecules25102314>.

Ewles M, Goodwin L (2011) Bioanalytical approaches to analyzing peptides and proteins by LC--MS/MS. *Bioanalysis* 3(12):1379–1397. <https://doi.org/10.4155/bio.11.112>.

Falcão F, Viegas E, Carmo I, Soares J, Falcao M, Solano M, et al. (2021) A prospective, observational study to evaluate adverse drug reactions in patients with COVID-19 treated

- with remdesivir or hydroxychloroquine: a preliminary report. *European journal of hospital pharmacy* Published Online First: 15 January 2021. <https://doi.org/10.1136/ejhpharm-2020-002613>.
- Feickert M, Burckhardt BB (2019)** A design of experiments concept for the minimization of nonspecific peptide adsorption in the mass spectrometric determination of substance P and related hemokinin-1. *Journal of separation science* 43(4):818–828. <https://doi.org/10.1002/jssc.201901038>.
- Franciosi L, Govorukhina N, Hacken N ten, Postma D, Bischoff R (2011)** Proteomics of epithelial lining fluid obtained by bronchoscopic microprobe sampling. *Nanoproteomics* 790:17–28. https://doi.org/10.1007/978-1-61779-319-6_2.
- Gangnus T, Burckhardt BB (2020)** Improving sensitivity for the targeted LC-MS/MS analysis of the peptide bradykinin using a design of experiments approach. *Talanta* 218:121134. <https://doi.org/10.1016/j.talanta.2020.121134>.
- Gangnus T, Burckhardt BB (2021a)** Sensitive mass spectrometric determination of kinin-kallikrein system peptides in light of COVID-19. *Scientific Reports* 11:3061. <https://doi.org/10.1038/s41598-021-82191-7>.
- Gangnus T, Burckhardt BB (2021b)** Stabilization of short-lived peptides of the kallikrein-kinin system in human plasma to facilitate use as promising biomarkers. *Clinical chemistry* 67(9):1287–1289. <https://doi.org/10.1093/clinchem/hvab129>.
- Gangnus T, Burckhardt BB (2021c)** Targeted LC-MS/MS platform for the comprehensive determination of peptides in the kallikrein-kinin system. *Analytical and bioanalytical chemistry* 413(11):2971–2984. <https://doi.org/10.1007/s00216-021-03231-9>.
- Gangnus T, Burckhardt BB (2022)** Reliable measurement of plasma kinin peptides: Importance of preanalytical variables. *Research and Practice in Thrombosis and Haemostasis* 6(1). <https://doi.org/10.1002/rth2.12646>.
- Garvin MR, Alvarez C, Miller JI, Prates ET, Walker AM, Amos BK, et al. (2020)** A mechanistic model and therapeutic interventions for COVID-19 involving a RAS-mediated bradykinin storm. *Elife* 9. <https://doi.org/10.7554/eLife.59177>.
- Gasteiger E, Hoogland C, Gattiker A, Duvaud S, Wilkins MR, Appel RD, et al. (2005)** Protein Identification and Analysis Tools on the ExPASy Server. In: Walker JM, editor. *The Proteomics Protocols Handbook*. Totowa, NJ: Humana Press Inc, p 571–607.
- Gobeil F, Neugebauer W, Nguyen-Le XK, Nea Allogho S, Pheng LH, Blouin D, et al. (1997)** Pharmacological profiles of the human and rabbit B1 receptors. *Canadian journal of physiology and pharmacology* 75(6):591–595.

- Goebel-Stengel M, Stengel A, Taché Y, Reeve JR (2011)** The importance of using the optimal plasticware and glassware in studies involving peptides. *Analytical biochemistry* 414(1):38–46. <https://doi.org/10.1016/j.ab.2011.02.009>.
- Golias C, Charalabopoulos A, Stagikas D, Charalabopoulos K, Batistatou A (2007)** The kinin system - bradykinin: biological effects and clinical implications. Multiple role of the kinin system - bradykinin. *Hippokratia* 3:124–128.
- Hahne H, Pachi F, Ruprecht B, Maier SK, Klaeger S, Helm D, et al. (2013)** DMSO enhances electrospray response, boosting sensitivity of proteomic experiments. *Nature methods* 10(10):989–991. <https://doi.org/10.1038/nmeth.2610>.
- Harbeck HT, Mentlein R (1991)** Aminopeptidase P from rat brain. Purification and action on bioactive peptides. *European journal of biochemistry* 198(2):451–458. <https://doi.org/10.1111/j.1432-1033.1991.tb16035.x>.
- Hassis ME, Niles RK, Braten MN, Albertolle ME, Ewa Witkowska H, Hubel CA, et al. (2015)** Evaluating the effects of preanalytical variables on the stability of the human plasma proteome. *Analytical biochemistry* 478:14–22. <https://doi.org/10.1016/j.ab.2015.03.003>.
- Hecht ES, Oberg AL, Muddiman DC (2016)** Optimizing mass spectrometry analyses: A tailored review on the utility of design of experiments. *Journal of the American Society for Mass Spectrometry* 27(5):767–785. <https://doi.org/10.1007/s13361-016-1344-x>.
- Hendriks D, Meester I de, Umiel T, Vanhoof G, van Sande M, Scharpé S, et al. (1991)** Aminopeptidase P and dipeptidyl peptidase IV activity in human leukocytes and in stimulated lymphocytes. *Clinica Chimica Acta* 196(2-3):87–96. [https://doi.org/10.1016/0009-8981\(91\)90061-G](https://doi.org/10.1016/0009-8981(91)90061-G).
- Henion J, Brewer E, Rule G (1998)** Sample preparation for LC/MS/MS: analyzing biological and environmental samples. *Analytical chemistry* 70(19):650A-656A. <https://doi.org/10.1021/ac981991q>.
- Hicks BM, Fillion KB, Yin H, Sakr L, Udell JA, Azoulay L (2018)** Angiotensin converting enzyme inhibitors and risk of lung cancer: Population based cohort study. *British Medical Journal* 4:k4209. <https://doi.org/10.1136/bmj.k4209>.
- Hilgenfeldt U, Linke R, Riester U, König W, Breipohl G (1995)** Strategy of measuring bradykinin and kallidin and their concentration in plasma and urine. *Analytical biochemistry* 228(1):35–41. <https://doi.org/10.1006/abio.1995.1311>.
- Hoang MV, Turner AJ (1997)** Novel activity of endothelin-converting enzyme: hydrolysis of bradykinin. *Biochemical Journal* 327(Pt 1):23–26. <https://doi.org/10.1042/bj3270023>.

- Hoffmann M, Kleine-Weber H, Schroeder S, Krüger N, Herrler T, Erichsen S, et al. (2020)** SARS-CoV-2 cell entry depends on ACE2 and TMPRSS2 and is blocked by a clinically proven protease inhibitor. *Cell* 181(2):271-280.e8.
<https://doi.org/10.1016/j.cell.2020.02.052>.
- Hofman Z, Maat S de, Hack CE, Maas C (2016)** Bradykinin: Inflammatory product of the coagulation system. *Clinical reviews in allergy & immunology* 51(2):152–161.
<https://doi.org/10.1007/s12016-016-8540-0>.
- Hoofnagle AN, Wener MH (2009)** The fundamental flaws of immunoassays and potential solutions using tandem mass spectrometry. *Journal of immunological methods* 347(1-2):3–11. <https://doi.org/10.1016/j.jim.2009.06.003>.
- Hoofnagle AN, Whiteaker JR, Carr SA, Kuhn E, Liu T, Massoni SA, et al. (2016)** Recommendations for the generation, quantification, storage, and handling of peptides used for mass spectrometry-based assays. *Clinical chemistry* 62(1):48–69.
<https://doi.org/10.1373/clinchem.2015.250563>.
- Hopfgartner G (2020)** Bioanalytical method validation: How much should we do and how should we document? *Analytical and bioanalytical chemistry* 412(3):531–532.
<https://doi.org/10.1007/s00216-019-02334-8>.
- Horby P, Lim WS, Emberson JR, Mafham M, Bell JL, Linsell L, et al. (2020)** Dexamethasone in hospitalized patients with COVID-19 - preliminary report. *The New England journal of medicine* 384(8):693–704. <https://doi.org/10.1056/NEJMoa2021436>.
- Huang C, Wang Y, Li X, Ren L, Zhao J, Hu Y, et al. (2020)** Clinical features of patients infected with 2019 novel coronavirus in Wuhan, China. *The Lancet* 395(10223):497–506.
[https://doi.org/10.1016/S0140-6736\(20\)30183-5](https://doi.org/10.1016/S0140-6736(20)30183-5).
- Hubers SA, Kohm K, Wei S, Yu C, Nian H, Grabert R, et al. (2018)** Endogenous bradykinin and B1-B5 during angiotensin-converting enzyme inhibitor-associated angioedema. *The Journal of allergy and clinical immunology* 142(5):1636-1639.e5.
<https://doi.org/10.1016/j.jaci.2018.06.032>.
- International Council for Harmonisation (1995)** ICH Topic Q2 (R1) Validation of Analytical Procedures: Text and Methodology (CPMP/ICH/381/95).
https://www.ema.europa.eu/en/documents/scientific-guideline/ich-q-2-r1-validation-analytical-procedures-text-methodology-step-5_en.pdf, last check: 07.04.2021.
- International Council for Harmonisation (2019)** ICH M10 Guideline on bioanalytical method validation step 2b. <https://www.ema.europa.eu/en/documents/scientific->

guideline/draft-ich-guideline-m10-bioanalytical-method-validation-step-2b_en.pdf, last check: 07.04.2021.

Ion V, Imre S, Carje A-G, Balint A, Muntean D-L (2017) LC-MS/MS analysis for peptides using human bradykinin and two of its fragments as model molecules. *Farmacia* 65(3):435–442.

John H, Walden M, Schäfer S, Genz S, Forssmann W-G (2004) Analytical procedures for quantification of peptides in pharmaceutical research by liquid chromatography-mass spectrometry. *Analytical and bioanalytical chemistry* 378(4):883–897.
<https://doi.org/10.1007/s00216-003-2298-y>.

Kang L, Weng N, Jian W (2020) LC-MS bioanalysis of intact proteins and peptides. *Biomedical chromatography* 34(1):e4633. <https://doi.org/10.1002/bmc.4633>.

Kaplan AP, Ghebrehiwet B (2021) Pathways for bradykinin formation and interrelationship with complement as a cause of edematous lung in COVID-19 patients. *The Journal of allergy and clinical immunology* 147(2):507–509.
<https://doi.org/10.1016/j.jaci.2020.10.025>.

Kaplan AP, Maas C (2017) The search for biomarkers in hereditary angioedema. *Frontiers in medicine* 4:206. <https://doi.org/10.3389/fmed.2017.00206>.

Kashuba E, Bailey J, Ailsup D, Cawkwell L (2013) The kinin-kallikrein system: physiological roles, pathophysiology and its relationship to cancer biomarkers. *Biomarkers* 18(4):279–296. <https://doi.org/10.3109/1354750X.2013.787544>.

Kaulbach H, White M, Igarashi Y, Hahn B, Kaliner M (1993) Estimation of nasal epithelial lining fluid using urea as a marker. *Journal of Allergy and Clinical Immunology* 92(3):457–465. [https://doi.org/10.1016/0091-6749\(93\)90125-Y](https://doi.org/10.1016/0091-6749(93)90125-Y).

Kinsey SE, Machin SJ (1989) The role of the contact system in the pathophysiology of ARDS. In: Vincent JL, editor. Update in intensive care and emergency medicine. Berlin: Springer-Verlag, p 39–47.

Kristensen K, Henriksen JR, Andresen TL (2015) Adsorption of cationic peptides to solid surfaces of glass and plastic. *PLoS one* 10(5):e0122419.
<https://doi.org/10.1371/journal.pone.0122419>.

Kutz A, Conen A, Gregoriano C, Haubitz S, Koch D, Domenig O, et al. (2021) Renin-angiotensin-aldosterone system peptide profiles in patients with COVID-19. *European journal of endocrinology* 184(4):543–552. <https://doi.org/10.1530/EJE-20-1445>.

Lame ME (2013) Development of a quantitative SPE LC-MS/MS assay for bradykinin in human plasma.

<http://www.waters.com/waters/library.htm?cid=511436&lid=134773810&locale=101>, last check: 07.04.2021.

Lame ME, Chambers EE, Fountain KJ (2016) An improved SPE-LC-MS/MS method for the quantification of bradykinin in human plasma using the ionKey/MS system.

<https://www.waters.com/webassets/cms/library/docs/720004945en.pdf>, last check: 07.04.2021.

Lawrence JB (2003) Preanalytical variables in the coagulation laboratory. *Laboratory Medicine* 34(1):49–57. <https://doi.org/10.1309/ER9P-64EB-MCFR-47KY>.

Lee R (2019) Statistical design of experiments for screening and optimization. *Chemie Ingenieur Technik* 91(3):191–200. <https://doi.org/10.1002/cite.201800100>.

Lindström M, Valkonen M, Tohmola N, Renkonen R, Strandin T, Vaheri A, et al. (2019) Plasma bradykinin concentrations during septic shock determined by a novel LC-MS/MS assay. *Clinica Chimica Acta* 493:20–24. <https://doi.org/10.1016/j.cca.2019.02.023>.

Lipsey M, Persson B, Eriksson O, Blom AM, Fromell K, Hultström M, et al. (2021) The outcome of critically ill COVID-19 patients is linked to thromboinflammation dominated by the kallikrein-kinin system. *Frontiers in immunology* 12: 627579. <https://doi.org/10.3389/fimmu.2021.627579>.

Lippi G, Meyer A von, Cadamuro J, Simundic A-M (2020a) PREDICT: a checklist for preventing preanalytical diagnostic errors in clinical trials. *Clinical chemistry and laboratory medicine* 58(4):518–526. <https://doi.org/10.1515/ccim-2019-1089>.

Lippi G, Plebani M, Henry BM (2020b) Thrombocytopenia is associated with severe coronavirus disease 2019 (COVID-19) infections: A meta-analysis. *Clinica Chimica Acta* 506:145–148. <https://doi.org/10.1016/j.cca.2020.03.022>.

Lippi G, Salvagno GL, Guidi GC (2005) No influence of a butterfly device on routine coagulation assays and D-dimer measurement. *Journal of thrombosis and haemostasis* 3(2):389–391. <https://doi.org/10.1111/j.1538-7836.2005.01163.x>.

Liu Y, Gu Y, Ng S, Deng Z, Lyon CJ, Koay EJ, et al. (2020) Circulating levels of hydroxylated bradykinin function as an indicator of tissue HIF-1 α expression. *Science Bulletin* 65(18):1570–1579. <https://doi.org/10.1016/j.scib.2020.04.023>.

Loeffen R, Kleinegriss M-CF, Loubele STBG, Pluijmen PHM, Fens D, van Oerle R, et al. (2012) Preanalytical variables of thrombin generation: Towards a standard procedure and validation of the method. *Journal of thrombosis and haemostasis* 10(12):2544–2554. <https://doi.org/10.1111/jth.12012>.

- Lortie M, Bark S, Blantz R, Hook V (2009)** Detecting low-abundance vasoactive peptides in plasma: progress toward absolute quantitation using nano liquid chromatography-mass spectrometry. *Analytical biochemistry* 394(2):164–170.
<https://doi.org/10.1016/j.ab.2009.07.021>.
- Maat S de, Mast Q de, Danser AJ, van de Veerdonk FL, Maas C (2020)** Impaired breakdown of bradykinin and its metabolites as a possible cause for pulmonary edema in COVID-19 infection. *Seminars in Thrombosis and Hemostasis* 46(07):835–837.
<https://doi.org/10.1055/s-0040-1712960>.
- Maes K, Smolders I, Michotte Y, van Eeckhaut A (2014a)** Strategies to reduce aspecific adsorption of peptides and proteins in liquid chromatography-mass spectrometry based bioanalyses: An overview. *Journal of chromatography A* 1358:1–13.
<https://doi.org/10.1016/j.chroma.2014.06.072>.
- Maes K, van Liefferinge J, Viaene J, van Schoors J, van Wansele Y, Béchade G, et al. (2014b)** Improved sensitivity of the nano ultra-high performance liquid chromatography-tandem mass spectrometric analysis of low-concentrated neuropeptides by reducing aspecific adsorption and optimizing the injection solvent. *Journal of chromatography. A* 1360:217–228. <https://doi.org/10.1016/j.chroma.2014.07.086>.
- Magerl M, Bader M, Gompel A, Joseph K, Kaplan AP, Kojda G, et al. (2014)** Bradykinin in health and disease: Proceedings of the Bradykinin Symposium 2012, Berlin 23-24 August 2012. *Inflammation research* 63(3):173–178. <https://doi.org/10.1007/s00011-013-0693-1>.
- Magnette A, Chatelain M, Chatelain B, Cate H ten, Mullier F (2016)** Pre-analytical issues in the haemostasis laboratory: guidance for the clinical laboratories. *Thrombosis Journal* 14(1):49. <https://doi.org/10.1186/s12959-016-0123-z>.
- Malin JJ, Spinner CD (2021)** DGI recommendations for COVID-19 pharmacotherapy. *Infection* 49(2):369–370. <https://doi.org/10.1007/s15010-020-01519-z>.
- Mann AM, Tighe BJ (2012)** A potent pain producing peptide-bradykinin in tears and contact lens wear. *Contact Lens and Anterior Eye* 35:Supplement 1, e31.
<https://doi.org/10.1016/j.clae.2012.08.096>.
- Mansour E, Bueno FF, Lima-Júnior JC de, Palma A, Monfort-Pires M, Bombassaro B, et al. (2021)** Evaluation of the efficacy and safety of icatibant and C1 esterase/kallikrein inhibitor in severe COVID-19: study protocol for a three-armed randomized controlled trial. *Trials* 22(1):71. <https://doi.org/10.1186/s13063-021-05027-9>.
- Marceau F, Bachelard H, Bouthillier J, Fortin J-P, Morissette G, Bawolak M-T, et al. (2020)** Bradykinin receptors: Agonists, antagonists, expression, signaling, and adaptation

- to sustained stimulation. *International Immunopharmacology* 82:106305.
<https://doi.org/10.1016/j.intimp.2020.106305>.
- Marceau F, Regoli D (2004)** Bradykinin receptor ligands: Therapeutic perspectives. *Nature reviews. Drug discovery* 3(10):845–852. <https://doi.org/10.1038/nrd1522>.
- Martens CP, van Mol P, Wauters J, Wauters E, Gangnus T, Noppen B, et al. (2021)** Dysregulation of the kallikrein-kinin system in lungs of patients with COVID-19. *EBioMedicine (under review)*.
- Martinu T, Koutsokera A, Benden C, Cantu E, Chambers D, Cypel M, et al. (2020)** International Society for Heart and Lung Transplantation consensus statement for the standardization of bronchoalveolar lavage in lung transplantation. *The Journal of Heart and Lung Transplantation* 39(11):1171–1190.
<https://doi.org/10.1016/j.healun.2020.07.006>.
- Mathé C, Devineau S, Aude J-C, Lagniel G, Chédin S, Legros V, et al. (2013)** Structural determinants for protein adsorption/non-adsorption to silica surface. *PloS one* 8(11):e81346. <https://doi.org/10.1371/journal.pone.0081346>.
- Maurer M, Bader M, Bas M, Bossi F, Cicardi M, Cugno M, et al. (2011)** New topics in bradykinin research. *Allergy* 66(11):1397–1406. <https://doi.org/10.1111/j.1398-9995.2011.02686.x>.
- McCarthy DA, Potter DE, Nicolaidis ED (1965)** An in vivo estimation of the potencies and half-lives of synthetic bradykinin and kallidin. *Journal of Pharmacology and Experimental Therapeutics* 148(1):117.
- McLean PG, Perretti M, Ahluwalia A (2005)** Kinin B 1 receptors as novel anti-inflammatory targets. *Emerging Therapeutic Targets* 4(2):127–141.
<https://doi.org/10.1517/14728222.4.2.127>.
- Meini S, Zanichelli A, Sbrojavacca R, Iuri F, Roberts AT, Suffritti C, et al. (2020)** Understanding the pathophysiology of COVID-19: Could the contact system be the key? *Frontiers in immunology* 11:2014. <https://doi.org/10.3389/fimmu.2020.02014>.
- Meyer KC, Raghu G, Baughman RP, Brown KK, Costabel U, Du Bois RM, et al. (2012)** An official American Thoracic Society clinical practice guideline: The clinical utility of bronchoalveolar lavage cellular analysis in interstitial lung disease. *American journal of respiratory and critical care medicine* 185(9):1004–1014.
<https://doi.org/10.1164/rccm.201202-0320ST>.

- Miladinović SM, Fornelli L, Lu Y, Piech KM, Girault HH, Tsybin YO (2012)** In-spray supercharging of peptides and proteins in electrospray ionization mass spectrometry. *Analytical chemistry* 84(11):4647–4651. <https://doi.org/10.1021/ac300845n>.
- Moore JB, June CH (2020)** Cytokine release syndrome in severe COVID-19. *Science* 368(6490):473–474. <https://doi.org/10.1126/science.abb8925>.
- Moreau ME, Garbacki N, Molinaro G, Brown NJ, Marceau F, Adam A (2005)** The kallikrein-kinin system: current and future pharmacological targets. *Journal of pharmacological sciences* 99(1):6–38. <https://doi.org/10.1254/jphs.srj05001x>.
- Mould DR, Upton RN (2013)** Basic concepts in population modeling, simulation, and model-based drug development-part 2: introduction to pharmacokinetic modeling methods. *CPT: pharmacometrics & systems pharmacology* 2(4):e38. <https://doi.org/10.1038/psp.2013.14>.
- Murphey LJ, Hachey DL, Oates JA, Morrow JD, Brown NJ (2000)** Metabolism of bradykinin in vivo in humans: Identification of BK 1-5 as a stable plasma peptide metabolite. *The Journal of pharmacology and experimental therapeutics* 294(1):263–269.
- Murphey LJ, Hachey DL, Vaughan DE, Brown NJ, Morrow JD (2001)** Quantification of BK1-5, the stable bradykinin plasma metabolite in humans, by a highly accurate liquid-chromatographic tandem mass spectrometric assay. *Analytical biochemistry* 292(1):87–93. <https://doi.org/10.1006/abio.2001.5073>.
- NCT04422509** Lanadelumab for treatment of COVID-19 disease (COVID_LAN). <https://clinicaltrials.gov/ct2/show/NCT04422509?term=Icatibant&cond=Covid19&draw=2&rank=2>, last check: 19.05.2021.
- NCT04460105** Lanadelumab in participants hospitalized with COVID-19 pneumonia. <https://clinicaltrials.gov/ct2/show/NCT04460105>, last check: 18.05.2021.
- Nicola H (2017)** The role of contact system in septic shock: the next target? An overview of the current evidence. *Journal of Intensive Care* 5:31. <https://doi.org/10.1186/s40560-017-0228-x>.
- Nicola S, Rolla G, Brussino L (2019)** Breakthroughs in hereditary angioedema management: a systematic review of approved drugs and those under research. *Drugs in context* 8:212605. <https://doi.org/10.7573/dic.212605>.
- Nicolau LAD, Magalhães PJC, Vale ML (2020)** What would Sérgio Ferreira say to your physician in this war against COVID-19: How about kallikrein/kinin system? *Medical Hypotheses* 143:109886. <https://doi.org/10.1016/j.mehy.2020.109886>.

- Nielsen MD, Nielsen F, Kappelgaard AM, Giese J (1982)** Double-antibody solid-phase radioimmunoassay for blood bradykinin. *Clinica Chimica Acta* 125(2):145–156. [https://doi.org/10.1016/0009-8981\(82\)90191-7](https://doi.org/10.1016/0009-8981(82)90191-7).
- Nokkari A, Abou-El-Hassan H, Mechref Y, Mondello S, Kindy MS, Jaffa AA, et al. (2018)** Implication of the Kallikrein-Kinin system in neurological disorders: Quest for potential biomarkers and mechanisms. *Progress in neurobiology* 165-167:26–50. <https://doi.org/10.1016/j.pneurobio.2018.01.003>.
- Nussberger J, Cugno M, Amstutz C, Cicardi M, Pellacani A, Agostoni A (1998)** Plasma bradykinin in angio-oedema. *The Lancet* 351(9117):1693–1697. [https://doi.org/10.1016/S0140-6736\(97\)09137-X](https://doi.org/10.1016/S0140-6736(97)09137-X).
- O'Leary H, Ou X, Broxmeyer HE (2013)** The role of dipeptidyl peptidase 4 in hematopoiesis and transplantation. *Current opinion in hematology* 20(4):314–319. <https://doi.org/10.1097/MOH.0b013e32836125ac>.
- Parasher A (2020)** COVID-19: Current understanding of its pathophysiology, clinical presentation and treatment. *Postgraduate medical journal* 97(1147):312–320. <https://doi.org/10.1136/postgradmedj-2020-138577>.
- Pellacani A, Brunner HR, Nussberger J (1992)** Antagonizing and measurement: Approaches to understanding of hemodynamic effects of kinins. *Journal of Cardiovascular Pharmacology* 20 Suppl 9:S28-34.
- Pellacani A, Brunner HR, Nussberger J (1994)** Plasma kinins increase after angiotensin-converting enzyme inhibition in human subjects. *Clinical Science* 87(5):567–574.
- Piccoli SP, Sauer JM, Writing Group, Critical Path Institute (2019)** Points to consider document: Scientific and regulatory considerations for the analytical validation of assays used in the qualification of biomarkers in biological matrices. <https://c-path.org/wp-content/uploads/2019/06/evidconsid-whitepaper-analyticalsectionv20190613-1.pdf>, last check: 16.04.2021.
- Pitrez PMC, Brennan S, Turner S, Sly PD (2005)** Nasal wash as an alternative to bronchoalveolar lavage in detecting early pulmonary inflammation in children with cystic fibrosis. *Respirology* 10(2):177–182. <https://doi.org/10.1111/j.1440-1843.2005.00649.x>.
- Proud D, Togias A, Naclerio RM, Crush SA, Norman PS, Lichtenstein LM (1983)** Kinins are generated in vivo following nasal airway challenge of allergic individuals with allergen. *Journal of Clinical Investigation* 72:1678–1683.
- Qin L, Du Y, Ding H, Haque A, Hicks J, Pedroza C, et al. (2019)** Bradykinin 1 receptor blockade subdues systemic autoimmunity, renal inflammation, and blood pressure in

- murine lupus nephritis. *Arthritis research & therapy* 21(1):12.
<https://doi.org/10.1186/s13075-018-1774-x>.
- Rai AJ, Vitzthum F (2006)** Effects of preanalytical variables on peptide and protein measurements in human serum and plasma: implications for clinical proteomics. *Expert review of proteomics* 3(4):409–426. <https://doi.org/10.1586/14789450.3.4.409>.
- Ranasinghe T, Freeman WD (2014)** 'ICU vampirism' - time for judicious blood draws in critically ill patients. *British journal of haematology* 164(2):302–303.
<https://doi.org/10.1111/bjh.12613>.
- Reed GA (2016)** Stability of drugs, drug candidates, and metabolites in blood and plasma. *Current Protocols in Pharmacology* 75(1):7.6.1-7.6.12. <https://doi.org/10.1002/cpph.16>.
- Regoli D, Rhaleb NE, Drapeau G, Dion S, Tousignant C, D'Orléans-Juste P, et al. (1989)** Basic pharmacology of kinins: pharmacologic receptors and other mechanisms. *Advances in experimental medicine and biology* 247A:399–407. https://doi.org/10.1007/978-1-4615-9543-4_61.
- Rennard SI, Basset G, Lecossier D, O'Donnell KM, Pinkston P, Martin PG, et al. (1986)** Estimation of volume of epithelial lining fluid recovered by lavage using urea as marker of dilution. *Journal of applied physiology* 60(2):532–538.
<https://doi.org/10.1152/jappl.1986.60.2.532>.
- Ricciardolo FLM, Folkerts G, Folino A, Mognetti B (2018)** Bradykinin in asthma: Modulation of airway inflammation and remodelling. *European Journal of Pharmacology* 827:181–188. <https://doi.org/10.1016/j.ejphar.2018.03.017>.
- Rocha e Silva M, Beraldo WT, Rosenfeld G (1949)** Bradykinin, a hypotensive and smooth muscle stimulating factor released from plasma globulin by snake venoms and by trypsin. *The American journal of physiology* 156(2):261–273.
<https://doi.org/10.1152/ajplegacy.1949.156.2.261>.
- Roche JA, Roche R (2020)** A hypothesized role for dysregulated bradykinin signaling in COVID-19 respiratory complications. *FASEB journal* 34(6):7265–7269.
<https://doi.org/10.1096/fj.202000967>.
- Rübsam K, Davari MD, Jakob F, Schwaneberg U (2018)** KnowVolution of the polymer-binding peptide LCI for improved polypropylene binding. *Polymers* 10(4):423.
<https://doi.org/10.3390/polym10040423>.
- Rutkowska-Zapała M, Suski M, Szatanek R, Lenart M, Węglarczyk K, Olszanecki R, et al. (2015)** Human monocyte subsets exhibit divergent angiotensin I-converting activity. *Clinical and experimental immunology* 181(1):126–132. <https://doi.org/10.1111/cei.12612>.

- Schmaier AH (2003)** The kallikrein-kinin and the renin-angiotensin systems have a multilayered interaction. *American journal of physiology. Regulatory, integrative and comparative physiology* 285(1):R1-13. <https://doi.org/10.1152/ajpregu.00535.2002>.
- Schmaier AH (2016)** The contact activation and kallikrein/kinin systems: Pathophysiologic and physiologic activities. *Journal of thrombosis and haemostasis* 14(1):28–39. <https://doi.org/10.1111/jth.13194>.
- Schmidt RL, Simonović M (2012)** Synthesis and decoding of selenocysteine and human health. *Croatian medical journal* 53(6):535–550. <https://doi.org/10.3325/cmj.2012.53.535>.
- Seip KF, Bjerknes KC, Johansen HT, Nielsen EW, Landrø L, Reubsaet L (2014)** Bradykinin analysis revived - a validated method for determination of its stable metabolite in whole blood by LC-MS/MS. *Journal of Chromatography B* 947-948:139–144. <https://doi.org/10.1016/j.jchromb.2013.12.033>.
- Sheikh IA, Kaplan AP (1986)** Studies of the digestion of bradykinin, lysyl bradykinin, and kinin-degradation products by carboxypeptidases A, B, and N. *Biochemical Pharmacology* 35(12):1957–1963. [https://doi.org/10.1016/0006-2952\(86\)90727-6](https://doi.org/10.1016/0006-2952(86)90727-6).
- Sheikh IA, Kaplan AP (1989)** Mechanism of digestion of bradykinin and lysylbradykinin (kallidin) in human serum: Role of carboxypeptidase, angiotensin-converting enzyme and determination of final degradation products. *Biochemical Pharmacology* 38(6):993–1000. [https://doi.org/10.1016/0006-2952\(89\)90290-6](https://doi.org/10.1016/0006-2952(89)90290-6).
- Sodhi CP, Wohlford-Lenane C, Yamaguchi Y, Prindle T, Fulton WB, Wang S, et al. (2018)** Attenuation of pulmonary ACE2 activity impairs inactivation of des-Arg9 bradykinin/BKB1R axis and facilitates LPS-induced neutrophil infiltration. *American journal of physiology. Lung cellular and molecular physiology* 314(1):L17-L31. <https://doi.org/10.1152/ajplung.00498.2016>.
- Spronk HMH, Dielis AWJH, Panova-Noeva M, van Oerle R, Govers-Riemslog JWP, Hamulyák K, et al. (2009)** Monitoring thrombin generation: is addition of corn trypsin inhibitor needed? *Thrombosis and haemostasis* 101(6):1156–1162.
- Stejskal K, Potěšil D, Zdráhal Z (2013)** Suppression of peptide sample losses in autosampler vials. *Journal of proteome research* 12(6):3057–3062. <https://doi.org/10.1021/pr400183v>.
- Steve Unger, Wenkui Li, Jimmy Flarakos, Francis L.S. Tse (2013)** Roles of LC-MS Bioanalysis in Drug Discovery, Development, and Therapeutic Drug Monitoring. In: Unger S, Li W, Flarakos J, Tse FLS, editors. *Handbook of LC-MS Bioanalysis*: John Wiley & Sons, Ltd, p 1–13.

- Stevens NT, Anderson-Cook CM (2019)** Design and analysis of confirmation experiments. *Journal of Quality Technology* 51(2):109–124. <https://doi.org/10.1080/00224065.2019.1571344>.
- Stolina M, Bolon B, Middleton S, Dwyer D, Brown H, Duryea D, et al. (2009)** The evolving systemic and local biomarker milieu at different stages of disease progression in rat adjuvant-induced arthritis. *Journal of clinical immunology* 29(2):158–174. <https://doi.org/10.1007/s10875-008-9238-8>.
- Suessenbach FK, Makowski N, Feickert M, Gangnus T, Tins J, Burckhardt BB (2020)** A quality control system for ligand-binding assay of plasma renin activity: Proof-of-concept within a pharmacodynamic study. *Journal of pharmaceutical and biomedical analysis* 181:113090. <https://doi.org/10.1016/j.jpba.2019.113090>.
- Sungnak W, Huang N, Bécavin C, Berg M, Queen R, Litvinukova M, et al. (2020)** SARS-CoV-2 entry factors are highly expressed in nasal epithelial cells together with innate immune genes. *Nature medicine* 26:681–687. <https://doi.org/10.1038/s41591-020-0868-6>.
- Taddei S, Bortolotto L (2016)** Unraveling the pivotal role of bradykinin in ACE inhibitor activity. *American Journal of Cardiovascular Drugs* 16(5):309–321. <https://doi.org/10.1007/s40256-016-0173-4>.
- Thakare R, Chhonker YS, Gautam N, Alamoudi JA, Alnouti Y (2016)** Quantitative analysis of endogenous compounds. *Journal of pharmaceutical and biomedical analysis* 128:426–437. <https://doi.org/10.1016/j.jpba.2016.06.017>.
- Tiwari G, Tiwari R (2010)** Bioanalytical method validation: An updated review. *Pharmaceutical methods* 1(1):25–38. <https://doi.org/10.4103/2229-4708.72226>.
- Tolouian R, Vahed SZ, Ghiyasvand S, Tolouian A, Ardalan M (2020)** COVID-19 interactions with angiotensin-converting enzyme 2 (ACE2) and the kinin system; looking at a potential treatment. *Journal of Renal Injury Prevention* 9(2):e19. <https://doi.org/10.34172/jrip.2020.19>.
- Turner PJ, Dear JW, Foreman JC (2000)** Involvement of kinins in hyperresponsiveness induced by platelet activating factor in the human nasal airway. *British journal of clinical pharmacology* 129:525–532. <https://doi.org/10.1038/sj.bjp.0703095>.
- Ullman AJ, Keogh S, Coyer F, Long DA, New K, Rickard CM (2016)** 'True Blood' The Critical Care Story: An audit of blood sampling practice across three adult, paediatric and neonatal intensive care settings. *Australian critical care* 29(2):90–95. <https://doi.org/10.1016/j.aucc.2015.06.002>.

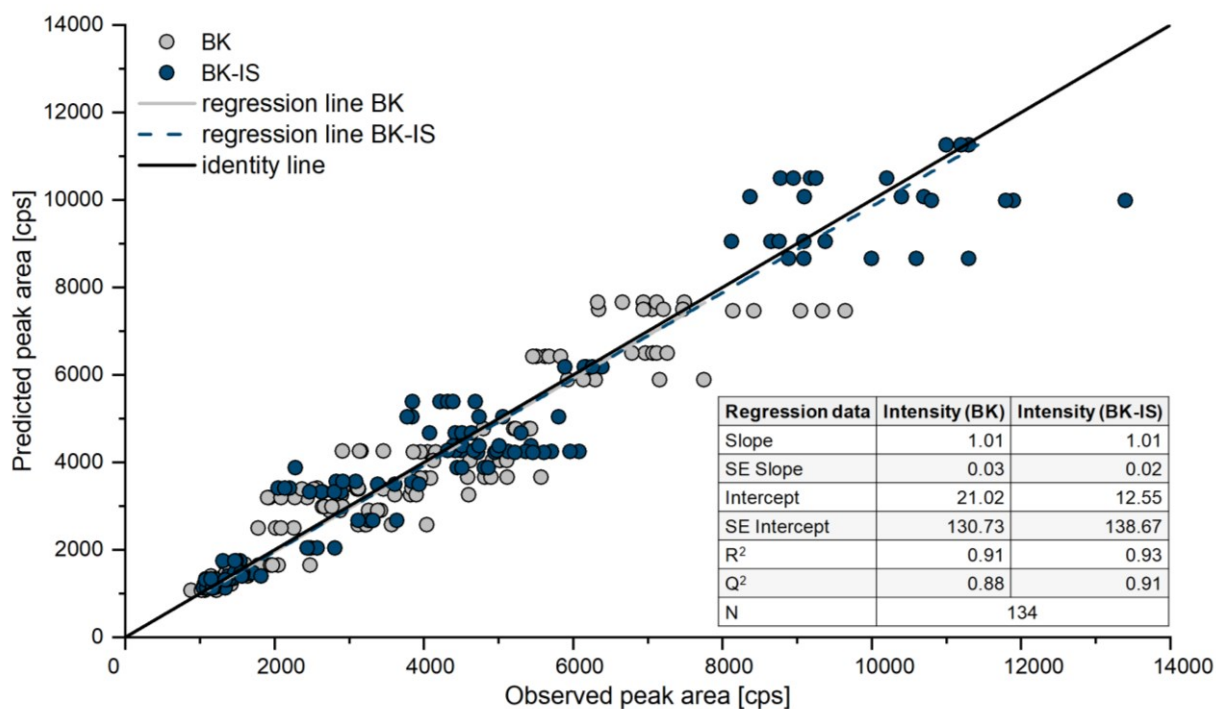
- United States Pharmacopeia Validation and Verification Expert Panel (2017)** Proposed New USP General Chapter: The Analytical Procedure Lifecycle (1220).
https://www.uspnf.com/sites/default/files/usp_pdf/EN/USPNF/revisions/s201784.pdf, last check: 15.04.2021.
- US Food and Drug Administration (2018)** Bioanalytical Method Validation Guidance for Industry. <https://www.fda.gov/files/drugs/published/Bioanalytical-Method-Validation-Guidance-for-Industry.pdf>, last check: 07.04.2021.
- van de Veerdonk FL, Kouijzer IJE, Nooijer AH de, van der Hoeven HG, Maas C, Netea MG, et al. (2020a)** Outcomes associated with use of a kinin B2 receptor antagonist among patients with COVID-19. *JAMA Network Open* 3(8):e2017708.
<https://doi.org/10.1001/jamanetworkopen.2020.17708>.
- van de Veerdonk FL, Netea MG, van Deuren M, van der Meer, J. W. M., Mast Q de, Brüggemann RJ, et al. (2020b)** Kallikrein-kinin blockade in patients with COVID-19 to prevent acute respiratory distress syndrome. *Elife* 9(e57555).
<https://doi.org/10.7554/eLife.57555>.
- van den Broek I, Sparidans RW, Schellens JHM, Beijnen JH (2010)** Quantitative assay for six potential breast cancer biomarker peptides in human serum by liquid chromatography coupled to tandem mass spectrometry. *Journal of Chromatography B* 878(5-6):590–602.
<https://doi.org/10.1016/j.jchromb.2010.01.011>.
- van Midwoud PM, Rieux L, Bischoff R, Verpoorte E, Niederländer HAG (2007)** Improvement of recovery and repeatability in liquid chromatography-mass spectrometry analysis of peptides. *Journal of proteome research* 6(2):781–791.
<https://doi.org/10.1021/pr0604099>.
- van Wanseele Y, Viaene J, van den Borre L, Dewachter K, Vander Heyden Y, Smolders I, et al. (2017)** LC-method development for the quantification of neuromedin-like peptides. Emphasis on column choice and mobile phase composition. *Journal of pharmaceutical and biomedical analysis* 137:104–112. <https://doi.org/10.1016/j.jpba.2017.01.014>.
- van Winden AWJ, van den Broek I, Gast M-CW, Engwegen JYMN, Sparidans RW, van Dulken EJ, et al. (2010)** Serum degradome markers for the detection of breast cancer. *Journal of proteome research* 9(8):3781–3788. <https://doi.org/10.1021/pr100395s>.
- Vanassche T, Engelen MM, van Thillo Q, Wauters J, Gunst J, Wouters C, et al. (2020)** A randomized, open-label, adaptive, proof-of-concept clinical trial of modulation of host thromboinflammatory response in patients with COVID-19: the DAWn-Antico study. *Trials* 21(1):1005. <https://doi.org/10.1186/s13063-020-04878-y>.

- Vickers C, Hales P, Kaushik V, Dick L, Gavin J, Tang J, et al. (2002)** Hydrolysis of biological peptides by human angiotensin-converting enzyme-related carboxypeptidase. *Journal of Biological Chemistry* 277(17):14838–14843. <https://doi.org/10.1074/jbc.M200581200>.
- Vujosevic S, Simó R (2017)** Local and systemic inflammatory biomarkers of diabetic retinopathy: An integrative approach. *Investigative Ophthalmology & Visual Science* 58(6):BIO68-BIO75. <https://doi.org/10.1167/iovs.17-21769>.
- Wakamatsu A, Ochiai S, Suzuki E, Yokota Y, Ochiai M, Kotani Y, et al. (2018)** Proposed selection strategy of surrogate matrix to quantify endogenous substances by Japan Bioanalysis Forum DG2015-15. *Bioanalysis* 10(17):1349–1360. <https://doi.org/10.4155/bio-2018-0105>.
- Wang D, Hu B, Hu C, Zhu F, Liu X, Zhang J, et al. (2020)** Clinical characteristics of 138 hospitalized patients with 2019 novel coronavirus-infected pneumonia in Wuhan, China. *JAMA* 323(11):1061–1069. <https://doi.org/10.1001/jama.2020.1585>.
- Werle E, Götze W, Kappler A (1937)** Über die Wirkung des Kallikreins auf den isolierten Darm und über eine neue darmkontrahierende Substanz. *Biochemische Zeitschrift* 289:217–233.
- Wheelock KM, Cai J, Looker HC, Merchant ML, Nelson RG, Fufaa GD, et al. (2017)** Plasma bradykinin and early diabetic nephropathy lesions in type 1 diabetes mellitus. *PloS one* 12(7):e0180964. <https://doi.org/10.1371/journal.pone.0180964>.
- Wu Z, McGoogan JM (2020)** Characteristics of and important lessons from the coronavirus disease 2019 (COVID-19) outbreak in China: Summary of a report of 72 314 cases from the Chinese Center for Disease Control and Prevention. *Journal of the American Medical Association* 323(13):1239–1242. <https://doi.org/10.1001/jama.2020.2648>.
- Yarovaya GA, Neshkova EA (2015)** Kallikrein-kinin system. Long history and present. (To 90th anniversary of discovery of the system). *Bioorganicheskaia khimiia* 41(3):275–291. <https://doi.org/10.1134/s1068162015030115>.
- Yu P, Hahne H, Wilhelm M, Kuster B (2017)** Ethylene glycol improves electrospray ionization efficiency in bottom-up proteomics. *Analytical and bioanalytical chemistry* 409(4):1049–1057. <https://doi.org/10.1007/s00216-016-0023-x>.
- Zhou F, Yu T, Du R, Fan G, Liu Y, Liu Z, et al. (2020)** Clinical course and risk factors for mortality of adult inpatients with COVID-19 in Wuhan, China: A retrospective cohort study. *The Lancet* 395(10229):1054–1062. [https://doi.org/10.1016/S0140-6736\(20\)30566-3](https://doi.org/10.1016/S0140-6736(20)30566-3).

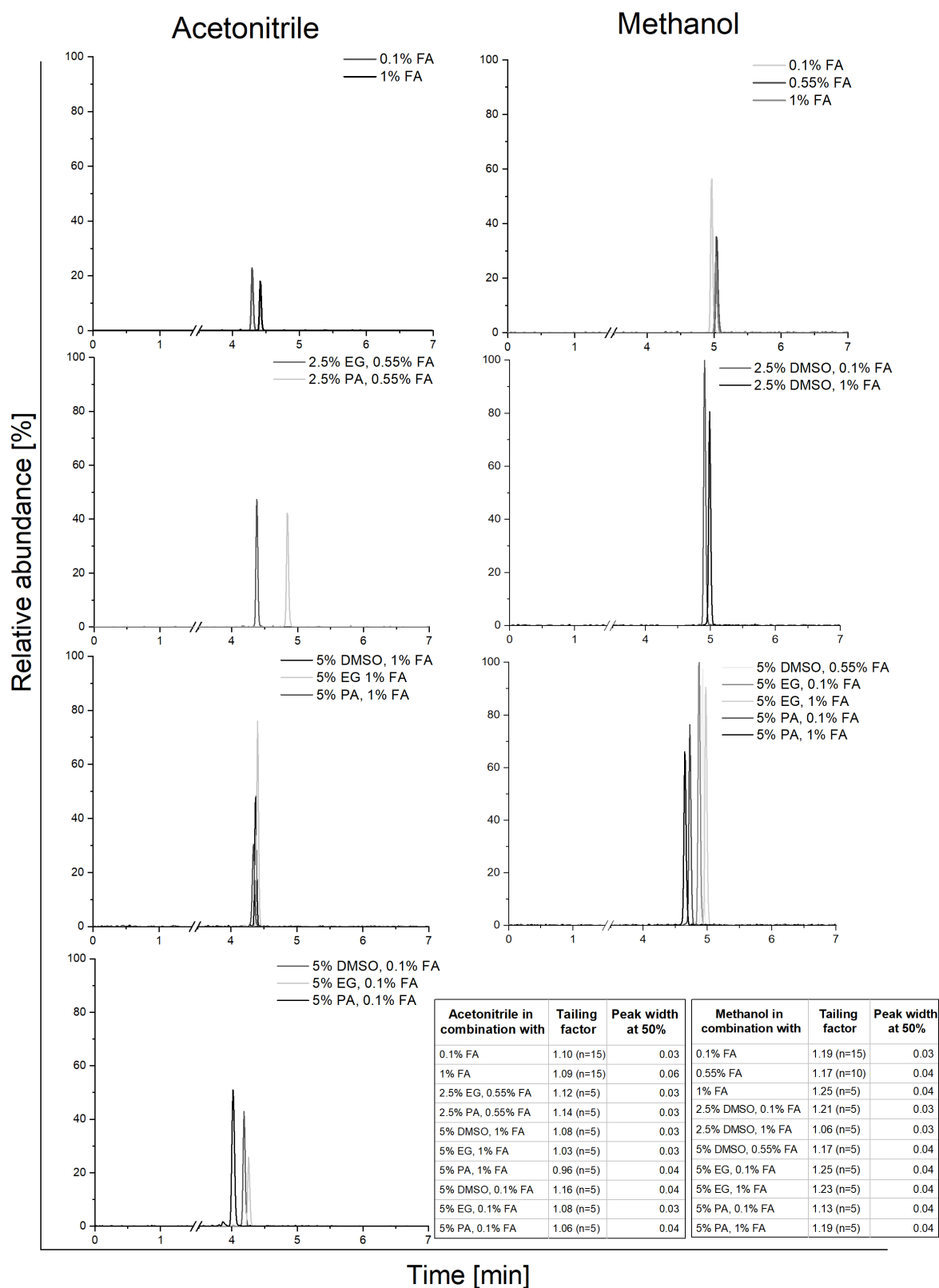
- Zhou W, Yang S, Wang PG (2017)** Matrix effects and application of matrix effect factor. *Bioanalysis* 9(23):1839–1844. <https://doi.org/10.4155/bio-2017-0214>.

12. Appendix

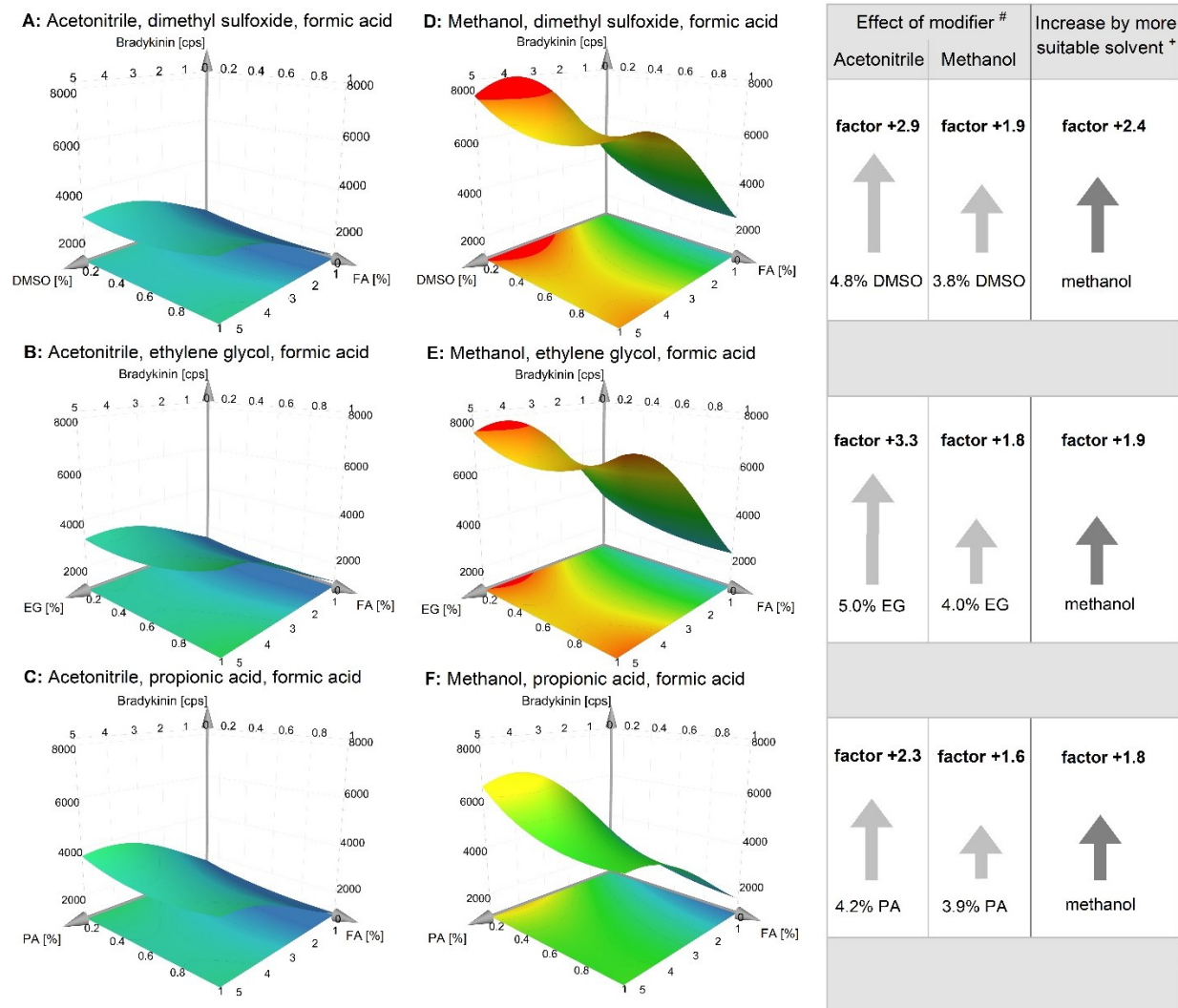
Appendix 1.	Observed versus predicted plot of the D-optimal of the mobile phase optimization.....	152
Appendix 2.	Example chromatograms of the conducted experiments of the D-optimal optimisation of the mobile phase composition.	153
Appendix 3.	Response surface plots of the mobile phase optimization.....	154
Appendix 4.	Example chromatograms of the confirmation runs for the mobile phase optimization using methanol as the organic mobile phase.	155
Appendix 5.	Observed versus predicted plot of the full-factorial screening of injection solvent and container materials.	156
Appendix 6.	Example chromatograms of distinct conditions investigated within the full-factorial screening on injection solvent and sample collection materials.	157
Appendix 7.	Observed versus predicted plot of the D-optimal for the injection solvent optimisation.....	158
Appendix 8.	Example chromatograms of the confirmation runs in the distinct materials for the injection solvent optimisation.	159
Appendix 9.	Unnormalized data of kinin levels in nasal lavage fluid of healthy volunteers.	160
Appendix 10.	Questionnaire for healthy volunteers participating in the study for collection of reference ranges.....	161
Appendix 11.	Conversion factors for calculation of the molar kinin concentration from the mass concentration considering the molecular weight.	162
Appendix 12.	Kinin levels in COVID-19 patients and controls.	163



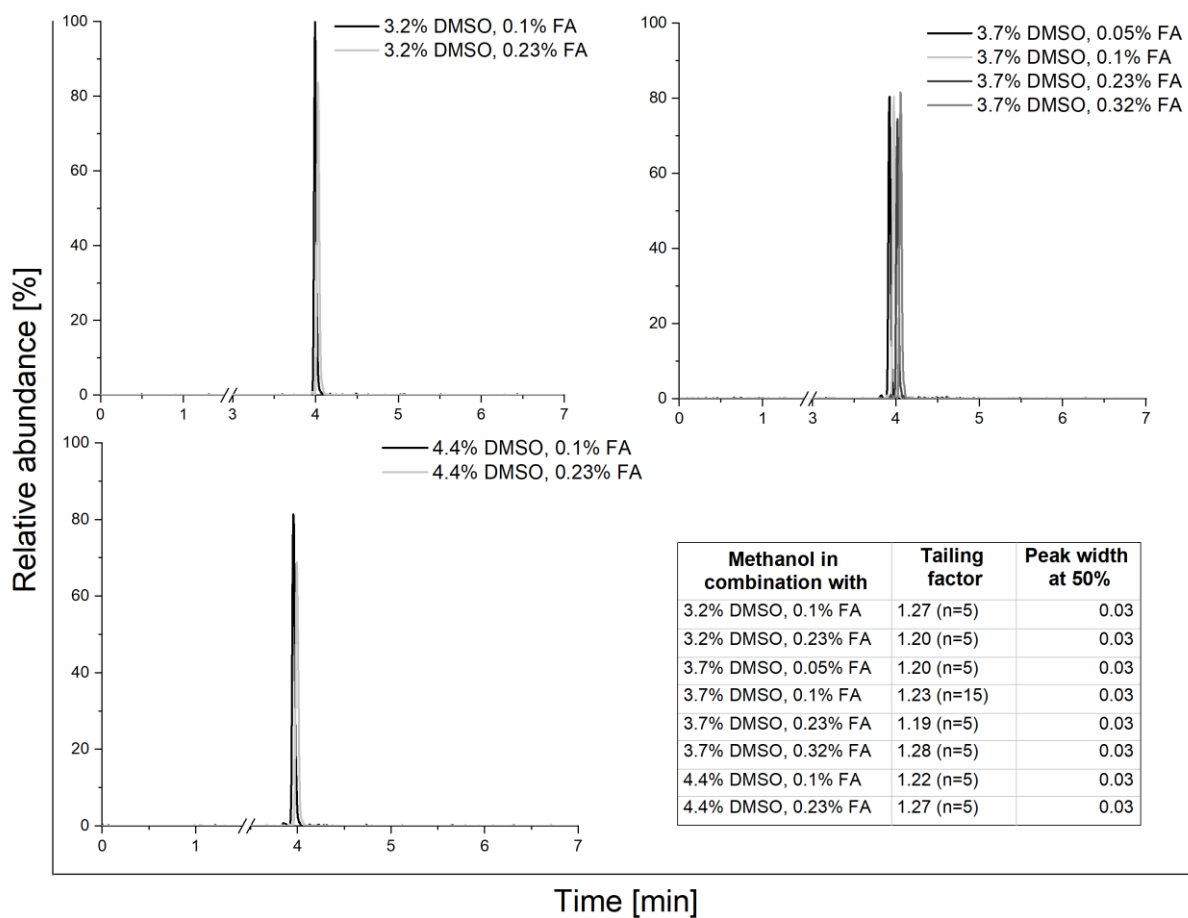
Appendix 1. Observed versus predicted plot of the D-optimal of the mobile phase optimization. BK: Bradykinin, BK-IS: internal standard of bradykinin, SE: standard error, N: number of experiments, R²: Goodness of fit, Q²: Goodness of prediction



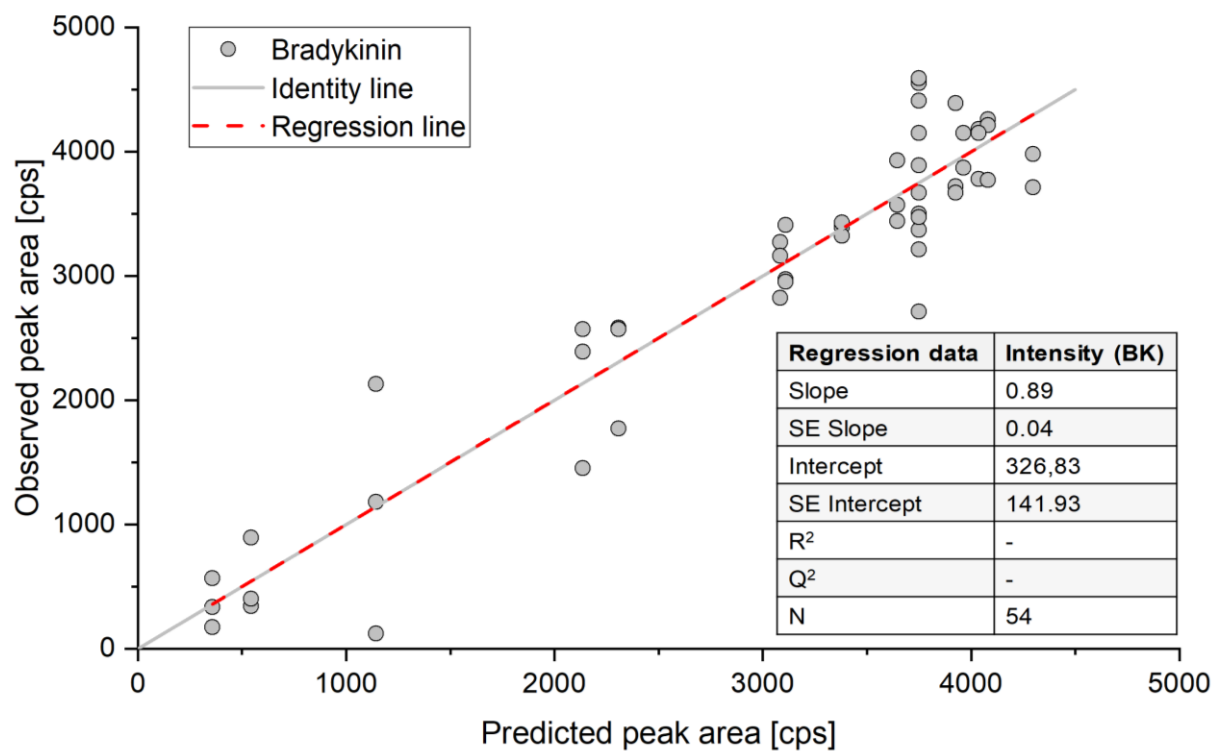
Appendix 2. Example chromatograms of the conducted experiments of the D-optimal optimisation of the mobile phase composition. DMSO: dimethyl sulfoxide, EG: ethylene glycol, FA: formic acid, PA: propionic acid



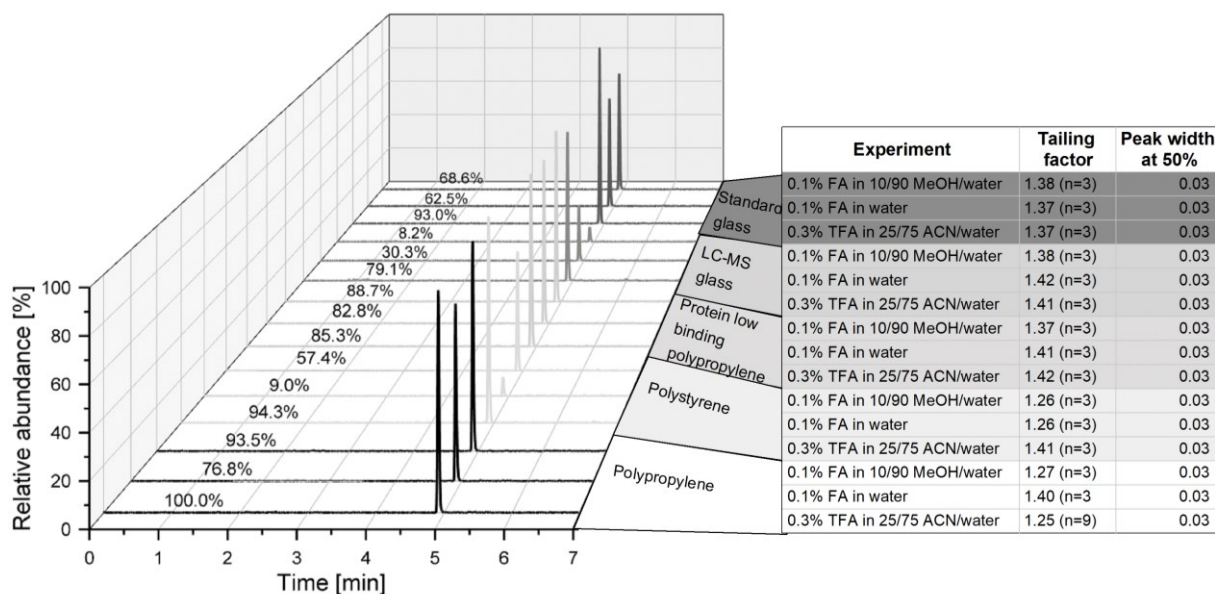
Appendix 3. Response surface plots of the mobile phase optimization. # Improvement when adding the optimized modifier concentration to optimized acid concentration; + Improvement when changing from acetonitrile to methanol using the respective optimized compositions. DMSO: dimethyl sulfoxide, EG: ethylene glycol, PA: propionic acid, FA: formic acid



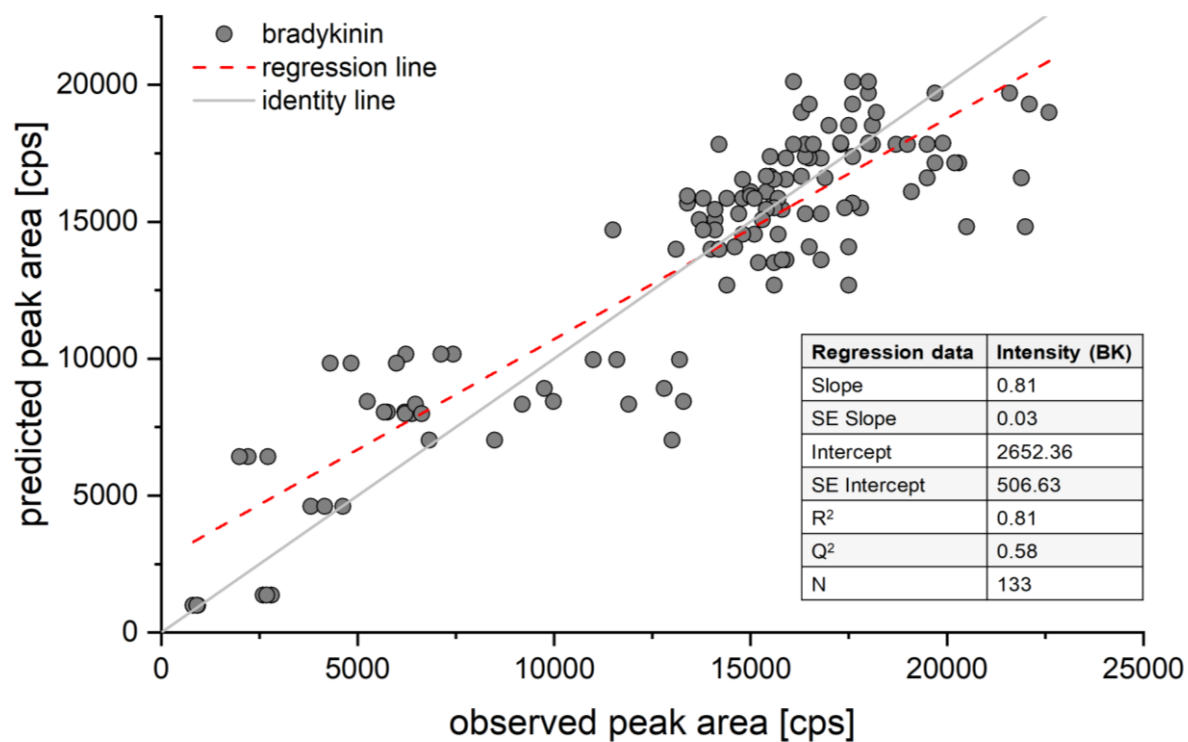
Appendix 4. Example chromatograms of the confirmation runs for the mobile phase optimization using methanol as the organic mobile phase. The retention time shift of one minute in comparison to the D-optimal optimization is due to a change in the LC-system. DMSO: dimethyl sulfoxide, FA: formic acid.



Appendix 5. Observed versus predicted plot of the full-factorial screening of injection solvent and container materials. BK: Bradykinin, SE: standard error, N: number of experiments, R²: Goodness of fit, Q²: Goodness of prediction

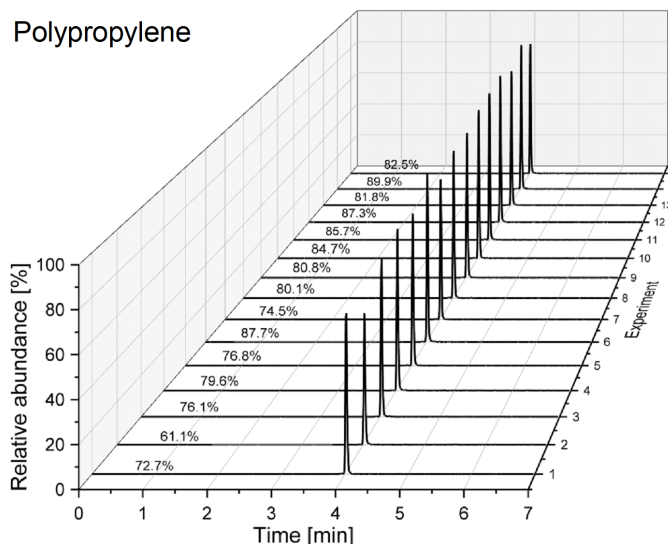


Appendix 6. Example chromatograms of distinct conditions investigated within the full-factorial screening on injection solvent and sample collection materials. ACN: acetonitrile, FA: formic acid, LC-MS: liquid chromatography coupled to mass spectrometry, MeOH: methanol, TFA: trifluoroacetic acid



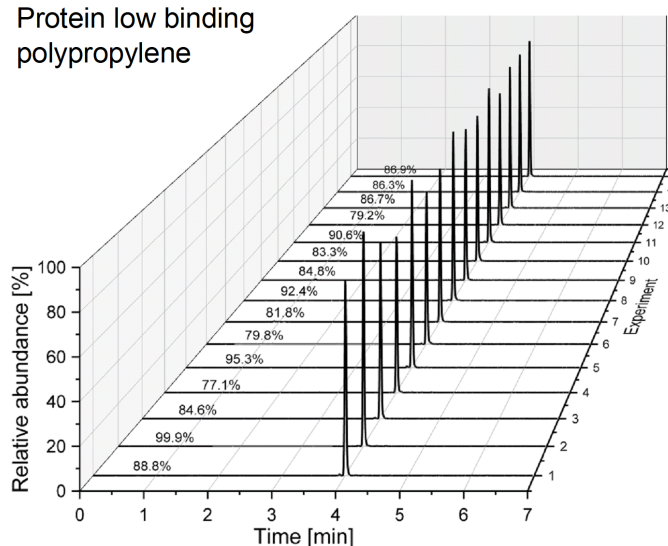
Appendix 7. Observed versus predicted plot of the D-optimal for the injection solvent optimisation. BK: Bradykinin, SE: standard error, N: number of experiments, R²: Goodness of fit, Q²: Goodness of prediction

Polypropylene



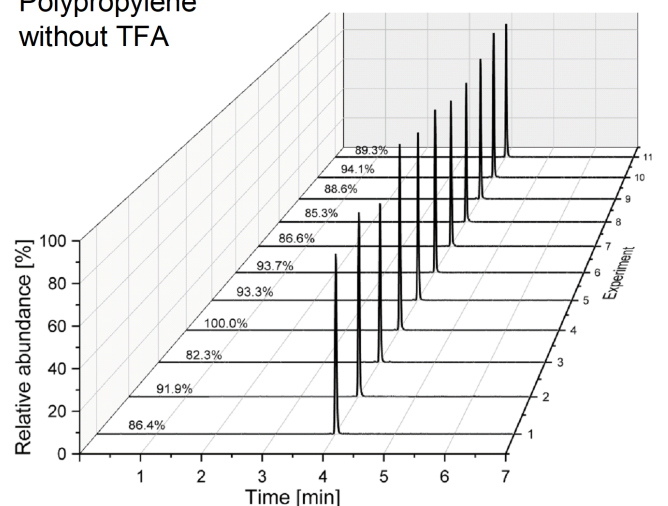
Experiment	Tailing factor	Peak width at 50%
15	1.22 (n=3)	0.03
14	1.18 (n=3)	0.03
13	1.27 (n=3)	0.03
12	1.13 (n=3)	0.03
11	1.19 (n=3)	0.03
10	1.17 (n=3)	0.03
9	1.15 (n=3)	0.03
8	1.22 (n=12)	0.03
7	1.26 (n=3)	0.03
6	1.30 (n=3)	0.03
5	1.19 (n=3)	0.03
4	1.23 (n=3)	0.03
3	1.20 (n=3)	0.03
2	1.25 (n=3)	0.03
1	1.23 (n=3)	0.03

Protein low binding polypropylene



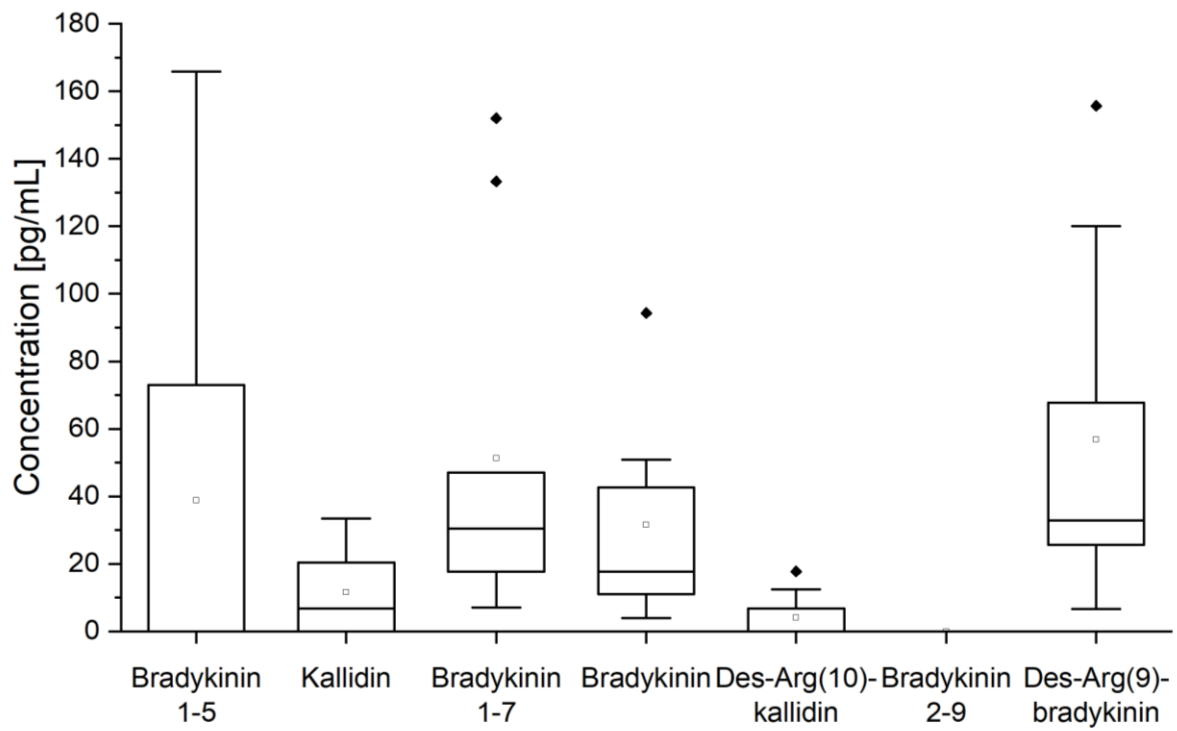
Experiment	Tailing factor	Peak width at 50%
15	1.24 (n=3)	0.03
14	1.22 (n=3)	0.03
13	1.24 (n=3)	0.03
12	1.19 (n=3)	0.03
11	1.18 (n=3)	0.03
10	1.20 (n=3)	0.03
9	1.22 (n=9)	0.03
8	1.21 (n=3)	0.03
7	1.17 (n=3)	0.03
6	1.18 (n=3)	0.03
5	1.08 (n=3)	0.03
4	1.26 (n=3)	0.03
3	1.17 (n=3)	0.03
2	1.20 (n=3)	0.03
1	1.19 (n=3)	0.03

Polypropylene without TFA



Experiment	Tailing factor	Peak width at 50%
11	1.17 (n=3)	0.03
10	1.18 (n=3)	0.03
9	1.20 (n=3)	0.03
8	1.20 (n=3)	0.03
7	1.18 (n=3)	0.03
6	1.19 (n=12)	0.03
5	1.21 (n=3)	0.03
4	1.15 (n=3)	0.03
3	1.21 (n=3)	0.03
2	1.09 (n=3)	0.03
1	1.25 (n=3)	0.03

Appendix 8. Example chromatograms of the confirmation runs in the distinct materials for the injection solvent optimisation. The retention time shift in comparison to the D-optimal optimisation is due to a change in the LC-system. ACN: acetonitrile, DMSO: dimethyl sulfoxide, FA: formic acid, MeOH: methanol, TFA: trifluoroacetic acid



Appendix 9. Unnormalized data of kinin levels in nasal lavage fluid of healthy volunteers. $n=9$, ■: interquartile range, T: 1.5 interquartile range, -: median, □: mean, ◆: outlier.

Appendix 10. Questionnaire for healthy volunteers participating in the study for collection of reference ranges.

Durchführung einer Nasenspülung und Blutabnahme im Rahmen der Evaluation der Bestimmbarkeit endogener Signalpeptide im Renin-Angiotensin-Aldosteron-System und angrenzenden Systemen (Angiotensin I, Angiotensin II, Bradykinin) mittels Massenspektrometrie

Angaben Studienteilnehmer

Studien-ID	___ __ _
Geschlecht	<input type="radio"/> weiblich <input type="radio"/> männlich
Alter	___ Jahre
COVID-19	<p>Hatten Sie in den letzten 14 Tagen Kontakt zu einem bestätigten COVID-19 Fall? <input type="radio"/> ja <input type="radio"/> nein</p> <p>Sind Sie in den letzten 14 Tagen in einem internationalen Risikogebiet oder in einem besonders betroffenen Gebiet in Deutschland gewesen? <input type="radio"/> ja <input type="radio"/> nein</p>
Erkrankungen	<p>Haben Sie allgemeine Erkältungssymptome (z.B. Fieber, Husten, Schnupfen)? <input type="radio"/> ja <input type="radio"/> nein</p> <p>Haben Sie Allergien? <input type="radio"/> ja <input type="radio"/> nein Wenn ja, welche: _____</p> <p>Leiden Sie unter Asthma oder einer anderen Atemwegserkrankung? <input type="radio"/> ja <input type="radio"/> nein</p> <p>Leiden Sie unter Herz-Kreislaufkrankungen? <input type="radio"/> ja <input type="radio"/> nein Wenn ja, welche: _____</p>
Arzneimittel	<p>Nehmen Sie regelmäßig Arzneimittel ein? <input type="radio"/> ja <input type="radio"/> nein Wenn ja, welche: _____</p>

Appendix 11. Conversion factors for calculation of the molar kinin concentration from the mass concentration considering the molecular weight. The molar concentration is calculated by division of the mass concentration by the conversion factor (Equation 6).

Kinin peptide	Conversion factor
Kallidin	1.188
(Hyp4)-kallidin	1.205
Des-Arg(10)-kallidin	1.032
Bradykinin	1.060
(Hyp3)-bradykinin	1.077
Des-Arg(9)-bradykinin	0.904
Bradykinin 1-7	0.756
Bradykinin 1-5	0.573
Bradykinin 2-9	0.904

Equation 6. Calculation of molar concentration:

$$\text{Concentration (pM)} = \frac{\text{Concentration } \left(\frac{\text{pg}}{\text{mL}}\right)}{\text{Conversion factor}}$$

Appendix 12. Kinin levels in COVID-19 patients and controls. Pg/mL values and respective pM values are expressed as median and [min – max] range.

Kinin	Unit	Control (n = 19)	COVID-19 (n = 21)	p-value
Kallidin	pM	6.0 [0.0 – 142.6]	6.1 [0.0 – 180.6]	0.751
	pg/mL	7.1 [0.0 – 120.0]	7.3 [0.0 – 152.0]	
Des-Arg(10)-kallidin	pM	5.1 [0.0 – 74.9]	5.1 [0.0 – 111.5]	0.415
	pg/mL	5.3 [0.0 – 72.6]	5.3 [0.0 – 108.0]	
Bradykinin	pM	13.5 [0.0 – 486.5]	12.0 [0.0 – 276.7]	0.432
	pg/mL	14.3 [0.0 – 459.0]	12.7 [0.0 – 261.0]	
des-Arg(9)-bradykinin	pM	0.0 [0.0 – 783.8]	19.6 [0.0 – 632.8]	0.062
	pg/mL	0.0 [0.0 – 867.0]	17.7 [0.0 – 700.0]	
Bradykinin 1-7	pM	37.6 [2.5 – 348.2]	128.6 [0.0 – 2,712.0]	0.056
	pg/mL	28.4 [3.3 – 460.0]	97.2 [0.0 – 3,583.0]	
Bradykinin 1-5	pM	0.0 [0.0 – 215.4]	156.6 [0.0 – 1,833.3]	0.001
	pg/mL	0.0 [0.0 – 374.0]	89.6 [0.0 – 2,425.0]	

13. Curriculum vitae

Personal Details

First name/ Last name	Tanja Gangnus
Date and place of birth	30.06.1993 in Schwetzingen
Address	Universitätsstr. 1, 40225 Düsseldorf, Germany
Telephone	+49 211 8113840
Fax	+49 211 8110741
E-Mail	Tanja.gangnus@hhu.de
Nationality	German

Professional experience

since 11/2017	Institute for Clinical Pharmacy and Pharmacotherapy, Heinrich Heine University Düsseldorf PhD-student / scientific co-worker
11/2016 – 04/2017	Bahnhof-Apotheke Pasing, Munich, Germany „Pharmazeut im Praktikum“ (pre-registration pharmacist)
05/2016 – 10/2016	Institute for Forensic Medicine, Freiburg, Germany „Pharmazeut im Praktikum“ (pre-registration pharmacist)
10/2015 – 12/2015	Kasoa Polyclinic, Kasoa-central region, Ghana Volunteer in hospital pharmacy

Education

07/2017	Certification as registered pharmacist in Germany (Apothekerkammer Bayern) and final state examination
10/2011 – 04/2016	Ludwig-Maximilians-University, Munich, Germany Pharmaceutical sciences
04/2016	Second state examination
08/2013	First state examination
07/2011	Abitur (equivalent to A-levels), Gymnasium Tutzing, Tutzing, Germany

Volunteering

02/2009 – 04/2017	TSV Herrsching e.V., Herrsching, Germany Youth handball coach
-------------------	--

14. List of publications

Parts of this thesis have already been published in peer-reviewed international journals or were presented at international conferences:

14.1. Publications in international peer-reviewed journals

- I. **Gangnus T and Burckhardt BB (2022)** Reliable measurement of plasma kinin peptides: Importance of preanalytical variables. *Research and Practice in Thrombosis and Haemostasis* 6(1): e12646 <https://doi.org/10.1002/rth2.1246>
- II. **Gangnus T and Burckhardt BB (2021)** Stabilization of short-lived peptides of the kallikrein-kinin system in human plasma to facilitate use as promising biomarkers. *Clinical chemistry* 67(9):1287-1289. <https://doi.org/10.1093/clinchem/hvab129>
- III. **Gangnus T, Burckhardt BB (2021)** Targeted LC-MS/MS platform for the comprehensive determination of peptides in the kallikrein-kinin system. *Analytical and bioanalytical chemistry* 413(11):2971–2984. <https://doi.org/10.1007/s00216-021-03231-9>.
- IV. **Gangnus T, Burckhardt BB (2021)** Sensitive mass spectrometric determination of kinin-kallikrein system peptides in light of COVID-19. *Scientific Reports* 11, 3061. <https://doi.org/10.1038/s41598-021-82191-7>
- V. **Gangnus T, Burckhardt BB, CARS consortium (2021)** Low-volume LC–MS/MS method for the pharmacokinetic investigation of carvedilol, enalapril and their metabolites in whole blood and plasma: Application to a paediatric clinical trial. *Drug Testing and Analysis* 13(3):694-708. DOI: 10.1002/dta.2949
- VI. **Gangnus T, Burckhardt BB (2020)** Improving sensitivity for the targeted LC-MS/MS analysis of the peptide bradykinin using a design of experiments approach. *Talanta*. 218:121134. <https://doi.org/10.1016/j.talanta.2020.121134>
- VII. **Suessenbach FK, Makowski N, Feickert M, Gangnus T, Tins J, Burckhardt BB; LENA consortium (2020)** A quality control system for ligand-binding assay of plasma renin activity: Proof-of-concept within a pharmacodynamic study. *Journal of Pharmaceutical and Biomedical Analysis*. 181:113090. <https://doi.org/10.1016/j.jpba.2019.113090>

- VIII. **Gangnus T, Burckhardt BB (2019)** Potential and Limitations of Atrial Natriuretic Peptide as Biomarker in Pediatric Heart Failure-A Comparative Review. *Frontiers in Pediatrics*. 6:420. <https://doi.org/10.3389/fped.2018.00420> Publications in revision in international peer-reviewed journals

14.2. Publications in revision in international peer-reviewed journals

- IX. **Gangnus T, Bartel A, Burckhardt BB.** Mass spectrometric study of variation in kinin peptide profiles in nasal fluids and plasma of adult healthy individuals. *Journal of Translational Medicine*.
- X. **Martens CP, Van Mol P, Wauters J, Wauters E, Gangnus T, Noppen B, Callewaert H, Feyen JHM, Liesenborgs L, Jansen S., Heylen E, Velasquez Pereira LC, Kraisin, S, Guler I, Engelen MM, Ockerman A, Van Herck A, Vos R, Vandembrielle C, Meersseman P, Hermans G, Wilmer A, Martinod K, Burckhardt BB, Vanhove M, Verhamme P, Neyts J, Vanassche T.** Dysregulation of the kallikrein-kinin system in lungs of patients with COVID-19. *EBioMedicine*.

14.3. Oral presentations

- I. **Gangnus T, Bartel A, Burckhardt BB (2021)** Comprehensive kinin peptide profiles in nasal fluids and plasma for a reliable healthy collective. Presented at *e-KININ 2021*, 8 June; online conference

14.4. Poster presentations

- I. **Gangnus T and Burckhardt BB (2020)** Facilitating insights into the pathophysiology of SARS-CoV-2: LC-MS/MS method for peptides of the kinin-kallikrein system. Poster presented at *36th symposium on Microscale Separations and Bioanalysis (e-MSB)*; 27-30 September; virtual edition
- II. **Gangnus T and Burckhardt BB (2020)** Hematocrit-independent low-volume LC-MS/MS assay for enalapril, carvedilol and their metabolites using whole blood for a paediatric clinical study. Poster presented at *12th Annual Congress on Mass Spectrometry and Advances in the Clinical Lab (MSACL US)*; 29 March - 2 April; Palm Springs, USA
- III. **Gangnus T and Burckhardt BB (2019)** A lean approach to examine surface adsorption of the low-abundant peptide bradykinin and to increase its signal intensity in LC-MS/MS:

A design of experiments concept. Poster presented at *Euroanalysis*; 1-5 September; Istanbul, Turkey

- IV. **Gangnus T and Burckhardt BB (2019)** Mobile phase optimization applying a design of experiments approach to increase the signal response of bradykinin and its internal standard. Poster presented at 48th *International Symposium on High-Performance Liquid Phase Separations and Related Techniques (HPLC)*; 16-20 June; Milan, Italy
- V. **Gangnus T, Suessenbach FK, Makowski N, Burdman I, Laeer S., Burckhardt BB (2019)** P37 Reference ranges of blood NT-proBNP in paediatric heart failure and healthy controls: compilation of literature data. *Archives of Disease in Childhood*;104:e32. Poster presented at *European Society for Developmental Perinatal and Paediatric Pharmacology (ESDPPP) Congress*; 2019 May 28-31; Basel, Switzerland
- VI. **Suessenbach FK, Gangnus T, Makowski N, Laeer S., Burckhardt BB (2019)** P95 Compilation of available plasma renin activity levels in the healthy and cardiac diseased paediatric population. *Archives of Disease in Childhood* 2019; 104:e56.2-e57. Poster presented at *European Society for Developmental Perinatal and Paediatric Pharmacology (ESDPPP) Congress*; May 28-31; Basel, Switzerland

14.5. Awards

- I. **Best oral presentation** at the **e-KININ 2021** for the talk entitled:

“Comprehensive kinin peptide profiles in nasal fluids and plasma for a reliable healthy collective.”

at the *e-KININ 2021*, 8 June; online conference

- II. **3rd Place** at the **Springer Poster Pitches Presentations Award** for the poster entitled:

“A lean approach to examine surface adsorption of the low-abundant peptide bradykinin and to increase its signal intensity in LC-MS/MS: A design of experiments concept”

at the *Euroanalysis 2019* conference, 1-5 September; Istanbul, Turkey